

Institut für Tierwissenschaften, Abt. Tierzucht und Tierhaltung  
der Rheinischen Friedrich – Wilhelms – Universität Bonn

---

**Functional analysis of microRNA-130b in bovine oocyte maturation and  
preimplantation embryo development**

Inaugural – Dissertation  
zur Erlangung des Grades

Doktor der Agrarwissenschaft  
(Dr. agr.)

der

Hohen Landwirtschaftlichen Fakultät

der

Rheinischen Friedrich – Wilhelms – Universität  
zu Bonn

vorgelegt im Mai 2011

von

Pritam Bala Sinha

aus

Ranchi, Indien

Diese Dissertation ist auf dem Hochschulschriftenserver der ULB Bonn

[http://hss.ulb.uni-bonn.de/diss\\_online](http://hss.ulb.uni-bonn.de/diss_online) elektronisch publiziert

E-mail: [diss-online@ulb.uni-bonn.de](mailto:diss-online@ulb.uni-bonn.de)

Universitäts- und Landesbibliothek Bonn

© Landwirtschaftliche Fakultät – Jahrgang 2011

Zugl.: ITW; Bonn, Univ., Diss., 2011

D 98

Referent: Prof. Dr. Karl Schellander

Korreferent: Prof. Dr. Jens Léon

Tag der mündlichen Prüfung: 11<sup>th</sup> July 2011

*Dedicated*

*To my Papa, my husband Bimal and my beloved daughter Vaishnawi*

## Funktionelle Analyse der microRNA miR-130b während der bovinen Oozytenmaturation und der preimplantativen Embryonalentwicklung

MicroRNAs (miRNAs) sind dafür bekannt, dass sie eine regulatorische Rolle in verschiedenen biologischen Prozessen, wie in der Embryonalentwicklung spielen. Es wird angenommen, dass das Expressionsmuster von miRNAs zwischen immaturren und *in vitro* maturierten bovinen Oozyten variiert, wobei gezeigt wurde, dass miR-130b in unreifen Oozyten hoch reguliert ist. Allerdings ist seine funktionelle Rolle in der Zellvitalität, Proliferation und Transkription während der bovinen Oozytenmaturation und der Präimplantationsembryoentwicklung noch nicht bekannt. Daher war das Ziel dieser Studie die Bedeutung von miR-130b in der Maturation von Oozyten-, Granulosa- und Kumuluszellen und in der präimplantativen Embryoentwicklung zu untersuchen. Dafür wurde das Expressionsmuster der miR-130-Familie im bovinen embryonalen Präimplantationsstadium erstellt. MiR-130b war in Kumulus- und Granulosazellen, in unreifen Oozyten sowie im Morula- und Blastozystenstadium höher exprimiert. Die miR-130b Zielgen-Identifizierung erfolgte mittels der *In silico* Analyse und der experimentellen Validierung durch den Luciferase-Assay. Dementsprechend konnten MSK1, SMAD5, MEOX2, DOC1R und EIF2C4 als Zielgene von miR-130b ermittelt werden. Um den Einfluss der miR-130b während der Maturation der Oozyten zu untersuchen, wurden in unreifen Oozyten pre-miR-130b und sequenz-spezifische miR-130b Antisense (Inhibitor) mikroinjiziert, während mit scrambled miRNA injizierte und nicht injizierte Oozyten als Kontrolle dienten. 24 Stunden nach der Mikroinjektion wurde der Reifungsstatus der Oozyten mittels der ersten Polkörper-Extrusion festgestellt. Sie betrug 86,3, 73, 85, und 84,6% bei Oozyten mit injizierter pre-miR-130b, anti-miR-130b, scramble RNA und nicht injizierter Kontrolle. Die Mehrheit der anti-miR-130b injizierten Oozyten blieb in der Telophase 1 (22%) stehen. Darüber hinaus konnte eine höhere mitochondriale Aktivität in pre-miR-130b und eine niedrigere in anti-miR-130b injizierten Oozyten im Vergleich zu scramble RNA und nicht injizierten Oozyten gefunden werden. Dies konnte mit der Zunahme der Proteinexpression der miR-130b Zielgene SMAD5 und MSK1 assoziiert werden. Oozyten Companionzellen sind für die Oozytenmaturation erforderlich. Der Einfluss der miR-130b konnte bei der Zellproliferation, Laktatproduktion und beim Cholesterinspiegel durch die Transfektion der miR-130b Precursor RNA oder anti-miR-130b RNA in Kumulus- und Granulosazellen beobachtet werden. Mit der Reduktion der miR-130b folgte eine Reduzierung in der Zellproliferation und der Laktatproduktion, allerdings keine Änderungen im Cholesterinspiegel in Granulosa- oder Kumuluszellen. Neben der Maturation der Oozyten und der Oozyten Companionzellfunktion wurde die Rolle der miR-130b während der präimplantativen Embryoentwicklung nach einer Mikroinjektion der miR-130b Precursor oder – Inhibitor in Zygoten untersucht. Das Ergebnis zeigte, dass die erste Teilungsrate unbeeinflusst vom Knockdown oder der Überexpression der miR-130b war, jedoch war die Morula/Blastozysten rate der anti-miR-130b injizierten Eizellen signifikant reduziert. Diese Studie liefert Hinweise dafür, dass die miR-130b während der bovinen Oozytenmaturation, der Granulosazellproliferation und der Morula- und Blastozystenformation funktionell beteiligt ist.

## Functional analysis of microRNA-130b in bovine oocyte maturation and preimplantation embryo development

MicroRNAs (miRNAs) are well known to regulate the proteins involved in various biological processes including development. The expression pattern of miRNAs is believed to vary between immature and *in vitro* matured bovine oocytes. Among these, miR-130b was reported to be upregulated in immature compared to matured oocytes. However, its functional role in cell viability, proliferation or transcription during bovine oocyte maturation and preimplantation embryo development is not known. Therefore, this experiment was aimed to investigate the functional role of miR-130b in oocyte maturation and oocyte surrounding cells and its involvement in preimplantation embryo development. For this, the spatiotemporal expression pattern of miR-130 family was performed throughout the bovine preimplantation stage embryos. Accordingly, miR-130b was found to be highly expressed in cumulus and granulosa cells, immature oocyte, morula and blastocyst stage embryos. Once the expression pattern of miR-130b was evaluated, its target genes were *in silico* analyzed and experimentally validated. Accordingly, MSK1, SMAD5, MEOX2, DOC1R and EIF2C4 were found to be the real targets of miR-130b.

To investigate the involvement of miR-130b during oocyte maturation, immature oocytes were microinjected with pre-miR-130b (precursor) or sequence specific antisense (inhibitor) of miR-130b, while scramble miRNA injected and uninjected oocytes were used as controls. The maturational status of the oocytes and the level of miR-130b target genes expression were assessed 22 hours post microinjection. The result showed that the first polar body extrusion was 86.3, 73, 85 and 84.6% in oocytes injected with pre-miR-130b, anti-miR-130b, scramble and uninjected controls, respectively. Similarly, mitotic staining showed that majority of oocytes injected with anti-miR-130b remains arrested at the telephase I stage (22%) and significantly reduced to reach Metaphase II compared to other oocyte groups. In addition, the mitochondrial activity was higher in pre-miR-130b and lower in anti-miR-130b injected oocytes compared to scramble and uninjected oocytes. This was associated with the reduction of miR-130b and increase of its target genes SMAD5 and MSK1 expression. Furthermore, oocyte surrounding cells are required for oocyte maturation, the involvement of miR-130b in cumulus and granulosa cell proliferation, lactate production and cholesterol level was assessed after transfection of pre-miR-130b or anti-miR-130b in both cell types. The inhibition of miR-130b resulted in reduction of cell proliferation and lactate production. However, knockdown of miR-130b did not change the cholesterol level in the granulosa or cumulus cells.

Apart from oocyte maturation and oocyte companion cell function, the role of miR-130b was investigated during preimplantation embryo development by microinjecting zygotes with pre-miR-130b or anti-miR-130b. The result has shown that the first cleavage rate was unaffected by knockdown or ectopic expression of miR-130b, but the rate of morula and blastocyst were significantly reduced in anti-miR-130b injected zygotes. Therefore this study provides the significant evidence that miR-130b may be required during bovine oocyte *in vitro* maturation and granulosa cell proliferation, morula and blastocyst formation, further functional in depth studies are necessary to understand whether miR-130b is involved in bovine oocyte *in vivo* maturation or embryo implantation.

Contents		Page
Abstract		v-vi
List of abbreviations		xii
List of tables		xvi
List of figures		xvii
1	Introduction	1
2	Literature review	3
2.1	MicroRNAs	3
2.1.1	Discovery of miRNAs	4
2.1.2	Biogenesis of microRNA	5
2.1.3	RNA induces silencing complex assembly	7
2.1.4	Principle of miRNA target prediction	9
2.1.5	Regulatory mechanism of microRNA in animals	11
2.2	Biological functions of miRNAs in animals	12
2.3	Expression and role of miRNA in mammalian folliculogenesis and embryogenesis	14
2.3.1	Involvement of miRNA in follicular development	14
2.3.2	Gamete formation and the involvement of miRNA	18
2.3.2.1	Expression and role of miRNA in oocyte maturation	18
2.3.2.2	Expression and role of miRNA in spermatogenesis	23
2.4	Role of miRNAs in fertilization and preimplantation embryo development	24
2.5.1	MicroRNA miR-130b family in embryonic stem cells	27
2.5.2	Impact of miR-130b in different cell types	28
3	Materials and methods	30
3.1	Materials	30
3.1.1	Embryos	30
3.1.2	Materials for laboratory analysis	30
3.1.2.1	Chemicals, kits, biological and other materials	30

3.1.2.2	List of equipment	33
3.1.2.3	Used softwares	34
3.1.2.4	Reagents and media	35
3.2	Methods	41
3.2.1	<i>In vitro</i> embryo production	41
3.2.1.1	Oocytes recovery and <i>in vitro</i> maturation	41
3.2.1.2	Sperm preparation and capacitation	42
3.2.1.3	<i>In vitro</i> fertilization of oocytes	42
3.2.1.4	<i>In vitro</i> culture of embryos	43
3.2.1.5	Oocytes denudation and storage	43
3.2.2	Plasmid DNA preparation	43
3.2.2.1	Primers design and gene cloning	43
3.2.2.2	Colony screening and sequencing	45
3.2.2.3	Plasmid DNA isolation and serial dilution	49
3.2.2.4	Cloning of 3'UTR amplicons in pmirGLO vector	50
3.2.2.5	Sequencing of 3'UTR and plasmid isolation	52
3.2.3	Cell culture	53
3.2.4	Transient transfection	54
3.2.5	Target validation	56
3.2.5.1	miRNA target prediction and site selection	56
3.2.5.2	DNA constructs	57
3.2.5.3	Reporter assays and preparation of luminometer	57
3.2.6	Microinjection	58
3.2.6.1	Design and synthesis of precursor, inhibitor and scramble RNA	58
3.2.6.2	Preparation of miRNA for injection	58
3.2.6.3	Microinjection of oocytes	58
3.2.6.4	Microinjection of zygotes	59
3.2.7	Oocytes and embryos collection	60
3.2.8	RNA isolation and cDNA synthesis	60
3.2.9	Expression profile of miRNA using qRT-PCR	61
3.2.10	Quantitative real-time PCR analysis for transcript	62
3.2.11	Localization of miRNA in ovary and embryos	63
3.2.12	Protein detection in oocyte and ovary cryosection	64

3.2.13	Western blot	66
3.2.13.1	Protein extraction	66
3.2.13.2	Protein separation and transfer	66
3.2.14	Mitochondrial assay	67
3.2.15	Cell proliferation assays	67
3.2.16	Cholesterol assay	68
3.2.17	Determination of glycolytic rate	69
3.2.18	Statistical analysis	69
4	Results	70
4.1	Expression profile of miR-208 and miR-130b in oocyte and surrounding cells	70
4.2	The expression pattern of miR-130 family	70
4.2.1	Expression of miR-130 family in oocytes and surrounding somatic cells	71
4.2.2	In situ detection of miR-130b in different stages of follicular cells	73
4.2.3	The expression profiling of miR-130 family in preimplantation embryo	74
4.2.4	In situ localization of miR-130b in preimplantation embryo development	76
4.3	In silico analysis and experimental validation of target gene	77
4.3.1	Identification of the appropriate gene as a target of miR-130b in oocyte maturation and preimplantation	77
4.3.2	Expression profiling of selected target genes in preimplantation embryo	81
4.3.3	Transfection of cells with different concentration of construct plasmid and miR-130b for further experimental validation	83
4.3.4	Experimental validation of cloned genes EIF2C1, EIF2C4, DDX6, SMAD5, MEOX2, MARCH2 and DOCR1	85
4.3.5	Expression of SMAD5 and MSK1 transcript in oocyte and companion cells	88
4.3.6	Localization of selected target proteins in follicular cells and COC	88



4.4	Effect of miR-130b in oocyte maturation and its surrounding cell function	89
4.4.1	Direct regulation of SMAD5 and MSK1 by miR-130b in oocyte maturation	89
4.4.2	Role of miR-130b on oocyte maturation	91
4.4.2.1	Polar body extrusion in miR-130b injected oocyte groups	91
4.4.2.2	Effect of miR-130b in mitotic division of oocytes	91
4.4.2.3	miR-130b affects the mitochondrial activity during oocyte maturation	92
4.4.3	Effect of miR-130b in oocyte surrounding cells	93
4.4.3.1	Regulation of SMAD5 and MSK1 by miR-130b in cumulus cells	93
4.4.3.2	Effect of miR-130b in cumulus cell proliferation	95
4.4.3.3	Regulation of SMAD5 and MSK1 by miR-130b in granulosa cells	95
4.4.3.4	Granulosa cell proliferation is influenced by miR-130b	96
4.4.3.5	miR-130b controls glycolysis in oocyte surrounding cells	98
4.4.3.6	Influence of miR-130b in cholesterol biosynthesis	99
4.5	Effects of miR-130b on <i>in vitro</i> embryos development	100
4.5.1	Effect of miR-130b on <i>in vitro</i> blastocyst formation	101
4.5.2	Effect of miR-130b on expression of SMAD5 and MSK1 in blastocyst derived from injected zygotes	102
4.5.3	Apoptotic effect of miR-130b	104
5	Discussion	105
5.1	Functional analysis of miRNA in bovine preimplantation	105
5.2	Selection of miRNA for functional analysis study	105
5.3	Differentially regulation of miR-130 family in oocyte, oocyte surrounding somatic cells and preimplantation embryos	106
5.4	Recognition of target genes and their validation	107
5.5	The role of miR-130b in oocyte maturation	110
5.6	Influence of miR-130b in oocyte surrounding cells proliferation and cholesterol biogenesis	112
5.7	Influence of miR-130b in glycolysis of oocyte surrounding cells	113
5.8	Effect of miR-130b on blastocyst formation and apoptosis	114

6	Summary	116
7	Zusammenfassung	121
8	Reference	126
9	Acknowledgements	I
10	Curriculum Vitae	III

A	Adenine
A570/650	Absorbance at 570/650 nm wavelength (UV light)
ACC. No	Gene bank accession number
AGO	Argonaute
APS	Alkaline phosphatase
T <sub>A</sub>	Annealing temperature
ATP	Adenosine triphosphate
BLAST	Basic local alignment search
BME	Basal medium eagle
bp	Base pairs
BSA	Bovine serum albumin
bta	Bos taurus
cDNA	complementary deoxy ribonucleic acid
<i>C. elegans</i>	<i>Caenorhabditis elegans</i>
CLSM	Confocal laser scanning microscope
CO <sub>2</sub>	Carbondioxide
COCs	Cumulus oocyte complex
Ct	Threshold cycle
CR1	Charles rosenkrans medium
cRNA	Complementary ribonucleic acid
Cy3	Cyanine 3 fluorescent dye
DAPI	4',6-Diamidin-2'-phenylindoldihydrochlorid
ddH <sub>2</sub> O	Distilled and deionised water
DEPC	Diethylpyrocarbonate
DMEM	Dulbecco's modified eagle's medium
DMSO	Dimethyl sulfoxide
DNA	Deoxyribonucleic acid
DNase	Deoxyribonuclease
dNTP	Deoxynucleotide triphosphate
DTCS	Dye terminator cycle sequencing
DTT	Dithiothreitol
<i>E.coli</i>	<i>Escherichia coli</i>

E <sub>2</sub>	Estradiol
EDTA	Ethylenediaminetetraacetic acid
EGA	Embryonic genome activation
ESC	Embryonic stem cell
ESTs	Expressed sequence tags
EtBr	Ethidium bromide
EtOH	Ethanol
FCS	Fetal calf serum
FITC	Fluorescein isothiocyanate
FSH	Follicle stimulating hormone
GAPDH	Glyceraldehyde 3-phosphate dehydrogenase
GFP	Green fluorescent protein
GnRH	Gonadotropin-releasing hormone
GO	Gene ontology
GTP	Guanosine triphosphate
GV	Germinal vesicle
GVBD	Germinal vesicle break-down
hCG	Human chorionic gonadotropin
ICM	Inner cell mass
hpi	Hours post insemination
IPTG	Isopropyl β-D-1-thiogalactopyranoside
IVC	<i>In vitro</i> culture
IVF	<i>In vitro</i> fertilization
IVM	<i>In vitro</i> maturation
IVP	<i>In vitro</i> production
ISH	<i>In situ</i> hybridization
KDa	Kilo dalton
LB	Lysogeny broth or Luria-Bertani broth
LH	Luteinizing hormone
LNA	Locked nucleic acid
MEM	Minimum essential medium
min	Minute
miRNA	MicroRNA

MAPK	Mitogen activated protein kinase
MPF	Maturation promoting factor
mRNA	Messenger ribonucleic acid
MSK	Mitogen and stress activated kinase
MI	First meiosis
MII	Second meiosis
MW	Molecular weight
MZT	Maternal to zygotic transition
NaOAc	Sodium oxaloacetic acid
NCBI	National center for biotechnological information
No	Number
nt	nucleotide
OD	Optical density
PAGE	Polyacrylamide gel electrophoresis
P4	Progesterone
PBS	Phosphate buffer saline
PBST	Phosphate buffer saline tween
PCR	Polymerase chain reaction
PFA	Paraformaldehyde
PGC	primordial germ cells
PVP	Polyvinyl pyrrolidone
QRT-PCR	Quantitative real time polymerase chain reaction
r	Correlation coefficient
RNA	Ribonucleic acid
RNasin	Ribonuclease inhibitor
rpm	Revolution per minute
RISC	RNA induced silencing complexes
SAS	Statistical analysis system
SD	Standard deviation
SDS	Sodium dodecyl sulphate
s.e.m.	Standard error of mean
SLS	Sample loading solution
SSC	Sodium chloride sodium citrate

SVM	Support vector machine
TAE	Tris acetate ethylenediamin tetra acetat
TE	Tris-ethylenediamin-tetra acetat
TEMED	N, N, N', N'-Tetramethylenediamine
tRNA	Transfer ribonucleic acid
TUNEL	Terminal deoxynucleotidyl transferase dUTP nick end labelling
X-gal	5-bromo-4-chloro-3-indolyl-beta-D-galactopyranoside
3'UTR	Three prime untranslated region
UV	Ultra-violet light
V/V	Volume per volume
W/V	Weight per volume

<b>List of tables</b>	<b>Page</b>
Table 1: The genes involved in SMAD signalling pathway during folliculogenesis and oocyte maturation.	20
Table 2: miRNA sequence of miR-130 family in human.	28
Table 3: List of primers (5' to 3') used in this study.	47
Table 4: List of 3'UTR primer (5' to 3') used for the validation of miR-130b target genes.	48
Table 5: The number of cells taken per millilitre medium to generate standard curve for cell proliferation assay using MTT.	56
Table 6: Samples and amount taken for RNA isolation.	61
Table 7: List of microRNA in bta-mir-130 family and their similarity to bta-mir-130b.	71
Table 8: List of selected bta-mir-130b target genes with its target sites.	78
Table 9: The polarbody extrusion rate of injected and uninjected oocytes groups.	91
Table 10: First cleavage of the zygote injected with miR-130b precursor, inhibitor and scramble compared to the uninjected control group.	100

<b>List of figures</b>	<b>Page</b>
<p>Figure 2.1: miRNA biogenesis: a. Transcription: The primary miRNA transcripts (pri-miRNA), are transcribed as individual miRNA genes, from different location of DNA, b. Nuclear processing: Processing of the nascent transcript to ~70-nt stem-loop precursor miRNA (pre-miRNA), c. Nuclear exporting: Export of the pre-miRNA from the nucleus, d. Cytoplasmic processing: Processing of ~22-bp miRNA duplex, e. Release of the ~22-nt mature miRNA and assembly of the miRNA-induced silencing complex (miRISC), f. Transcriptional repression or mRNA degradation by miRNA binding to the 3'UTR of target mRNA (adapted from van Rooij and Olson 2007).</p>	6
<p>Figure 2.2: RNA induces silencing complex assembly and binding to siRNA or miRNA. siRISC binds to its target mRNA by perfectly matching base pairs, cleaves the target mRNA, recycles the complex, and does not require P-body structures for its function. Multiple numbers of miRISC bind to target mRNA by forming a bulge sequence in the middle that is not suitable for RNA cleavage, accumulate in P-bodies, and repress translation by exploiting global translational suppressors such as RCK/p54. The translationally repressed mRNA is either stored in P-bodies or enters the mRNA decay pathway for destruction. Depending upon cellular conditions and stimuli, stored mRNA can either re-enter the translation or mRNA decay pathways (from Herrera-Esparza et al. 2008).</p>	9
<p>Figure 2.3: The schematic description of the miRNA seed sequence binding to target mRNA. The perfect seed binding extended with 3' site ends with mRNA cleavage. Imperfect binding of seed sequence is not enough for mRNA degradation but suppress the function.</p>	



- Wobble (G:U) pairing in seed sequence don't allow the complementary binding of miRNA and mRNA. 11
- Figure 2.4: Different approaches used to identify the miRNA genes, target genes and functions of miRNAs in animals with an example. Ce: *Caenorhabditis elegans*; Dm: *Drosophila melanogaster*; Dr: *Danio rerio*; Hs: *Homo sapiens*; Mm: *Mus musculus* (from Wienholds and Plasterk 2005). 14
- Figure 2.5: Stages of mammalian oogenesis and folliculogenesis. PGD: primordial germ cells, n: chromosomal and C: DNA content (from Picton et al. 1998). 15
- Figure 2.6: Crosstalk between the oocyte and granulosa cells (both cumulus and mural) is integral for various stages of folliculogenesis. Oocyte-derived factors act via SMAD 1/5/8 and SMAD 2/3 respectively, to elicit cellular responses that are essential for successful folliculogenesis and ovulation (from Myers and Pangas 2010). 21
- Figure 2.7: Schematic diagram of *in vitro* preimplantation embryo development in bovine. 25
- Figure 3.1: pmirGLO Dual-Luciferase miRNA Target Expression Vector. PGK promoter for firefly with multiple cloning site and SV40 promoter for renilla luciferase expression. Amp<sup>r</sup>: ampicillin resistance; MCS: multiple cloning site; PKG: phosphoglycerate kinase. 51
- Figure 4: The expression profile of miR-130b and miR-208 in granulosa cells, immature cumulus and mature cumulus cells. The vertical axis indicates the fold change of miRNA using the minimum value as one and normalized to the geometric mean of U6 and Snod48. Error bars show miRNA mean  $\pm$  SD. Significant differences (a:b – p < 0.05). GC: granulosa cell; ICC : immature

cumulus cell; MCC : mature cumulus cell. 70

Figure 4.1: The expression profile of miR-130 family in granulosa cells, mature and immature cumulus cells. The vertical axis indicates the fold change of miRNA using the minimum value as one and normalized to the geometric mean of U6 and Snod48. Error bars show miRNA mean  $\pm$  SD. Significant differences (a:b –  $p < 0.05$ ) IM: immature; M: mature. 72

Figure 4.2: The expression pattern of miR-130 family in immature and mature oocytes (A), miR-130b across the cumulus cells, granulosa cells, immature and mature oocyte (B). The vertical axis indicates the fold change of miRNA using the minimum value as one and normalized to geometric mean of U6 and Snod48. Error bars show the miRNA mean  $\pm$  SD. Significant differences (a:b:c –  $p < 0.05$ ) and (\*\* $p < 0.001$ ). GC: granulosa cell, CC: cumulus cell, IMO: immature oocytes, MO : mature oocytes. 73

Figure 4.3: In-situ detection of miR-130b in the ovarian sections using 3'-digoxigenin labelled locked nucleic acid (LNA) microRNA probes for miR-130b, U6 and scramble miRNA. A and B: miR-130b, C: U6 (positive control) and D: scramble (negative control). A: preantral follicle, B, C and D: antral follicle, Red signal stands for miRNA (miR-130b, U6 and scramble) and blue signal represents nuclear staining, DAPI: 4',6-diamidino-2-phenylindole. Scale bar represents 20  $\mu$ m. 74

Figure 4.4: The expression pattern of miR-130 family across the preimplantation stage embryos. The vertical axis indicates the fold change of miRNA using the minimum value as one and normalized to the geometric mean of U6 and Snord48. Error bars show miRNA mean  $\pm$  SD. Significant differences (a:b:c –  $p < 0.05$ ) and (\* $p < 0.001$ ). 75

- Figure 4.5: Whole-mount in-situ detection of miR-130b in COCs and preimplantation embryo stage using 3'-digoxigenin labelled locked nucleic acid (LNA) based microRNA probes for miR-130b and scramble miRNA and nucleus was stained with DAPI. 2D, 2 dimensional; 3D, 3 dimensional; scr, scramble; miR, miR-130b; DAPI, 4',6-diamidino-2-phenylindole. Red and blue colours indicate miRNA expression and nuclear staining respectively. 76
- Figure 4.6: Bovine miR-130b and predicted 3'UTR of the target gene. Blue: target gene, Red: miR-130b. A: DDX6; B: RPS6KA5; C: EIF2C1; D: EIF2C4; E: MARCH2; F: SMAD5; G: MEOX2; H: DOC1R. 80
- Figure 4.7: Expression profiling of selected transcripts across the preimplantation stage embryos. MO: Mature oocyte; Z: Zygote; 2C: 2-Cell; 4C: 4-cell; 8C: 8-Cell; Mo: Morula; Bl: Blastocyst. 82
- Figure 4.8: (A) The miR-130b concentrations (15 nM, 30 nM and 50 nM) transfected with 800 ng/ml MSK1Glo construct plasmid. (B) Different controls used to validate the target accuracy. (C-D) Cotransfection of 500 ng pMJGreen vector with miR-130b shows transfection efficiency > 60%. Forty-eight hours post transfection the activity of F-luc was normalized by R-luc expression and the error bar show mean  $\pm$  SD of four independent experiments. Significant differences (a:c –  $p < 0.05$ ) and (\* $p < 0.01$ ) versus cumulus cells transfected with mismatch vector construct control. RE, relative expression; FL, firefly luminescent; RL, renilla luminescent. 84
- Figure 4.9: Validation of genes as target of miR-130b with luciferase reporter activity. Cumulus cells were cotransfected with pmirGLO vector construct with 30 nM miR-130b/ml precursor or inhibitor. Forty-eight hours post transfection the activity of F-luc was normalized

by R-luc expression and the error bar show mean  $\pm$  SD of four independent experiments. Significant differences (\* $p < 0.05$ ) and (\*\* $p \leq 0.005$ ) versus cumulus cells transfected with mismatch vector construct control. RE, relative expression; FL, firefly luminescent; RL, renilla luminescent.

86

Figure 4.10: Validation of genes targeted by miR-130b using luciferase reporter activity. Cumulus cells were cotransfected with pmirGLO vector construct with 30 nM miR-130b/ml mimic or inhibitor. Forty-eight hours post transfection the activity of F-luc was normalized by R-luc expression and the error bar show mean  $\pm$  SD of four independent experiments. Significant difference (\* $p < 0.05$ ) versus cumulus cells transfected with mismatch vector construct control). FL, firefly luminescent; RL, renilla luminescent.

87

Figure 4.11: Relative abundance of SMAD5 (A) and MSK1 (B), in mature and immature oocyte and its corresponding cumulus cells. Error bar show mean  $\pm$  SD of three independent experiments. Significant difference (\* $p < 0.05$ ) related to corresponding cumulus cells.

88

Figure 4.12: Immunofluorescent analysis of SMAD5 and MSK1 in ovarian section shows the localization of protein. Green colour indicates the protein (SMAD5 and MSK1), where as, blue colour indicates the nucleus staining with DAPI. Scale bar represents 20  $\mu$ m.

89

Figure 4.13: Expression levels of miR-130b (A), MSK1 (B), and SMAD5 (C), in miR-130b precursor, miR-130b inhibitor and scramble injected oocytes and uninjected oocyte control. (D) Western blot analysis showing the protein expression of MSK1 and SMAD5 genes in miR-130b precursor, miR-130b inhibitor and scramble injected oocyte groups. (E) Immunofluorescent indicating spatial localization of MSK1 protein in different injected groups of oocytes. Scale bar represents 20  $\mu$ m.

90

- Figure 4.14: Mitotic divisions of oocyte observed 22 hours post injection. GV: Germinal vesicle; MI: Metaphase I; TI: Telophase I; MII: Metaphase II. 92
- Figure 4.15: The fluorescent quenching in mitochondria of injected oocytes with miR-130b precursor, miR-130b inhibitor, scrambled and uninjected after 22 hours of injection. Scale bar represents 20  $\mu\text{m}$ . 93
- Figure 4.16: (A) The ectopic expression of miR-130b showed significantly high level of miR-130b after 24 hrs in transfected cumulus cells. (B) MSK1, (C) SMAD5, expression in 130b precursor, miR-130b inhibitor and scramble transfected cumulus cells after 24 hours. Significant difference (\* $p < 0.05$ ). (D) The protein level of MSK1 and SMAD5 in miR-130b precursor, miR-130b inhibitor and scramble control groups after 48 hrs of transfection. GAPDH was used as loading control. 94
- Figure 4.17: The number of live cells was determined in cumulus cells by trypan blue vital cell count after 24 hours and 48 hours of transfection. . Error bars represent the mean  $\pm$  SD for three independent experiments. Significant differences (\* $p \leq 0.05$ ) and (\*\*  $p < 0.01$ ). 95
- Figure 4.18: Relative abundance of MSK1 (A) and SMAD5 (B) mRNA in miR-130b precursor, miR-130b inhibitor and scramble transfected granulosa cells. Significant difference (\* $p < 0.05$ ). (C) The protein level of MSK1 and SMAD5 in miR-130b precursor, miR-130b inhibitor and scramble control transfected granulosa cells. GAPDH was used as loading control. 96
- Figure 4.19: The live cell count in granulosa cells was determined by trypan blue vital cell count after 24 hours and 48 hours of transfection. Error bars represented the mean  $\pm$  SD for three independent experiments. Significant difference (\* $p < 0.01$ ). 97

- Figure 4.20: Effects of miR-130b overexpression and suppression on granulosa cell proliferation using MTT assay. Error bars represent the mean  $\pm$  SD for four replicates. Significant difference ( $*p \leq 0.05$ ), hrs: hours. 98
- Figure 4.21: Lactate production in miR-130b precursor, inhibitor and scramble RNA transfected cells. The OD was taken at 460 nm calibrated with untransfected cells. Error bars represent the mean  $\pm$  SD for four replicates. Significant differences ( $*p < 0.01$ ) and ( $**p < 0.005$ ). 99
- Figure 4.22: The graph shows cholesterol concentration in miR-130b precursor, inhibitor, scramble and untransfected groups of cells and medium. Concentration was calculated by referring standard curve. RFU: Relative Fluorescence Units. 99
- Figure 4.23: (A) The proportion of 4-Cell and 8-Cell stage embryos 72 hours post insemination in different zygote injected groups (B) The proportion of day 5 morula in different zygote injected groups. Error bars represent the mean  $\pm$  SD for four replicates. Significant difference ( $*p < 0.05$ ). 101
- Figure 4.24: The proportion of day 7 blastocyst formation rate derived from miR-130b precursor, inhibitor and scramble injected and uninjected zygotes groups. Error bars represent the mean  $\pm$  SD for four replicates. Significant difference ( $*p < 0.05$ ). 102
- Figure 4.25: (A) The expression of miR-130b in blastocysts derived from miR-130b precursor, inhibitor and scramble injected and uninjected zygotes groups. The relative expression level of MSK1 (B) and SMAD5 (C) mRNA transcript in blastocysts derived from miR-130b precursor, miR-130b inhibitor, scramble injected and uninjected zygotes. (D) Western blot analysis showing the expression difference of SMAD5 in 130b precursor,

inhibitor and scramble injected, where as GAPDH used as endogenous control. 103

Figure 4.26: The total number of blastocyst cell and apoptotic index of blastocysts stage derived from zygote injected with different treatment groups. 104

## 1 Introduction

MicroRNAs (miRNAs) are non-coding genetically transcribed small molecule which post-transcriptionally fine-tunes the protein regulation in the range of living being from prokaryotes to eukaryotes (Abrahante et al. 2003, Bartel 2004, Gottesman 2004, Lewis et al. 2005, Lim et al. 2003, Wienholds et al. 2005). miRNAs are conserved in eukaryotic organisms that are believe to be a dynamic and evolutionarily ancient component of genetic regulation (Kren et al. 2009, Lee et al. 2007, Tanzer and Stadler 2004), which can target about 60% of human genome (Friedman et al. 2009). Mainly it down regulates the gene expression in a range of manners, including translational repression, mRNA cleavage, and deadenylation. In animals, miRNAs have shown diverse biological functions including ovarian function, spermatogenesis, embryonic development, abnormal endometrium, organ development, granulose cells proliferation and function and stem cells differentiation (Hayashi et al. 2008, Houbaviy et al. 2003, Lagos-Quintana et al. 2002, Lei et al. 2010, Otsuka et al. 2008, Pan and Chegini 2008, Yao et al. 2010a, Zhao and Srivastava 2007). In addition, evidences indicated that the expression pattern of miRNAs is associated with their specific biological process or molecular functions.

Apart from their significant contribution in different biological or cellular process, the role of miRNAs during oocyte maturation and preimplantation embryo development has been a focus of research. Development of an embryo depends on the proper genetic programming during preimplantation period starts even before fertilization during gametogenesis. This genetic programming includes mRNA transcription, miRNA transcription and degradation of maternal transcripts (Bashirullah et al. 1999, Bushati et al. 2008, Tadros et al. 2007). For instance, some reports have showed the importance of miRNAs in oocyte maturation and preimplantation embryo development (Giraldez et al. 2006, Sempere et al. 2003). Furthermore, Byrne and Warner (2008) indicated the involvement of miRNA in the regulation of early development in mice. Additionally, a report of Tesfaye et al., (2009) showed expressional differences of miRNAs between immature and *in vitro* matured bovine oocytes, using a heterologous miRNA array platform. Accordingly the authors indicated that miR-130b was upregulated in immaturred oocytes compared to matured oocyte. This may suggest being miR-130b as one of the candidate miRNA required to play some significant function during oocyte



maturation. This miRNA is known to be conserved in vertebrates and belongs to miR-130 family by sharing similar seed sequence (Houbaviy et al. 2003, Ma et al. 2010b). High expression of miR-130b has been reported in different cancerous cells as, mouse mammary tumor (Sun et al. 2009), liver cancer (Jiang et al. 2008, Krutovskikh and Herceg 2010), and transformation of mouse cells (Watashi et al. 2010). These reports suggest the involvement of miR-130b in controlled or uncontrolled cell proliferation. Moreover, miR-130b has been found to be involved in different functions in diverse cell types including; mesenchymal stromal cells (Gao et al. 2011), fibroblast cells (Mosakhani et al. 2010), gastric cells (Lai et al. 2010), human mammary epithelial cells (Borgdorff et al. 2010), gliomas cells (Malzkorn et al. 2010). Despite its functional role in different cell types, whether this miRNA involves in cell viability, proliferation and transcription during bovine oocyte maturation is not yet known. Therefore, the main objectives of this study were

1. To investigate the expression pattern of miR-130b and its related miRNAs in bovine oocytes, oocyte companion cells and preimplantation embryo.
2. To identify and experimentally validate the genes targeted by miR-130b during oocyte maturation, granulosa cell proliferation and preimplantation embryo development.
3. To highlight the role of miR-130b in bovine oocyte maturation and cultured granulosa and cumulus cells.
4. To uncover the role of miR-130b during bovine preimplantation *in vitro* development.

## 2 Literature review

In this section the discussion of microRNA discovery, biogenesis, mechanism and the principle of target binding is focused. The fundamental knowledge on regulation of miRNA has been described. A review on the expression and functional aspect of miRNA on mammalian embryogenesis, folliculogenesis, maternal and embryonic transcript is accumulated. A brief introduction for the fundamental aspects of miRNA in gamete formation, fertilization, preimplantation and the role on embryonic stem cell development has been discussed. Moreover, a review on embryonic stem cells microRNA, miR-130 family and its role is also added in the later section of this chapter. The literature focused on the involvement of the miRNA on embryogenesis. In the end the research gap and the mission of the research has reviewed.

### 2.1 MicroRNAs

MicroRNAs (miRNAs) are small single-stranded, noncoding, endogenous with 19-24 nucleotides (nt) in length which regulates the expression of genes by binding to the 3'-untranslated regions (3'-UTR) of specific mRNAs. Till date thousands of miRNAs have been identified in virus to plants and animals (Abrahante et al. 2003, Besecker et al. 2009, Gottesman 2004, Jia et al. 2008, Jung et al. 2009, Lewis et al. 2005, Zhang et al. 2006) . miRNA can form the largest part of ~1% of total genome and can control the regulation of more than 30% of protein coding genes (Lewis et al. 2005). miRNAs can play important regulatory roles in posttranscriptional gene regulation by regulating their targets by translational inhibition and mRNA destabilization. miRNAs comprise one of the most abundant classes of gene regulatory molecules in multicellular organisms and likely influence the output of many protein-coding genes. These mechanisms are conserved in animal from signaling to chromatin remodeling and transcription (Zhao and Srivastava 2007). A single miRNA can target numerous mRNAs or a single mRNA can be targeted by numerous miRNAs. MicroRNAs were discovered in 1993 by Victor Ambros, Rosalind Lee and Rhonda Feinbaum during a study of *C. elegans* development and the first published description was given by Lee and colleagues in 1993 (Ambros et al. 2003b, Bushati and Cohen 2007, Lee et al. 1993), however the term miRNA was coined in 2001 (Lagos-Quintana et al. 2001).

In higher eukaryotes hundreds of miRNA genes are predicted to be present and a single miRNA having the ability to regulate multiple genes (Lim et al. 2003a). These miRNAs may act as key regulators for several processes even for early development by posttranscriptional modification (Reinhart et al. 2000), cell proliferation and cell death (Brennecke et al. 2003), cell differentiation and apoptosis (Carletti et al. 2010, Hirai et al. 2010). miRNAs are also found in brain development (Krichevsky et al. 2003), chronic lymphocytic leukemia (Calin et al. 2004), colonic adenocarcinoma, Burkitt's Lymphoma (Pfeffer et al. 2004) and some reports have shown the possible links between miRNAs and viral disease, neurodevelopment and cancer (Zhang et al. 2007a). Now it is clear that miRNA plays a vital role in post transcriptional gene regulation but still specific functions of specific miRNAs is an area of research and very few works has been done in this field. Although, *in silico* analysis, based on target predictions using a variety of bioinformatics approaches shows several targets of a specific miRNA ranging from one to hundreds (Artzi et al. 2008,minutes.and Yoon 2010), still in physiological condition targets are largely unknown.

### 2.1.1 Discovery of miRNAs

The first microRNA was uncovered through classical genetic methods to identify a mutation responsible for abnormal development of the nematodes namely, *Caenorhabditis elegans* (*C. elegans*) by Ambros and coworkers (Ambros et al. 2003a, Ambros et al. 2003b, Reinhart et al. 2000, Wightman et al. 1993). They found that the gene *lin-4* was essential for post-embryonic development in *C. elegans* and negatively regulates the protein Lin-14. Markingly, when the open reading frame of the *lin-4* was analyzed it didn't show any encoding of proteins. Further investigation of *lin-4* led to the conclusion that it has sequence complementarity with the repeated sequence in the 3' untranslated region (UTR) of the *lin-14* messenger RNA (mRNA) and thus the speculation made for *lin-4* may function via an antisense RNA-RNA mechanism by that an entirely unexpected class of genes and a novel regulatory mechanism was discovered (Bagga et al. 2005, Olsen and Ambros 1999). This discovery of posttranscriptional gene regulation has given a new apparatus of gene regulation during development. Initially, it was believed that miRNA were unique to *C. elegans*, however, after several years in 2000, the second miRNA characterized, *let-7* (*let*=lethal) in *C. elegans* having 22-nt that regulates the expression of protein-coding genes, i.e. *lin-41*, *daf-12*, *lin-14*, *lin-28*, and

lin-42 by targeting the 3' UTR target sites during development of *C. elegans* (Pasquinelli et al. 2000, Reinhart et al. 2000). Initially it was believed that the existence of miRNA was limited to *C. elegans* but later on let-7 was found to be conserved in many species. In fact, now miRNAs have known to be present in diverse range of organisms from bacteria and viruses to plants and animals (Cai et al. 2005, Chen 2005, Nielsen et al. 2009, Reinhart et al. 2002, Zhang et al. 2004).

### 2.1.2 Biogenesis of microRNA

Biogenesis of miRNA is complicated and differs in plant and animal system. In mammals miRNA processing pathway leads to a series of several biochemical steps from primary miRNA transcripts to mature functional miRNA. The ~22-nt, mature forms of miRNAs arise from multiple processing steps of longer substrate RNAs. Around 70% of the mammalian miRNAs are located in intergenic transcription units (TU) i.e. intronic and exonic miRNAs (Golan et al. 2010, Rodriguez et al. 2004). Moreover, 61% of miRNAs are located in protein coding region, the localization rules are discussed further in this section. RNA polymerase II is the transcription factor for most of the miRNAs, but the miRNAs located within Alu-repetitive elements are transcribed by RNA polymerase III (Chen and Rajewsky 2007, Zeng et al. 2003). They also apparently undergo 5'-end 7-methyl guanosine capping, 3'-end polyadenylation and splicing (Bracht et al. 2004, Bushati and Cohen 2007). The pri-miRNA with RNA hairpin structure of 60-120 nt is processed within the nucleus by a multiprotein complex called Microprocessor, whose core components are RNase III enzyme (Drosha) and the double-stranded RNA-binding domain protein pasha (DGCR8) (Gregory et al. 2004, Han et al. 2004, Landthaler et al. 2004). These proteins are conserved in insects upto mammals. Drosha cleaves the pri-miRNA stem from the distance of the single-stranded/double-stranded RNA junction (Han et al. 2006) and binding protein helps to produce a ~60-70-nt hairpin precursor miRNA (pre-miRNA) 2-nt 3' overhang (Lee et al. 2002), which is a specific characteristic of RNase III enzyme. This cleavage recognized by Exportin- 5, and transported into the cytoplasm via a Ran-GTP-dependent mechanism (Han et al. 2006, Lee et al. 1993, Lund et al. 2004) shown in (Figure 2.1), presence of Ran-GTP cofactor is important for binding of Exportin- 5 to pre-miRNA (Yi et al. 2003).

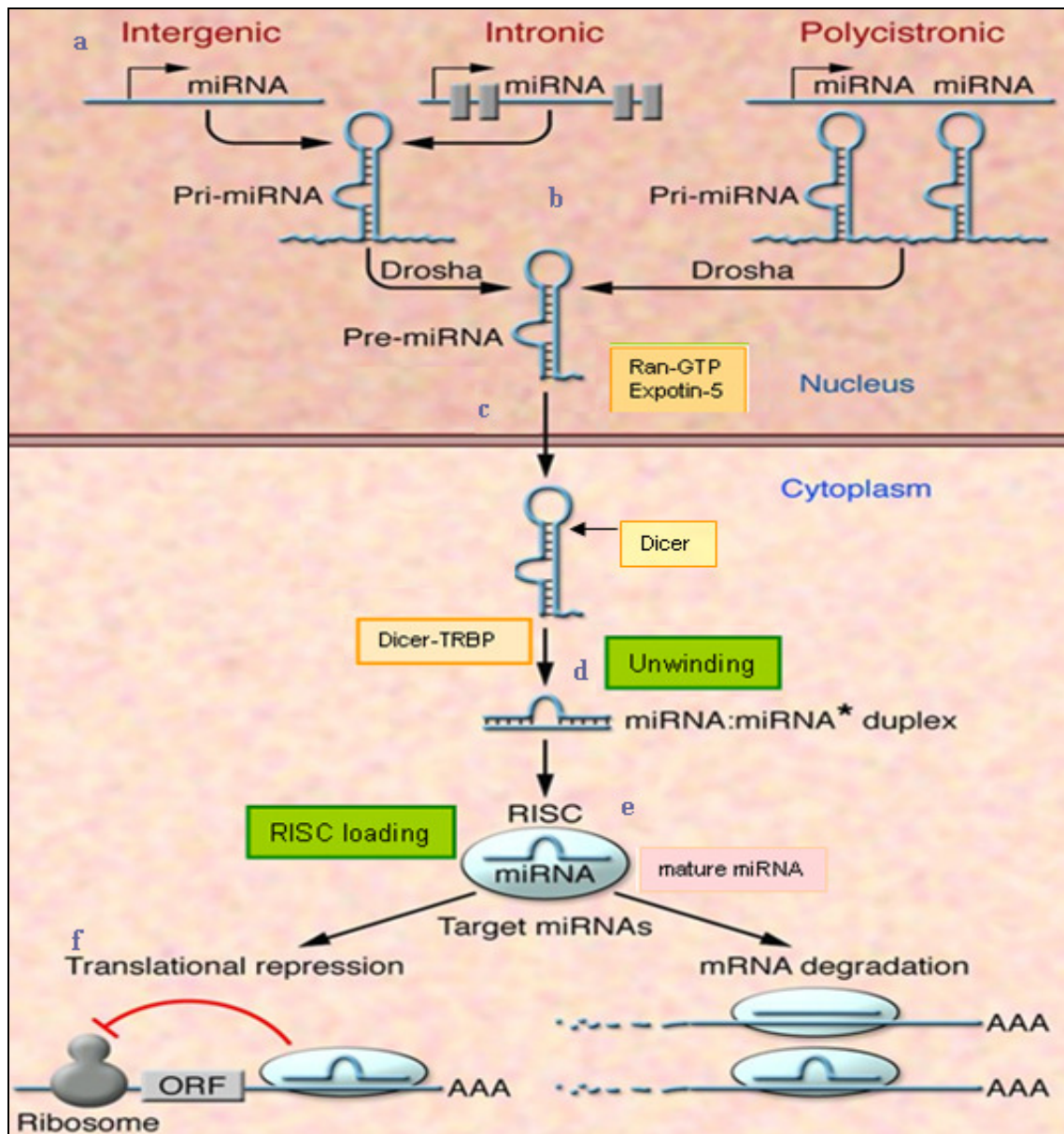


Figure 2.1: miRNA biogenesis: a. Transcription: The primary miRNA transcripts (pri-miRNA), are transcribed as individual miRNA genes, from different location of DNA, b. Nuclear processing: Processing of the nascent transcript to ~70-nt stem-loop precursor miRNA (pre-miRNA), c. Nuclear exporting: Export of the pre-miRNA from the nucleus, d. Cytoplasmic processing: Processing of ~22-bp miRNA duplex, e. Release of the ~22-nt mature miRNA and assembly of the miRNA-induced silencing complex (miRISC), f. Transcriptional repression or mRNA degradation by miRNA binding to the 3'UTR of target mRNA (adapted from van Rooij and Olson 2007).

Now, the one end of mature miRNA is defined by Drosha and the next end crunched by another RNase III enzyme, Dicer. Dicer produce the mature ~22-nt miRNA: miRNA\* duplex, by slicing, which interacts with TRBP/Loquacious, a dsRBD proteins (Chendrimada et al. 2005, Forstemann et al. 2005, Lee et al. 1993). Subsequently, TRBP binds directly to Dicer through its C-terminal domain and recruits the trimeric complex to the assembly of RNA-induced silencing complex a ribonucleoprotein complex (Daniels et al. 2009, Forstemann et al. 2005, Gregory et al. 2005, Ketting et al. 2001). Overall the whole biogenesis is completed in four major steps: 1. Transcription, 2. nuclear processing, 3. nuclear exporting and 4. cytoplasmic process (Figure 2.1).

The localization of miRNA genes within genomes are systematically governed and can be grouped as:

- The miRNAs transcribed with their own promoters as pri-miRNAs are Intergenic miRNAs. For example: mir-30a, mir-21, mir-10a, let-7, (Griffiths-Jones 2004, Lee et al. 2004).
- The miRNAs located in intronic regions of protein-coding genes in the sense or antisense orientation like, mir-93, mir-186, mir-126 (Lagos-Quintana et al. 2001, Lagos-Quintana et al. 2003, Rodriguez et al. 2004).
- Intronic miRNAs located out of protein-coding genes, mir-26a-1, mir-26a-2, mir-26b, mir-28 and mir-126 are good examples (Kim and Kim 2007, Lin et al. 2005, Rodriguez et al. 2004).
- Most of the miRNA genes (about 50%) are polycistronic in nature and transcribe in cluster form from the genome. Examples of such clusters are well known such as let family, miR-17-92 clusters (Hayashita et al. 2005, Lagos-Quintana et al. 2001, Lau et al. 2001, Mourelatos et al. 2002).
- Some miRNA comes in an exon of the non-coding RNA. For example, miR-10, is located in the Hox gene cluster in insects, zebrafish, mouse and human (Lagos-Quintana et al. 2003).

### 2.1.3 RNA induces silencing complex assembly

The RNA-induced silencing complex assembles on short interfering (si) RNA fragments and cleaves target mRNAs that hybridize with the siRNA RISC forms through an ATP-dependent assembly pathway that includes a siRNA-unwinding step

(Figure 2.1). The relative thermodynamic stabilities of the ends of the siRNA duplex help to specify the strand that will ultimately assemble into RISC. RISC is a multiple-turnover, divalent-metal-ion-dependent enzyme that hydrolyses the target phosphodiester linkage, leaving 3'-hydroxyl and 5'-phosphate perfection (Krol et al. 2004, Sontheimer 2005).

The miRNA strand with relatively lower stability of base-pairing at its 5' end is incorporated into RISC, whereas the miRNA\* strand is degraded (Ambros et al. 2003a, Du and Zamore 2005). According to some thermodynamic arguments the selection of mature miRNA strand was performed and the 5' end that is more easily peeled away from its antisense is incorporated into a stable complex and the other half is unprotected and degraded (Khvorova et al. 2003). The position of the stem-loop may also influence strand choice (Lin et al. 2005). Finally, the assembly of RISC and miRNA recognize the 3'UTR site of mRNA and binds to it (Figure 2.2). Argonautes are needed for miRNA-induced silencing and having two RNA binding domains. These domains are conserved and known as PAZ and PIWI (structurally same to ribonuclease-H). PAZ domain having the ability to interact the 3' end of a single strand in the mature miRNA and PIWI domain which binds to the 5' end of the guide strand. They bind the mature miRNA and orient it for interaction with a target mRNA. Among argonautes, Ago2 is important for direct cleavage of target transcripts (Cifuentes et al. 2010). Argonautes may also activate some other unknown proteins which help to achieve translational repression (Pratt and MacRae 2009). In human genome argonaute proteins are eight types among that each four have sequence similarities into two families: AGO (EIF2C/Ago), and PIWI (Schwarz and Zamore 2002). Here, these proteins make the fate of mRNA cleavage or suppression. In the process of mRNA cleavage, the miRNA pathway appears to be biochemically very much similar to the RNA silencing pathway known as RNA interference (RNAi) (Fire et al. 1998, Zeng et al. 2003). In the last step RISC identifies its targets by the perfect complementarity between the miRNA and the mRNA and cleaved directly by Argonaute2 (AGO2) protein (Bushati and Cohen 2007, Choe et al. 2010). It is assumed that in mammal the most common complementarity is imperfect match and leads for translation suppression in spite of mRNA cleavage. These uncleaved mRNA accumulates within discrete cytoplasmic foci called Processing bodies (P-bodies) where they are inaccessible to the translational machinery and

destroyed by RNA-degrading enzymes (Sen and Blau 2005). The RISC binding to miRNA and further process to p-body has shown in figure 2.2.

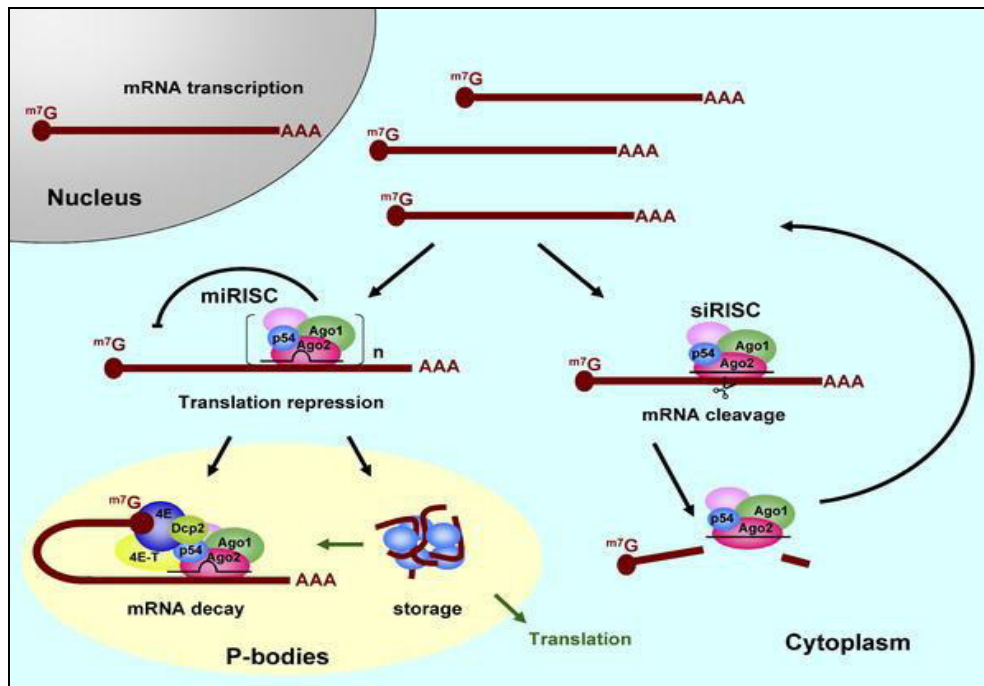


Figure 2.2: RNA induces silencing complex assembly and binding to siRNA or miRNA. siRISC binds to its target mRNA by perfectly matching base pairs, cleaves the target mRNA, recycles the complex, and does not require P-body structures for its function. Multiple numbers of miRISC bind to target mRNA by forming a bulge sequence in the middle that is not suitable for RNA cleavage, accumulate in P-bodies, and repress translation by exploiting global translational suppressors such as RCK/p54. The translationally repressed mRNA is either stored in P-bodies or enters the mRNA decay pathway for destruction. Depending upon cellular conditions and stimuli, stored mRNA can either re-enter the translation or mRNA decay pathways (from Herrera-Esparza et al. 2008).

#### 2.1.4 Principle of miRNA target prediction

The prediction of miRNA targets is critical and several approaches are available to predict the miRNA target gene. It is known that a miRNA can able to target a number of genes and a single gene can be targeted by a number of miRNAs, but still, identification



and validation of the real targets is not an easy task. The efficacy of *in silico* validation to locate and grade the possible genomic binding sites is supported by the relatively high degree of miRNA complementarity to experimentally determine the binding sites. The prediction of miRNA target is depending upon the sequence binding or miRNA/mRNA interaction. This interaction depends upon the 5' seed sequence match of miRNA, conservation of the sequence and the thermodynamic stability between miRNA and mRNA (Krol et al. 2004, Ni et al. 2010). Several target prediction programs are available based on the above mentioned criteria. The most popular site for target prediction is miRanda ([www.microrna.org/microrna/home.do](http://www.microrna.org/microrna/home.do)) which is based on the principle of sequence match and binding energy between the miRNA/mRNA and the evolutionary conservation of the gene target binding site. The estimated false positive rate for this program is approximately 24-39% (Enright et al. 2003). Next known target prediction site for mammalian miRNA targets is TargetScan ([www.targetscan.org](http://www.targetscan.org)). It is based on the 8 mer or 7 mer conserved sites that match the seed sequence of the miRNA and also on the free energy using the RNA fold algorithm. For this program, the estimated false positive rate is between 22-31% (Enright et al. 2003). In this site conserved targeting has also been detected within open reading frames (Lewis et al. 2005). The third well known target prediction site is PicTar ([pictar.bio.nyu.edu](http://pictar.bio.nyu.edu)) which is used to identify miRNA target genes in vertebrates, *Drosophila* and *C. elegans* (Grun et al. 2005, Krek et al. 2005, Lall et al. 2006). The estimated false positive rate for this program is approximately 30%. Moreover, these programs identify targets for single miRNA as well as targets that are regulated by several miRNAs in a coordinated manner. This suggests that miRNA and target network might be more complicated than originally expected and the experimental validation should be performed carefully. However, prediction programs don't account for all of the criteria by mutated target binding sites of the 5' seed region of the miRNA. This 5' seed, consisting of 2-8 nts, must bind perfectly to the target mRNA sequence. The Cohen laboratory reported the minimal target site for miRNA function. They mentioned that seven or more sequences that are complementary at the 5' end of the miRNA are enough to show function. If the 3' sequence has weaker binding, then the 3' compensatory binding is required (Vella et al. 2004). The possibility of miRNA:mRNA binding was schematically described in (Figure 2.3).

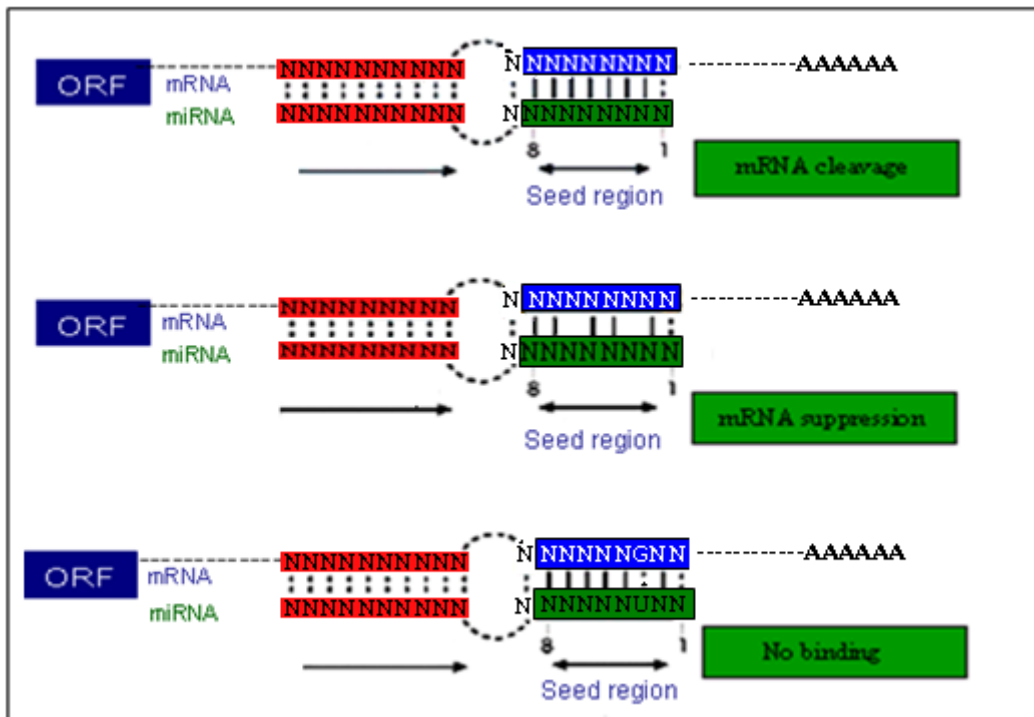


Figure 2.3: The schematic description of the miRNA seed sequence binding to target mRNA. The perfect seed binding extended with 3' site ends with mRNA cleavage. Imperfect binding of seed sequence is not enough for mRNA degradation but suppress the function. Wobble (G:U) pairing in seed sequence don't allow the complementary binding of miRNA and mRNA.

### 2.1.5 Regulatory mechanism of microRNA in animals

When the miRNA is incorporated into the miRISC, it interacts with specific sites of the 3'UTR of target mRNAs and downregulates their expression, either by translational repression or by mRNA degradation in animals (Ambros 2004, Bartel 2004). In nearly-perfect complementarity, the miRNA with nearly-perfect complementarity to target sites cleaves the mRNA directly, as like as siRNA. In partial complementarity, the miRNA complement to the target site of 3'UTR of the mRNA but not binds to whole seed sequence, it can be 7 to 5 nt bond in seed region, which results in translational repression without mRNA cleavage (Ajay et al. 2010). Most of the animal miRNA binds with partial complementarity and repress the translation of protein (Fabian et al. 2010). But some miRNA in animals also make near-perfect complementarity, like miR-196 sequence binds nearly-perfect site to HOXB8 during vertebrate development

(Yekta et al. 2004). In some other cases also we show, miRNAs can guide mRNA cleavage in animals as in muscle stem cells, the 3'UTR of the Pax3 mRNA has some perfect sequence for miR-27b seed sequence, which leads to the initiation of cleavage of the Pax3 mRNA (Crist et al. 2009). The mechanism of regulation is determined by the degree of miRNA and mRNA binding, reviewed in (Huntzinger and Izaurralde 2011). However, the first model is most common for plant gene silencing with mRNA cleavage and the second model, translational repression is consider being more prevalent in animals.

Several mechanistic studies of translational repression have led to different conclusions. In the original studies of the lin-4/lin14 interaction in *C. elegans* presented that repression occurs after translational initiation. The lin-14 mRNA was found to be stably associate with polysomes, suggesting either an arrest of translational elongation (ribosomal stalling), or cotranslational peptide degradation (Olsen and Ambros 1999). In contrast, Pillai and colleagues have evidenced that inhibition of translational initiation occurs by let-7 in human cells. They evaluated that: i) mRNA which is targeted by miRNA accumulates in P-bodies. ii) the mRNAs which falls in P-bodies unable to undergo translation; and iii) miRNAs don't allow the mRNA to load into polysomes (Pillai et al. 2005). In addition, alteration of translation initiation, can make the mRNA resistant to miRNA-induced repression, for example when mRNA binds to the translational factors Eukaryotic translation initiation factor 4E or Eukaryotic translation initiation factor 4G directly it resist to miRNA repression (Hoeffler et al. 2011, Valencia-Sanchez et al. 2006). It leaves further some uncovered questions related to the target of the miRNA/mRNA complex in P-bodies, whether it is the site of translational inhibition by the miRNA machinery, or if P-bodies represent only as a storage area for repressed mRNA (Valencia-Sanchez et al. 2006).

## 2.2 Biological functions of miRNAs in animals

In animals, miRNAs have shown diverse biological functions. There are several approaches which lead to the evidence of the function of miRNAs in animals (Figure 2.4). At first, several miRNAs in *C. elegans* and *D. melanogaster* were identified by forward genetics (loss- and gain-of-function genetic screens). The study in *C. elegans* showed, miRNA effects the early developmental timing (Lee et al. 1993, Moss et al. 1997, Wightman et al. 1993) where lin-4 targets lin-14 and lin-28, let-7 targets lin-41

and *daf-12* that affects late developmental timing (Lin et al. 2003, Reinhart et al. 2000), miR-273 affects neuronal left/right asymmetry (Chang et al. 2004). In *Drosophila* miR-14 regulates programmed cell death and metabolism (Brennecke et al. 2003, Xu et al. 2003), miR-7 regulates notch signalling (Lai et al. 2005, Stark et al. 2003), and in zebrafish miR-430 affects brain morphogenesis (Giraldez et al. 2005). Some other helpful approaches to find the function of miRNAs are reverse genetic approaches and computational predictions. Reverse genetic approaches for miRNA includes miRNA knockout or knockdown (Hutvagner et al. 2004, Lecellier et al. 2005, Meister et al. 2004a). Which showed, different roles for argonaute proteins in small RNA-directed RNA cleavage pathways (Okamura et al. 2004) and sequence-specific inhibition of small RNA function (Hutvagner et al. 2004). By computational predictions, almost all miRNAs target genes are analyzed (Huang et al. 2010, Koscianska et al. 2007, Lai 2004, Mosakhani et al. 2010). According to computational analysis, hundreds of genes can be predicted to be targeted by each miRNA (Enright et al. 2003). However, the molecular details of the suppression of genes via miRNA-mediated suppression are still being investigated using forward and reverse genetic approaches. In addition, the miRNA expression profiles using microarray, real-time PCR and in situ localization have revealed specific miRNA expression patterns, which can clue the functions of the specific miRNA in specific tissue or organ. For example, mir-155, mir-130b, mir-21 are highly regulated in cancerous tissues which avail the role of these miRNA as oncomiR (Jiang et al. 2010, Medina et al. 2010, Yeung et al. 2008). Whereas, minimization of tumour in hepatoma cell lines was observed by miR-199-5p miRNA which targets discoidin domain receptor-1 (DDR1) tyrosine kinase. The downregulation of miR-199-5p allow the DDR1 to deregulate and increase cell invasion (Shen et al. 2010a). Few genes responsible for disease have been identified using forward and reverse genetic screens approached by experimental validation, such as, miR-155 targets the suppressor of cytokine signaling 1 and induces breast cancer in mammals and by targeting SMAD2 miR-155 modulates the response of macrophages to transforming growth factor-beta (Jiang et al. 2010, Louafi et al. 2010), miR-21 blocked NF- $\kappa$ B activity and promoted IL-10 by regulating PDCD4 expression after LPS stimulation of human peripheral blood mononuclear cells (Sheedy et al. 2010). Some recent research shows that miRNAs can also potentially bind to complementary sequences in the open reading frame (Borgdorff

et al. 2010) or to 5' UTR of an mRNA (Zhang et al. 2004). The different approaches to achieve the function of miRNA in animals are shown in figure 2.4.

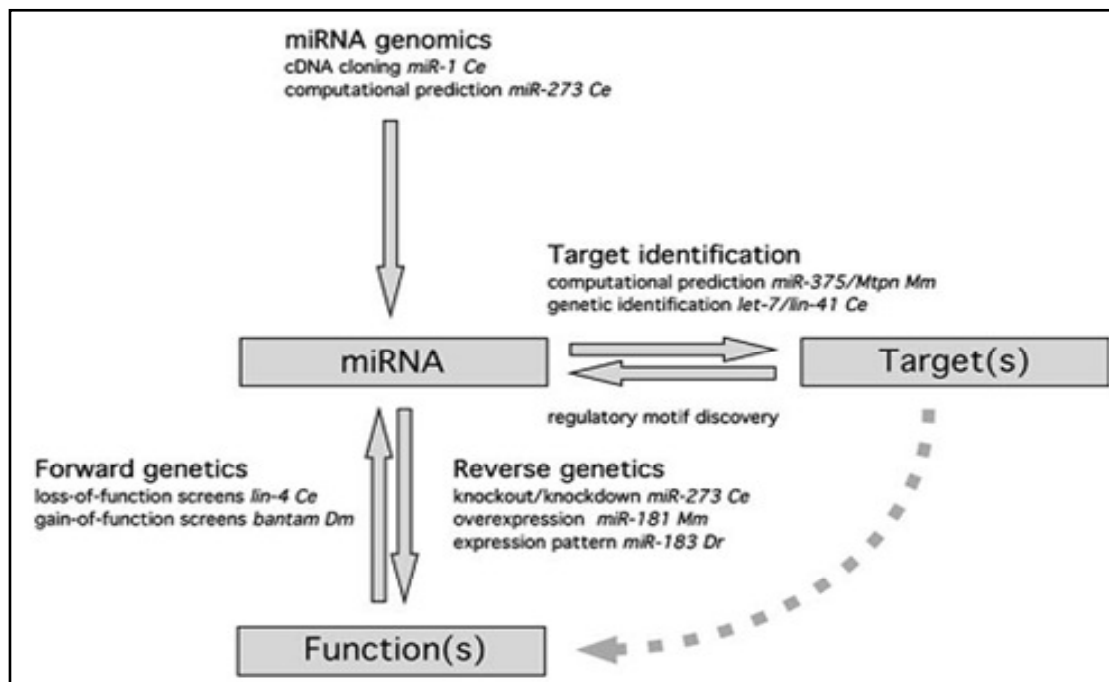


Figure 2.4: Different approaches used to identify the miRNA genes, target genes and functions of miRNAs in animals with an example. Ce: *Caenorhabditis elegans*; Dm: *Drosophila melanogaster*; Dr: *Danio rerio*; Hs: *Homo sapiens*; Mm: *Mus musculus* (from Wienholds and Plasterk 2005).

### 2.3 Expression and role of miRNA in mammalian folliculogenesis and embryogenesis

The following section highlights the accessible information of miRNA in fundamentals of mammalian folliculogenesis and preimplantation embryo development.

#### 2.3.1. Involvement of miRNA in follicular development

Early folliculogenesis in mammalian ovary begins with the breakdown of germ cell clusters and formation of primordial follicles. Each follicle has immature oocytes surrounded by flat and squamous granulosa cells that are separated from the oocyte's environment by the basal lamina. Primordial follicles are able to maintain dormant phase by few weeks to several years in cattle and shows a little or no biological activities (Choi and Rajkovic 2006, Knight and Glister 2001). Later it undergoes for

developmental process in which primordial follicle activated and develops to a preovulatory size following growth and differentiation of the oocyte (Choi and Rajkovic 2006, Gougeon 1996, Salama et al. 2010). Throughout puberty, the pools of primordial follicles are continuously growing and the primordial follicles from a resting to a growing stage can be observed throughout life. After puberty, gonadotrophin-dependent growth occurs in a cohort of antral follicles and follicle depletion starts at a very high rate. At birth, millions of primordial follicles remain which requires very few follicles to reach up to the ovulatory stage, where by most non-ovulatory follicles undergoes for atresia. During folliculogenesis atresia is a common phenomenon observed *in vivo* and *in vitro* (Fujino et al. 1996, Grotowski et al. 1997, Matsuda et al. 2011, Perez et al. 1997, Wang et al. 2011). During the time of development, it achieves several stages namely, primary, secondary, tertiary and graafian (Hutt and Albertini 2007, Smitz and Cortvrindt 2002). These stages are characterised according to the follicle and oocyte size, development and antrum formation, shown in figure 2.5.

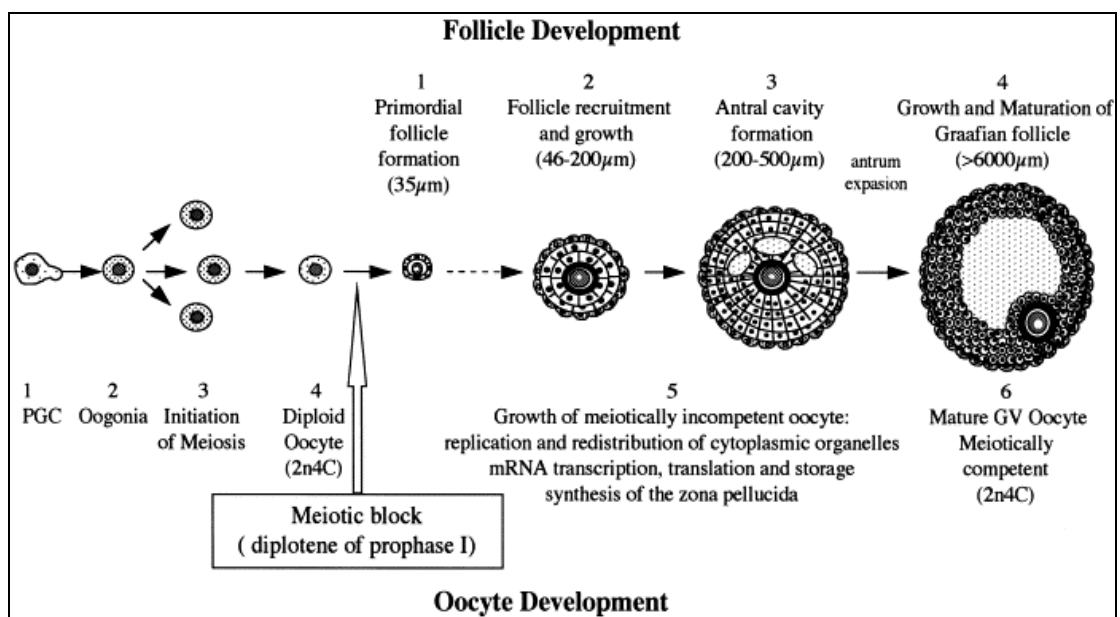


Figure 2.5: Stages of mammalian oogenesis and folliculogenesis. PGD: primordial germ cells, n: chromosomal and C: DNA content (from Picton et al. 1998).

In the process of follicular growth, the oocyte plays an important role in genetically programming and coordination of the multiple events during folliculogenesis and embryogenesis (Dean et al. 2001, Madan et al. 2003). Similarly, oocyte surrounding

granulosa cells also plays a major role for the development and growth of oocyte. The granulosa cells are uniform in developing follicles but after the antrum formation mostly at preovulatory stage these granulosa cells are differentiated in theca granulosa, mural granulosa and cumulus granulosa cells (Gilchrist et al. 2001, Hutt and Albertini 2007). The cells adjacent to the oocyte during ovulation are known as cumulus cells. The cumulus cells and oocytes are tightly connected to each other and facilitate heterologous interactions as, metabolites, ions and small signalling molecules exchange (Nicholson 2003). Cumulus cells provide metabolites, cholesterol, steroids, epidermal growth factor (EGF) and hormones to growing oocytes (Nyholt de Prada et al. 2009, Zamah et al. 2010). During this growth granulosa cells are highly proliferated and undergo several metabolic changes by the influence of transforming growth factors (TGFs) which involves SMADs protein signaling pathway. In oocyte and granulosa cells SMAD signaling pathway involves three different ligands (Table 1) with receptor I and II and further leads to the phosphorylation of transcriptional factor (Kawabata and Miyazono 1999, Myers and Pangas 2010), MSK1 gene has also been reported to be involved in the TGF- $\beta$  activated SMAD signaling pathway. In folliculogenesis gene transcription, posttranscriptional modification, protein synthesis and storage play a vital role. Several reports indicated that SMAD5 increases granulosa cell mitosis, stimulates preantral follicular growth and its function in rodent (Myers and Pangas 2010), but for ruminants and also in pigs the SMAD pathway shows mildly or even inhibitory effect in respect to both cell proliferation and function (Gilchrist et al. 2008). In bovine, SMAD pathway is highly active in preantral follicles and it performs for suppression of granulosa cell proliferation and promotes apoptosis (Zheng et al. 2009). Investigation of the biological role of SMAD family shows their influence on estradiol (E2) and progesterone (P4) biosynthesis in bovine granulosa cells by targeting the steroidogenic enzymes and inhibits luteinization in cultured bovine granulosa cells further leads to increased apoptosis (Yu et al. 2004, Zheng et al. 2008, Zheng et al. 2009)

Recently, some evidences showing the presence of miRNA in follicular cells (Carletti et al. 2010, Yao et al. 2010b) and the role of miRNA in ovarian function was well reviewed by Christenson (2010). Presence of miRNA and small RNA library construction was conformed in new born and 2 weeks old mouse ovary (Ahn et al. 2010, Alvarez-Garcia and Miska 2005, Ro et al. 2007a, Ro et al. 2007b) and also in bovine ovaries, the miRNA and small RNA library was constructed with the findings of

some novel miRNAs (Hossain et al. 2009, Tripurani et al. 2010). Conditional inactivation of Dicer1 in follicular granulosa cells leads to increased primordial follicle numbers and increased early follicle recruitment (Huang and Yao 2010, Lei et al. 2010). Dicer1 knockout shows female infertility due to impaired growth of new vessels in the corpus luteum (Otsuka et al. 2008).

Regarding the male fertility and folliculogenesis, miRNAs show their importance in many aspects; Dicer lacking male (where biogenesis of miRNA was interrupted) shows delayed in fertility, reduced proliferation of primordial germ cells and spermatogonia leading to spermatogenic arrest (Hayashi et al. 2008, Maatouk et al. 2008). While female lacking Dicer is infertile and decreased ovulation (Hong et al. 2008, Nagaraja et al. 2008). In regard to the specific cells of follicles, several investigations has done to find the factors involved in regulation of miRNA or the factors regulated by miRNA during folliculogenesis. A recent report shows that human chorionic gonadotrophin (hCG) supplementation and vitamin C status alter the miRNA expression profiles in oocytes and granulosa cells during *in vitro* growth of murine follicles (Kim et al. 2010b). FSH-mediated progesterone secretion of cultured granulosa cells has alternated the expression of around 31 miRNA showing pleiotropic effects of FSH (Yao et al. 2010b). There are some other reports which indicated the role of miRNA in granulosa cell proliferation by the regulation of SMAD signalling pathway. TGF- $\beta$ , BMP and Activin are the key regulators of SMAD signalling pathway. TGF- $\beta$  treatment during *in vitro* culture of mouse preantral granulosa cells has shown the up-regulation of 3 miRNAs and down regulation of 13 miRNAs in were down-regulated the report also shows the regulation of SMAD4 was under the control of miR-224 in granulosa cells (Yao et al. 2010a). miRNA can play a role as apoptotic marker as well as these miRNA can controls the apoptotic pathway in ovarian cells which is witnessed by the work showing increase in the apoptotic markers as, caspase 3 and control of apoptosis in ovarian cells and increased ovulation by miR-21 (Carletti et al. 2010). Several other reports have shown the regulation of ovarian function, prevention of granulosa cell apoptosis, control of hormonal secretion in granulosa cells via some miRNA (Hawkins and Matzuk 2010, Hennebold 2010, Sirotkin et al. 2009). Dicer1 plays important roles in follicular cell development through the differential regulation of gene expression. Recently a report has indicated for the involvement of TGF- $\beta$  regulates miRNA



regulation (Yao et al. 2010a) or vice versa (Davis et al. 2008, Kahata et al. 2004, Rogler et al. 2009).

### 2.3.2. Gametes formation and the involvement of miRNA

Gametes formation is a biological process by which diploid or haploid precursor cells undergo cell division and differentiation to form mature haploid gametes. In female it is called oogenesis or development of oocyte and in male it is known as spermatogenesis.

#### 2.3.2.1 Expression and role of miRNA in oocyte maturation

Mammalian oocytes are arrested at prophase I of meiosis before induction of maturation by the preovulatory luteinizing hormone (LH) surge at the stage of puberty. It is known that the oocyte plays an important role in the progression of follicle growth and granulosa cell differentiation. The bidirectional communication promotes oocyte to secrete soluble paracrine growth factors which are uptaken by companion granulosa cells, and help for oocyte development. This oocyte-cumulus cell interacts with each other and prevents luteinization of cumulus cells by suppressing luteinizing hormone receptor expression and promoting growth factor, steroidogenesis and inhibin synthesis (Eppig 1985, Gilchrist et al. 2004). During embryogenesis the maternally-inherited RNAs and proteins are stored within the oocyte, these RNAs and proteins are essential for completion of the meiotic cell cycle, initial cleavage divisions and the establishment of an embryonic genome and regulation of preimplantation embryo development (Bilodeau-Goeseels 2003, Lieberfarb et al. 1996, Mtango et al. 2008, Pepling 2010, Schier 2007).

Oocyte maturation is a complex event in which the oocyte break it's quiescent and progress to the MII stage (nuclear maturation) from the stage of diplotene of prophase I. The surge of LH evokes the resumption of meiosis in oocytes. The oocytes in meiosis were relaxed and structurally forms vesicle known as germinal vesicle. This GV arrest is continuing until the puberty and after that the meiosis resumes occurs. In cattle, the age of puberty is 7-18 months in males and 18-24 months in heifers. As the meiosis revive reductive division starts, the GV disappears and the chromatin is recondensed, the pairs of homologous chromosomes are separated in half and a part with reduced amount of cytoplasm forming the first polar body. Here again the meiosis interrupted

(in metaphase II). The starting of the complex process of maturation attends with GV breaking and further follow with several other steps which are discuss further and completed by the formation of the first polar body, with the outcome of a mature and fertile oocyte (Dekel et al. 1989, Homa 1995), that are able to be fertilized by sperm. All mammals having approximate same process of mitotic activation but the timing of the cycle differs in each species. In cattle the timing taken for maturation can be divided as GVBD: 6 hrs, metaphase I: 12-14hrs, telophase: 18 -20 hrs, nuclear maturation: 22-24 hrs. Here the oocyte remains arrested at the MII stage until the fertilization takes place (Hunter and Moor 1987, Sato et al. 1990). Meanwhile, cytoplasmic maturation also takes place which involves organelle reorganization and storage of mRNAs, proteins and transcription factors that controls the whole maturation process, fertilization and early embryogenesis (Ferreira et al. 2009, Liehman et al. 1986). The meiotic maturation depends on a high level of cAMP within the oocyte too, *in vitro* culture of bovine oocyte shows the prominent amount of cAMP is important to regulate resumption of meiosis (Lee et al. 2010, Sanbuissho et al. 1992). Once the oocyte gets mature it get arrested in MII stage until it gets fertilized within certain timing. The arrest is managed by the constantly high activity of cyclin B and the protein kinase p34<sup>cdc2</sup> (MPF) with the entry of M-phase by activation of MPF, (Fan et al. 2004, Gavin et al. 1999, Palmer et al. 1998, Palmer and Nebreda 2000). MPF is necessary to maintain MII arrest and to sustain MPF Cytostatic Factor (CSF) function is required (Dumont et al. 2005). MAPK plays a crucial role in the activation of CFS (Fissore et al. 1996). The MAPK has a role in promoting MPF activation and in assisting meiotic resumption (Fissore et al. 1996, Ohashi et al. 2003). The activation of MAPK mediates the activation of MPF, a key regulator of the M phase and results in the induction of GVBD in xenopus (Gotoh and Nishida 1995, Hehl et al. 2001), mouse (de Vantery Arrighi et al. 2000), bovine (Fissore et al. 1996) and porcine (Ohashi et al. 2003). MSK1 (RPS6KA5) is a downstream protein of MAPK which phosphorylates the transcriptional factors. MSK1 is required for CREB and ATF1 phosphorylation after mitogenic stimulation of mouse ES cells (Arthur and Cohen 2000) fibroblasts (Wiggin et al. 2002). MSK1 is also involved in TGF- $\beta$  mediated pathway, here the capability of SMAD3 to mediate TGF- $\beta$  induced transcriptional responses was blocked by suppressing the proshorylation of MSK1 (Abecassis et al. 2004). It also illustrates the involvement of MSK1 in SMAD signalling pathway. In the ovulating follicle, oocyte-

secreted factors also play vital roles in enabling cumulus cell expansion and regulating extracellular matrix stability, thus facilitating ovulation. The identity of these oocyte-secreted growth factors regulating such key ovarian functions remain unknown, although growth differentiation factor-9 (GDF-9), bone morphogenetic protein-15 (BMP-15) are likely candidate molecules, probably forming complex local interactions with other related members of the TGF- $\beta$  superfamily shown in Table 1.

Table 1: The genes involved in SMAD signalling pathway during folliculogenesis and oocyte maturation.

Ligands	BMP	TGF $\beta$	Activin
Signaling Receptors:	ALK2	ALK2	ALK2
Type I	ALK3 ALK6	ALK5	ALK4
Binding Receptors: (Type II)	BMPR2	TGFBR2	ACVR2A ACVR2B
Receptor Smads:	SMAD1 SMAD5 SMAD8	SMAD2 SMAD3	SMAD2 SMAD3
Common Smad:	SMAD4	SMAD4	SMAD4
Suppressor Smads:	SMAD7 SMAD6	SMAD7	SMAD7

Oocyte-derived bone morphogenetic protein 15 (BMP15) and growth differentiation factor 9 (GDF9) are key regulators of follicular development (Paulini and Melo, Paulini and Melo 2011), in the transient of the primary follicle to secondary follicle, growth differentiation factor 9 (GDF9) in mouse (Sasseville et al. 2010) and bone morphogenetic protein 15 (BMP15) (Galvin et al. 2010) in sheep (Xu et al. 2010) are essential and playing an important role in animal fertility. GDF9 and BMP15 are the regulation members of the TGF- $\beta$  superfamily that play crucial roles in mammals (Chang et al. 2002, Otsuka et al. 2011). These transcriptions are most closely homologous to each other in the family and are synthesized in oocytes beginning of the recruitment of primordial follicles (Elvin et al. 2000). The SMAD signalling pathway is a key regulator of TGF- $\beta$  signalling and involved in the regulation of cumulus cell

metabolism, particularly glycolysis and cholesterol biosynthesis before the preovulatory surge of luteinizing hormone (Gilchrist et al. 2004). The better understanding of the relationship between the oocyte and its companion somatic cells are changing as we are gaining the appropriate greater understanding of these factors in folliculogenesis (Su et al. 2008). The crosstalk between oocyte and its surrounding cells are shown in figure 2.6.

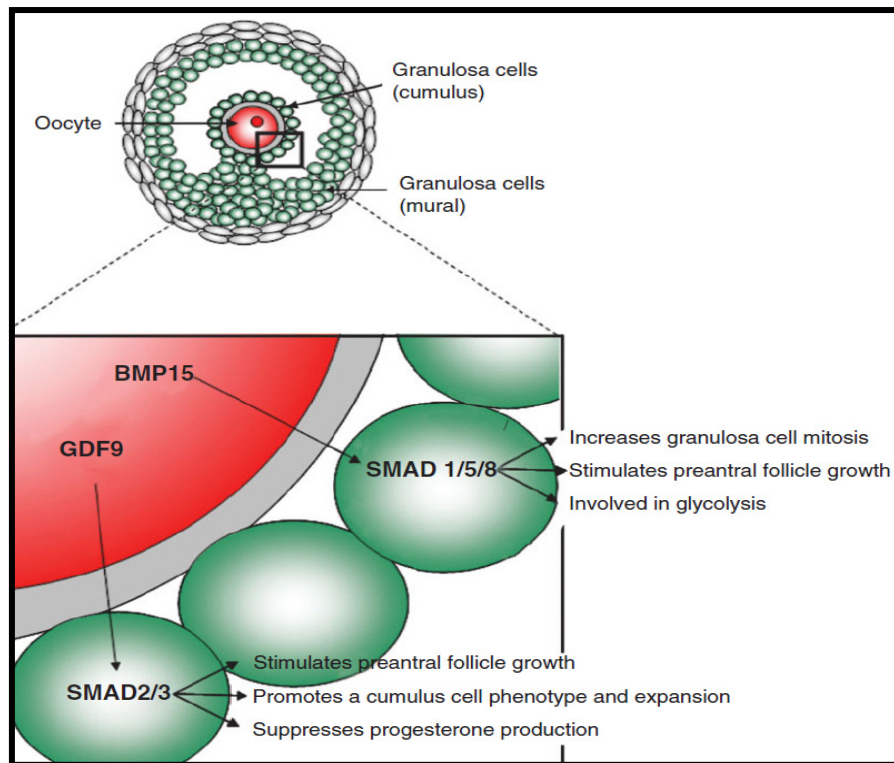


Figure 2.6: Crosstalk between the oocyte and granulosa cells (both cumulus and mural) is integral for various stages of folliculogenesis. Oocyte-derived factors act via SMAD 1/5/8 and SMAD 2/3 respectively, to elicit cellular responses that are essential for successful folliculogenesis and ovulation (from Myers and Pangas 2010).

Presence of miRNA in oocyte is vital and well known. There are several evidences which show the presence and function of miRNA in oocyte. The role of miRNA in oocyte was first identified by the group of Nakahara in drosophila and they found that the accumulation of 40S ribosomal protein and S2 protein is inhibited by miRNAs during oocyte maturation by global suppression of miRNA (Nakahara et al. 2005). Identification and expression of miRNA in oocyte were done by adapting RT-PCR

based miRNA detection using homologous or heterologous approaches in mouse (Choi et al. 2007, Tam et al. 2008) and bovine (Tesfaye et al. 2009). However, Watanabe and co-workers managed to clone miRNA with two other small noncoding RNAs, retrotransposon-derived siRNAs from mouse oocyte and germline small RNAs in male germline (Watanabe et al. 2006). Expression profiling of miRNA in oocyte and the surrounding cumulus cells (Giraldez et al. 2006) has shown a differential regulation of miRNA in oocyte and its surrounding communicating cells (Hawkins and Matzuk 2010).

Cloning of miRNA was been possible during oocyte development in bovine by Tripurani et al. in 2010. In which, bta-mir424 and bta-mir-10b showed high expression patterns during oocyte maturation and preimplantation development of bovine embryos, both the miRNAs were abundant in GV and Metaphase II stage oocytes (Tripurani et al. 2010). Degradation of maternal transcripts in zebrafish has reported by manipulation a single miRNA miR-430 in oocytes (Giraldez et al. 2006). As, the miRNA processing genes directly related to the function and biogenesis of miRNA, here an importance of maternal transcript argonaute 2 is reported being essential for early mouse development is shown by argonaute2 knockout mouse (Lykke-Andersen et al. 2008). Dicer is well known for the notching of siRNA and miRNA both. The abnormal spindle assembly in oocyte and the aberrant chromosomal organization has attended the important and markable role during oogenesis and were essential for meiotic completion (Liu et al. 2010). Dicer1 is highly expressed and functionally important in the oocytes during folliculogenesis as well as in the mature oocytes. Dicer lacking in growing oocytes shown the importance of maternal miRNA for zygote formation resulted in an arrest of zygotic development mice, arrest in meiosis I with multiple disorganized spindles and severe chromosome congression defects defective spindle organization and further embryonic development. This analysis had also shown the misregulation of several transcripts and proteins in Dicer1 knockout oocytes, which demonstrates that the maternal miRNAs are essential for the early stage embryonic development in mouse (Murchison et al. 2007, Tang et al. 2007, Watanabe et al. 2008). The Dicer-knockout models in oocytes are not only evidence the imperative role of miRNAs in the oocyte but also indicate that the regulations of maternal transcripts are fine tuned by the influence of miRNA. Although there are some recent report which shows the limited role of miRNA in oocyte and preimplantation development in mouse (Suh et al. 2010),

there is a wide spectrum to analyze a specific miRNA showing role in oocyte maturation and further development. Specially the functional characterization for the bovine oocyte and corresponding cumulus cells are remains to be articulated.

### 2.3.2.2 Expression and role of miRNA in spermatogenesis

Spermatogenesis is the process by which male primary germ cells divide and produce a number of cells of same type termed spermatogonia. This spermatogonia forms primary spermatocytes and end to two secondary spermatocytes. Further, secondary spermatocytes divide into two spermatozoa. These spermatozoa develop and mature to form sperm cells. Spermatozoa are the mature male gametes in many sexually reproducing organisms (O'Donnell et al. 2001). Thus, spermatogenesis is the complex biological process tightly regulated with stage-specific genes transcriptions and remodelling (Johnston et al. 2008). Identification and function of miRNA in mammalian sperms were reported by different researchers (Bouhallier et al. 2010, Hayashi et al. 2008, Yan et al. 2009). In porcine miRNA has shown a high degree of sequence conservation among other mammalian species (Curry et al. 2009). A different study of miRNA expression profile using microarray analysis in testis tissues from immature rhesus monkey indicate that miRNAs are extensively involved in spermatogenesis (Yan et al. 2009). Furthermore, some studies showed the specific gene regulation by miRNA. Here, RNA –binding protein, Dead end 1 (Dnd1), is essential for fetal male germ cell development which prevents the miRNA-mediated repression of cell cycle-related target mRNAs (Cook et al. 2011, Kedde et al. 2007). Recently a study in mouse pachytene spermatocytes and round spermatids cells showed the expression of miR-34c could enhance spermatogenesis (Bouhallier et al. 2010). Another study of specific miRNA member of oncomir-1 cluster family, miR-18 directly targets the heat shock factor 2 and affects the transcription factor in spermatogenesis (Bjork et al. 2010). Similar study of individual miRNA has shown the regulation of Tnp2 (a gene involved in chromatin remodeling) during spermatogenesis by miR-122a (Yu et al. 2005). For the study of miRNA function miRNA processing genes also been manipulated. Dicer (a cytoplasmic protein function for miRNA and siRNA stemloop cleavage) deletion results in a loss of sperm and validates the importance of miRNA for proper proper differentiation of the male germline (Hayashi et al. 2008, Maatouk et al. 2008) Similarly, the deletion of Argonaute 2 (Ago2), has shown not significant different

phenotype of testis (Hayashi et al. 2008). The presence of miRNA in sperm was shown by Amanai group (Amanai et al. 2006). Although, the role of miRNA derived from sperm was limited in fertilization and embryo formation in comparison to oocyte derived miRNAs even miRNAs are playing role for spermatogenesis and there regulation.

#### 2.4 Role of miRNAs in fertilization and preimplantation embryo development

In the process of bovine fertilization, the fusion of an oocyte with a sperm occurs either *in vivo* or *in vitro*, which finally leads to the development of an embryo. *In vivo* fertilization performed by millions of sperms deposited into the vagina during mating. The sperms make their way through the cervix into the uterus and then on to the fallopian tubes where mature oocyte waits for it. During this all process the number of sperm decline and only few hundred sperms get close to the oocyte. Once inside the fallopian tube, the sperm attracts towards the oocyte (surrounded by cumulus cells and zona pellucida) by releasing a chemical substrate (Krug et al. 2009). Where as, *in vitro* fertilization occur in a petri plate, where a number of sperms are allowed to interact with oocyte. The cumulus cells allow the sperm to interact and the zona pellucida interrupt polyfertility and allow only one sperm to penetrate it. Head of the sperm releases its genetic contents, which fuses with the nucleus of oocyte and the fertilization, occurs. The embryo formed is known as zygote. The early embryo development starts with eventual cleavage and forming blastomeres (Fields et al. 2011). In the early development of bovine embryo the preimplantation period remains from day 1 to day 8 surrounded with zona pellucida (Panigel et al. 1975). The embryos enter into several divisions after fertilization. The zygote is large cell, having a low nuclear to cytoplasmic ratio (Figure 2.6). To attain a ratio similar to somatic cells, cell divisions occur without an increase in cell mass. This process is referred as cleavage. The cleavage starts 2 days post fertilization and reaches to expended blastocyst by day 9 or 10 with containing 250 cells. In between day 3 and 4 after fertilization the embryo with 8-16 cells and by 5 to 6 days it reaches to 32-64 cell stage which known as morula stage. It forms early blastocyst in 7 days with ~128 cells (all stages of preimplantation embryos are shown in Figure 2.7).

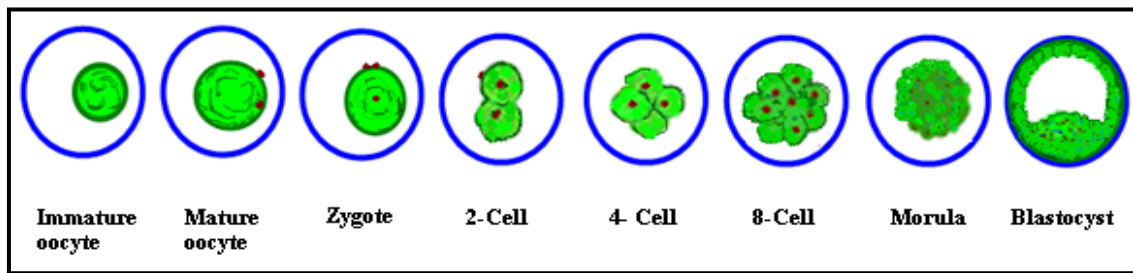


Figure 2.7: Schematic diagram of *in vitro* preimplantation embryo development in bovine

Here after the embryo undergoes compaction and forms blastocyst with blastocoelic cavities by reaching the day 8. Blastocyst formation (cavitation) is essential for implantation and subsequent development and implantation failure is a principal cause of early pregnancy loss (Starbuck et al. 2004) in cow (Ealy and Yang 2009, Khatib et al. 2009, Pretheeban et al. 2009). The blastocoelic cavity and compaction allows the cells to differentiate into inner cell mass (ICM) and trophoblast (TE) cells, the blastomeres remaining in contact with the outside are destined to form the TE cells lineage while the blastomeres inside the embryo are destined to form the ICM. The ICM later forms the fetus, with fated three germinal layers. Early embryonic development is characterized by the number of nuclei (blastomere) present within the developing embryo. The initial development of the number of nuclei (blastomere) present within the developing embryos is controlled by maternally inherited molecules in the oocyte. The minor embryonic genome activation which begins at 2-cell stage and major embryonic genomic activation starts at 8-cell stage in bovine. During this early embryogenesis an eventually developmental control is purchased (Maddox-Hyttell et al. 2003). This shift from maternal to zygotic genomic control is referred to as the maternal/zygotic transition (MZT). A unique feature of these early embryonic cells is the ability by which a single cell can able to form a whole organism, which is termed as totipotency. Blastomeres maintain complete totipotency until the 16-cell stage of development, here after the differentiation of cell happens in the embryo which prevents the complete totipotency of an embryo (Kurosaka et al. 2004).

For the formation of zygote both the gametes (male and female) are contributing 50-50% of the nuclear content but approximate whole cytoplasmic content was taken from



female. So, the contribution of transcripts are more from female gametes and also the cytoplasmic miRNA contribution which known to be abundant in oocyte in comparison to sperms. Amanai group has shown that miRNAs derived from sperms plays no role or if any, the role is limited in mammalian fertilization or early preimplantation development (Amanai et al. 2006). Identification of miRNAs in cattle embryos was obtained by cloning, microarray or qRT-PCR profiling (Castro et al. 2010, Coutinho et al. 2007, Long and Chen 2009, Tripurani et al. 2010). A total of 390 miRNAs had shown temporal expression profiles during prenatal development at specific stages of mouse embryonic development (Mineno et al. 2006). The group working in zebra fish embryonic development found that the embryos lack let-7 miRNA, phenotypically they have shown delay in early growth and after 8 days of fertilization the embryo was lethargic and the development was arrested (Wienholds et al. 2003). The effect of miRNAs during embryonic development in different embryonic tissues was determined by microarray analysis. These identified miRNAs are responsible for development and control of stem cell in zebrafish (Wienholds et al. 2005). Expression difference of miRNA was shown by Tripurani et al in 2010. They showed the high expression of bta-mir424 and bta-mir-10b in early stages of preimplantation embryos and some of the novel miRNA were relatively less in early stages but higher in blastocysts stage (Tripurani et al. 2010). Dicer is a key enzyme in processing of mature miRNA, so lack of dicer interrupts the biogenesis of miRNA. Dicer1<sup>-/-</sup> embryos have shown the drop in the expression of miRNAs in mouse development (Bernstein et al. 2003). As the knockout of Dicer1 reduces miRNA expression, it leads to the embryonic lethal and depletion of stem cell development in mice (Bernstein et al. 2003). Female fertility and embryo development were also been affected by the involvement of Dicer1/miRNA mediated posttranscriptional gene regulation in reproductive somatic tissues (Hong et al. 2008). In bovine, nuclear transfer and *in vitro* fertilized embryo were taken at day 17 to find the differentially regulated miRNA in both group using microarray screening and qRT-PCR. Additionally, it also has shown the nuclear reprogramming in somatic cloning (Castro et al. 2010). A study in human describes the infertility of male and female with its transferable quality of blastocysts and correlation of the miRNA expression in the male factor infertility and polycystic ovaries (McCallie et al. 2010). Further more, functional analysis of microRNA in preimplantation embryo development will facilitate the contribution of miRNA in biological processes and disease in

embryos. The study specially will help to understand the mystery of the gene expression controlled by miRNA in maternal to embryonic gene transition and the study also facilitate the knowledge of miRNA expression pattern in different stages of development. Some functional work has been done in preimplantation stage of different other species but not yet in bovine. This study will lead to prevent the embryo loss in bovine and will develop some therapeutic applications which can be useful in future.

### 2.5.1 MicroRNA miR-130b family in embryonic stem cells

MicroRNA 130 family was first identified in embryonic stem cell (ESC) and known as ESC miRNAs (Houbaviy et al. 2003). It has four members in family namely: miR.130a, miR-130b, miR-301a and miR-301b. The annotated sequences for all four family members of miR-130/301 family in human are shown in (Table 2). miR-130a was initially been identified by cloning studies in mouse (Lagos-Quintana et al. 2002). miR-130b was first identified in mouse embryonic cells (Houbaviy et al. 2003). Later on these miRNAs were identified in human embryonic stem cells (hES) and believed to serve as molecular markers for the early embryonic stage and for undifferentiated hES cells (Suh et al. 2004). Different functions have been found for the family members of miR-130. Regarding to other cells miR-130b was verified to be present in human BC-1 cells (Cai et al. 2005). Additionally, in human disease the expression of miR-130b was seen higher in schizophrenic compared with normal individuals (Burmistrova et al. 2007). Furthermore, reduction of adipogenesis was observed by miR-130 which regulates PPARgamma biosynthesis (Lee et al. 2011). In human vascular endothelial cells, miR-130a, is a regulator of the angiogenic phenotype by targeting *GAX* and *HOXA5* and regulating there expression (Chen and Gorski 2008). miR-130a plays a role in the regulation of cardiac development by the regulation of FOG-2, a transcriptional co-factor, protein (Kim et al. 2009). A recent report shows the family members of miR-130 (miR-130/301), binds to a conserved site in the 3'UTR of CD69 mRNA and down-regulates its expression in activated CD8+ cells (Zhang and Bevan 2010). Furthermore, regarding to human disease miR-130b found in the development and progression of melanoma (Stark et al. 2010). The family members of miR-130/301 were known to be oncomiR (Shi et al. 2011, Yeung et al. 2008). Recently, a report has shown miR-301 is located in an intron of the *SKA2* gene and act as a novel oncogene in LNN breast cancer

and targets Col2A1, PTEN, FoxF2, and BBC3 mRNAs in human breast cancer that acts through multiple pathways and mechanisms to promote nodal or distant relapses (Shi et al. 2011).

Table 2: miRNA sequence of miR-130 family in human

miRNA	Family	Sequence (seed sequence)
hsa-miR-130b	mir-130	CAGUGCAAUGAUGAAAGGGCAU
hsa-miR-130a	mir-130	CAGUGCAAUGUAAAAGGGCAU
hsa-miR-301a	mir-130	CAGUGCAAUAGUAUUGUCAAAAGC
hsa-miR-301b	mir-130	CAGUGCAAUGAUAUUGUCAAAAGC

miR-130b\* sequence is the complementary sequence of miR-130b and located in the negative strand of chromosome, It was identified as a miRNA candidate using RAKE and MPSS techniques (Berezikov et al. 2006). The expression of miR-130b\* was later confirmed by cloning (Landgraf et al. 2007).

MicroRNA miR-130a, miR-130b and miR-301 were first known in bovine through the web-server for miRNA gene which provides homologous tool for animals (Artzi et al. 2008, Strozzi et al. 2009). The conserve region of genes are stable and miR-130a, 130b are highly conserved in mammalian species (Jin et al. 2009). Expression profiling using heterologus approaches of miRNA had shown a high expression of miR-130b in immature oocyte in comparison to mature oocyte (Tesfaye et al. 2009).

### 2.5.2 Impact of miR-130b in different cell types

The miRNA miR-130b was known to be an oncomir regarding various researches (Ma et al. 2010b, Watashi et al. 2010, Yeung et al. 2008). The role of miR-130b was been observe in Human HTLV-1–transformed T-cell lines for regulating cell proliferation and survival in HTLV-1 transformed cells by targeting TP53INP1. Here, miR-130b known to regulate cell growth and established by conducting experiments which showed that enhanced TP53INP1 expression increased apoptosis in HTLV-1 transformed cells (Yeung et al. 2008). Functional studies of miR-130b on lentiviral-

transduced CD133-cells demonstrated high resistance to chemotherapeutic agents, enhanced tumorigenicity *in vivo*, and also provide a better possibility for self renewal of cells. So, this report shows increase in miR-130b reduces the expression of TP53INP1, a known miR-130b target and regulate CD133+ liver TICs which enhance self renewal and tumorigenicity in CD133-cells (Ma et al. 2010b). miR-130/301, were up-regulated T-cell and targets to down-regulate CD69 transcript expression via binding to a conserved site in the 3'UTR of CD69 mRNA (Zhang and Bevan 2010). A recent study shows the tumorigenesis induced by miR-130b can be reprogrammed by some small molecules which affects the biogenesis pathway of miRNA targeting two different compounds; one impaired Dicer activity and the other blocked small RNA-loading into AGO2 complex. These small molecules could potentially reverse tumorigenesis induced by miR-130b (Watashi et al. 2010). In a report a specific miRNA can regulate the miR-130b which can be correlated with the reprogramming during newt regeneration and the stem or germ cells reprogramming (Nakamura et al. 2010). This all reports show that, miR-130b is an embryonic stem cell specific miRNA. It is a conserved and an important miRNA in animal system which also able to induce tumour or proliferation in different cell types including stem cells but the function of miR-130b is still uncovered for the preimplantation embryos including oocytes and its surrounding cells.

### 3 Materials and methods

#### 3.1 Materials

##### 3.1.1 Embryos

For this study, bovine oocytes were obtained from local slaughter house and embryos were obtained by *in vitro* production (IVP) technologies after *in vitro* maturation, fertilization and culture.

##### 3.1.2 Materials for laboratory analysis

###### 3.1.2.1 Chemicals, kits, biological and other materials

Manufacturer/Supplier	Chemicals or biological materials
Acris Antibodies GmbH:	RPS6KA5 (MSK1) primary antibody anti rabbit
Abcam, Cambridge, MA, USA:	Fluorescein (FITC)-conjugated donkey anti-goat antibody, Lactate Colorimetric Assay Kit
Beckman Coulter, Krefeld, Germany:	CEQ™ 8000 Genetic Analysis System, Dye Terminator Cycle Sequencing (DTCS), Sample loading solution (SLS), Glycogen for sequencing
BioAssay System, USA:	Enzychrom AF Cholesterol Assay Kit (E2CH-100)
Biomol, Hamburg, Germany:	Phenol, Phenol/ Chlorophorm/Isoamyl alcohol (25:24:1)
Bio-Rad laboratories, Munich, Germany:	iTaq SYBR Green Supermix with ROX
Burlingame, CA, USA:	4', 6'-diamidino-2-phenylindole hydrochloride (DAPI)
Clontech, Takara Bio Europe /Clontech, France:	pMJGreen (pBEHpac18 + pEGFP-N1)
Dako Deutschland GmbH, Hamburg, Germany:	Fast Red Substrate System
Diagnostics GmbH, Mannheim, Germany:	Digoxigenin-AP Roche

Eppendorf Biopur, Hamburg:	Safe-Lock tubes 0.5 ml, epT.I.P.S. Singles 0.1-20 $\mu$ l, 2.5x RealMasterMix/ 20x SYBR Solution
Exiqon, Vedbaek, Denmark:	miRNA primer, Precursor, inhibitor, miRCURY™ LNA Detection probe
Gibco, Karlsruhe, Germany:	GIBCO® Opti-MEM I Reduced-Serum Medium (1x) liquid, Fetal Calf Serum (FCS)
Invitrogen Life Technologies, Karlsruhe, Germany:	Lipofectamine 2000, DMEM, DPBS, MEM NEAA 100x (non- essential amino acids), BME EAA 50x (essential amino acids), Gentamycin, FCS, Hoechst 33342, MitoTracker® Mitochondrion-Selective Probes
New England Biolabs Ipswich, MA, USA:	Pme1 and Xho1 Restriction Enzymes
Promega WI, USA :	Random primer, BSA, pGEM®-T vector. RNasin (Ribonuclease inhibitor), 2X rapid ligation buffer, 10x PCR buffer, Bovine serum albumin (BSA), T4 DNA ligase, pmirGLO Dual-Luciferase miRNA Target Expression Vector, Dual-Luciferase® Reporter Assay System (E1910), JM109 ( <i>Escherichia coli</i> ) competent cells
Qiagen, Hilden, Germany:	mirNeasy® Mini kit, QIAquick PCR Purification Kit, Mini Elute™ Reaction Cleanup Kit, RNase-free DNase, miScript Reverse Transcription Kit, miScript SYBR Green PCR Kit
Roth, Karlsruhe, Germany:	Acetic acid, Agar Agar, Ammonium persulfate (APS), Ampicillin, Boric acid, Bromophenol blue, Calcium chloride, Chloroform, dNTP, Dimethyl sulfoxide (DMSO), Ethylenediaminetetraacetic acid (EDTA), Ethanol, Ethidium bromide, DTT, Formaldehyde, Hydrochloric acid, Isopropyl - D-thiogalactoside (IPTG), Kohrsolin® FF Pepton, Nitric acid, Peptone, Potassium dihydrogen phosphate, Ponceau-S, Proteinase K, 2- Propanol, Roti®-Block-10x, Rotiphosese Gel 30 (37:5:1), Silver nitrate, Sodium acetate, Sodium carbonate, Sodium chloride, Sodium hydroxide, Sodium carbonate, Sodium chloride, Tris, N, N, N',

---

	N'-Tetramethylethylenediamine (TEMED), Tris-HCl, T-octylphenoxypolyethoxyethanol (Triton X-100), 5-bromo-4-chloro-3-indolyl-beta-D-galactopyranoside (X-Gal), Yeast extract
Santa Cruz Biotechnology, CA, USA:	Primary antibody SMAD1/5 anti goat, GAPDH anti goat, horseradish-peroxidase (HRP) conjugated donkey anti-rabbit secondary antibody, HRP-conjugated mouse anti-goat IgG
Sigma-Aldrich Chemie GmbH, Munich, Germany:	2-Mercaptoethanol, Acetic anhydride, Agarose, Ammonium acetate, anti-goat IgG FITC conjugated antibody, Calcium chloride, Calcium chloride dehydrate, Calcium lactate, Cell Growth Detection Kit MTT based, Dulbecco's phosphate buffered saline (D-PBS), Fast green, Formaldehyde, Fetal Bovine Serum, FSH, GenElute™ Plasmid Miniprep kit, Heparin, Hepes, Hydroxylamine, Hyaluronidase, Hypotaurin, Igepal, Isopropanol, Magnesium chloride, Magnesium chloride hexahydrate, Medium 199, Mineral oil, Penicillin, Phenol red solution, 10x PCR reaction buffer, Potassium chloride, Proteinase inhibitor, RIPA Buffer RNA later, Secondary anti-rabbit IgG FITC conjugated antibody, Sodium Dodecyl Sulfate (SDS), Sodium hydrogen carbonate, Sodium hydrogen phosphate, Sodium hydrogen sulfate, Sodium lactate solution (60%), Sodium pyruvate, Streptomycin sulfate, Taq DNA polymerase, Trypan Blue Solution (0.4%), Trypsin-EDTA, yeast tRNA
Thermo Scientific, USA:	SuperSignal West Pico Substrate
Whatman- Protran®, Schleicher & Schuell Bioscience:	Protran Nitrocellulose Transfer Membrane
USB, Ohio, USA:	ExoSAP-IT
Vector laboratories, Burlingame, CA:	DAPI

---

## 3.1.2.2 List of Equipment

---

ABI PRISM® 7000 SDS	Applied Biosystems, Foster city, USA
4-well, 24-well and 96-well plate	Thermo Fisher Scientific, Nunc, Roskilde, Denmark
Agilent 2100 bioanalyzer	Technologies , CA, USA
ApoTome microscope	Carl Zeiss MicroImaging, Germany
Carbon dioxide incubator (BB16)	Heraeus, Hanau, Germany
Carbon dioxide incubator (MCO-17AI)	Sanyo, Japan
Centrifuge	Hermle Labortechnik, Wehingen
CEQ™ 8000 Genetic Analysis System	Beckman Coulter GmbH, Krefeld
Confocal laser scanning microscope-510	Carl Zeiss, Germany
Cryotube Nunc	Roskilde, Germany
Epifluorescence microscope (DM-IRB)	Leica, Bensheim, Germany
Gel-documentation unit	BioRad, Munich, Germany
HERA safe Bioflow safety hood	Heraeus Instruments, Meckenheim
Icycler	Bio-Rad Laboratories, München
Incubator	Heraeus, Hanau, Germany
Inverted microscope	Leica DM –IRB, Germany
Inverted microscope, ECLIPSE TS100	Nikon, Japan
Injection capillary (K-MPIP-3335-5)	Cook, Ireland
Luminofluorescent reader	Centro LB 960, Berthold Technologies, Germany
Millipore apparatus	Millipore corporation, USA
Multiplate reader	Molecular Device, Germany
NanoDrop 8000 spectrophotometer	NanoDrop, Wilmington, USA
Nitrocellulose transfer membrane (Protran®)	BioScience, Germany
PCR thermocycler (PTC100)	MJ Research, USA & BioRad, Germany
pH meter	Kohermann, Germany



---

Power Supply Mini-Protan®	BioRad, Munich, Germany
Power supply PAC 3000	Biorad, Munich, Germany
Savant SpeedVac®	TeleChem International, Sunnyvale
Slide SuperFrost® Plus	Braunschweig, Germany
SHKE6000-8CE refrigerated Shaker	Thermoscientific, IWA, USA
Stereomicroscope SMZ 645	Nikon, Japan
Thermalshake Gerhardt	John Morris scientific, Melbourne
Trans/Blot® Semi/Dry transfer Cell	BioRad, CA, USA
Tuttnauer autoclave	Connections unlimited, Wetzlar
Ultra low freezer (-80 °C)	Labotect GmbH, Göttingen, Germany

---

### 3.1.2.3 Used softwares

---

BLAST program	<a href="http://www.ncbi.nlm.nih.gov/BLAST">http://www.ncbi.nlm.nih.gov/BLAST</a>
ENSEMBL genome browser	<a href="http://www.ensembl.org/index.html">http://www.ensembl.org/index.html</a>
Entrez Gene	<a href="http://www.ncbi.nlm.nih.gov/entrez/query.fcgi?db=gene">www.ncbi.nlm.nih.gov/entrez/query.fcgi?db=gene</a>
Gene Ontology	<a href="http://www.geneontology.org">http://www.geneontology.org</a>
microRNA.org, target prediction	<a href="http://www.microrna.org/microrna/home.do">http://www.microrna.org/microrna/home.do</a>
Mitarget	<a href="http://cbit.snu.ac.kr/~miTarget/">http://cbit.snu.ac.kr/~miTarget/</a>
PicTar target prediction	<a href="http://www.pictar.org/">http://www.pictar.org/</a>
Targetscan, target prediction	<a href="http://www.targetscan.org/">http://www.targetscan.org/</a>
miRBase_12.0	<a href="http://microrna.sanger.ac.uk/sequences/">http://microrna.sanger.ac.uk/sequences/</a>
Multiple Sequence Alignment	<a href="http://searchlauncher.bcm.tmc.edu/">http://searchlauncher.bcm.tmc.edu/</a>
Primer Express® software v2.0	Applied Biosystems, Foster city, CA, USA
SAS (version 9.2)	SAS Institute Inc., NC, USA

---

## 3.1.2.4 Reagents and media

All solutions used in this study were prepared using deionized and demineralised millipore water (ddH<sub>2</sub>O) and when required the pH was adjusted with sodium hydroxide (NaOH) or hydrochloric acid (HCl). For some of the sensitive experiment, the solutions or buffers were filtered through 0.2 µm filter and autoclaved at 120 °C for 20 minutes.

General reagents

DEPC-treated water	DEPC	1.0 ml
	Water added to	1,000.0 ml
LB-agar plate	Sodium chloride	8.0 g
	Peptone	8.0 g
	Yeast extract	4.0 g
	Agar	12.0 g
	Sodium hydroxide (40 mg/ml)	480.0 µl
	ddH <sub>2</sub> O added to	800.0 ml
LB-broth	Sodium chloride	8.0 g
	Peptone	8.0 g
	Yeast extract	4.0 g
	Sodium hydroxide (40 mg/ml)	480.0 µl
	ddH <sub>2</sub> O added to	800.0 ml
	10x TBE buffer	Tris base
Boric acid		55.0 g
EDTA (0.5 M)		40.0 ml
ddH <sub>2</sub> O added to		1,000.0 ml
50X TAE buffer, pH 8.0		Tris
	Acetic acid	57.1 ml
	EDTA (0.5 M)	100.0 ml

	ddH <sub>2</sub> O added to	1,000.0 ml
1X TE buffer	Tris (1 M)	10.0 ml
	EDTA (0.5 M)	2.0 ml
	ddH <sub>2</sub> O added to	1,000.0 ml
X-gal	X-gal	50.0 mg
	N, N'-dimethylformamide	1.0 ml
10X PBS	NaCl	8.77 g
	Na <sub>2</sub> HPO <sub>4</sub>	1.50 g
	NaH <sub>2</sub> PO <sub>4</sub>	2.04 g
	Water added to	1,000.0 ml
1X PBS	10X PBS	100.0 ml
	Water added to	1,000.0 ml
1X PBS-Tween (PBST)	PBS	999.50 ml
	Tween®20	0.50 ml
PBS + PVA (50 ml)	Polyvinyl alcohol (PVA)	300.0 mg
	PBS upto	50.0 ml
Physiological saline solution	Sodium chloride	9.0 g
	Water upto	1,000.0 ml
Agarose loading buffer	Bromophenol blue	0.0625 g
	Xylencyanol	0.0625 g
	Glycerol	7.5 ml
	ddH <sub>2</sub> O added to	25.0 ml
Lysis buffer	Igepal	0.8 µl
	RNasin	5.0 µl
	DTT	5.0 µl
	Water added to	100.0 µl
SDS solution	Sodium dodecylsulfat in ddH <sub>2</sub> O	10% (w/v)

Proteinase K solution	Proteinase K in 1X TE buffer	2% (w/v)
dNTP solution	dATP (100 mM)	10.0 $\mu$ l
	dCTP (100 mM)	10.0 $\mu$ l
	dGTP (100 mM)	10.0 $\mu$ l
	dTTP (100 mM)	10.0 $\mu$ l
	ddH <sub>2</sub> O added to	400.0 $\mu$ l
IPTG solution	IPTG	1.2 g
	ddH <sub>2</sub> O added to	10.0 ml
3M Sodium Acetate, pH 5.2	Sodium Acetate	123.1 g
	ddH <sub>2</sub> O added to	500.0 ml
1M EDTA, pH 8.0	EDTA	37.3 g
	ddH <sub>2</sub> O added to	1,000.0 ml
Phenol Chloroform	Phenol : Chloroform	1 : 1 (v/v)
	ddH <sub>2</sub> O added to	10.0 ml
3M Sodium Acetate, pH 5.2	Sodium Acetate	123.1 g
	ddH <sub>2</sub> O added to	500.0 ml
20X SSC	NaCl	87.65 g
	Sodium citrate	44.1 g
	Water upto	500.0 ml
1 M Tris-HCl (1M)	Tris	121.14 g
	Water added to	1,000.0 ml
4% PFA, pH 7.3	Para-formaldehyde	4.00 g
	1X PBS	100.0 ml
Brought to 65 °C under ventilation hood. 5 $\mu$ l of 5 M NaOH was added for solution to become clear. Stored in light protected place upto 2 weeks.		

20X SSC, pH 7.0	NaCl	87.65 g
	Sodium citrate	44.12 g
	Water upto	500.0 ml
0.5M Sucrose/PBS (30% sucrose)	Sucrose	85.57 gm
	1X PBS upto	500.0 ml
Acetylation solution	Triethanolamine	2.33 ml
	Acetic anhydride	500.0 $\mu$ l
	DEPC water upto	200.0 ml
Yeast tRNA (10 mg/ml)	Yeast tRNA	25.0 mg
	DEPC-treated H <sub>2</sub> O	2.50 ml
Hybridization solution	Formamide 65%	32.25 ml
	5X SSC	12.5 ml
	Tween-20, 0.1%	50.0 $\mu$ l
	1M citric acid	460.0 $\mu$ l
	Heparin, 50 $\mu$ g/ml	2.5 mg
	tRNA, 500 $\mu$ g/ml	2.5 ml
	DEPC water upto	50.0 ml
Hybridization wash solution	Formamide, 65%	65.0 ml
	5X SSC,	25.0 ml
	Tween-20, 0.1%	100.0 $\mu$ l
	1M citric acid	1.2 $\mu$ l
	DEPC water upto	100.0 ml
50% Formamide/SSC	Formamide	1,000.0 ml
	1X SSC	1,000.0 ml
50% Formamide/Tween-20/SSC	Formamide, 50%	500.0 ml

	Tween-20, 0.1%	1.0 ml
	1X SSC	499.0 ml
5X SSC	20X SSC	250.0 ml
	DEPC water	750.0 ml
2X SSC	20X SSC	100.0 ml
	DEPC water	900.0 ml
1X SSC	20X SSC	100.0 ml
	DEPC water	1,900.0 ml
0.2X SSC	20X SSC	10.0 ml
	DEPC water	990.0 ml
1X PBST	1X PBS	999.0 ml
	Tween-20	1.0 ml
Blocking solution	FCS	2.0 ml
	B1 solution	18.0 ml
B1 solution	1M Tris, pH7.5	100.0 ml
	5M NaCl	30.0 ml
Stop solution	EDTA, 1mM	14.61 mg
	PBS, pH 5.5 upto	50.0 ml
10N NaOH	NaOH	40.0 gm
	dd H <sub>2</sub> O upto	100.0 ml
0.2% Triton-X100	Triton	2.0 ml
	10X PBS added to	1,000.0 ml
0.3% BSA in PBS	BSA	3.0 g
	10X PBS added to	1,000.0 ml
3% BSA in PBS	BSA	30.0 g
DMEM	DMEM	129.0 ml
	Sodium pyruvate, 1%	1.5 ml

	Non-Essential amino acid, 1%	1.5 ml
	L-Glutamine, 1%	1.5 ml
	PenicillinStreptomycin, 1%	1.5 ml
	Fungizone/Amphothericin, 1%	1.5 ml
	2-mercaptomethanol	1.5 µl
	Fetus Calf Serum, 10%	1.5 ml
Cryoprotectant	FCS, 90%	9.0 ml
	DMSO, 10%	1.0 ml
Fertilization medium	Sodium chloride	330 .0 mg
	Potassium chloride	117.0 mg
	Sodium hydrogen carbonate	105.0 mg
	Sodium dihydrogen phosphate	2.1 mg
	Penicillin	3.2 mg
	Magnesium chloride hexahydrate	5.0 mg
	Calcium chloride dihydrate	15.0 mg
	Sodium lactate solution, 60%	93.0 µl
	Phenol red solution, 5% (in DPBS)	100.0 µl
	Water upto	50.0 ml
Modified parker medium	HEPES	140.0 mg
	Sodium pyruvate	25.0 mg
	L-Glutamine	10.0 mg
	Gentamicin	500.0 µl
	Medium 199	99.0 ml
	Hemi calcium lactate	60.0 mg
	Water upto	110.0 ml
Permeabilizing solution(10 ml)	Triton X-100	5.0 µl
	Glycine + PBS added	10.0 ml

PHE medium	Physiological saline, 0.9%	16.0 ml
	Hypotaurin solution	10.0 ml
	Epinephrin solution	4.0 ml
CR1-aa culture medium (50 ml)	Hemi-calcium lactate	273.0 mg
	Streptomycin sulphate	3.9 mg
	Penicillin G	1.9 mg
	Sodium chloride	315.6 mg
	Potassium chloride	11.2 mg
	Sodium hydrogen carbonate	105.0 mg
	Sodium pyruvate	2.2 mg
	L-Glutamine	7.3 mg
	Phenol red solution	100.0 µl
	Sodium hydrogen carbonate	80.0 mg

## 3.2 Methods

Functional analysis of miR-130b in preimplantation embryo development is conducted in several steps of experiments and beside this cumulus cell culture was conducted for the validation of miRNA target.

### 3.2.1 *In vitro* embryo production

#### 3.2.1.1 Oocytes recovery and *in vitro* maturation

Bovine ovaries were obtained from the local abattoirs and transported to the laboratory within 2-3 hours in a thermo flask (30-35 °C) having physiological saline (0.9% NaCl), supplemented with 0.5 ml Steptocombin® per liter. Before aspiration of cumulus oocyte complex (COC), the ovaries were surface sterilized with 70% EtOH followed with twice washing with 0.9% physiological saline and dried with sterile paper. COC were aspirated from antral follicles (2-8 mm diameter) using an 18-gauge needle and a 10 ml syringe containing ~2 ml aspiration media (Hepes-buffered Tissue Cultured Medium-



199). This aspirated fluid was collected in 50 ml tubes and kept at 37 °C for 15 minutes to allow the precipitation of COC. The competent COCs were picked out and separated using glass-pipette under a stereomicroscope (Nikon) and washed three times in drops of pre-warmed maturation medium (Modified Paker Medium, MPM). The medium was taken with 12% heat-inactivated oestrus cow serum (OCS), 0.5 mM L-glutamine, 0.2 mM sodium pyruvate, 50 µg/ml gentamycin sulphate, and 12% FSH (Sigma-Aldrich Chemie GmbH). The COCs were transferred in groups of 50/well in 400 µl maturation medium under mineral oil (Sigma) in four well dishes (Nunc). Oocytes with evenly granulated cytoplasm and multiple layers of cumulus cells surrounded were *in vitro* matured. During the IVM procedure, these competent COCs were culture in TCM-199 as basic medium at 37 °C in incubator with humidified atmosphere of 5% CO<sub>2</sub> in air for 22-24 hours.

#### 3.2.1.2 Sperm preparation and capacitation

According to the oocyte number the semen straws were taken (2-4) from the known breeding bull and thawed. To obtain the best quality of motile spermatozoa swim-up procedure (Parrish et al. 1988). During the swim-up procedure the frozen thawed sperm cell were incubated in a tube containing 5 ml capacitating medium supplemented with heparin for 50 minutes under 39 °C in an incubator with humidified atmosphere of 5% CO<sub>2</sub> in air. The motile sperm cells found in the upper layer of the solution were transferred into new falcon tube. The sperm cells were pelleted by centrifugation at 10,000 rpm for 10 minutes. The resulting pellet was washed two times and finally resuspended in already prepared 3.5 ml capacitating medium for IVF.

#### 3.2.1.3 *In vitro* fertilization of oocytes

Matured oocytes were washed twice in the fertilization medium and transferred into a four-well dish containing 400 µl of fertilization medium supplement with 6 mg/ml bovine serum albumin (BSA), 2.2 mg/ml sodium pyruvate and 1 mg/ml heparin. Ten microliter of PHE medium was added to each well to initiate sperm motility and covered with mineral oil (Sigma). Motile spermatozoa were selected according to the procedure explained above in 3.2.1.2. The final concentration of  $1 \times 10^6$  spermatozoa/ml was taken in the fertilization medium. These diluted spermatozoa were added to a group

of 50 oocytes in each well and co-cultured for 18 hrs at standard incubation conditions with 39 °C and humidified atmosphere containing 5% CO<sub>2</sub> in air (Tesfaye et al. 2010).

#### 3.2.1.4 *In vitro* culture of embryos

The mature oocytes were *in vitro* fertilized and then the presumptive zygotes were collected into 15 ml of falcon tube with 1 ml of culture medium (CR1aa) (Rosenkrans and First 1994) with 10% OCS, 10 µl/ml BME (essential amino acids) and 10 µl/ml MEM (non essential amino acids). The presumptive zygotes were gently vortexed for the separation of dead spermatozoa and cumulus cells. The cumulus free zygotes were screened and washed twice with culture medium. Then transferred in the group of 50-60 zygotes each well into four-well dish, each of this well was filled with pre-warmed 400 µl culture medium cover with mineral oil. The first cleavage rate was observed 48 hours post fertilization followed by incubating for the consecutive days of the embryos to collect different stages of preimplantation stages embryos.

#### 3.2.1.5 Oocytes denudation and storage

For the separation of oocytes from the cumulus cells, mature and immature COCs were taken in 15 ml falcon tube separately in TCM or maturation medium supplemented with hyaluronidase (1 mg/ml) (Sigma) and vortexed for 4 minute. Oocytes were carefully picked out and corresponding cumulus cells were collected by centrifugation. Oocytes and the cumulus cells of each group were washed two times in PBS (Sigma) and frozen separately in cryo-tubes containing 20 µl of lysis buffer [0.8% IGEPAL (Sigma), 40 U/µl RNasin (Promega Madison WI, USA), 5 mM dithiothreitol (DTT) (Promega Madison WI, USA)]. Finally, samples were grouped according to experiment and stored at -80 °C until RNA extraction.

### 3.2.2 Plasmid DNA preparation

#### 3.2.2.1 Primers design and gene cloning

For this study the genes selected as the target were first quantified in all stages of embryos and cells. For that sequence specific primers were designed using Primer Express® Software v2.0 (Applied Biosystems, Foster City, CA, USA) or from the online software primer 3.0 (<http://frodo.wi.mit.edu/primer3/>). Used primer sequences,

the GenBank accession number, size of amplified products and the annealing temperature are shown in (Table 3). For designing 3'UTR primers were constructed with restriction digestion sequence. Primers for 3' UTR were listed in (Table 4). To balance the GC content some more bases were added. All primers were purchased from Eurofins MWG synthesis GmbH (MWG Biotech, Eberberg, Germany) and diluted at 100 pmole as a stock solution. The selected gene sequence were amplified from genomic DNA or cDNA using Polymerase Chain Reaction (PCR) with 20  $\mu$ l final volume containing 2  $\mu$ l of 10X PCR buffer (Sigma), 0.5  $\mu$ l of each primer (10 pmole), 0.5  $\mu$ l of dNTP (50  $\mu$ M), 0.5 U of Taq DNA polymerase (Sigma), 14.4  $\mu$ l millipore H<sub>2</sub>O which finally added to 2  $\mu$ l of cDNA templates or 50 ng/ $\mu$ l genomic DNA and Millipore water (2  $\mu$ l) was used as negative control. The PCR reactions were carried out in a PT-100 Thermocycler and the thermal cycling program was set as: denaturation at 95 °C for 5 min, followed by 35 cycles at 95 °C for 30 sec, annealing at the corresponding temperature, as shown in table 3, for 30 seconds and extension at 72 °C for 1 min, final extension step at 72 °C for 10 minutes. Finally, 5  $\mu$ l of loading buffer were added to PCR products and loaded on agarose gel (2% for cDNA checking; 0.8% for PCR product extraction) in 1X TAE buffer by staining with ethidium bromide. The amplified PCR products were electrophoresed for 23 minutes at 120 voltages and visualized under Gel-documentation unit (BioRad) and the gel that have the DNA fragment of interest was cut if needed. The PCR product was extracted using QIAquick PCR purification kit (Qiagen) for the qRT-PCR primers using the manufacturer protocol.

Ligation was performed using pGEM-T Vector System I ligation kit for the entire specific gene fragment amplified by PCR and purified. According to the manufacturer instruction, ligation was performed in a 6  $\mu$ l reaction mix containing 3  $\mu$ l of 2X rapid ligation buffer, 0.5  $\mu$ l of pGEM vector (50 ng/ $\mu$ l), 0.5  $\mu$ l of T4 DNA ligase (3 units/ $\mu$ l), and 2  $\mu$ l of gel purified PCR product. The reaction was then incubated at 4 °C overnight or 1 hour at 37 °C. Transformation was performed by combining 3  $\mu$ l of ligation reaction with 60  $\mu$ l of JM109 (*Escherichia coli*) competent cells in a 2 ml tube and incubating on ice for 30 minutes. After incubation, the mixture was then heat-shocked briefly in a 42 °C water bath for 60 seconds and immediately returned to ice for 2 minutes. Then, 650  $\mu$ l of LB broth was added to the previous mixture and all together was shaken with speed of 90 rpm at 37 °C for 90 minutes in SHKE6000-8CE refrigerated Stackable

Shaker (Thermoscientific, IWA, USA). Meanwhile, plates of LB-agar with ampicillin (4 mg / 100 ml) were prepared. About 20 minutes prior to use 20  $\mu$ l of 0.5 M IPTG and 20  $\mu$ l of 50 mg/ml X-Gal was spread over the surface of LB-ampicillin plates with a glass spreader. And by 90 minutes of incubation, 300  $\mu$ l of inoculums were transferred in each plate and incubated at 37 °C overnight till the colonies become visible.

#### 3.2.2.2 Colony screening and sequencing

The positive bacteria having DNA insert in the pGEM-T vectors were screened by the presence of  $\beta$ -galactosidase activity.  $\beta$ -galactosidase is an enzyme produced by lacZ gene in pGEM®-T vector which interacts with IPTG to produce a blue colony. On the other hand, the insert of DNA disrupts the lacZ gene which failure to produce  $\beta$ -galactosidase, which results in white colonies. So the appearance of white colony shows the success of cloning. Four white colonies in addition to one blue colony were picked up and suspended in 30  $\mu$ l 1X PCR buffer for M13 reaction for further confirmation of transformation and sequencing. At the same time, colonies were also cultured in 600  $\mu$ l LB-broth with ampicillin (4 mg / 100 ml) in a shaking incubator 90 rpm at 37 °C for 90 minutes. On the other hand, bacteria that were suspended in 30  $\mu$ l 1X PCR were lysed by heating at 95 °C for 15 minutes. The colonies were screened for the insert by performing a PCR with primers designed in M13 promoter region of the vector. 20  $\mu$ l of reaction volume containing 10  $\mu$ l of lysate, 0.5  $\mu$ l dNTPs (10 mM), 0.5  $\mu$ l of each of primer 0.5 U of Taq polymerase (Sigma) in 1X PCR buffer were amplified in PTC 100 (MJ Research) thermal cycler for 35 cycles at 95 °C denaturation, 60 °C annealing and 72 °C extension followed by 10 minutes of final extension at 72 °C. The products were electrophoresed in 2% agarose gel. Clones having insert have higher molecular weight fragments than the blue clones. And the colonies with insert were then transferred to 15 ml tube and 5 ml of LB-broth with ampicillin were added and incubation continued overnight at the previous conditions for further plasmid isolation. The M13 PCR products from white colonies containing inserts were used as a template for subsequent sequencing to identify the proper sequence in the vector. A volume of 5  $\mu$ l of M13 products was purified by adding 1  $\mu$ l of ExoSAP-IT (USB Corporation) then incubated at 37 °C for 45 minutes followed by enzyme inactivation step at 80 °C for 15 minutes. The purified DNA product (6  $\mu$ l) was subsequently used as template for the sequencing

PCR which contains 8  $\mu$ l of millipore water, 2  $\mu$ l of 1.6 pmole M13 forward or reverse primer, 4  $\mu$ l of DTCS Quick Start Master Mix (Beckman Coulter). The PCR sequencing reaction was performed for 30 cycles at 96 °C for 20 seconds, 50 °C for 20 seconds and 60 °C for 4 minutes, followed by holding at 4 °C. The stop solution was prepared in a volume of 2  $\mu$ l of 3M NaOAc (pH = 5.2), 2  $\mu$ l of 100 mM EDTA (pH = 2.0) and 1  $\mu$ l of glycogen (20 mg/ml). The sequencing PCR product was transferred to a 1.5 ml sterile tube and mixed with 5  $\mu$ l stop solution. A volume of 60  $\mu$ l cold EtOH (98%) was added and mixed by vortex and then centrifuged for 15 minutes at 4 °C. The supernatant was removed and the pellet was washed 2 times with 200  $\mu$ l cold EtOH (70%) then centrifuged for 5 minutes at 4 °C. After removing the supernatant pellet was allowed to dry. The obtained pellets were dissolved in 40  $\mu$ l SLS and transferred to the sequencing plate, covered with mineral oil (Beckman Coulter, Krefeld, Germany) and immediately loaded to CEQ™ 8000 Genetic Analysis (Beckman Coulter, Krefeld, Germany) sequencing machine. The sequence similarity of the result was verified by blasting the sequence into NCBI/BLAST search tool (<http://blast.ncbi.nlm.nih.gov/Blast.cgi>).

Table 3: List of primers (5' to 3') used in this study

Gene	NCBI Accession No. (Bos Taurus)		Sequence of primer 5' to 3'	T <sub>A</sub> (°C)
MSK1 (RPS6KA5)	NM_001192023.1	F	CTTGATTCTAATGGCCACGTGA	53
		R	CATCAACAGTGAACGGAGATGC	
SMAD5	NM_001077107.2	F	CCATCAGCCCAACAACACT	52
		R	AGGCAGGAGGAGGAGTATCA	
EIF2C1	XM_002686476.1	F	AGAGTGGAGTATGCAGTGCTCG	51
		R	GGGCATCAACATCGTTGTCA	
EIF2C4	XM_606455.4	F	CACACATCCATCCGAGTTTG	54
		R	ACCGCACATAGGTGTGACAA	
DDX6	NM_001143867.1	F	AGGCAGGAACATCGAAATCGT	53
		R	AAGATGACCAAAGCGACCTGA	
DOC1R	NM_001035320.1	F	GCCCTTTCAGACCACTGTTT	51
		R	GGATCTCTTTGCCATCTCTT	
MEOX2	NM_001098045.1	F	GTTTGGAAACCGTCGTGAAGT	51
		R	GCAAGACGAGGAAGAAGTGG	
MARCH2	NM_001037589.1	F	GGTCTCATTCCGCTACCATT	54
		R	TGTCTCCTCAGCCACCTTCT	
GAPDH	NM_001034034	F	AATGGAAAGGCCATCACCATC	57
		R	GTGGTTCACGCCATCACA	
Histone	NM_174809.2	F	GCCGTATTCATCGACACCTGA	55
		R	CTCCACGAATAGCAAGTTGCAA	
pmirGLO		F	GTGGTGTGTGTTTCGTGGAC	58
		R	CTTTCGGGCTTTGTTAGCAG	
M13		F	TTGTAAACGCGGCCAGT	59
		R	CAGGAAACAGCTATGACC	

Table 4: List of 3'UTR primer (5' to 3') used for the validation of miR-130b target genes

Gene		Primer for 3'UTR 5' to 3' (underline bases shows restriction site)	Seq.	T <sub>A</sub> (°C)
SMAD5 (I. seed match sequence)	F	GTGCGG <u>TTTAAAC</u> GCTAGTGACAGTGCGTGCAT	194	Tdown 66.5
	R	GTCGGCCTCGAGAGGGGTACCAAGGAAGCAAG		
SMAD5 (II. & III. seed match sequence)	F	CGCTG <u>TTTAAAC</u> GATAAGGACTGGGGCTCACA	325	Tdown 57
	R	CTGT <u>CTCGAG</u> TGAAGCATGTTGCTAGAATTTCA		
SMAD5 (IV & V. seed match sequence)	F	CGCTG <u>TTTAAAC</u> CCATTGGAGATGATGTTGCTT	324	62
	R	CTGT <u>CTCGAG</u> TGAAGCATGTTGCTAGAATTTCA		
MSK1	F	CGCTG <u>TTTAAAC</u> AGTTTTGCACTGCTCTTTCC	483	56
	R	CGT <u>CTCGAG</u> TTGAGCTATACAAGTGCTCTGC		
	F	CGCTG <u>TTTAAAC</u> TTCAACAGCGACACTCACTC		
GAPDH	R	CGCT <u>CTCGAG</u> GGAAACATGTGGAAGTCAGG	266	56
DDX6	F	CGCTG <u>TTTAAAC</u> CTGTGACACATCGATTTTGG	249	58
	R	GCT <u>CTCGAG</u> AGGCACTTCGCACAAATAAG		
EIF2C4	F	CGCTG <u>TTTAAAC</u> CGAACTCGGAATAGTTGCAC	551	58
	R	CGTG <u>CTCGAG</u> AATTGCCTGTCTGAATCTGC		
EIF2C1	F	CGCTG <u>TTTAAAC</u> GCAGAACTGCAACCTTTTGT	206	57
	R	CGCT <u>CTCGAG</u> TGGCAATGGACTCAGGTTAT		
MEOX2	F	CGCTG <u>TTTAAAC</u> CCAGAGGTGTTGGTTGTGTG	422	65.1
	R	CTGT <u>CTCGAG</u> GCTGGTTCTGTTTGTTCATCG		
MARCH2	F	CGCTG <u>TTTAAAC</u> AGCCGATTCTGTGATTCCTG	324	Gradient PCR (52.3-59.6)
	R	CTGT <u>CTCGAG</u> GGGCTCCTTTTATTCATTCG		
DOCR1	F	CGCTG <u>TTTAAAC</u> CGACTCCACCTCAGCTTCTGG	199	Tdown 59
	R	CTGT <u>CTCGAG</u> CCTCGCTGCTAACTCTTTTCG		

T<sub>A</sub>, Aneline temperature; Seq, Sequence; Tdown, touchdown

### 3.2.2.3 Plasmid DNA isolation and serial dilution

Once the sequence were conformed for the gene of interest into the plasmid DNA the plasmid was isolated from the bacteria by using GenElute™ Plasmid Miniprep Kit (Sigma, Germany) based on the manufacturer's instructions. Briefly, 5 ml of bacterial culture were centrifuged at 12,000 g for 1 minute for harvesting cells. The supernatant was discarded and the pellet containing cells were collected. These cells were resuspended in 200 µl of resuspension solution under the laminar hood. Then 200 µl of lysis solution was added to lyses the bacteria. The mixture was subsequently mixed by inversion of tubes until it became clear and viscous. After incubating at room temperature (< 4 minutes), cell precipitation was done by adding 350 µl of neutralization buffer, mixed gently and centrifuged at 12000 rpm for 10 minutes. At the same time, the GeneElute Miniprep column was prepared by washing with 500 µl of preparation solution using centrifuge. After that, the clear supernatant of plasmid was transferred to this binding column and centrifuged at 12000 rpm for 1 minute. The flow-through was discarded and the column was washed with 750 µl of wash solution followed by centrifugation at 12000 rpm for 1 minute and discarding the flow. Access wash buffer was removed from the column by re-centrifuging at 14000 rpm for 1 minute. DNA was eluted from the column by transferring it into a fresh collection tube; 30 µl of ddH<sub>2</sub>O was added and centrifuged at 14000 rpm for 1 minute. The column was discarded and the plasmid DNA was then collected. For determination of plasmid size and quality, 5 µl of plasmid together with 2 µl loading buffer was checked by agarose gel electrophoresis. In addition, the quantity of plasmid was also measured by NanoDrop 8000 spectrophotometer (NanoDrop, Wilmington, Delaware, USA) at 260 nm. An aliquot of plasmid DNA was subjected to sequence check; the rest was stored at -20 °C to be used as template for setting up the standard curve in real-time PCR. The copy number per microlitre of plasmid DNA was calculated based on the size and concentration. The plasmid serial dilution was prepared by converting concentration of plasmid (ng/µl) into numbers of molecules using the website ([http://molbiol.ru/eng/scripts/01\\_07.html](http://molbiol.ru/eng/scripts/01_07.html)). Serial dilutions were then prepared from the concentration of 10<sup>9</sup> upto 10<sup>1</sup> copies /µl and were stored at -20 °C. To achieve suitable standard curve for Real-time PCR the template serial dilution was conformed by PCR.



#### 3.2.2.4 Cloning of 3'UTR amplicons in pmirGLO vector

Once the 3'UTR were cloned in pGEM-T Vector it was sequence confirmed and purified from bacteria as described above. For the 3'UTR amplicons into the pmirGLO Vector (Figure 3.1) the plasmid DNA were first digested with 0.5  $\mu$ l of *pme1* and 2  $\mu$ l of *Xho1* restriction enzyme with 2  $\mu$ l of BSA and incubated at 37 °C for 60 minutes. Now the restricted plasmid was loaded in 0.8% agarose gel at 120 Voltage for 15 minutes and the 3'UTR amplicon was extracted from 0.8% (W/V) agarose gel using phenol-chloroform. All centrifugation were performed at 4 °C with 12,000x g speed. The gel that have PCR fragment was sliced, heated at 42 °C with 0.5 ml of 1X TE buffer until it is completely dissolved. The extraction was carried out by vigorously vortexing the gel solution with 0.6 ml of phenol-chloroform. Centrifugation for 15 minutes allow the mixture to be separated into three phases having, a lower phenol-chloroform phase, an interphase of precipitated protein, and an upper aqueous phase containing the amplified gene product. Upper aqueous phase was transferred into a new tube, shaken vigorously with an equal volume of chloroform to remove possibly carried over phenol, and re-centrifuged for another 10 minutes. The cleared aqueous phase was precipitated by gentle mixing with 50  $\mu$ l (or 1/10 volume) of sodium acetate solution (3 M, pH 5.3) and 1.5 ml of 100% EtOH (or 2.5 volume). Precipitation was maximized by placing at -20 °C for 2 hour. The precipitated amplified PCR product was pelleted at 12,000x g for 30 minutes at 4 °C in universal centrifuge Z233MK (Hermle Labortechnik, Wehingen, Germany). The supernatant was then removed and the pellet was washed with 200  $\mu$ l of 70% ethanol and centrifuged for 5 minutes to remove the supernatant. The pellet was air dried and gently dissolved in 20  $\mu$ l of ddH<sub>2</sub>O and stored at -20 °C till ligation or ligation was performed immediately.

The 3'UTR fragment digested with restriction enzyme was religated with pre-digested pmirGLO vector. Ligation was performed in a 6  $\mu$ l reaction mix containing 3  $\mu$ l of 2X rapid ligation buffer, 0.5  $\mu$ l of pmirGLO vector (1 $\mu$ g/ $\mu$ l), 0.5  $\mu$ l of T4 DNA ligase (3 units/ $\mu$ l), and 50-120 ng of digested and gel purified 3'UTR fragment (according to the length of DNA with 3:1 ratio). The reaction was then incubated overnight at 4 °C. Transformation was performed by combining 6  $\mu$ l of ligation reaction with 80  $\mu$ l of JM109 (*Escherichia coli*) competent cells in a 2 ml tube and incubated on ice for 30 minutes. After incubation, the mixture was then heat-shocked briefly in a 42 °C water bath for 60 seconds and immediately returned to ice for 2 minutes. Then, 700  $\mu$ l of LB

medium was added to the previous mixture and all together was shaken with speed of 90 rpm at 37 °C for 90 minutes in SHKE6000-8CE refrigerated Stackable Shaker (Thermoscientific, IWA, USA). Meanwhile, LB-agar plates were prepared with ampicillin (4 µg/100 µl). For each gene two plates were prepared by adding about 400 µl of inoculums per plate and incubated at 37 °C overnight till the colonies become visible. As pmirGLO vector don't have lacZ gene it can't produce β-galactosidase enzyme to form blue colony so all about 20 white colonies were randomly been picked up and suspended in 30 µl 1X PCR buffer. At the same time, colonies were also transformed in 900 µl of ampicillin/LB-broth (4 mg /100 ml) in a shaking incubator 90 rpm at 37 °C for 90 minutes. The colonies in plate were stored at 4 °C if needed. The bacteria that were suspended in 30 µl 1X PCR were lysed by heating at 95 °C for 15 minutes and PCR amplified with gene specific primers and conforms the presence of the gene but it don't conforms the integration of fragment into the vector or the orientation of sequence.

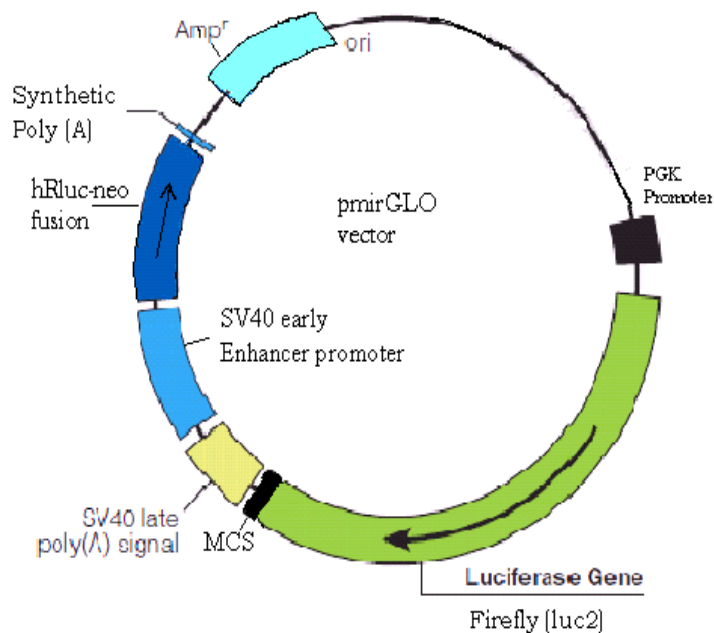


Figure 3.1: pmirGLO Dual-Luciferase miRNA Target Expression Vector. PGK promoter for firefly with multiple cloning site and SV40 promoter for renilla luciferase expression. Amp<sup>r</sup>: ampicillin resistance; MCS: multiple cloning site; PKG: phosphoglycerate kinase.

### 3.2.2.5 Sequencing and plasmid isolation of 3'UTR

The conformed colonies with gene specific primers were screened for the insert by performing a PCR with primers designed in pmirGLO vector. 20  $\mu$ l of reaction volume containing 10  $\mu$ l of lysate, 0.5  $\mu$ l dNTPs (10 mM), 0.5  $\mu$ l of each of primer, 0.5 U of Taq polymerase (Sigma) in 1X PCR buffer were amplified in PTC 100 (MJ Research) thermal cycler for 35 cycles at 95 °C denaturation, 58 °C annealing and 72 °C extension followed by 10 minutes of final extension at 72 °C. 5  $\mu$ l of the pmirGLO PCR products was purified by adding 1  $\mu$ l of ExoSAP-IT (USB Corporation) then incubated at 37 °C for 45 minutes followed by enzyme inactivation step at 80 °C for 15 minutes. The purified DNA product (6  $\mu$ l) was subsequently used as template for the sequencing PCR which contains 8  $\mu$ l of millipore water, 2  $\mu$ l of 1.6 pmole pmirGLO forward or reverse primer, 4  $\mu$ l of DTCS Quick Start Master Mix (Beckman Coulter). The PCR sequencing reaction was performed for 30 cycles at 96 °C for 20 seconds, , 50 °C for 20 seconds and 58 °C for 4 min, followed by holding at 4 °C. The stop solution was prepared in a volume of 2.0  $\mu$ l of 3M NaOAc (pH = 5.2), 2.0  $\mu$ l of 100 mM EDTA (pH = 2.0) and 1.0  $\mu$ l of glycogen (20 mg/ml). The sequencing PCR product was transferred to a 1.5 ml sterile tube and mixed with 5  $\mu$ l stop solution. A volume of 60  $\mu$ l cold EtOH (98%) was added and mixed by vortex and then centrifuged for 15 minutes at 4 °C. The supernatant was removed and the pellet was washed 2 times with 200  $\mu$ l cold EtOH (70%) and centrifuged for 5 minutes at 4 °C. After removing the supernatant pellets were allowed for dry. The obtained pellets were dissolved in 40  $\mu$ l SLS and transferred to the sequencing plate, covered with mineral oil (Beckman Coulter, Krefeld, Germany) and immediately loaded to CEQ™ 8000 Genetic Analysis (Beckman Coulter, Krefeld, Germany) sequencing machine. The sequence similarity of the result was verified by blasting the sequence into NCBI/BLAST search tool (<http://blast.ncbi.nlm.nih.gov/Blast.cgi>). After the confirmation of insert and sequence orientation the colonies with insert were then transferred to 50 ml tube and 25 ml of LB-broth with ampicillin (4 mg / 100 ml) were added and incubation continued more then 16 hours at the previous conditions for further plasmid isolation (in 3.2.2.3).

For the determination of plasmid size and quality, 5  $\mu$ l of plasmid together with 2  $\mu$ l loading buffer was checked by agarose gel electrophoresis. In addition, the concentration and quality of plasmid were also measured by NanoDrop 8000 spectrophotometer (NanoDrop, Wilmington, Delaware, USA) at 260/280 nm. An

aliquot of DNA plasmid was subjected to sequencing for conformation as described above; the rest was stored at -20 °C to be used for transfection.

### 3.2.3 Cell culture

Granulosa/Cumulus cells were cultured using standard protocol of cell culture (Gutierrez et al. 1997, Portela et al. 2010) with slight modification. In Brief, Bovine ovaries were collected from local abattoirs and transported to the laboratory in a thermoflask containing 0.9% physiological saline (0.9% NaCl), at 30-35 °C. Ovaries were placed in 70% EtOH for 30 seconds and then rinsed twice with 0.9% physiological saline, for surface sterilization. Granulosa cells were harvested from follicular fluid by aspiration in 50 ml falcon tube containing 10 ml TCM media. Cells debris was allowed to settle down and upper liquid part was taken in 15 ml falcon tube and centrifuged at 250x g for 4 minute. The pellet containing cells were collected and the supernatant was discarded. The pellet was resuspended in 4 ml in Dulbecco Modified Eagle Medium (DMEM), sodium bicarbonate (10 mmol/L), sodium selenite (4 ng/mL), bovine serum albuminates.(BSA), (0.1%; Sigma-Aldrich), penicillin (100 U/mL), streptomycin (100 mg/mL), transferrin (2.5 mg/mL) without FCS. Where as cumulus cells were collected by vortexing the COC in 500 µl tissue culture medium (TCM) 199 supplemented with 0.1% BSA (A- 3311, Sigma), 0.2 mM pyruvate and 50 µg/ml gentamycin sulphate (Sigma) for 4 minute and were washed 3 times in DMEM containing penicillin/streptomycin (200 U/mL) and fungizone (100 mg/mL). Cells were resuspended in Dulbecco Modified Eagle Medium (DMEM), sodium bicarbonate (10 mmol/L), sodium selenite (4 ng/mL), bovine serum albuminates.(BSA), (0.1%; Sigma-Aldrich), penicillin (100 U/mL), streptomycin (100 mg/mL), transferrin (2.5 mg/mL), 10% FCS, with essential and nonessential amino acid. Viability of freshly harvested cells was 40%–50%, estimated by 0.4% trypan blue staining (Sigma). Cultures were maintained at 37 °C in 5% CO<sub>2</sub> in air by changing medium every 2 days. After 16 hours of culture the medium should be changed to remove red blood corpuscles. Cells were cultured according to their demand in each experiment. All experiments were conducted in primary cells and miRNA target validation at between 2-3 passage cells.

According to Sutton et al. (2003) the metabolic activities of cumulus and granulosa cells were unaffected by the presence or absence of bovine oocytes so all the experiments for cumulus and granulosa cells were performed without co-culture with oocytes.

### 3.2.4 Transient transfection

Prior to transfection the cultured cells were washed twice with perwarmed DPBS or phosphate saline buffer (PBS) without calcium and magnesium supplemented and transfection was performed for several different experiments:

1. Validation of miRNA target: The cumulus cells ( $8 \times 10^4$  cells/ well) were seeded in DMEM medium with 10% FCS in 24 wells plate and incubated at 37 °C in 5% CO<sub>2</sub> air for 24 hours prior to transfection. At more then 80% confluence, cells were co-transfected with construct DNA at final concentration of 800 ng /ml and miR-130b precursor, inhibitor or scramble control (30 pmole/ml) with 2 µl/ml Lipofectamine 2000 reagent (Invitrogen) according to the manufacturer's instructions. In brief, cultured cells of 2-3 passage were washed twice in pre warmed DMEM without FCS and penicillin/streptomycin. 200 µl of prewarmed Opti-MEM medium IX Reduced Serum Media was added and placed into the incubator, meanwhile in RNase-free tube 50 µl/well Opti-MEM medium was taken with DNA or RNA and in other tube mix was prepared with 1 µl Lipofectamine and 50µl/well medium. Both mixes were incubated for 5 minute and combined together to mix with each other. Prepared mix was incubated at RT for 20 minutes then 100 µl of mix was distributed to each well accordingly and the total volume for per well was made upto 500 µl. Transfected cells were incubated for 5 hrs at 37 °C in a humidified, 5% CO<sub>2</sub> incubator. After 5hrs of incubation the transfected cells were washed twice in pre warmed DMEM without FCS and 500 µl of DMEM with 10% FCS was added.

Cell Lysate preparation: After 48 hours of transfection 5X Passive Lysis Buffer (PLB Promega) was thawed and 1X PLB was prepared in distilled water. The cells were taken from incubator and media was aspirated. Cells were gently washed with PBS and 100 µl of 1X PLB was added to each well and gently shaken for 15 minutes at room temperature. After centrifugation the pellet was discarded and buffer with protein was either directly analyzed or stored in -20 °C for luciferase assay.

2. Cumulus cells were separated from oocytes and cultured as described above. For the effect of miR-130b in cumulus and granulose cells the transfection was preformed after 16 hrs of culture with miR-130b (precursor or inhibitor) and lipofectamin 2000 as described above but without any plasmid DNA. The cells were harvester after 24 and 48

hours for RNA and protein analysis respectively. The cells were collected in RIPA buffer with 1% protease inhibitor (Sigma) for protein analysis.

3. Cell proliferation assay was conducted using Growth Detection Kit MTT (Sigma) as described by manufacturer. In brief, primary granulosa/cumulus cells were seeded in 96 wells plate in the concentration of  $7.5 \times 10^4$ /ml. For standard curve generation cells were seeded as shown in table 5. The transfection process was same as described above.

4. For glycolysis assay granulosa and cumulus cell were cultured as described by Sutton et al. 2003 with slight modification. Primary granulosa and cumulus cells were co-cultured ( $2 \times 10^5$  cells /ml in 24 wells plate) in Dulbecco Modified Eagle Medium (DMEM), sodium bicarbonate (10 mmol/L), sodium selenite (4 ng/mL), bovine serum albumin (BSA), (0.1%; Sigma-Aldrich), penicillin (100 U/mL), streptomycin (100 mg/mL), transferrin (2.5 mg/mL), 10% FCS, with essential and nonessential amino acid. 16 hrs post seeding transfection was performed in serum free medium as mentioned above. 24 hrs post transfection medium was collected directly and the cells were washed twice in PBS and homogenized in the assay buffer. The cell lysate was centrifuge to remove the insoluble materials and stored in  $-80^\circ\text{C}$  until use.

5. For cholesterol assay granulosa cells were cultured same as for glycolysis (mentioned above). 16 hrs post seeding transfection was performed in serum free medium. After 24 hrs of transfection media was collected and the cells were washed twice in PBS and collected. After centrifugation PBS was discarded and 1:2 Methanol: chloroform was added to 20 volumes for cells and 6 volumes for medium and homogenized strongly. The homogenate was, then centrifuged at  $800 \times g$  for 3 minutes and lower phase was collected. The solution containing lipids were dried in vacuum dry (Savant SpeedVac) and stored in  $-80^\circ\text{C}$  upto use.

Table 5: The number of cells taken per millilitre medium to generate standard curve for cell proliferation assay using MTT.

	Cells /ml	Media in 96wells plate
1.	$8 \times 10^5$	100 $\mu$ l
2.	$4 \times 10^5$	100 $\mu$ l
3.	$2 \times 10^5$	100 $\mu$ l
4.	$1 \times 10^5$	100 $\mu$ l
5.	$5 \times 10^4$	100 $\mu$ l
6.	$2.5 \times 10^4$	100 $\mu$ l
7.	$1.25 \times 10^4$	100 $\mu$ l
8.	$6.25 \times 10^3$	100 $\mu$ l

For the experiment cells taken  $2.5 \times 10^4$ /well, with 50 nM/well miRNA concentration

### 3.2.5 Target validation

MicroRNA targets a number of mRNA in biological system but it always depends on the expression of gene and the cell type where the miRNA and the gene can express. To clarify it we use the cumulus cells as model cell and computational prediction and experimental validation was carried out.

#### 3.2.5.1 miRNA target prediction and site selection

The predicted targets are annotated in miRBase (<http://www.microrna.sanger.ac.uk>) bioinformatic tools namely PicTar (<http://www.pictar.org>), miRanda ([www.microrna.org/microrna/home.do](http://www.microrna.org/microrna/home.do)) and TargetScan (<http://www.targetscan.org>) (Griffiths-Jones 2004, Grun et al. 2005, Lewis et al. 2005). The selected bovine mRNA was uploaded on the software miTarget (<http://cbit.snu.ac.kr/~miTarget/>) which give the support vector machine (SVM) score for the target site (Kim et al. 2006). For constructing the vector mRNA secondary structure was also kept in mind and analyzed by Mfold (Zuker 2003). By selecting the appropriate site, the primers were designed with restriction enzymes (PmeI and XhoI) for all the genes. Partial segments (200–600 nucleotides) of the mRNA 3' untranslated region (UTR) containing the miR-130b-binding sequences shown in table 8 were PCR amplified from genomic DNA of bovine. Gene Ontology (<http://www.geneontology.org>) analysis of miRNA target genes was performed in order to predict the possible biological processes and functions.

### 3.2.5.2 DNA constructs

Validation of mRNA as a target of miRNA was done by pmirGLO Dual-Luciferase miRNA Target Expression Vector (Cat.No. E1330, Promega). Although the vector was not yet been published even it was selected because of its dual nature of expression of luciferase. It had firefly as well as renilla expression genes in the same vector which minimize the transfection difference in primary cell system. The amplicons were cloned to the downstream of firefly which have the human phosphoglycerate kinase promoter and renilla with the promoter of SV40 in the same backbone of vector. The pmirGLO Dual-Luciferase miRNA Target Expression Vector is designed to quantitatively evaluate microRNA activity by the insertion of miRNA target sites to 3'UTR of the firefly luciferase gene. This vector is based on Promega dual-luciferase technology with firefly luciferase used as the primary reporter to monitor mRNA regulation and Renilla luciferase acting as a control reporter for normalization and selection.

### 3.2.5.3 Reporter assays and preparation of luminometer

Either the freshly prepared lysate or frozen lysate was taken for luminofluorescent assay. The luminescent activity of each sample was measured in an Opticom II luminometer (Bretford Instruments) using Dual-Luciferase reporter assay as advised by the manufacturer. In brief, 20 µl of cell Lysate was taken in each well of 96 wells plate, where untransfected cell lysate was used as blank. The instrument was set with injector 1 and 2 to dispense 100 µl of LAR II and Stop & Glo reagent respectively. For measurement, using 2 second premeasurement delay and 10 second integration to detect luciferase for both reagents. Firefly luciferase activity was normalized by dividing renilla luciferase activity. All luciferase values represent average SD format with performing minimum quadruplicate transfections using SAS software.

Injectors were prepared by placing 50 ml Falcon tubes containing ddH<sub>2</sub>O to both the injectors and from the program WASH INJECTORS (1, 2) was selected with (30 injections) and OK. Continued with 70% EtOH PRIME and left the EtOH for 30 minutes. Then washed with ddH<sub>2</sub>O (30 injections). As mentaioned above the reagents were plased accordingly to injector 1 and injector 2. After the completion of detection the luminometer was washed same as the preparation and the water was returned out to dry the injector before leaving it.



### 3.2.6 Microinjection

#### 3.2.6.1 Design and synthesis of precursor, inhibitor and scramble RNA

All the synthetic miRNA- precursors and inhibitors for miR-130b (pre-mir-130b and anti-miR-130b) and scramble miRNA were purchased by company from Ambion, USA. Precursors are double stranded miRNA resemble the precursor stem-loop of miRNA, where inhibitors are single stranded miRNA that makes perfect complementary to mature miR-130b and scramble control was the sequence of miRNA which don't target any annotated genes used as negative control.

#### 3.2.6.2 Preparation of miRNA for injection

RNA was prepared to perform microinjection. 50  $\mu$ M of miRNA precursor or inhibitor or scramble were mixed separately with 1% of Fast green (F7258, Sigma) to give the final concentration of 45  $\mu$ M of miRNA and 0.1% fast green in a safe-lock eppendorf tubes using epT.I.P.S single tips. The mix were mixed well and centrifuged before injection. Fast green was used for the injection control.

#### 3.2.6.3 Microinjection of oocytes

Competent oocytes were selected on the bases of cumulus compactibility. Once the oocytes were selected, the cumulus cells were partially removed by vortexing to avoid technical difficulties during microinjection. Stripping of cumulus cells was done by vortexing the COC in 500  $\mu$ l phosphate saline buffer (PBS) without calcium and magnesium supplemented with 1 mg/ml hyaluronidase (H-2251, Sigma) for 4 minutes. Then, oocytes were kept in a tissue culture medium (TCM) 199 supplemented with 0.1% BSA (A- 3311, Sigma), 0.2 mM pyruvate and 50  $\mu$ g/ml gentamycin sulphate (Sigma) having humidified atmosphere with 5% CO<sub>2</sub> at 39 °C until it was used. Prior to injection, immature oocytes were incubated for 20 minutes in TCM-199 medium supplemented with cytochalasin B (8  $\mu$ g/ml) was used to reduce the mechanical damage during injection (Paradis et al. 2005). As mentioned above, the immature oocytes were categorized into four groups namely: miR-130b precursor, miR-130b inhibitor and scramble injected with control uninjected group. Microinjection was performed on an inverted microscope (Leica DM-IRB) at 200x magnification. The group of 50-60

immature oocytes were placed in a 10  $\mu$ l droplet of HEPES-buffered tissue culture medium 199 (H-TCM) supplemented with 8  $\mu$ g/ml cytochalasin B under mineral oil. Injection was performed by aspiration of the miR-130b precursor, inhibitor, and scramble into the separate injection capillary (Cook, Ireland, K-MPIP-3335-5). The inner diameter of the injection capillary was 5  $\mu$ m. The injection volume of  $\sim$ 7 pl (picoliter) was estimated from the displacement of the meniscus of mineral oil in the capillary (Nganvongpanit et al. 2006). The different experimental groups were injected one after the other.

Subsequently, in each injection for three experimental replications, a total of 400 immature oocytes were categorized for each group: miR-130b precursor injected (n = 100), inhibitor injected (n = 100), scramble injected (n = 100) and uninjected control (n = 100) in each injection. Likewise, at least 6 injections have been performed for different analysis. After microinjection all groups of oocytes were washed twice in TCM-199 and set back into culture (in 3.2.1.4). After 3-4 hours the oocytes degenerated due to mechanical injury were separated and remaining oocytes were kept for further culture.

#### 3.2.6.4 Microinjection of zygotes

For the injection in zygote the *in vitro* fertilized zygotes (3.2.1.3) were selected and grouped into 3 about 100 each. Zygotes were placed into injection medium (HTCM) for injection with miR-130b precursor, inhibitor or scramble with an uninjected control. Microinjection was performed on an inverted microscope (Leica DM-IRB) at 200x magnification same as described in (3.2.6.3). After injection all groups of zygotes were washed twice in CR1aa medium and set back into culture in (3.2.1.4). The zygotes were checked for survival 3-4 hr after injection. For this experiment, zygotes were produced and injected in the category of miR-130b precursor (100), inhibitor (100) and scramble (100) with uninjected control (n = 100) for each injection.

### 3.2.7 Oocytes and embryos collection

In order to calculate the effect of miR-130b the oocytes and embryos were collected after specific time of treatment to analyze mRNA and protein using real-time quantitative PCR and western blotting analysis, respectively. Immature oocytes were cultured and collected after 22 hours of microinjection to observe the role of miR-130b in oocyte maturation. Zygotes were injected with miR-130b precursor, inhibitor or scramble RNA and uninjected controls were cultured *in vitro* until day 8 blastocyst stages to assess development and resulting blastocysts from each treatment group were collected for mRNA and protein analysis to determine the role of miR-130b in preimplantation embryo formation. Prior to freezing, all oocytes and embryos were washed twice with PBS (Sigma) and treated with acidic Tyrode pH 2.5-3 (Sigma) to dissolve the zona pellucida. The zona free embryos were further washed two times in drops of PBS and frozen in cryo-tubes containing minimal amounts of lyses buffer with 1% protease inhibitor (Sigma). Until used for RNA isolation (in 3.2.8) or western blotting (in 3.2.13), all embryos were stored at -80 °C.

### 3.2.8 RNA isolation and cDNA synthesis

Total RNA containing microRNAs was isolated from three independent pools of immature and *in vitro* matured oocytes, corresponding cumulus cells, *in vitro* produced embryos: zygote, 2-cell, 4-Cell, 8-cell, morula, blastocyst and cultured (granulosa and cumulus) cells (Table 6) using miRNeasy mini kit (Qiagen, Hilden, Germany) following manufacturer's protocol. In brief, cells or gametes of embryos were homogenated nicely using 700 µl chilled QIAzol Lysis Reagent and incubated at room temperature (RT) for 4-5 minutes. Then to the homogenate 140 µl chloroform was added and mixed gently and centrifuged at 12,000x g for 15 minutes at 4 °C after a short incubation at RT. Here, after the upper aqueous phase was collected in a new tube and remaining down phase was stored at -20 °C for protein extraction. 1.5 volumes of 100% EtOH was added to the aqueous phase and pipetted to spin columns to centrifuge. The further procedure was followed by washing and oncolumn DNA digest using RNase-free DNase (Qiagen). The total RNA was eluted with 30 µl of RNase free water. Total RNAs were assessed by NanoDrop 8000 spectrophotometer (NanoDrop, Wilmington, Delaware, USA). Total RNA isolation from injected oocytes, blastocysts and transfected cells was performed

by same method using miRNeasy mini kit (Qiagen, Hilden, Germany). Total number of embryos and cells was shown in table 6. Total RNAs (containing miRNA) was reverse transcribed using a miScript reverse transcription kit (Qiagen, Hilden, Germany) as described by manufacturer's protocol. In brief, 4  $\mu$ l of 5X miScript RT Buffer (Includes  $Mg^{2+}$ , dNTPs, and primers) was taken in PCR strips and miScript Reverse Transcriptase Mix (1  $\mu$ l) was added to it. Template RNA was made to the final concentration of 200 ng with RNase-free water. Total reaction mix (20  $\mu$ l) was incubated for 60 minutes at 37 °C and the mix was inactivated at 95 °C for 5 minutes and place immediately on ice. After synthesis, the cDNA was either used immediately or stored in -20 °C.

Table 6: Samples and amount taken for RNA isolation

RNA Isolation	Groups	No. per replicate
Oocyte	Immature and mature	100
Embryos	Zygote, 2-cell	100
Embryos	4-cells	75
Embryos	8-cells	50
Embryos	Morula, Blastocyst	30
Cells	IMCC, MCC, GC	$1.0 \times 10^6$
Injected oocytes (after maturation)	Precursor, Inhibitor, Scramble, Uninjected	100-120
Zygote injected (Blastocyst)	Precursor, Inhibitor, Scramble, Uninjected	30
Transfected cells	Precursor, Inhibitor, Scramble, Untransfected	$1.0 \times 10^6$

IMCC: immature cumulus cells, MCC: mature cumulus cells, GC: granulosa cells, No.: Number.

### 3.2.9 Expression profile of miRNA using qRT-PCR

For the detection of miRNA real-time RT-PCR was carried out in an ABI Prism® 7000 SDS instrument based on the changes in fluorescence proportional to the increase of product. SYBR® Green, which emits a fluorescent signal upon binding to double stranded DNA, was used as a detector. Fluorescence values were recorded during every cycle representing the amount of product amplified to a point known as threshold cycle

(Ct). The higher the initial transcript amount, the sooner accumulated product was detected in the PCR. Triplicate reactions were performed for each miRNA to quantify the abundance of miRNA in each sample with miRscript SYBR Green PCR kit (Cat: 218073, Qiagen, Valencia, CA). miRNAs are amplified using the miScript Universal Primer together with the miRNA-specific primer (the miScript Primer Assay). Mature miRNA-specific primers were purchased from (Qiagen) and the universal reverse primer provided by the manufacturer. In brief, real-time PCR was performed using 2.5  $\mu$ L template cDNA with 12.5  $\mu$ L of SYBRGreen mix, 10X miScript Universal Primer and 10X miScript Primer Assay in 25  $\mu$ l of final volume. The thermocycler was set at 50 °C for 2 seconds, 95 °C for 10 min, followed by 40 amplification cycles at 95 °C for 15 seconds and at 60 °C for 1 minute. At the end of the last cycle, dissociation curve was generated by starting the fluorescence acquisition at 60 °C following standard protocol of the manufacturer in 7000 Real Time PCR system (Applied Biosystem, USA) and the Ct were calculated using Sequence Detection Software (SDS v1.2.1, Applied Biosystem, USA) using normalization to the geometric mean of U6 and Snod48 snRNA. Fold change was calculated as compared with the calibrator after normalization of the transcript level to the endogenous control, following the  $2^{-\Delta\Delta Ct}$  method (Livak and Schmittgen 2001). All experiments were conducted in triplicate.

### 3.2.10 Quantitative real-time PCR analysis for mRNA

Quantitative RT-PCR was performed for mRNAs using gene-specific primers and iTaq SYBR Green Supermix with ROX (Bio-Rad laboratories, Munich, Germany) in ABI Prism 7000 apparatus (Applied Biosystems, Foster City, CA). The detection was done by emission of fluorescent signal when amplification starts with primer extension. The higher the initial transcript amount, the sooner accumulated product was detected in the PCR. Prior to quantification, the optimum primer concentration was performed with different combinations of primer from 200 nM to 600 nM. Among then the lowest threshold cycle and minimum non-specific amplification was selected for subsequent reaction. After selection of primer concentration, a final assay consisted of 2  $\mu$ l cDNA as template, up and downstream primers and SYBR Green Universal PCR Master Mix containing SYBR Green I Dye, AmpliTaq Gold DNA polymerase, dNTPs with dUTP, passive reference and optimized buffer components were performed in a total volume of

20  $\mu$ l reaction. The PCRs were performed in 20  $\mu$ l reaction volumes containing 10  $\mu$ l SYBR Green universal master mix (Sigma) and 2  $\mu$ l of template cDNA. A universal thermal cycling parameter (initial activation step at 95 °C for 3 min, 45 cycles of denaturation at 95 °C for 15 s and 60 °C for 45 s) were used to quantify each gene of interest. After the end of the last cycle, a dissociation curve was generated by starting the fluorescence acquisition at 60 °C. Genes of each group was quantified in comparison with geometric mean of GAPDH and Histone as endogenous control. The list of primers was indicated in (Table 3). Standard curves were generated for all genes and endogenous control genes using serial dilution of plasmid DNA ( $10^1$ – $10^9$ ) molecules. To determine the relative abundance of transcripts as fold change compared to the calibrator sample. Finally quantitative analysis was done using the relative standard curve method and results were reported as the relative expression or fold change as compared to the calibrator after normalization of the transcript level to the endogenous control. The quantification of genes was performed based on the relative standard curve method. The relative expression data were analyzed using General Linear Model (GLM) of the Statistical Analysis System (SAS) software package version 9.2 (SAS Institute Inc., NC, USA). Differences among the mean values were tested using ANOVA followed by a multiple pair wise comparison using *t*-test. A probability of  $P \leq 0.05$  was considered to be expressed with significant difference.

### 3.2.11 Localization of miRNA in ovary and embryos

Whole mount in situ hybridization of miRNAs was conducted with at least 5 COC or *in vitro* produced embryos (zygotes, 2-cell, 4-cell, 8-cell, morula and blastocyst) of each stage were taken. The embryos were collected and washed twice in PBS then fixed overnight in 4% paraformaldehyde. For hybridization embryos were rehydrated in series of methanol/PBS. Acetylation (2.33 ml triethanolamine, 500  $\mu$ l acetic anhydride, H<sub>2</sub>O up to 200 ml, readily prepared and treated for 10 minutes) and proteinase K treatment (10  $\mu$ g/ml, 10 minutes) were performed with 3 times brief washing (10 minutes) in PBS for each step. Two hours of pre-hybridization was performed at 52 °C in hybridization solution (50% formamide, 5 $\times$  SSC, 0.1% Tween-20, 50  $\mu$ g/ml heparin, and 500 mg/ml yeast tRNA). Embryos were incubated overnight with 3'-Digoxigenin (DIG) labeled LNA-modified oligonucleotide probes (1 pM) for miR-130b and scramble RNAs

(Exiqon, Vedbaek, Denmark) in hybridization buffer in a humidified chamber at the temperature 20 °C below the  $T_m$  of probes. After overnight incubation, embryos were washed briefly in wash buffer (similar to hybridization buffer but without tRNA) and serial wash in 2X SSC/wash buffer (each time 10 minutes) to final three washes in 0.2X SSC each for 30 minutes at hybridization temperature was performed. Blocking, incubation with anti-DIG-AP antibody, washing and color development (Fast Red substrate reaction) was performed as described previously (Obernosterer et al. 2007). Embryos were mounted individually with VectaShield containing DAPI (Vector laboratories, Burlingame, CA) and analyzed by confocal laser scanning microscope (CLSM LSM-510, Carl Zeiss, Germany).

Localization of miRNA in cryosections of ovary was performed with chopped ovary serially in 10  $\mu$ m sections at -20 °C using rapid sectioning cryostat (Leica microsystem Nussloch GmbH, Heidelberg, Germany) which were prior embedded in Tissue-Tek (Sakura Finetek Europe, Zoeterwoude, Netherlands). The sections were mounted on poly-L-lysine coated slides (Menzel GmbH & Co. KG, Braunschweig, Germany) then directly fixed in 4% (w/v) paraformaldehyde in PBS for 15 minutes at room temperature. The fixed specimens were washed three times in PBS for 5 minutes of each. The sections were incubated in an ascending alcohol series of 50%, 70%, 90% and 100% EtOH (v/v) for 5 minutes each (prepared fresh in DEPC-treated H<sub>2</sub>O), followed by a descending alcohol series of 90%, 70%, 50% EtOH (v/v) for 5 minutes each, respectively. The sections were washed in 1X PBS for 5 minutes, blocked in 0.6% (v/v) H<sub>2</sub>O<sub>2</sub> diluted in 1X PBS for 1 hour washed twice with 1X PBS for 5 minutes of each. The acetylation was performed by incubation of sections in 0.1 M TEA buffer with 0.25% acetic anhydride for 10 minutes. The samples were equilibrated in 2X SSC for 10 minutes. Blocking, incubation (with anti-DIG-AP antibody), washing and color development with Fast Red substrate reaction were performed as described previously (Obernosterer et al. 2007). Specimen were mounted with VectaShield containing DAPI (Vector laboratories, Burlingame, CA) and analyzed by confocal laser scanning microscope (CLSM LSM-510, Carl Zeiss, Germany).

### 3.2.12 Protein detection in oocyte and ovary cryosection

The ovarian sections were taken from the same serial number taken for miR-130b detection. The specimens were brought to room temperature for 10 to 15 minutes to dry

and washed twice in PBS for 5 minutes then fixed in 4% (w/v) paraformaldehyde in PBS for 45 minutes at room temperature. The slides now were permeabilized with 0.2% (v/v) Triton-X100 (Sigma) in PBS for 5 minutes and washed thrice in PBS. Non-specific binding was minimized by blocking in 3% (w/v) bovine serum albumin (BSA) in PBS for 1 hr at 37 °C. Meanwhile, anti-SMAD1/5 (1:100) and anti-MSK1 (1:100) were prepared in 0.3% (w/v) BSA in PBS and covered over tissue section and were incubated overnight at 4 °C. To remove the unbound primary antibody specimens were washed three times with PBS. Secondary antibody fluorescein (FITC)-conjugated goat anti-rabbit antibody (Sigma) and fluorescein (FITC)-conjugated donkey anti-goat antibody (Abcam) in 0.3% (w/v) BSA /PBS with dilution 1:100 used for 1 hr at 37 °C and negative controls were processed in the same manner by omitting the primary antibody. The specimen were washed three times with PBS and mounted with VectaShield containing DAPI (Vector laboratories, Burlingame, CA) and analyzed by confocal laser scanning microscope (CLSM LSM-510, Carl Zeiss, Germany).

For the detection of protein in COCs and oocytes atleast 20 COCs or oocytes were taken. After washing with PBS with PVA the specimen were fixed in 4% paraformaldehyde overnight at 4 °C. The COCs or oocytes were washed in Glycin-PBS (G-PBS) for twice and permeabilized with 0.5% (v/v) Triton-X100 (Sigma) in PBS for 2 ½ hrs at room temperature. The washing was continued for three times with PVA in PBS. The samples were blocked in 3% (w/v) bovine serum albumin (BSA) with 0.3% (v/v) donkey serum in PBS for 1 hr at 37 °C. The primary antibody was prepared in 10 times diluted blocking solution with anti-SMAD1/5 (1:100) or anti-MSK1 (1:100). COCs and oocytes were incubated overnight with primary antibody at 4 °C. Unbound antibody was removed by washing with G-PBS three times. Secondary antibody fluorescein (FITC)-conjugated goat anti-rabbit antibody (Sigma) and fluorescein (FITC)-conjugated donkey anti-goat antibody (Abcam) in ten times diluted blocking solution with dilution 1:100 prepared. COCs and oocytes were incubated for 1 hr at 37 °C and negative controls were also processed but without primary antibody. The COCs and oocytes were washed three times with PBS and mounted with VectaShield containing DAPI (Vector laboratories, Burlingame, CA) and analyzed under confocal laser scanning microscope (CLSM LSM-510, Carl Zeiss, Germany).



### 3.2.13 Western blot

#### 3.2.13.1 Protein extraction

As the injected embryos were limited the total RNA and protein were isolated with the same sample. Protein was extracted using miRNeasy mini kit (Qiagen, Hilden, Germany) from the embryos after the isolation of total RNA, although the adapted protocol was not mentioned by manufacturer. As per the manufacturers protocol the upper aqueous phase used for RNA isolation and the lower, red, organic phase was discarded. But here, the lower phase was been collected and proceeded for protein isolation. To the lower organic phase 150  $\mu$ l of 100% EtOH was added and allowed to stand for 2 to 3 minutes at room temperature then centrifuged at 12,000x g for 5 minutes. After centrifugation the supernatant was transferred to a new 2.0 ml tube and 750  $\mu$ l of isopropanol was added then allowed to stand 10 minutes at room temperature followed by centrifugation at full speed for 10 minutes. The protein pellet was washed three times in 1 ml of 0.3 M guanidine hydrochloride prepared in 95% EtOH solution and each wash had an incubation period of 20 minutes at room temperature and then was centrifuged at 7,500x g for 5 minutes. Afterward again three times washing was preformed with 100% EtOH. 1 ml of 100% EtOH was added and the mixture was allowed to stand for 20 minutes continued with centrifugation at 7,500x g for 5 minutes (all centrifuge was at 4 °C). Finally, the protein was air dried and dissolved in 200  $\mu$ l of sample buffer containing 1% protease inhibitor cocktail and stored at -20 °C for westernblot analysis. The transfected cultured cells 48 hours post transfection were washed two times with PBS without calcium and magnesium supplemented and 100  $\mu$ l RIPA buffer (Sigma) was added with 1% protease inhibitor cocktail (Sigma) and whole cells lysate was vortex by incubating on ice. The lysate was centrifuged and supernatant was collected as protein and stored at -20 °C for westernblot analysis.

#### 3.2.13.2 Protein separation and transfer

The protein loading buffer was added to each sample and was boiled at 95 °C for 5 minutes. Proteins were separated by 10% Polyacrylamide gel and then transferred onto nitrocellulose transfer membrane, pore size 0.45 mm (Whatmen Protran Nitrocellulos Membrane). The membrane was stained with Ponceau S to evaluate the transfer quality and blocked for 1 hr in 1X Roti-Block (Roth GmbH) with 1xTBS containing 0.1%

Tween-20. The membrane was then incubated at 4 °C overnight using the required antibody. The primary antibodies used were as follows, Rabbit polyclonal anti-RPS6KA5 (1:1000) (Acris Antibodies GmbH), goat polyclonal anti-SMAD1/5 (1:500), and goat polyclonal anti-GAPDH (1:500) (Santa Cruz Biotechnology) was prepared in 0.1X of Roti-Block buffer. After incubation with the primary antibody, the membrane was washed six times for 5 minutes in PBST and the hybridization with the appropriate secondary antibody at room temperature for 1 hour was performed. The horseradish-peroxidase (HRP) conjugated donkey anti-rabbit secondary antibody (Santa Cruz Biotechnology) and HRP-conjugated donkey anti-goat (Santa Cruz Biotechnology) were used with dilution factor 1:20000 in 0.1X Roti-Block buffer. The membrane was finally washed 6 times for 5 minutes in PBST. The protein and antibody binding was detected using the SuperSignal West Pico Chemiluminescent Substrate (Thermo Scientific) following the manufacturer's instructions and visualized using Kodak BioMax XAR film (Kodak) or BioRad (Germany).

#### 3.2.14 Mitochondrial assay

Mitochondrial probe detection was performed according to the manufacturer instruction. In brief, all groups of oocytes (miR-130b precursor or inhibitor or scramble and uninjected) were collected after 22hrs of injection and washed in maturation medium then incubated with 300 nM of mitochondrion-specific dye (MitoTracker® Mitochondrion-Selective Probes, invitrogen) for 10 minutes and washed thrice in maturation medium. After washing all oocytes were fixed with 4% paraformaldehyde for 30 minutes (Oubrahim et al. 2001) and washed three times in PBS for collecting the image on confocal laser scanning microscope (CLSM LSM-510, Carl Zeiss, Germany) at 579 nm to 599 nm wavelength.

This probe is cell-permeate mitochondrion-selective dyes which passively diffuse across the plasma membrane and accumulate in active mitochondria and remains associated with the mitochondria even after fixation.

#### 3.2.15 Cell proliferation assays

Cell proliferation was determined using a modified 3-(4,5-dimethyl-2-thiazolyl)-2,5-diphenyl-2H-tetrazolium, bromide (MTT) assay on live cells. As described in 3.2.12

cells were seeded in 96 wells plate and transfected 24 hours post seeding. MTT activity was assayed with Cell Growth Detection Kit (Sigma) according to manufacturer's instruction after 24 or 48 hours of treatment. In Brief, 24 hours and 48 hours post transfection the culture plate was taken and aseptically 10  $\mu$ l MTT SOLUTION was added in each well of culture and incubated 4 hours in incubator. Now the dead cells with media were removed carefully and 100  $\mu$ l of MTT SOLVENT was added to each well. Plate was gently stirring in a gyratory shaker in dark and the absorbance was read at 570 nm on a multiplate reader spectrophotometer (Molecular Device, Germany), with a 690 nm reference filter. All readings were taken within 30 minutes to 1 hrs and average was calculated. The  $\pm$ SEM (standard error of the mean) was calculated with the absorbance (OD) of the transfected wells with untransfected wells (Pregel et al. 2007). The viability of transfected cells were checked using (0.4%) Trypan Blue Solution (Sigma). The cells seeded by  $8 \times 10^4$  each well of 24 well plate and 50 nM of miR-130b precursor, inhibitor and scramble. After 24 hours and 48 hours of transfection the transfected cell were washed with were stained with tryphan blue solution and live cells were observed in haemocytometer under microscope (ECLIPSE TS100, Nikon).

### 3.2.16 Cholesterol assay

Primary granulose and cumulus cells were cultured in 24 wells plate in the concentration of  $2 \times 10^5$ /ml. The cells and the medium were dried stored at  $-80^\circ\text{C}$ . 1 hour prior to use the samples was resuspended in 1:1 Methanol: Chloroform solution with 20  $\mu$ l volume (Miah et al. 2011). 80  $\mu$ l Assay buffer was added to the solution from the EnzyChrom AF Cholesterol Assay Kit (E2CH-100). Further experiment was done according to the manufacturer. In brief, standard was prepared and 50  $\mu$ l of each standard and unknown samples were distributed in 96 will plate with about 5 replicates of each transfected group (precursor, inhibitor, scramble and control). Enzyme 1  $\mu$ l, Dye Reagent 1  $\mu$ l and Assay buffer 55  $\mu$ l pre well were mixed and aliquoted 50  $\mu$ l in each well. The plate was incubated at room temperature in dark for 30 minutes. Meanwhile, all setup was completed for the fluorescence reader. The reading was preformed with fluorescence at  $\lambda_{\text{ex}} = 530\text{nm}$  and  $\lambda_{\text{em}} = 585\text{nm}$ . Standard prepared with highest at 100 mg/dl, with different dilution and blank with 0.

$$\text{Cholesterol (mg/dL)} = [\text{F}_{\text{Sample}} - \text{F}_{\text{blank}}] / \text{Slope},$$

Where F stands for Fluorescent

### 3.2.17 Determination of glycolytic rate

The high glycolysis shows high metabolic activity. To determine the role of miR-130b in glycolysis the experiment was conducted using primary cell culture of granulosa and cumulus cell. The cells were transfected with 100 nM/ml of miR-130b precursor, inhibitor or scramble in 24 wells plate in serum free medium. After 24 hours of transfection the cells were collected in assay buffer and glycolytic rate was measured by using the Lactate Colorimetric Assay Kit (Abcam, Cambridge, MA, USA). All the reagents were preparation and stored as described by the manufacturer. Lactate assay was performed in 96 wells plate in multiplate reader (Molecular Device), The OD was taken at 450 nm and calibrated with untransfected cells. Standard was generated with assay buffer and provided standard from manufacturer, taken as: 0, 2, 4, 6, 8, and 10 nmol/well of the Lactate Standard. Plot was made with standard curve of nmol/well vs. OD 450 nm for the standard curve. Lactate concentrations were calculated for the test samples:

$$C = La/Sv \text{ (nmol/}\mu\text{l or mM)}$$

Where: La is the lactic acid amount (nmol) of the sample from standard curve. Sv is the sample volume ( $\mu\text{l}$ ) added into the well. Lactate concentration was normalized by sample cell number.

### 3.2.18 Statistical analysis

The general linear model procedure of General Linear Model (GLM) of Statistical Analysis System (SAS) version 9.2 was used to test the significant variation in the polarbody extrusion, cleavage rate, morula and blastocyst rates between the pre-miR-130b injected, anti-miR-130b injected, scrambled injected and uninjected oocytes or zygotes, cholesterol level, lactate concentration, cell proliferation in transfected cells and the list significant difference t-test was employed to separate means between all treatment groups. Moreover, the relative expression of miRNA and gene between the treatment groups was performed of t-test. A probability of  $p \leq 0.05$  was considered to be expressed with significant difference.

## 4 Results

### 4.1 Expression profile of miR-208 and miR-130b in oocyte and surrounding cells

The expression of miR-208 and miR-130b was performed in granulosa cells, mature and immature cumulus cells. U6 and Snord48 were used as endogenous control and Ct value was calculated. The results were according to figure 4. miR-130b was significantly high in granulosa cells and cumulus cells compared to miR-208 ( $p < 0.01$ ).

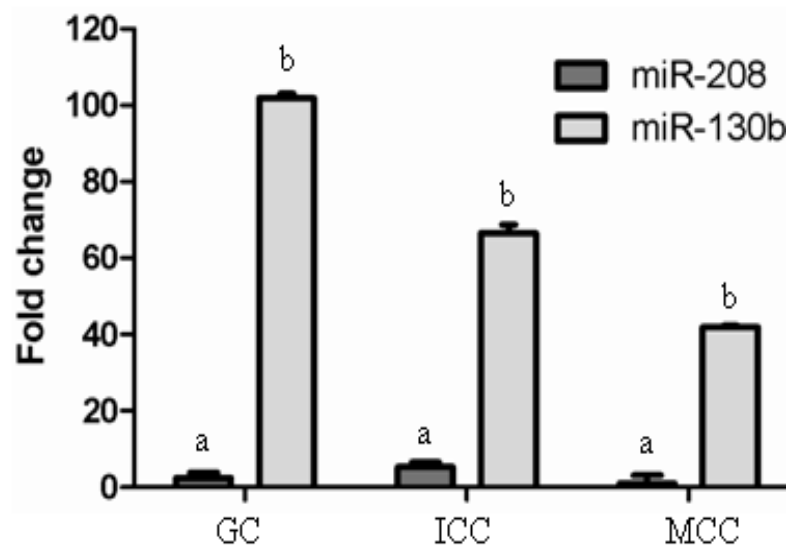


Figure 4: The expression profile of miR-130b and miR-208 in granulosa, immature cumulus and mature cumulus cells. The vertical axis indicates the fold change of miRNA using the minimum value as one and normalized to the geometric mean of U6 and Snod48. Error bars show each miRNA mean  $\pm$  SD. Significant differences (a:b –  $p < 0.05$ ). GC: granulosa cell; ICC : immature cumulus cell; MCC : mature cumulus cell.

### 4.2 The expression pattern of miR-130 family

MicroRNA miR-130 family shares same seed sequence and mostly have same targets. So, further, to verify the biogenesis of the miR-130 family members (miR-130a, miR-130b, miR-301a and miR-301b) *in silico* chromosomal analysis was performed. According to miRBase Version 15 database, miR-130b and miR-301b were located at chromosome 17 within 10kb and miR-130a and miR-301a were located at different

chromosomes of bovine genome (Table 7).

Table 7: List of microRNA in bta-mir-130 family and their similarity to bta-mir-130b.

miRNA	Acc No.	Family	Sequence	Ch	Sr (%)
<b>bta-miR-130b</b>	MIMAT0009224	<b>mir-130</b>	<u>CAGUGCAAUGAUGAAAGGGCAU</u>	17	100%
<b>bta-miR-130a</b>	MIMAT0009223	<b>mir-130</b>	<u>CAGUGCAAUGUAAAAGGGCAU</u>	15	90.9%
<b>bta-miR-301a</b>	MIMAT0009276	<b>mir-130</b>	<u>CAGUGCAAUAGUAUUGUCAAAAGCAU</u>	19	44%
<b>bta-miR-301b</b>	MIMAT0009277	<b>mir-130</b>	<u>CAGUGCAAUGAUAUUGUCAAAAGCAU</u>	17	48%

Acc No, Accession number; Ch, chromosomal location; Sr, similarity.

#### 4.2.1 Expression of miR-130 family in oocytes and surrounding somatic cells

After chromosomal localization of miR-130 family, the expression profiling was performed for the verification of transcription similarity in immature and mature oocytes and their surrounding cells (cumulus and granulosa). The expression profiling was conducted in triplicate using real time PCR and geometric mean of U6 and Snord48 was used as endogenous control. Accordingly, the expression result showed that the members of miR-130 family don't have any tendency to regulate in same pattern together (Figure 4.1- 4.2). The expression of miR-130b was significantly ( $p < 0.05$ ) high in granulosa and cumulus cells compared to other members of the miR-130 family (Figure 4.1).

The expression of miR-301a was the lowest in all cell type among the family members. miR-130a was about 3-fold high in immature cumulus cells and granulosa cells ( $p < 0.05$ ) when compared to mature cumulus cells. The expression of miR-301b was about 5-fold higher in granulosa cells compared to immature and mature cumulus cells ( $p < 0.05$ ). In granulosa cells miR-130a was 3-fold higher ( $p < 0.05$ ), miR-301b was 5-fold higher ( $p < 0.05$ ) and miR-130b was about 18-fold higher than compared to miR-301a ( $p < 0.05$ ). In immature cumulus cells miR-130a was 3-fold higher, miR-301b was 2-fold high and miR-130b was 13-fold higher ( $p < 0.05$ ) compared to 301a. Compared to all indicated miRNA miR-130b was significantly high in cumulus and granulosa cells. In mature cumulus cells miR-130a and miR-301a both expressed in low level where as miR-301b was 2-fold high compared to miR-301a ( $p \geq 0.05$ ). miR-130b was significantly high ( $p < 0.05$ ) with (> 12-fold) in mature cumulus cells compared to miR-301a (Figure 4.1).

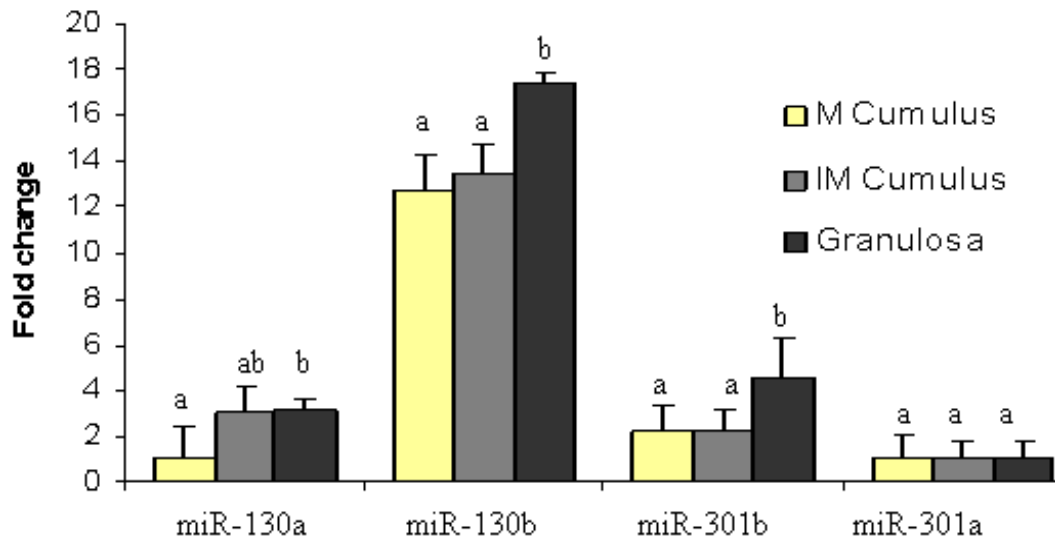


Figure 4.1: The expression profile of miR-130 family in granulosa cells, mature and immature cumulus cells. The vertical axis indicates the fold change of miRNA using the minimum value as one and normalized to the geometric mean of U6 and Snod48. Error bars show miRNA mean  $\pm$  SD. Significant differences (a:b –  $p < 0.05$ ). IM: immature; M: mature.

The expression pattern of miR-130 family in immature and mature oocytes showed that miR-301a was relatively low expressed in both oocyte groups. miR-301a and miR-130a were not differentially regulated in both immature and mature oocytes ( $p \geq 0.05$ ). Similarly, miR-301b was not differentially regulated in both mature and immature oocytes but 4-fold higher ( $p < 0.05$ ) than miR-301a. Whereas, miR-130b was significantly ( $p < 0.05$ ) higher compared to miR-301a in immature and mature oocytes. Coming to the comparison of miR-130 family in each group of oocyte, the expression of miR-301a was lowest in immature oocyte and used as calibrator. Whereas, miR-130a was 2-fold high, miR-130b was 10-fold ( $p < 0.005$ ) high and miR-301b was 5-fold high ( $p < 0.05$ ) compared to miR-301a in immature oocyte. And in mature oocyte miR-130a was 1.5-fold high and 130b was 5.5-fold ( $p < 0.05$ ), whereas, miR-301b was 5-fold higher ( $p < 0.05$ ) than miR-301a (Figure 4.2A). When miR-130b was compared among granulosa cells, cumulus cells, immature oocyte and mature oocyte, it was abundant in granulosa and cumulus cells with 59- and 54-fold respectively compared to mature oocytes ( $p < 0.001$ ) (Figure 4.2B). Additionally, when miR-130b expression compared

between immature and mature oocytes, it showed 2.8-fold high expression of immature than mature oocyte ( $p < 0.05$ ), as showed in figure 4.2B.

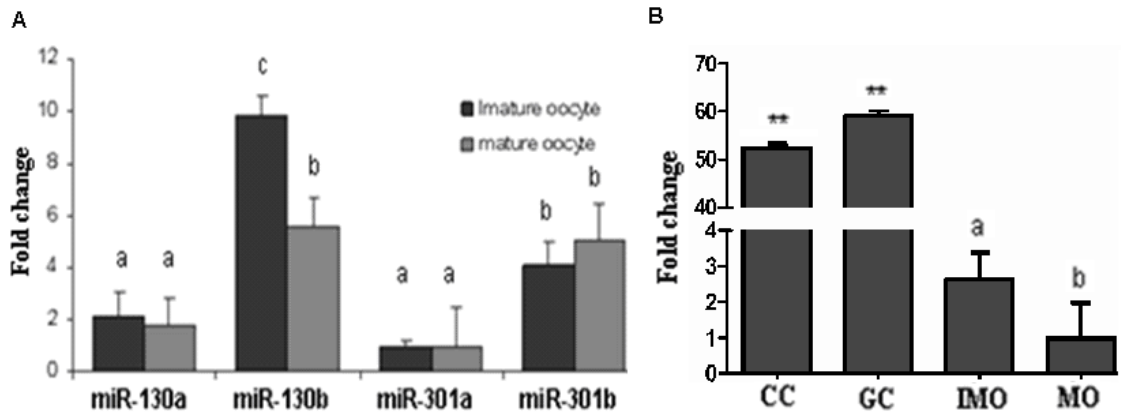


Figure 4.2: The expression pattern of miR-130 family in immature and mature oocytes (A), miR-130b across the cumulus cells, granulosa cells, immature and mature oocyte (B). The vertical axis indicates the fold change of miRNA using the minimum value as one and normalized to geometric mean of U6 and Snod48. Error bars show the miRNA mean  $\pm$  SD. Significant differences (a:b:c –  $p < 0.05$ ), and (\*\* $p < 0.001$ ). Significantly different (a:b:c –  $p < 0.05$ ) and (\*\* $p < 0.001$ ). GC: granulosa cell, CC: cumulus cell, IMO: immature oocytes, MO : mature oocytes.

#### 4.2.2 In situ detection of miR-130b in different stages of follicular cells

The expression of miR-130b was higher in granulosa and cumulus cells compared to oocyte, so further detection of miR-130b was conducted in different stages of follicular cells in ovarian section using 3'-digoxigenin labelled locked nucleic acid (LNA) microRNA probes and U6 was used as positive and scramble as negative controls. The in situ localization of miR-130b shows the detection of miR-130b in the granulosa cells, cumulus cells and oocytes of antral follicles in association with the early stages (preantral) follicles and other ovarian tissues (Figure 4.3).



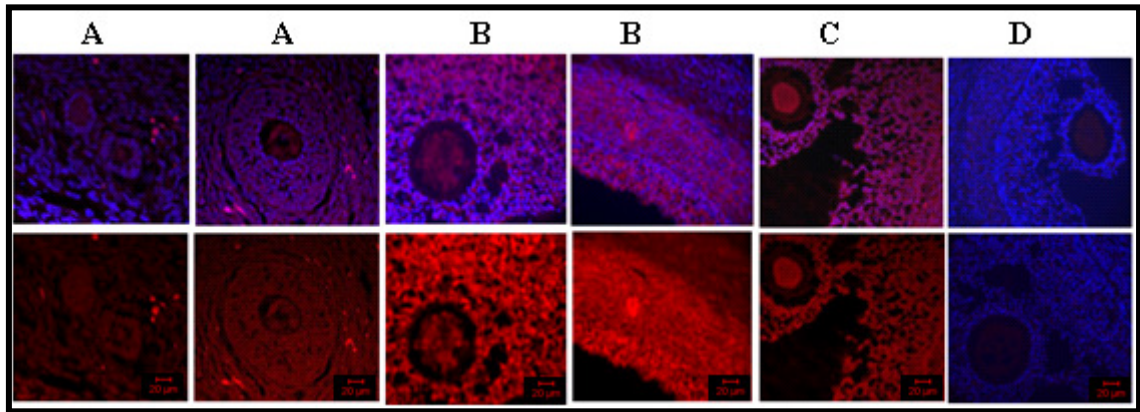


Figure 4.3: In-situ detection of miR-130b in the ovarian sections using 3'-digoxigenin labelled locked nucleic acid (LNA) microRNA probes for miR-130b, U6 and scramble miRNA. A and B: miR-130b, C: U6 (positive control) and D: scramble (negative control). A: preantral follicle, B, C and D: antral follicle, Red signal stands for miRNA (miR-130b, U6 and scramble) and blue signal represents nuclear staining, DAPI: 4',6-diamidino-2-phenylindole. Scale bar represents 20  $\mu\text{m}$ .

#### 4.2.3 The expression profiling of miR-130 family in preimplantation embryo

The expression pattern of miR-130 family was investigated in different stages of embryos (Zygote, 2-Cell, 4-Cell, 8-Cell, Morula and Blastocyst) using qRT-PCR with equal amount of cDNA for all stages of embryos. The experiment was performed in appropriate biological replicates and geometric mean of Snord48 and U6 were used as endogenous control. The result indicates the expression of each miRNA of miR-130 family was different at each stage. At the zygote stage, 301a was 1.5-fold higher compared to miR-130a. miR-130b was 4.7-fold higher where as miR-301b was 5.2-fold higher in association to miR-130a. At 2-cell embryo miR-130a was used as calibrator and expression of miR-130b, miR-301b and miR-301a were 2.4-fold, 2.5-fold and 2-fold high respectively. In 4-cell stage embryo, miR-130a, miR-130b and miR-301b were 2-fold, 13-fold and 17-fold high expressed respectively compared to miR-301a. At 8-cell embryo, miR-130a was 8-fold, miR-130b was 35-fold and miR-301b was 10-fold higher compared to miR-301a and the expression differences were significant ( $p < 0.05$ ) for all. At morula stage embryo, miR-301a and miR-130a were less expressed, where

as, miR-301b was 10-fold ( $p < 0.05$ ) higher and miR-130b was 87-fold ( $p < 0.001$ ) higher compared to miR-301a. Similarly, at blastocyst stage, miR-130a, miR-301a and miR-301b were expressed in low level but miR-130b was 60-fold higher ( $p < 0.001$ ) compared to miR-301a. However, when each miRNA of miR-130 family was compared across the preimplantation stage, the expression of miR-130a and 301a were limited through out preimplantation stage. Although, the expression of miR-130a was slightly increased in zygote, 2-cell, and 4-cell with 8-fold, 16-fold, and 6-fold respectively compared to the expression at blastocyst stage. Similarly, miR-301a was higher in zygote and 2-cell stage embryo compared to blastocyst stages embryo. Additionally, the expression patten of miR-301b was relatively higher in zygote, 2-cell and 4-cell ( $p < 0.05$ ) compared to blastocyst stage. Whereas, the expression of miR-130b was high throughout the implantation stage compared to other members of miR-130 family. However, the expression of miR-130b was comparatively low at zygote, 2-cell and 4-cell but increased after embryonic genomic activation. Expression of miR-130b at morula was 8-fold higher compared to zygote stage with significant difference ( $p < 0.05$ ) (Figure 4.4).

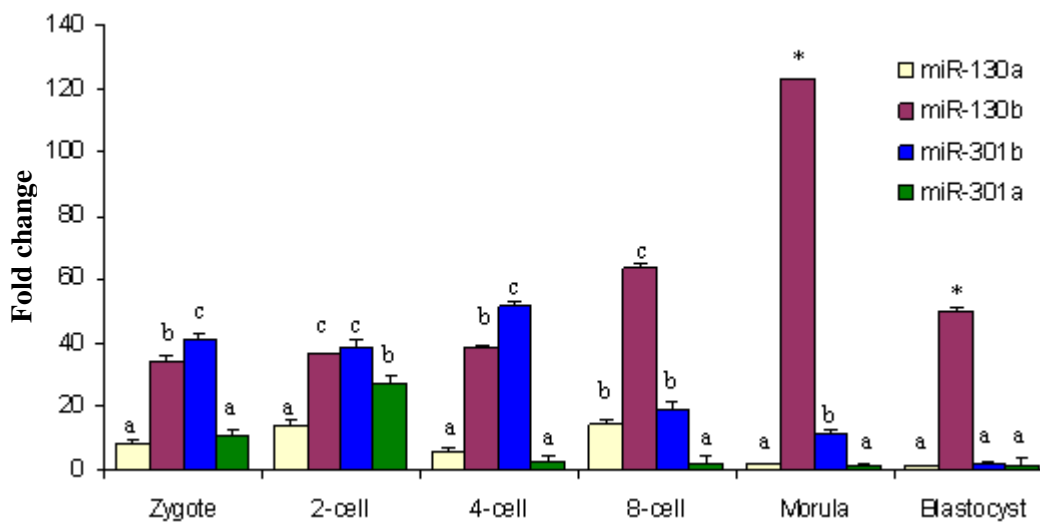


Figure 4.4: The expression pattern of miR-130 family across the preimplantation stage embryos. The vertical axis indicates the fold change of miRNA using the minimum value as one and normalized to the geometric mean of U6 and Snord48. Error bars show miRNA mean  $\pm$  SD. Significant differences (a:b:c –  $p < 0.05$ ), and (\* $p < 0.001$ ).

#### 4.2.4 In situ localization of miR-130b in preimplantation embryo development

The microRNA miR-130b was more imperative when compared to other family members as it shows the transcription at maternal as well as embryonic gene activation. Hence, this microRNA was further localization in all stages of embryos conducting Whole-mount in-situ detection. The result showed the high detection of miR-130b in the cumulus cells of mature and immature oocytes, immature oocytes and further at 8-cell, morula and blastocyst stage (Figure 4.5).

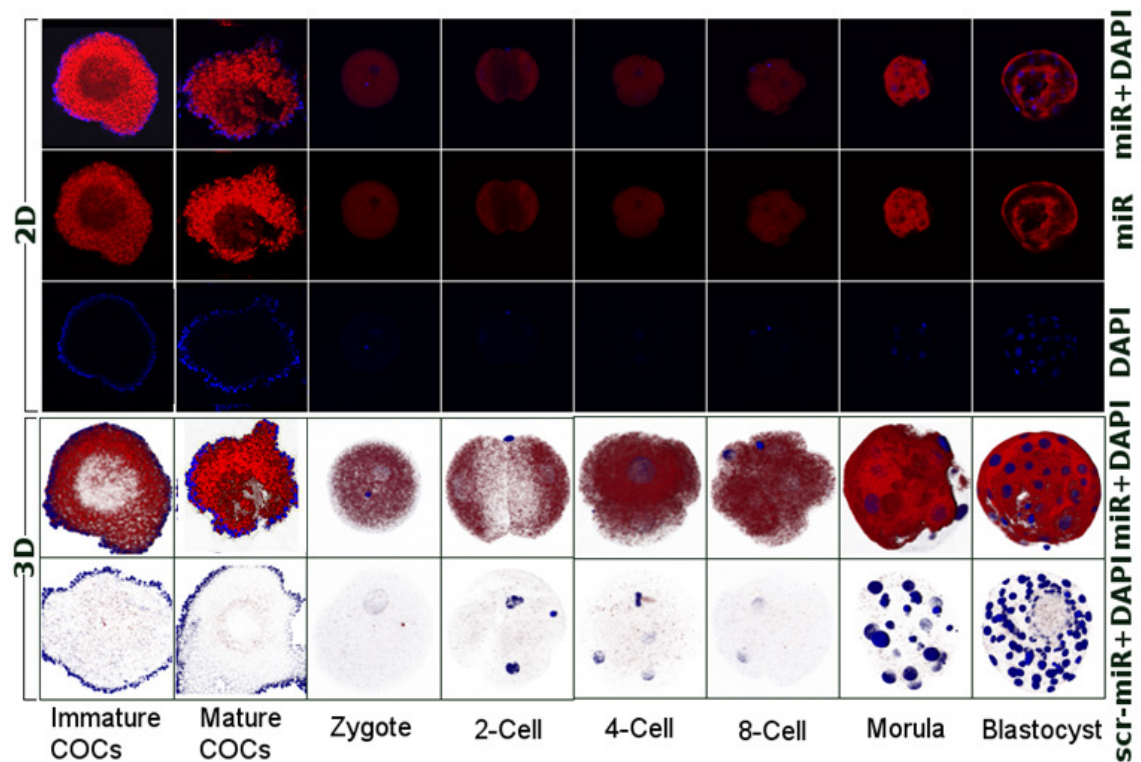


Figure 4.5: Whole-mount in-situ detection of miR-130b in COCs and preimplantation embryo stage using 3'-digoxigenin labelled locked nucleic acid (LNA) based microRNA probes for miR-130b and scramble miRNA and nucleus was stained with DAPI. 2D, 2 dimensional; 3D, 3 dimensional; scr, scramble; miR, miR-130b; DAPI, 4',6-diamidino-2-phenylindole. Red and blue colours indicate miRNA expression and nuclear staining respectively.

### 4.3 In silico analysis and experimental validation of target gene

#### 4.3.1 Identification of the appropriate gene as a target of miR-130b in oocyte maturation and preimplantation

In order to dissect the mechanisms of miR-130b in preimplantation development and function, it was necessary to determine the endogenous mRNA potential targets that are known to play a major role in function of granulosa cell, oocyte maturation and in preimplantation embryo development. To identify the direct target genes of miR-130b in oocyte maturation and granulosa cell function, PicTar, miRanda and TargetScan were used as a target prediction tool. The mentioned algorithms annotated on the database of the miRBase::Sequences program (<http://microrna.sanger.ac.uk>), on the bases of strong free thermodynamic energy and its SVM scoring. The function of the selected gene further analysed using Gene Ontology (GO) analysis associated with signal transduction, oocyte maturity, follicular growth and preimplantation development transcription factors. Accordingly, the selected genes were SMAD1, SMAD5, MEOX2, MARCH2, DDX6, EIF2C1, EIF2C4, RPS6KA5 and DOCR1. Furthermore, the selected genes were blasted using NCBI software to evaluate the sequence similarity in bovine. And, the result found were SMAD5, MEOX2, MARCH2, DDX6, EIF2C1, EIF2C4, RPS6KA5 and DOCR1 having the same target site as in human or mouse except SMAD1. SMAD1 is a target in human and mouse but the 3'UTR sequence was not similar to bovine. The selected target sequences were uploaded in miTarget with the bovine miR-130b to observe the specificity of target and sequence difference to each target site shown in (Table 8). The number of target sites at single gene by miR-130b was shown in figure 4.6.

Table 8: List of selected bta-mir-130b target genes with its target sites.

<b>RPS6KA5</b> Alignment	Position cloned	Free Energy (total)	SVM Score
3' - UACGGGAAAGUAGUAACGUGAC-5'   : :     :   :             5' ----GUUAUUGUUUUUAAUU---UUGCACUG-3'	1st vector 30	-14.20	0.531
3' - ACGGGAAAAUUGUAACGUGAC-5'   : : :       :             5' ----UGUUUUAAAGUAAUUAUUGCACU-3'	1st vector 108	-12.50	0.759
3' --UACG-G-GAAAGUA— GUA-ACGUGAC-5'         : : :       :       :       5'-GUGCACUCUUUAAAAGCAUAUGUACUG-3'	1st vector 173	-15.00	2.602
3'--- UACGGGAAAGUAGU--AACGUGAC-5'           :           :     5'----UUGCCUCACACCCCCUUGCGCUU-3'	1st vector 234	-17.30	2.300
3'--UACGGGAAAGUAGUAACGUGAC-5'           :           5'--CGGCCC- - - CAGAG - - GCACUG-3'	1st vector 291	-15.30	1.071
3'-UACGGGAA- AGUAGUAACGUGAC-5'   : : :       :             5'-GCGCUGUGCUCGUGGCUGCACUG-3'	1st vector 346	-18.30	3.769
<b><u>SMAD5</u></b>			
3'--UACG - - - GGAAAGUAGUAACGUGAC-5'         :     :               5'--AUGCAUUAUCUUUUUAAUUUGCACUU-3'	1st vector 860	-15.80	0.417
3'- UACGGGAAAGUA- GUAACGUGAC-5'       :         : :               5'-GUACCUGUUUAAAGUGUUGUACUU-3'	2nd vector 3480	-11.10	0.402
3'- UACGGGAAAGUAGUAACGUGAC-5'       : :         :       :       5 AUACUUUUUCUA--GUUGC-U-UG-3'	2nd vector 3545	-10.50	0.229
3' ----UACGGGAAAGUAGUAACGUGAC-5'     : :         :             :   5'-- GUGGUUGGUUAAAGUUGCAUUU-3'	3rd vector 4842	-11.00	0.238
'--UACG--GGAAAG— UAGU--AACGUGAC-5'     :             :           :   5'-UUGCAUUUUGAAAUCGCUUGCAUUA-3'	3rd vector 4860	-11.60	0.039
3'--UACGGGA-AAGUAGU-AACGUGAC-5'       :               :         5'--AGGUCUGCUUC-UUACUUGUACUU-3'	3rd vector 4999	-12.20	0.530
<b><u>MEOX2</u></b>			
3'—UACGGG----- AAAG-----UAGUAACGUGAC-5' : : :                             5'----GCCUUUGUGUUUGCUUUGCUUGCACUG-3'	1st vector 281	-16.10	1.174
3'--UACGGGAAAGUAGUAACGUGAC-5'       :               :               5'--UUGCUCUCGC-----UUGCACUG-3'	1st vector 433	-16.60	5.365

<b><u>MARCH2</u></b>	Position cloned	Free Energy (total)	SVM Score
3'-UACGGGAA-AGUAGUAA-----CG--UGAC-5'     : : :       :           5'---GCUUCCUCAUCCAACACCAGCUACUG-3'	1st vector 537	-10.70	0.160
3'---UACGGGAAAGUAGU-AACGUGAC-5' :           :                 5'---GUGCCAUA-CAGAGUUUGCAGUG-3'	1st vector 565	-13.50	1.274
3'---UACGGGAAA---GUAGUACGUGAC-5'     : :       :                 5'---AGGCUCUGCAGGCUUC-UUGCACUU-3'	1309	-15.50	1.964
<b><u>EIF2C1</u></b>			
3'-UACGGGAAAGUAGUAA-CGUGAC-5'   :                                     5'-AAAUCCAUGA-CAUUUGCACUU-3'	1st vector 281	-10.40	0.398
3'-UACGG-GAAAGUAGUA-----ACGUGAC-5'   5'--UCCCGCUUUCUCCACCUGC-CUG-3'	1st vector 380	-10.50	2.510
<b><u>EIF2C4</u></b>			
3'---UACGGGAAAGUAG--UAACGUGAC-5'   5'-CAGCAAC-UCGGAAUAGUUGCACUG-3'	1st vector 69	-14.80	1.401
3'--- UACGGGAAAGUAGUACGUGAC-5'   5' --- CUGCCAGG-CA-----AUUGCACUA-3'	1st vector 569	-15.40	3.712
<b><u>DDX6</u></b>			
3'--UACGGGAAAGU--AGU-----AACGUGAC-5' : : :       :                             5'---CCUUUUUUGUCCACUUGUUUGCACUG-3'	1st vector 244	-13.40	1.018
3'-UACGG--GAAA--GUAGU----AACGUGAC-5'                 :                         5'-GUGCUGACUGAACAUUAGUUGCACUA-3'	1st vector 271	-15.70	3.095
<b><u>DOC1R (CDK2AP2)</u></b>			
3'--UACGGGAAAGUAG--UAACGUGAC-5'   5'--UGGCCUUCACCCGAGUUGCACUU-3'	523	-15.64	4.160

SVM: Support Vector Machine

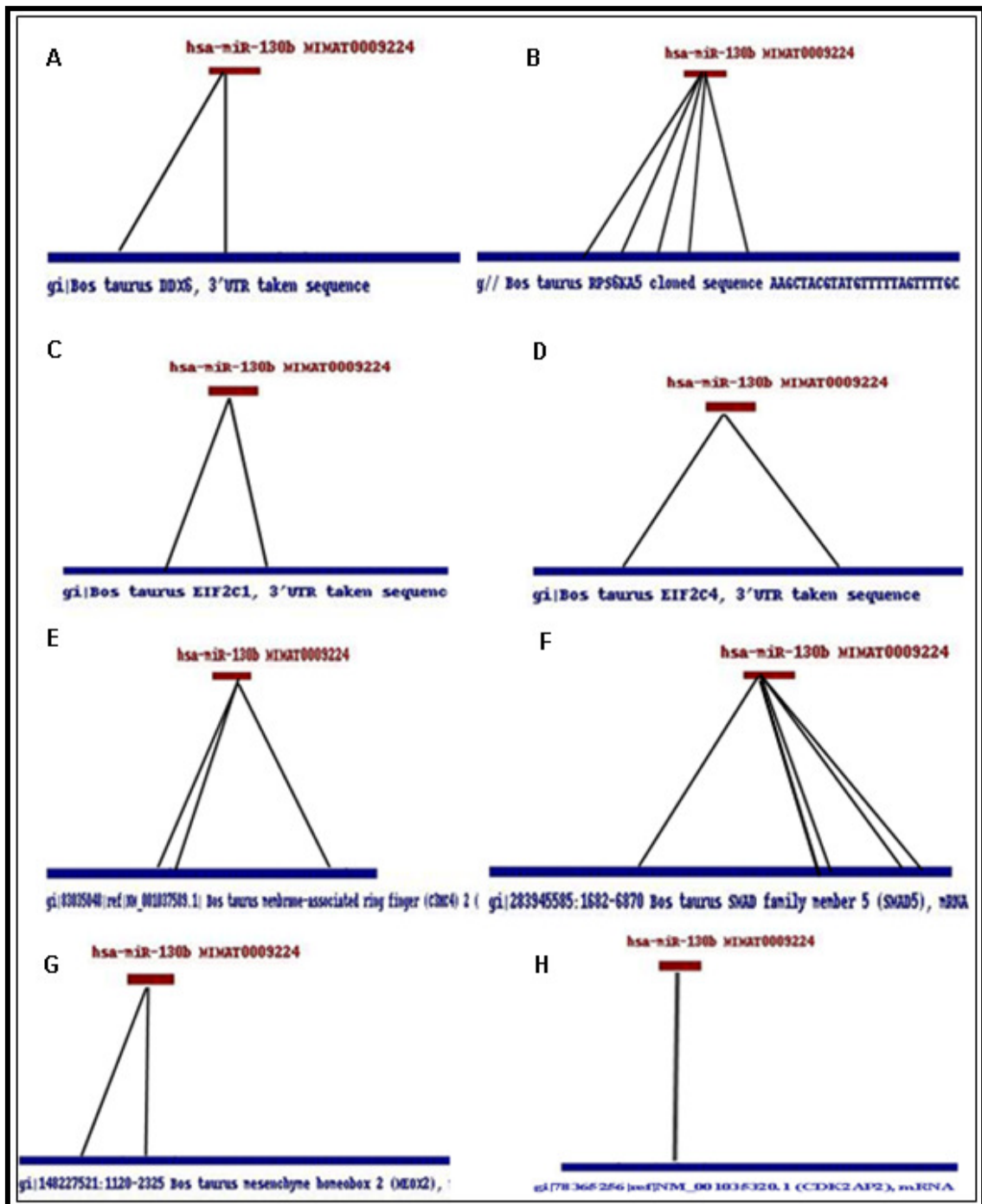


Figure 4.6: bovine miR-130b and predicted 3'UTR of the target gene. Blue: target gene, Red: miR-130b. A: DDX6; B: RPS6KA5; C: EIF2C1; D: EIF2C4; E: MARCH2; F: SMAD5; G: MEOX2; H: DOC1R.

#### 4.3.2 Expression profiling of selected target genes in preimplantation embryo

Once the targets were selected; the expression profiling of selected genes (EIF2C1, EIF2C4, DDX6, MARCH2, RPS6KA5 (MSK1), MEOX2, DOC1R and SMAD5) was conducted in preimplantation embryo using qRT-PCR. The expression was normalized to GAPDH transcript, an endogenous control. The mRNA abundance of EIF2C1, EIF2C4, DDX6, MARCH2, MSK1 and SMAD5 in all the stages (mature oocyte, zygote, 2-cell, 4-cell, 8-cell, morula and blastocyst) of preimplantation embryo was shown in (Figure 4.7). However the expression of MEOX2 and DOC1R were not detected in all stages of embryo except very low in morula and blastocyst. The expression of DDX6 was low at mature oocyte but increased at 2-cell followed by significantly decline expression at 8-cell and increase at morula stage ( $p < 0.05$ ). MARCH2 and SMAD5 were low at oocyte and zygote but increased at 2-cell upto 8-cell stage significantly ( $p < 0.05$ ). Where as, the detection reduced significantly ( $p < 0.05$ ) at morula and blastocyst stage EIF2C1 didn't show any significant difference ( $p \geq 0.05$ ) in expression among all stages of embryo but little increase at zygote and 2-cell stage embryo. Transcript of EIF2C4 was low from oocyte upto 8-cell stage but was significantly increased ( $p < 0.05$ ) at morula and blastocyst stage. RPS6KA5 was low at oocyte but significantly increased ( $p < 0.05$ ) at zygote which remains about constant upto 8-cell embryos and decrease of mRNA was detected at morula and blastocyst stage embryos ( $p < 0.05$ ).



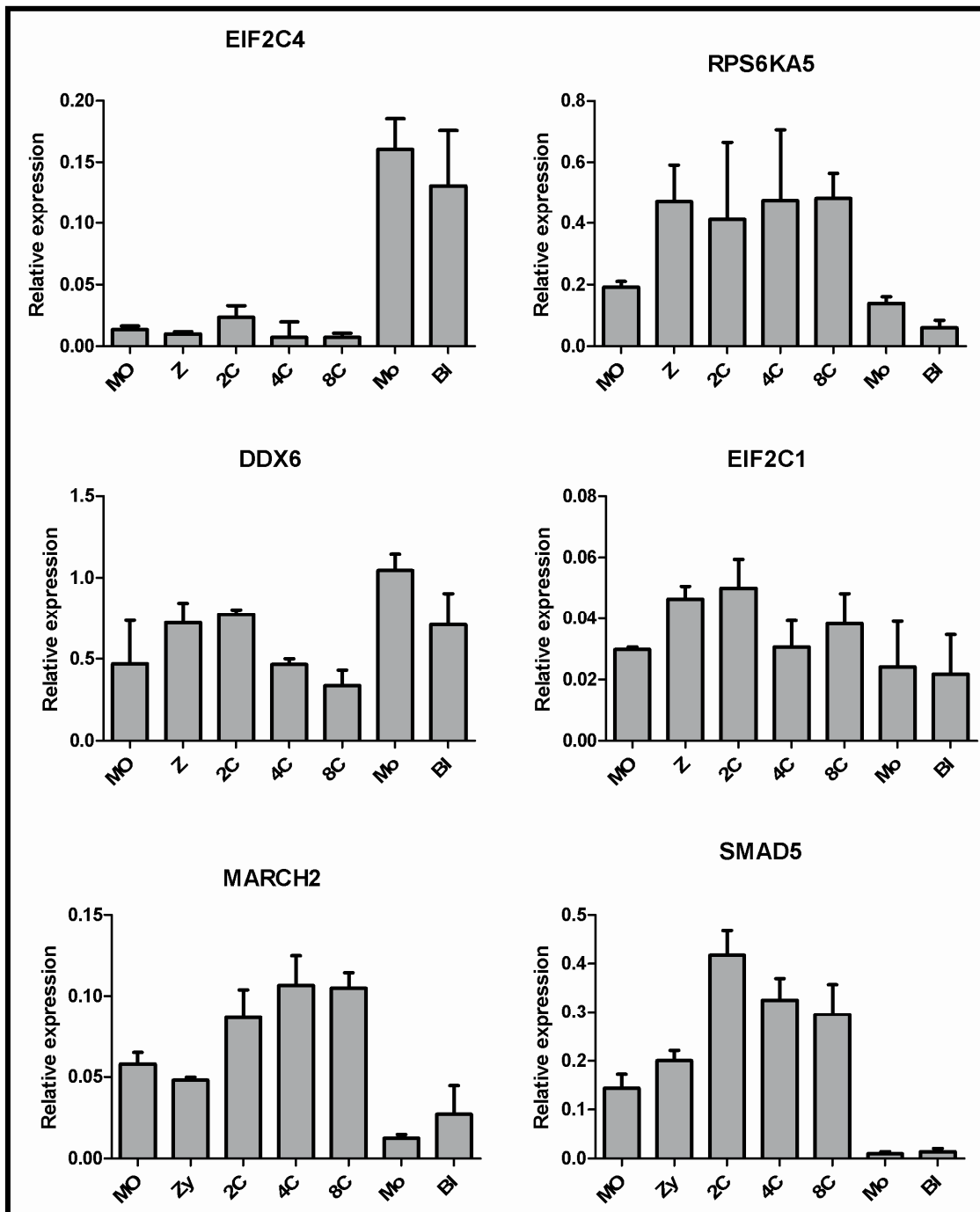


Figure 4.7: Expression profiling of selected transcripts across the preimplantation stage embryos. MO: Mature oocyte; Z: Zygote; 2C: 2-Cell; 4C: 4-cell; 8C: 8-Cell; Mo: Morula; Bl: Blastocyst. Error bars show the mean  $\pm$  SD.

#### 4.3.3 Transfection of cells with different concentration of construct plasmid and miR-130b for further experimental validation

To generate pmirGLO target vector, about 200 to 600bp of 3'UTR (according to the target site present) were cloned to the pmirGLO vector. As mentioned in materials and method. However, the procedure of miRNA target validation was done first time in our institute so optimization was needed for the transfection efficiency, DNA and miRNA optimal concentration. MSK1 (RPS6KA5) construct, a single construct with several target site was been selected for optimization. With different number of cells different concentration of vector-construct plasmid and different concentration (15 nM, 30 nM and 50 nM precursor) of miR-130b mimic or inhibitor were used. 24 hours and 48 hours post-transfection the luciferase activity was observed by firefly luciferase (F-luc) activity normalised with renilla luciferase (R-luc) activity. The cell concentration was selected where less cell death and more than 80% cell confluency was observed. Additionally, all wells showed uniform growth of cells at the concentration of  $8 \times 10^4$ . All concentration was used with same number of cells optimised. miR-130b 15 nM, 30 nM and 50 nM shows significantly decreased in the signalling of MSK1mirGlo construct vector compared the cells without miR-130b or with anti-miR-130b ( $p < 0.05$ ) (Figure 4.8A). The cumulus cells were co-transfected with 500 ng of PMJGreen vector to visualise transfection efficiency and the transfection efficiency was more then 60% (Figure 4.8C-D). Next experiment was done using several controls for cotransfection. The controls used were (1) mismatch construct, (2) mismatch vector with miR-130b, MSK1 without miR-130b (4) scramble RNA and (5) PMJGreen vector visible control. The result shows the cells cotransfected with 800 ng/ml MSK1mirGlo vector with 30 nM/ml of miR-130b precursor was significantly ( $p < 0.05$ ) reduced in the ratio of F-luc/R-luc activity compared to all the other controls (mismatch vector control, MSK1 without miR-130b control and scramble control). Where as cells transfected with MSK1mirGlo vector with 30 nM/ml miR-130b inhibitor showed significant ( $p < 0.05$ ) increase in F-luc/R-luc activity compared to MSK1mirGlo without miR-130b control (Figure 4.8B).

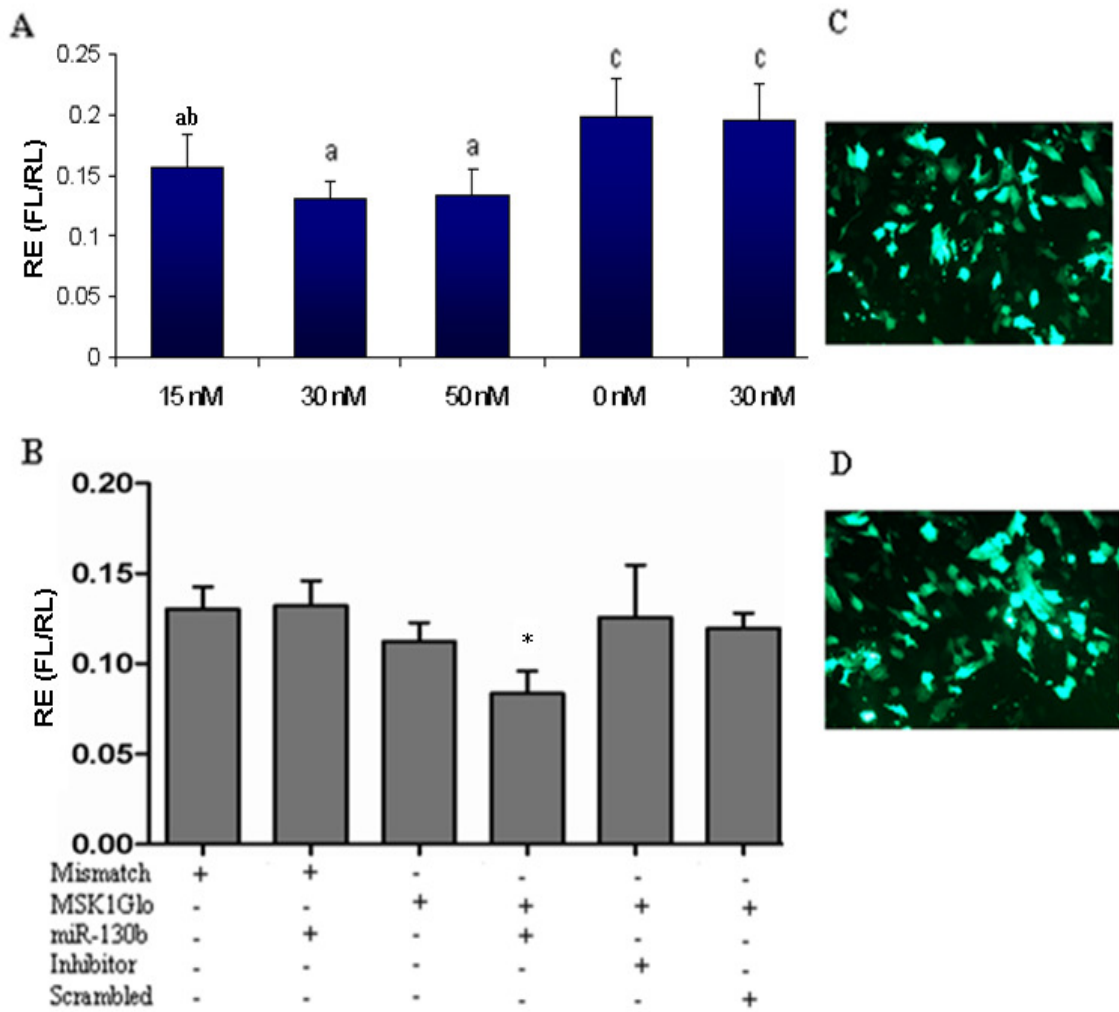


Figure 4.8: (A) The miR-130b concentrations (15 nM, 30 nM and 50 nM) transfected with 800 ng/ml MSK1Glo construct plasmid. (B) Different controls used to validate the target accuracy. (C-D) Cotransfection of 500 ng pMJGreen vector with miR-130b shows transfection efficiency > 60%. Forty-eight hours post transfection the activity of F-luc was normalized by R-luc expression and the error bar show mean  $\pm$  SD of four independent experiments. Significant differences (a:c –  $p < 0.05$ ), and (\* $p < 0.01$ ) versus cumulus cells transfected with mismatch vector construct control. RE, relative expression; FL, firefly luminescent; RL, renilla luminescent.

#### 4.3.4 Experimental validation of cloned genes EIF2C1, EIF2C4, DDX6, SMAD5, MEOX2, MARCH2 and DOCR1

The validation result shows that miR-130b triggered a strong and specific silencing effect on the target but not to all of the predicted genes. The 3'UTR of the SMAD5 gene contains all the predicted binding sites for miR-130b in 3 different clones and 3'UTR of the MSK1 gene with 3 sites with highly conserved regions was cloned in single vector. MEOX2, MARCH2, EIF2C1, DOCR1, DDX6 and EIF2C4 were constructed with one or two target site in single vector (Figure 4.6). To validate whether these genes are the real target of miR-130b, sites were cloned into the downstream of the firefly luciferase site of the pmirGLO vector and transiently transfected with minimum 4 individual replicates. The transfection was grouped in mismatch vector with miR-130b transfected cells, construct vector transfected cells, construct vector or miR-130b transfected cells and construct vector and inhibitor transfected cells.

The result shows MSK1 was reduced by 40% ( $p < 0.05$ ) in firefly luciferase expression in miR-130b precursor cotransfected with MSK1Glo vector cells compared to mismatch mirGlo vector and precursor cotransfected, whereas miR-130b inhibitor was 30% high signal in MSK1Glo co-transfected cells (Figure 4.8B).

The cells cotransfected with SMAD5Glo vector and miR-130b precursor with two target sites shows 60% reduction (Figure 4.9A) which was highly significant ( $p \leq 0.005$ ) and SMAD5\_site1Glo cotransfected with miR-130b inhibitor showed increase in firefly luciferase expression (20%). And the SMAD5\_site2 Glo construct cotransfected with miR-130b precursor showed reduction in signal ( $p \geq 0.05$ ) but the third construct SMAD5\_site3 didn't show any change in the signal (Figure 4.9B-C). DOCR1mirGlo cotransfected with miR-130b precursor showed reduction in signal by 35% in firefly luciferase expression compared to mismatch vector transfected with precursor ( $p < 0.05$ ) was significant (Figure 4.9D). EIF2C4 was constructed with 2 strong sites and cotransfected with miR-130b precursor was 35% reduced in firefly luciferase expression compared to mismatch vector transfected with precursor ( $p \leq 0.05$ ), whereas miR-130b inhibitor transfected with EIF2C4mirGlo increased by 20% high signal of firefly luciferase compared to EIF2C4mirGlo alone transfected (Figure 4.10E). MEOX2 was constructed with two strong target sites and gave about 30% reduction ( $p \leq 0.05$ ) in firefly luciferase signalling in miR-130b precursor transfected cells compared to

mismatch vector transfected with mir-130b precursor transfected cells, where as miR-130b inhibitor increased by 20% of firefly luciferase signal compared to mismatch cotransfected with miR-130b precursor (Figure 4.10C). EIF2C1, MARCH2 and DDX6 didn't show any reduction in firefly signal (Figure 4.10A-B, D). All transfection was controlled using PMJGreen vector with 70- 80% confluent and 50-60% transfection efficiency.

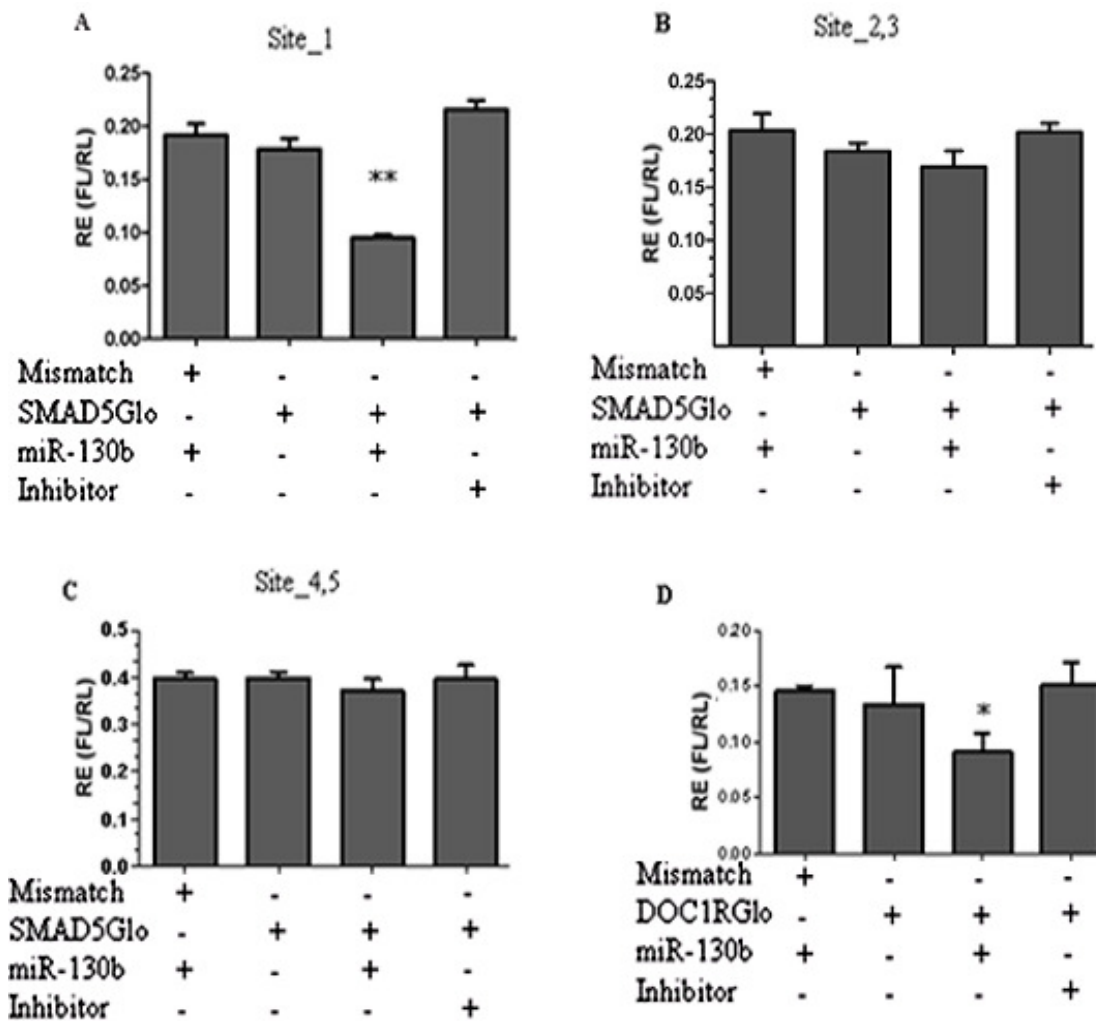


Figure 4.9: Validation of genes as target of miR-130b with luciferase reporter activity.

Cumulus cells were cotransfected with pmirGLO vector construct with 30 nM miR-130b/ml precursor or inhibitor. Forty-eight hours post transfection the activity of F-luc was normalized by R-luc expression and the error bar show mean  $\pm$  SD of four independent experiments. Significant differences (\* $p < 0.05$ ) and (\*\* $p \leq 0.005$ ) versus cumulus cells transfected with mismatch vector construct control. RE, relative expression; FL, firefly luminescent; RL, renilla luminescent.

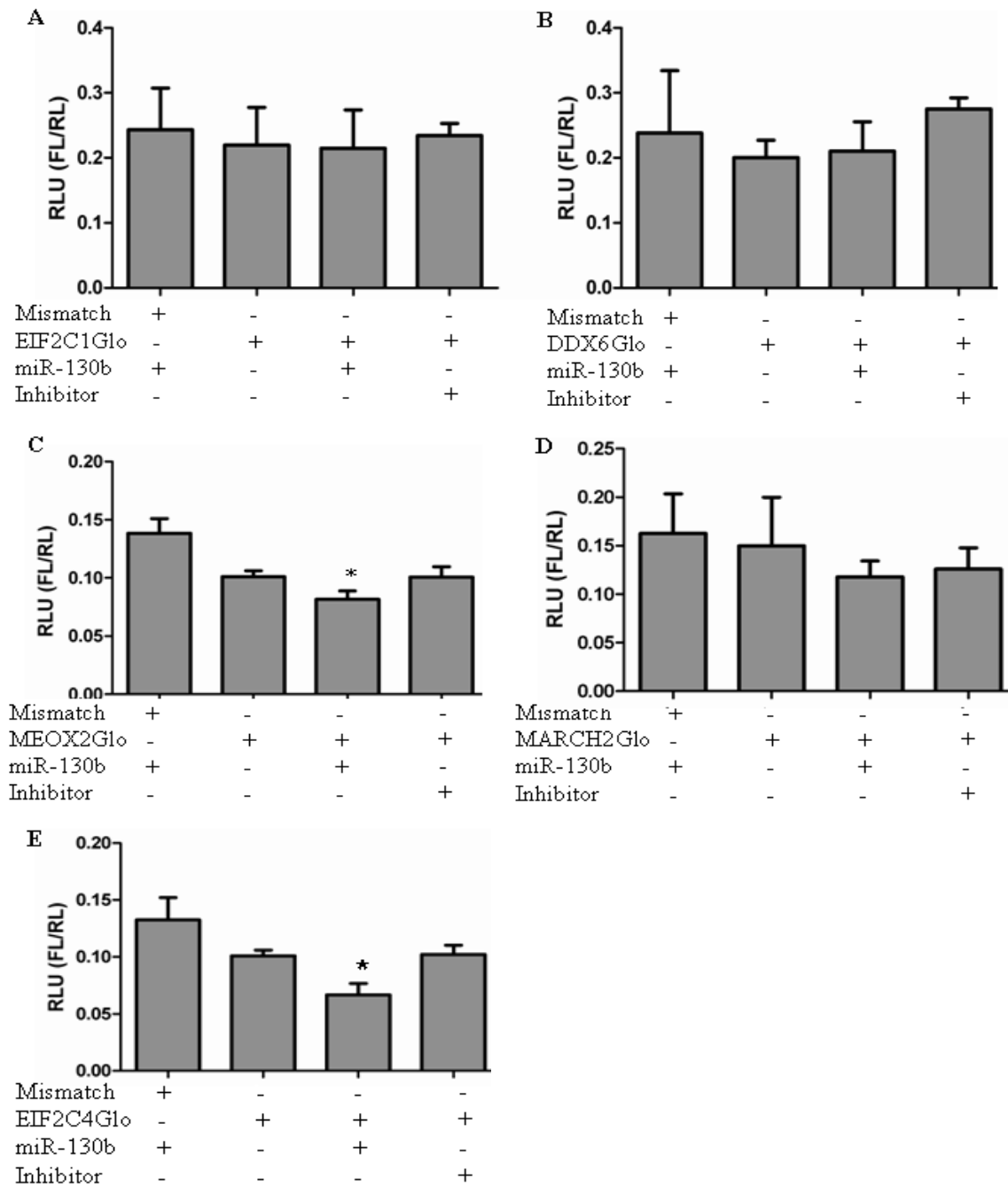


Figure 4.10: Validation of genes targeted by miR-130b using luciferase reporter activity. Cumulus cells were cotransfected with pmirGLO vector construct with 30 nM miR-130b/ml precursor or inhibitor. Forty-eight hours post transfection the activity of F-luc was normalized by R-luc expression and the error bar show mean  $\pm$  SD of four independent experiments. Significant differences (\* $p < 0.05$ ) versus cumulus cells transfected with mismatch vector construct control). FL, firefly luminescent; RL, renilla luminescent.

The results shows MSK1, SMAD5, MEOX2, EIF2C4 and DOC1R were experimentally validated as target of miR-130b where as EIF2C1, MARCH2 and DDX6 were not been validated as target by experimental analysis. Among the validated target MSK1 and SMAD5 were selected for further investigation

#### 4.3.5 Expression of SMAD5 and MSK1 transcript in oocyte and companion cells

The transcript abundance of SMAD5 and MSK1 was measured in mature and immature oocytes and its corresponding cumulus cells to observe there expression pattern which was as figure 4.11, high regulation of SMAD5 as well as MSK1 were observed in oocytes compared it its corresponding cumulus cells ( $p < 0.05$ ).

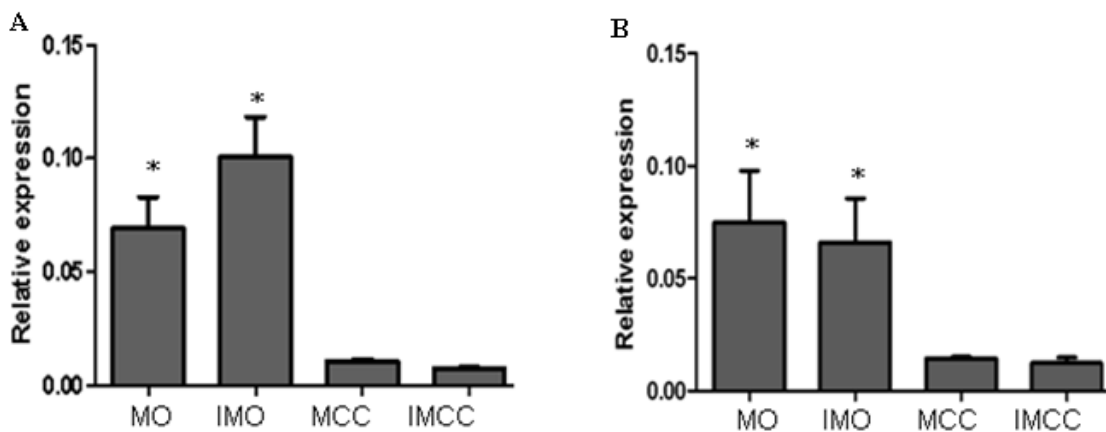


Figure 4.11: Relative abundance of SMAD5 (A) and MSK1 (B), in mature and immature oocyte and its corresponding cumulus cells. The error bar show mean  $\pm$  SD of three independent experiments. Significant differences ( $*p < 0.05$ ) related to corresponding cumulus cells. MO, mature oocyte; IMO, immature oocyte; MCC, mature cumulus cells; IMCC, immature cumulus cells.

#### 4.3.6 Localization of selected target proteins in follicular cells and COC

The spatial protein expression of MSK1 and SMAD5 were further investigated in ovarian tissue section and COCs using immunohistochemistry. Accordingly strong protein florescence signals were detected in oocyte and cumulus cells for MSK1. However, its signal was relatively lower in granulosa cells. On the other hand, the

protein signalling of SMAD5 was higher in cumulus cells and follicular granulosa cell (Figure 4.12).

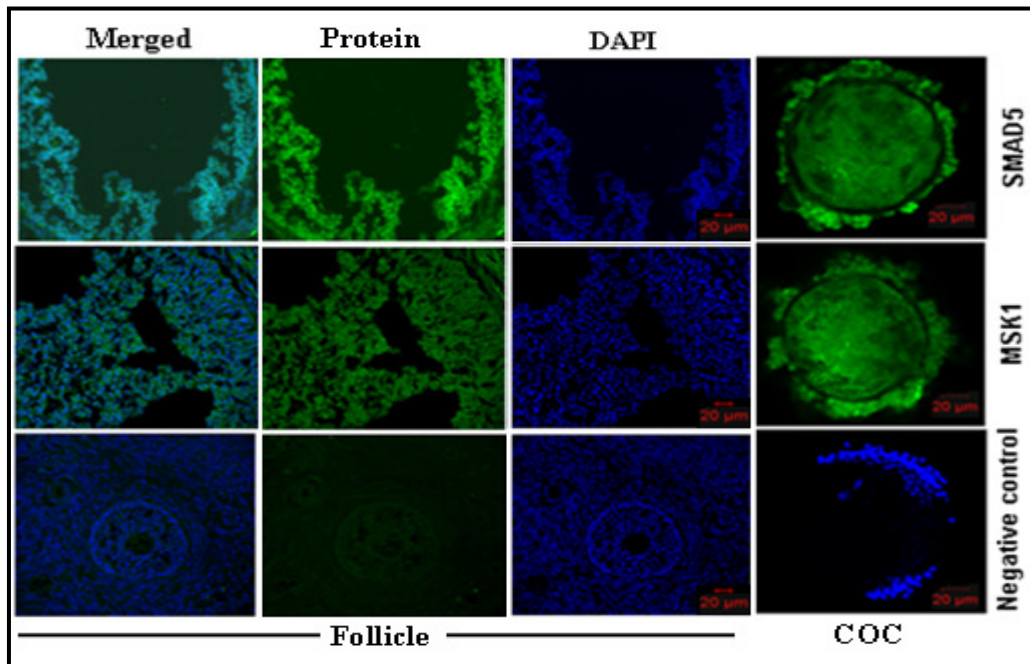


Figure 4.12: Immunofluorescent analysis of SMAD5 and MSK1 in ovarian section shows the localization of protein. Green colour indicates the protein (SMAD5 and MSK1), where as, blue colour indicates the nucleus staining with DAPI. Scale bar represents 20 μm.

#### 4.4 Effect of miR-130b in oocyte maturation and its surrounding cell function

The role of miR-130b was investigated in oocyte maturation and its surrounding somatic cells by overexpression and suppression of miR-130b.

##### 4.4.1 Direct regulation of SMAD5 and MSK1 by miR-130b during oocyte maturation

To observe the effect of miR-130b on its target gene function during oocyte maturation, miR-130b precursor and inhibitor were injected to the immature oocyte. Scramble injected and uninjected oocytes groups were used as a control. The result showed that after 22 hrs of injection, the expression of miR-130b was significantly ( $p < 0.001$ ) increased by 8000-fold in precursor injected group compared to uninjected oocyte group (Figure 4.13A). Furthermore, the gene expression analysis indicated that the mRNA ( $p < 0.05$ ) and protein expression of MSK1 and SMAD5 were significantly increased in



inhibitor injected compared to uninjected group (Figure 4.13B, 4.13C, 4.13D). Moreover, immunohistochemistry localization showed that the protein signal of MSK1 gene was reduced in precursor injected group and remarkable increased in inhibitor injected group compared to scramble injected and uninjected control groups (Figure 4.13C, 4.13D)

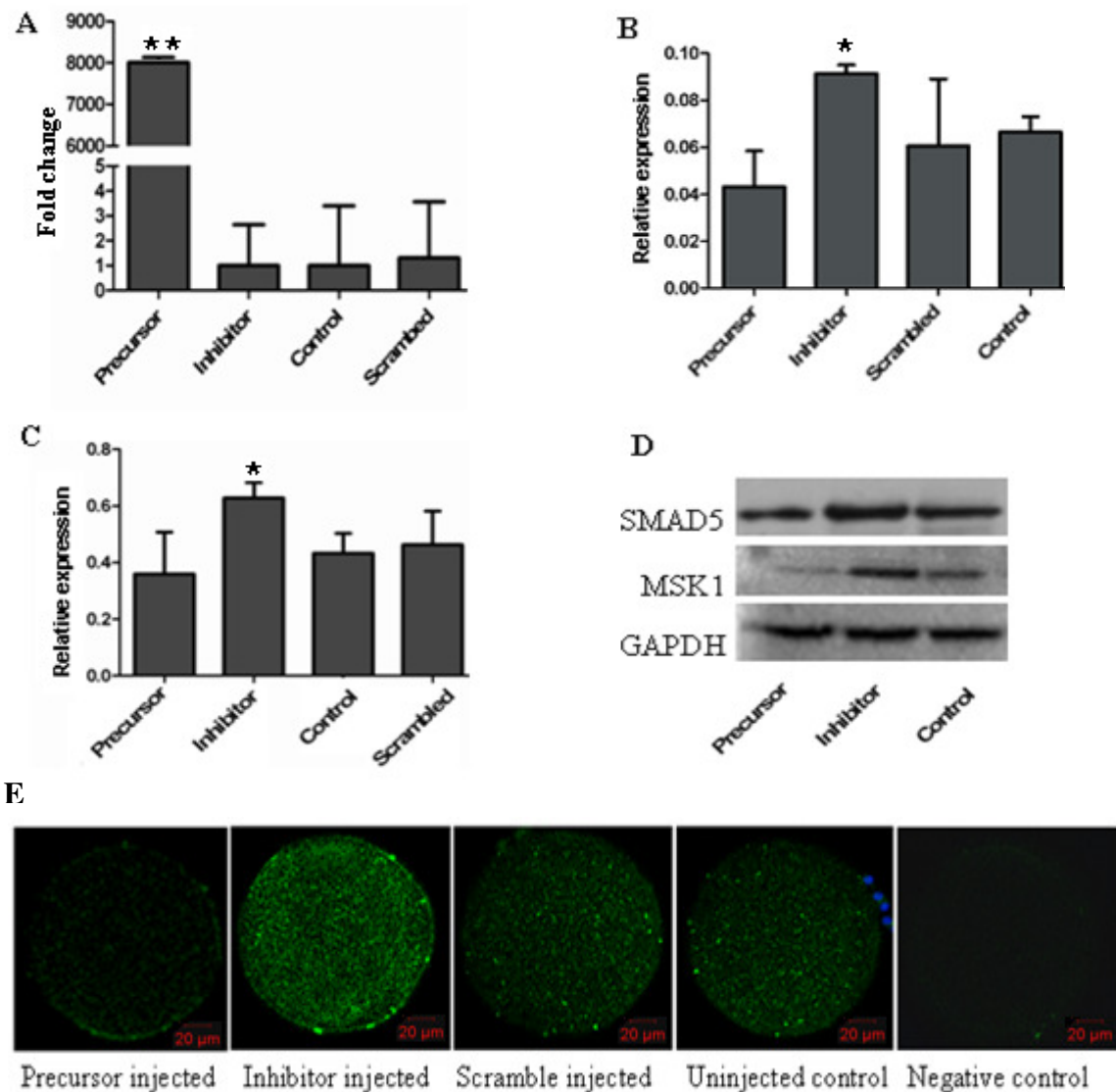


Figure 4.13: Expression levels of miR130b (A), MSK1 (B), and SMAD5 (C), in miR-130b precursor, miR-130b inhibitor and scramble injected oocytes and uninjected oocyte control. (D) Western blot analysis showing the protein expression of MSK1 and SMAD5 genes in miR-130b precursor, miR-130b inhibitor and scramble injected oocyte groups. (E) Immunofluorescent indicating spatial localization of MSK1 protein in different injected groups of oocytes. Scale bar represents 20  $\mu$ m. (\*\* $p < 0.001$ , \* $p < 0.05$ )

#### 4.4.2 Role of miR-130b on oocyte maturation

The oocytes injected with miR-130b precursor, miR-130b inhibitor, scramble and uninjected control group were observed during oocyte maturation to understand the role of miR-130b on oocyte maturation.

##### 4.4.2.1 Polar body extrusion in miR-130b injected oocyte groups

miR-130b was over-expressed or suppressed during oocyte maturation *in vitro* to understand the role of miR-130b during oocyte maturation. The results have showed that the ectopic expression of miR-130b in oocyte has increased the polar body extrusion and the suppression of endogenous miR-130b resulted in significant reduction of polar body extrusion (Table: 9). The comparative difference between inhibitor injected with other injected and uninjected groups was ( $p \leq 0.01$ ).

Table 9: The polarbody extrusion rate of injected and uninjected oocytes groups.

Injected groups	No. of oocytes	First polar body 24 h after injection (%)
miR-130b precursor	408	86.30 $\pm$ 4.02 <sup>a</sup>
miR-130b inhibitor	467	73.39 $\pm$ 6.59 <sup>b</sup>
Scramble	489	85.13 $\pm$ 3.91 <sup>a</sup>
Uninjected	401	84.65 $\pm$ 7.8 <sup>a</sup>

Different letters of superscripts in the same column indicate significant difference ( $p \leq 0.01$ ) between injected groups.

##### 4.4.2.2 Effect of miR-130b in mitotic division of oocytes

A group of oocyte injected with miR-130b precursor, inhibitor, scramble and uninjected (150 oocytes /group) were stained after 22 hours of injection with Hoechst to investigate the chromosomal position in the oocytes. The results have shown that 10-12% oocytes remains in GV stage in all injected groups, 22% of inhibitor injected and 8% precursor injected groups were arrested in Telophase I stage. On the other hand, the proportion of oocytes reached to MII stage were lower significantly ( $p \leq 0.05$ ) in inhibitor injected

compared to the control groups (Figure 4.14). But the proportion of oocytes reached to MII stage was high in miR-130b precursor injected oocytes compared to uninjected oocyte groups but not significant.

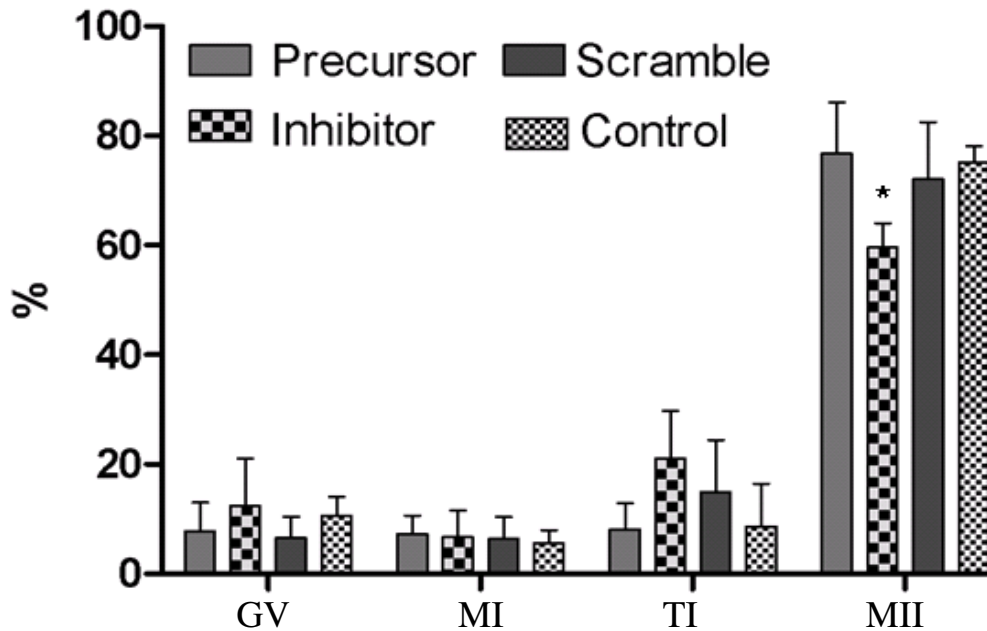


Figure 4.14: Mitotic divisions of oocyte observed 22 hours post injection.

GV: Germinal vesicle; MI: Metaphase I; TI: Telophase I; MII: Metaphase II.

#### 4.4.2.3 miR-130b affects the mitochondrial activity during oocyte maturation

As mitochondria are a powerhouse of cells, loss of mitochondrial activity shows the loss of cellular metabolism which leads to apoptosis. Hence, to understand whether loss of miR-130b was associated with loss of mitochondrial activity, mitochondrial activity assay was performed using MitoTracker probes. At least 20 oocytes per group were taken for microscopy and the experiment was done in triplicate. The staining has shown a clear reduction in the fluorescent quenching, in miR-130b inhibitor injected groups where as the miR-130b precursor injected groups has shown strong fluorescent signal compared to scramble or uninjected groups (Figure 4.15).

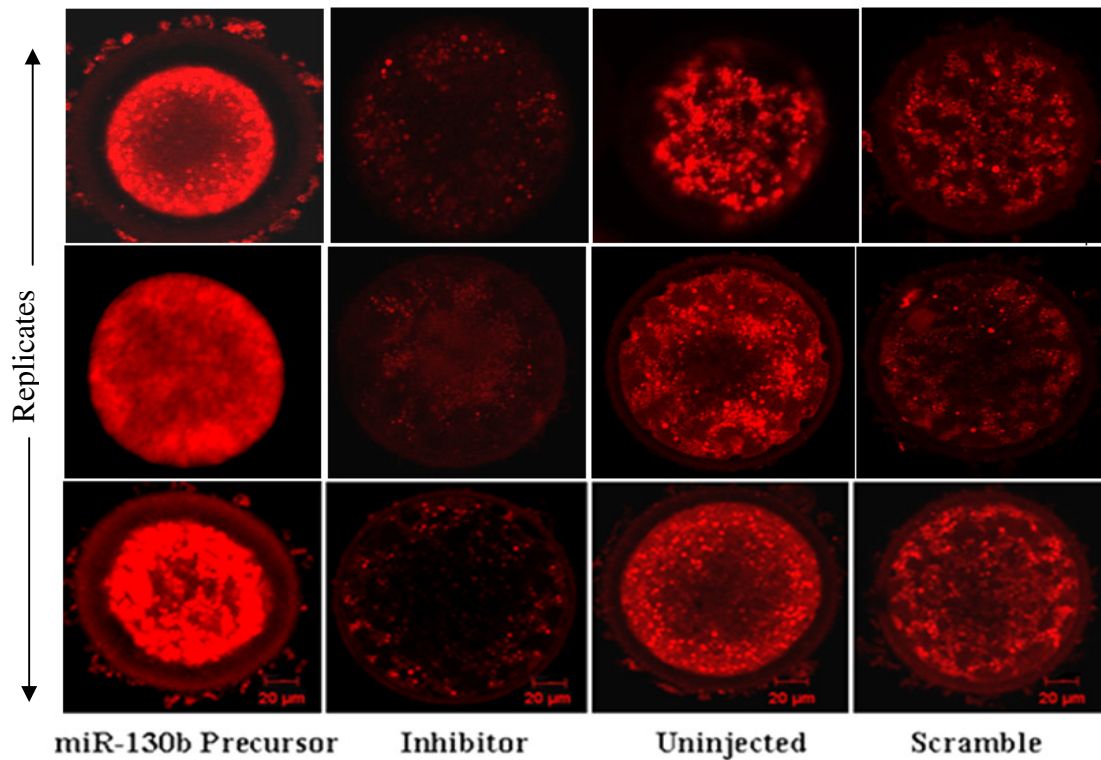


Figure 4.15: The fluorescent quenching in mitochondria of injected oocytes with miR-130b precursor, miR-130b inhibitor, scrambled and uninjected after 22 hours of injection. Scale bar represents 20  $\mu\text{m}$ .

#### 4.4.3 Effect of miR-130b in oocyte surrounding cells

The granulosa cells and cumulus cells were transfected with miR-130b precursor, miR-130b inhibitor, scramble and untransfected control were observed after 24 and 48 hours of transfection for cell proliferation, cholesterol and glycolysis.

##### 4.4.3.1 Regulation of SMAD5 and MSK1 by miR-130b in cumulus cells

The cumulus cells were transfected with miR-130b precursor, miR-130b inhibitor or scramble control. QRT-PCR analysis showed the significantly high level of miR-130b with 45-fold and 2-fold low in inhibitor transfected compared to untransfected group (Fig: 4.16A). Consequently, the mRNA level of MSK1 was significantly reduced in precursor transfected cells (Figure 4.16B). Similarly, the SMAD5 mRNA expression was reduced in miR-130b precursor transfected and also increased in inhibitor

transfected group when compared to control groups (Figure 4.16C). The protein level of MSK1 and SMAD5 has slightly been increased in inhibitor transfected and also slight reduction in precursor transfected cumulus cells (Figure: 4.16D).

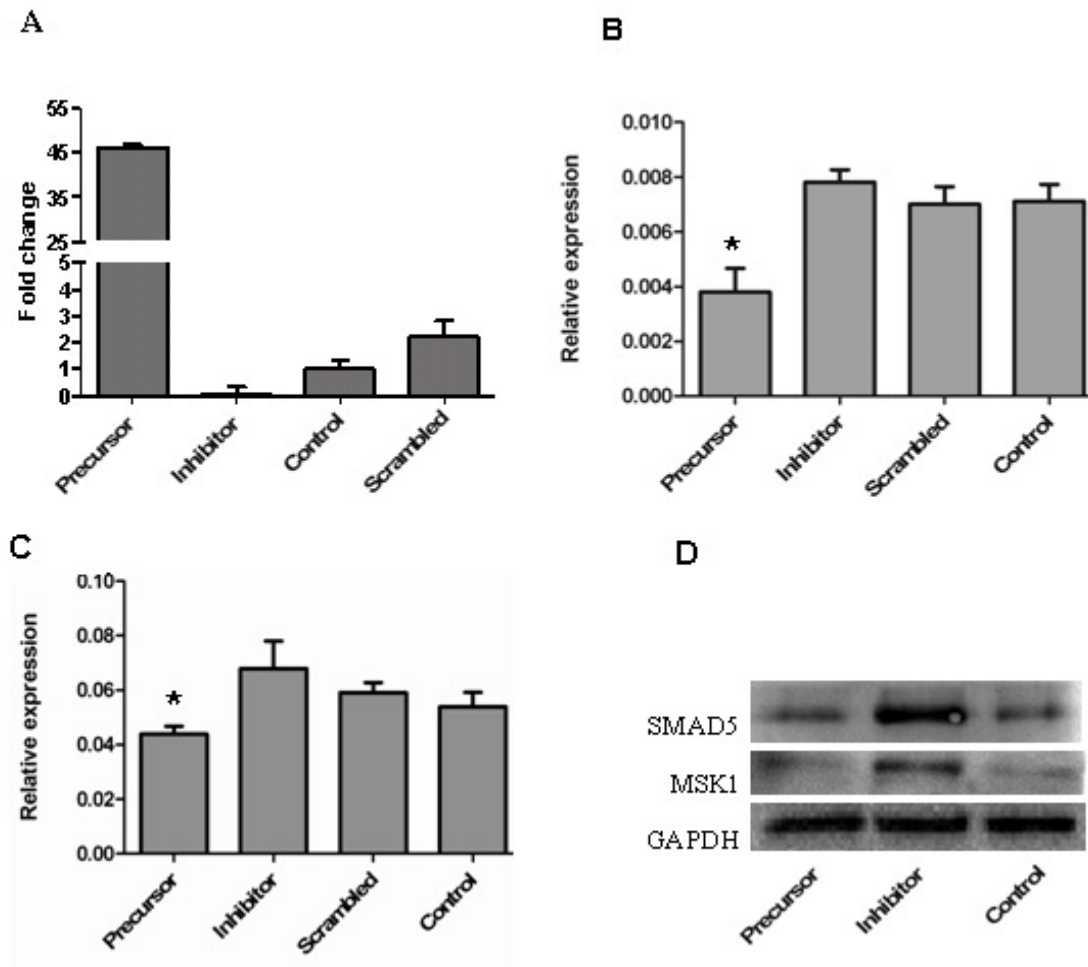


Figure 4.16: (A) The ectopic expression of miR-130b showed significantly high level of miR-130b after 24 hrs in transfected cumulus cells. (B) MSK1, (C) SMAD5, expression in 130b precursor, miR-130b inhibitor and scramble transfected cumulus cells after 24 hours. Significant difference (\* $p < 0.05$ ). (D) The protein level of MSK1 and SMAD5 in miR-130b precursor, miR-130b inhibitor and scramble control groups after 48 hrs of transfection. GAPDH was used as loading control.

#### 4.4.3.2 Effect of miR-130b in cumulus cell proliferation

The cumulus cells were cultured and transfected with miR-130b precursor, miR-130b inhibitor or scramble miRNA to observe the viability of cells at different time points. Live cell count was performed in triplicates and the cell count showed relatively higher cell number in precursor transfected cells and cell viability was less ( $p \leq 0.05$ ) in inhibitor transfected cells after 24 hours compared to untransfected control group. Where as after 48 hours of transfection the cell count in precursor transfected cells was significantly high ( $p < 0.05$ ) and relatively low in inhibitor ( $p < 0.01$ ) transfected cells compared to scramble transfected as well as untransfected control cells (Figure: 4.17).

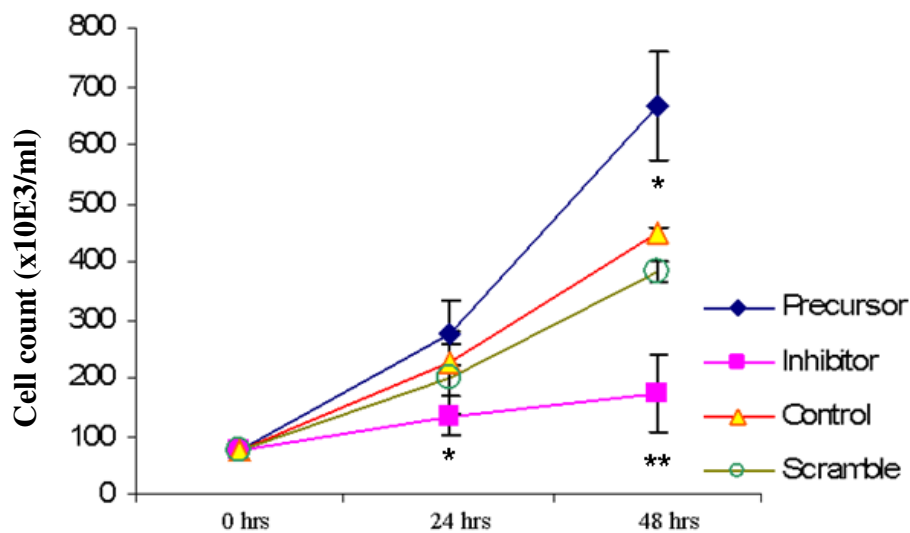


Figure 4.17: The number of live cells was determined in cumulus cells by trypan blue vital cell count after 24 hours and 48 hours of transfection. . Error bars represent the mean  $\pm$  SD for three independent experiments. Significant differences (\* $p \leq 0.05$ ) and (\*\*  $p < 0.01$ ).

#### 4.4.3.3 Regulation of SMAD5 and MSK1 by miR-130b in granulosa cells

The granulosa cells were transfected with pre-miR-130b, anti-miR-130b and scramble control and untransfected control. QRT-PCR analysis showed the mRNA level of MSK1 was reduced in precursor where as increased in inhibitor transfected cells (Figure 4.18A). Similarly, mRNA of SMAD5 was reduced in miR-130b precursor transfected

and slight increased in inhibitor transfected group when compared to control groups (Figure 4.18B). The protein level of MSK1 and SMAD5 has slightly been increased in inhibitor transfected and also slight reduction in precursor transfected granulosa cells (Figure: 4.18C).

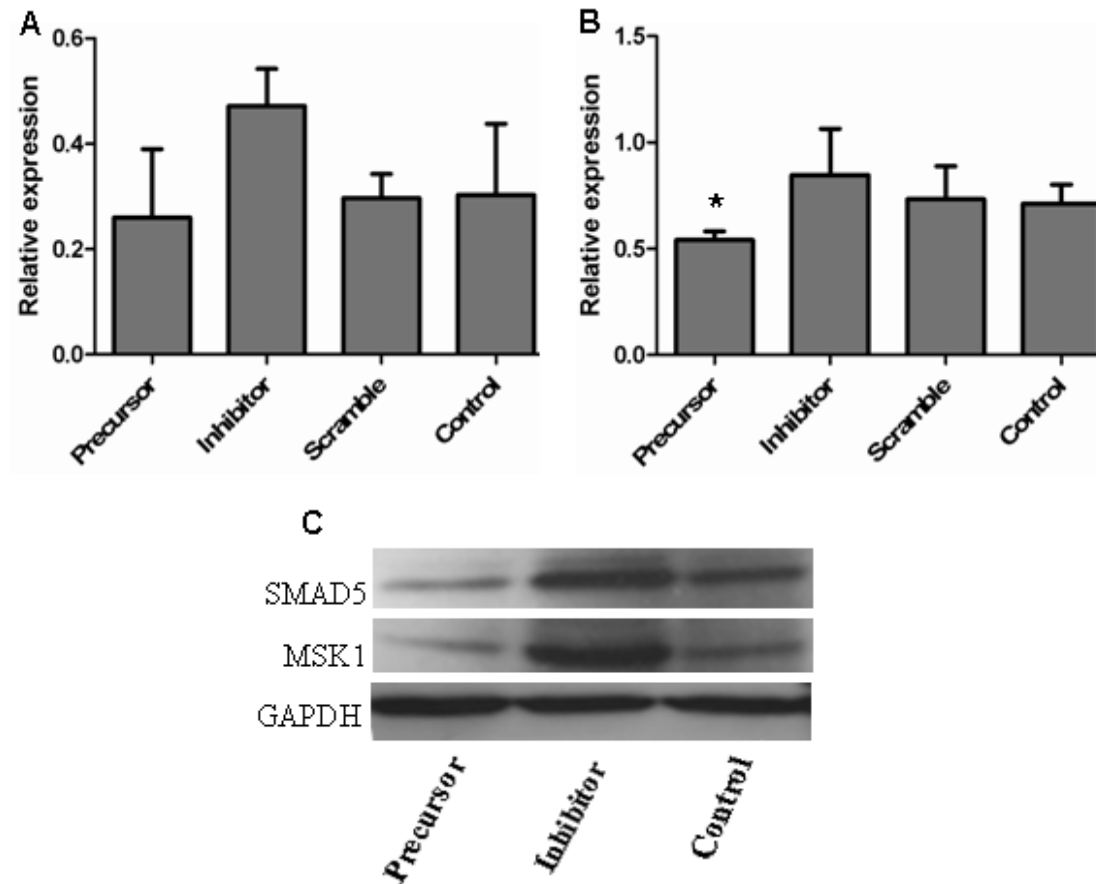


Figure 4.18: Relative abundance of MSK1 (A) and SMAD5 (B) mRNA in miR-130b precursor, miR-130b inhibitor and scramble transfected granulosa cells. Significant difference (\* $p < 0.05$ ). (C) The protein level of MSK1 and SMAD5 in miR-130b precursor, miR-130b inhibitor and scramble control transfected granulosa cells. GAPDH was used as loading control.

#### 4.4.3.4 Granulosa cell proliferation is influenced by miR-130b

The granulosa cells were cultured and transfected with miR-130b precursor, miR-130b inhibitor or scramble miRNA to observe the viability of cells at different time point 24 and 48 hours post transfection. Live cell count was performed under the microscope

using haemocytometer with minimum 4 replicates. The cell count showed relatively higher cell number in precursor transfected cells ( $*p < 0.01$ ) after 48 hrs of transfection where as lower in inhibitor transfected cells ( $*p < 0.01$ ) in both 24 and 48 hrs after transfection compared to scramble transfected and untransfected control cells (Figure 4.19).

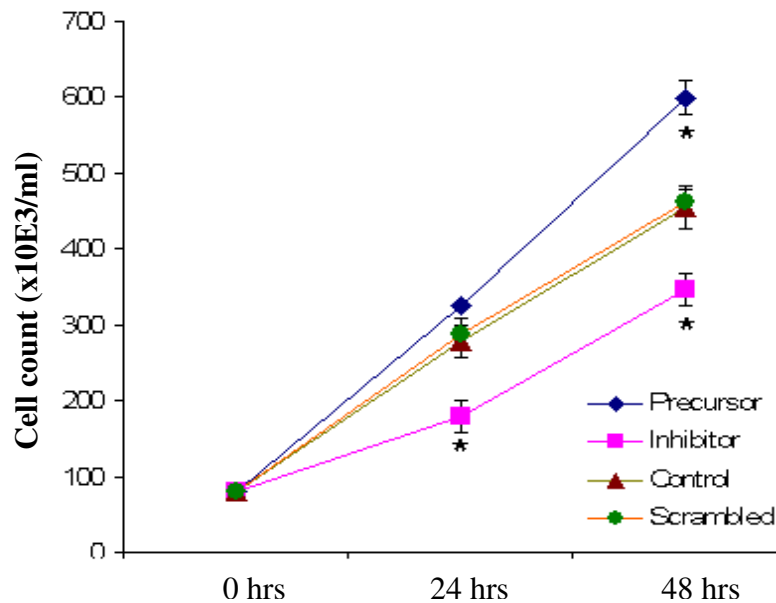


Figure 4.19: The live cell count in granulosa cells was determined by trypan blue vital cell count after 24 hours and 48 hours of transfection. . Error bars represent the mean  $\pm$  SD for three independent experiments. Significant differences ( $*p < 0.01$ ).

Following this, the result of the cell count was further validated by the cell proliferation assay using MTT assay. The primary granulosa cells were transfected with 50 nM/ml miR-130b precursor, miR-130b inhibitor or scramble and after 24 and 48 hours of transfection, the cell proliferation assay was performed. The result showed that miR-130b precursor transfected cells significantly ( $p \leq 0.05$ ) increased the level of cell proliferation potential after 48 hrs and the miR-130b inhibitor transfected cells were declined in the proliferation potential immediate after 24 hrs post transfection and continued upto 48 hrs post transfection significantly compared to scramble as well as untransfected control (Figure 4.20). The cell concentration was calculated by standard curve generated by OD verses cell number. Moreover, after 48 hours, granulosa cell



transfected with miR-130b precursor exhibited a higher proliferation potential of cells ( $p \leq 0.05$ ), where as miR-130b inhibitors transfected groups showed lower cell proliferation compared to untransfected cells ( $p \leq 0.05$ ).

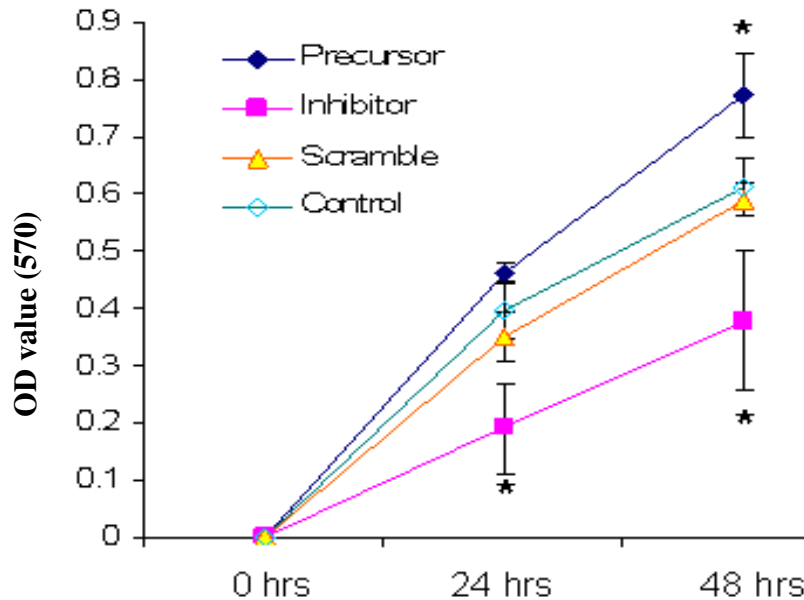


Figure 4.20: Effects of miR-130b overexpression and suppression on granulosa cell proliferation using MTT assay. Error bars represent the mean  $\pm$  SD for four replicates. Significant differences ( $*p \leq 0.05$ ), hrs: hours.

#### 4.4.3.5 miR-130b controls glycolysis in oocyte surrounding cells

To understand the role of miR-130b in glycolysis the primary granulosa and cumulus cells were transfected and lactate assay was performed 24 hours post transfection in 96 wells plate in ELISA reader. Addition of miR-130b to cultured cells lead to a significant elevation in lactate production ( $p < 0.005$ ) where as, inhibitor transfected cells showed a decreased ( $p < 0.01$ ) in lactate production compared to untransfected cells (Figure 4.21). Concentration of lactate was calculated using standard curve which was generated by OD verses dilution.

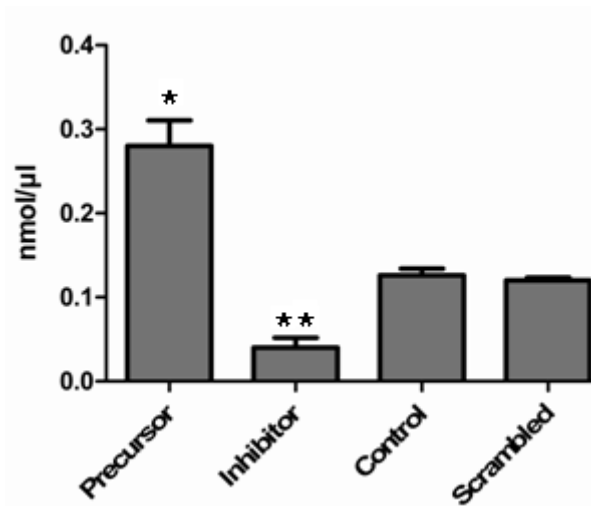


Figure 4.21: Lactate production in miR-130b precursor, inhibitor and scramble RNA transfected cells. The OD was taken at 460 nm calibrated with untransfected cells. Error bars represent the mean  $\pm$  SD for four replicates. Significant differences (\* $p < 0.01$ ) and (\*\* $p < 0.005$ ).

#### 4.4.3.6 Influence of miR-130b in cholesterol biosynthesis

The transfected cells and medium were collected 24 hours post transfection with miR-130b precursor and inhibitor with scramble and untransfected control. The fluorescent reading showed the cholesterol concentration to be very low in all groups of cells. Moreover in precursor transfected cells and medium the cholesterol level was less compared to untransfected cells and medium but not significant (Figure 4.22).

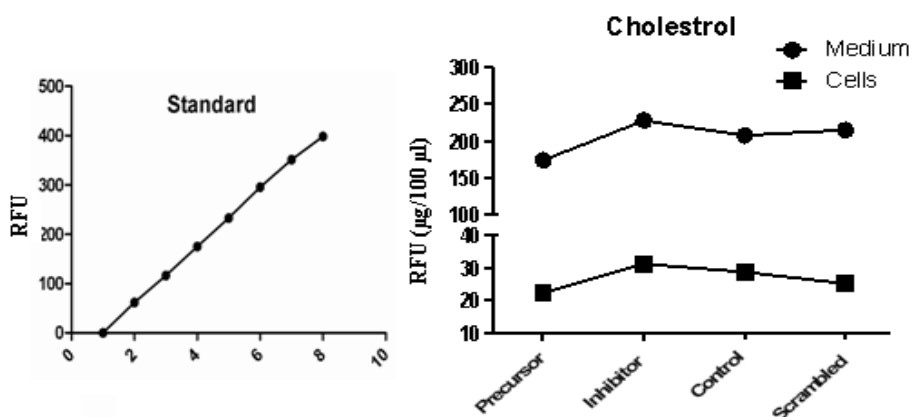


Figure 4.22: The graph shows cholesterol concentration in transfected and untransfected groups of cells and medium. Concentration was calculated by referring standard curve. RFU: Relative Fluorescence Units.

#### 4.5 Effects of miR-130b on *in vitro* embryos development

After microinjection the first cleavage rate obtained was 75% to 81% for all the embryos injected with miR-130b precursor, inhibitor, and scramble with uninjected control group (Table 10). However, these differences were not statistically significant ( $p > 0.05$ ).

Table 10: First cleavage of the zygote injected with miR-130b precursor, inhibitor and scramble compared to the uninjected control group.

Injected group	No. of cleaved embryo/total	First cleavage rate (%)
miR-130b precursor	664/878	75.66 ± 5.22
miR-130b inhibitor	623/814	75.45 ± 7.70
Scramble	676/837	80.79 ± 4.85
Uninjected	498/613	81.38 ± 6.16

hpi: hour post insemination. There was no significant difference among all injected groups ( $p > 0.05$ ).

72 hours post insemination, 68% embryos derived from precursor injected zygotes reached to 8-cell stages, and 16% were remains at 4-cell stage. On the other hand, embryos derived of inhibitor injected zygote reached to 8-Cell was 58% and 4-cell stage 28%, whereas 65% of scramble injected and 69% uninjected controls reached to 8-cell (Figure 4.23A). Moreover, 19% of scramble and 18% uninjected controls were at 4-cells ( $p > 0.05$ ). Similarly, the day 5 morula formation was 33% in precursor injected zygotes, 18% in inhibitor injected, 27% in scramble injected and 32% in uninjection control . However, the morula rate was ( $p \leq 0.05$ ) reduced in the suppression of miR-130b embryos compared to uninjected zygote derived morula (Figure 4.23B)

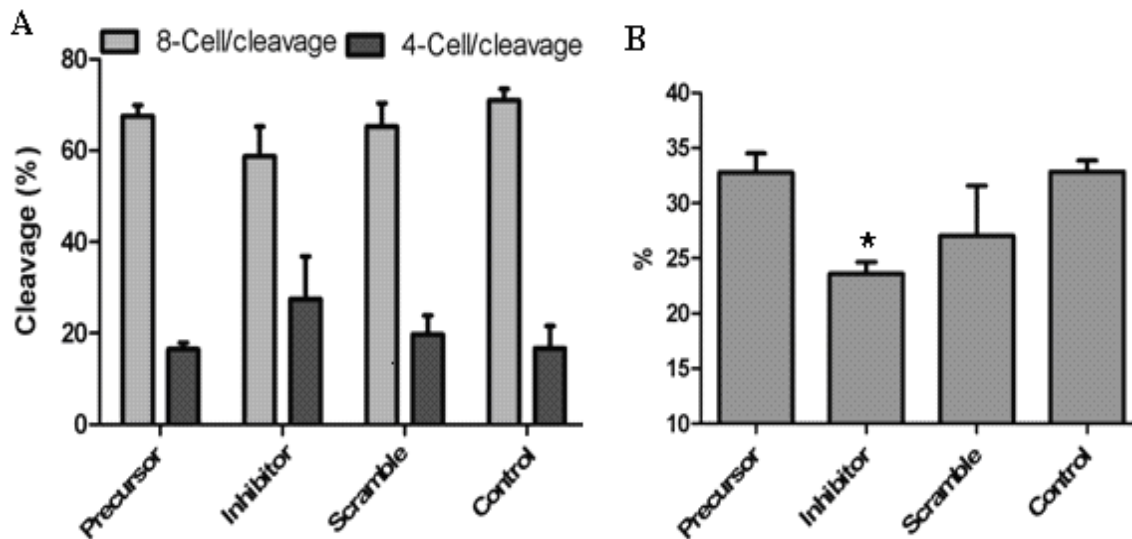


Figure 4.23: (A) The proportion of 4-Cell and 8-Cell stage embryos 72 hours post insemination in different zygote injected groups (B) The proportion of day 5 morula in different zygote injected groups. Error bars represent the mean  $\pm$  SD for four replicates. Significant difference (\* $p < 0.05$ ).

#### 4.5.1 Effect of miR-130b on *in vitro* blastocyst formation

The embryos reached to blastocyst stage were 22%, 14% 19% and 20% in miR-130b precursor, miR-130b inhibitor and scramble injected and uninjected zygote groups respectively (Figure 4.24). However, there was no significantly increase in blastocyst rate in precursor injected zygote groups ( $p > 0.05$ ), but suppression of miR-130b showed significant reduction of blastocyst formation ( $p \leq 0.05$ ).

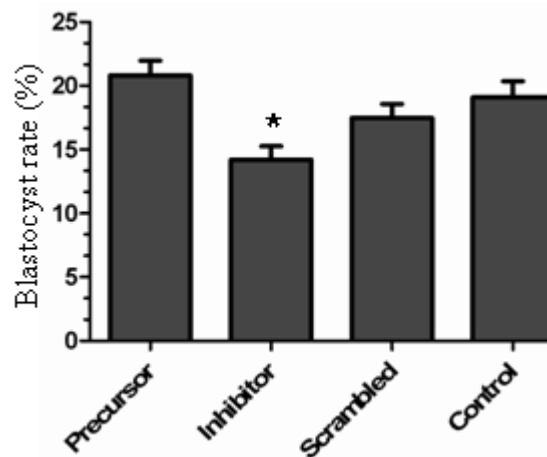


Figure 4.24: The proportion of day 7 blastocyst formation rate derived from miR-130b precursor, inhibitor and scramble injected and uninjected zygotes groups. Error bars represent the mean  $\pm$  SD for four replicates. Significant difference (\* $p < 0.05$ ).

#### 4.5.2 Effect of miR-130b on expression of SMAD5 and MSK1 in blastocyst derived from injected zygotes

To observe the effect of miR-130b on the target genes regulation at blastocysts stage embryos derived from zygotes injected with miR-130b precursor or miR-130b inhibitor and scramble injected and uninjected zygotes were used as controls. The results showed that the expression of miR-130b was (>55-fold) increased in miR-130b precursor injected whereas inhibitor injected showed reduction of miR-130b expression (Figure 4.25A). The expression of MSK1 mRNA was lower in blastocysts derived from miR-130b precursor injected zygotes. On the other hand, the expression of MSK1 was higher in blastocysts derived from inhibitor or scramble injected zygotes compared to blastocysts derived from uninjected zygotes groups (Figure 4.25B). Similarly, the mRNA and protein level of SMAD5 was found to be higher in blastocysts derived from miR-130b inhibitor injected zygotes and tended to be decreased in blastocysts derived from miR-130b precursor injected zygotes (Figure 4.25C, 4.25D). The SMAD5 protein was markedly increased in miR-130b inhibitor injected group blastocysts.

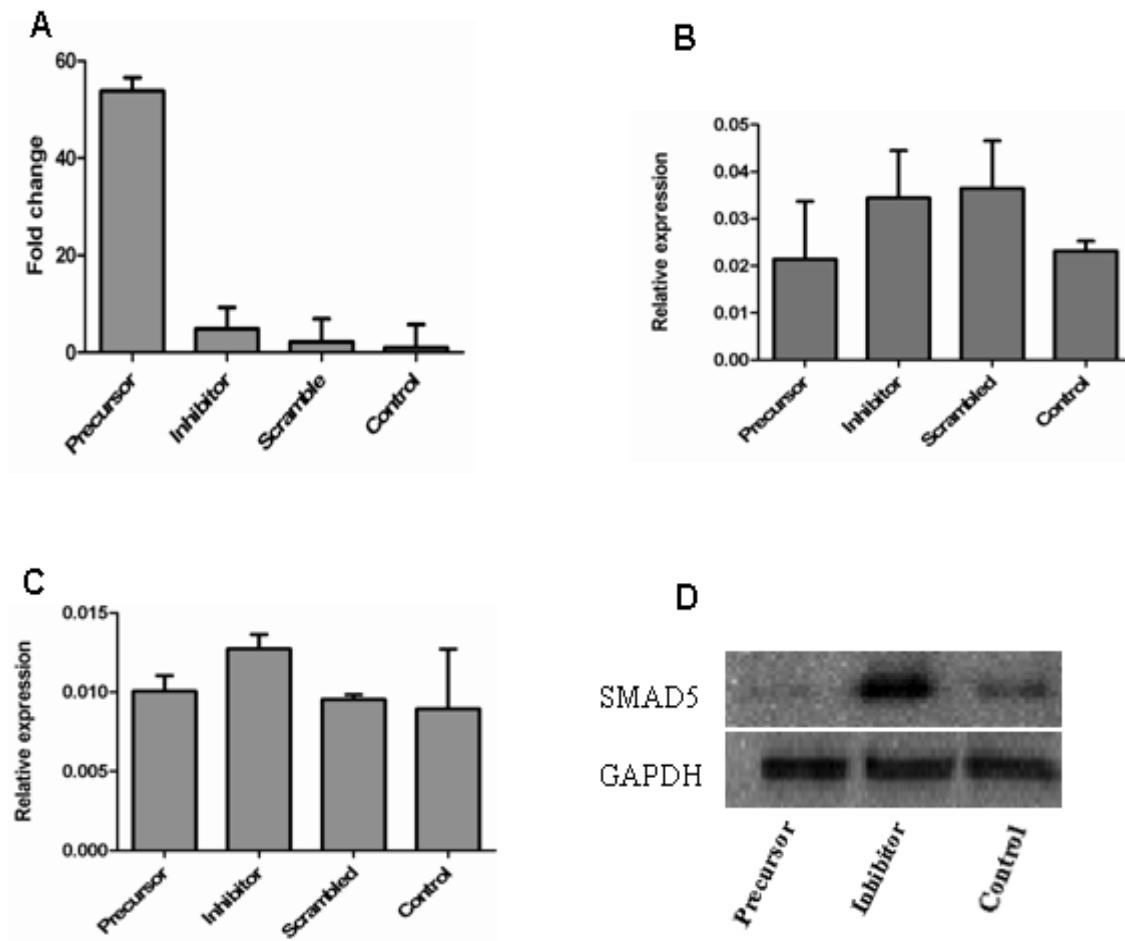


Figure 4.25: (A) The expression of miR-130b in blastocysts derived from miR-130b precursor, inhibitor and scramble injected and uninjected zygotes groups. The relative expression level of MSK1 (B) and SMAD5 (C) mRNA transcript in blastocysts derived from miR-130b precursor, miR-130b inhibitor, scramble injected and uninjected zygotes. (D) Western blot analysis showing the expression difference of SMAD5 in 130b precursor, inhibitor and scramble injected, where as GAPDH used as endogenous control.

#### 4.5.3 Apoptotic effect of miR-130b

Staining of DNA fragmentation was performed by TUNEL assay at blastocyst derived from the zygotes injected with miR-130b precursor, miR-130b inhibitor, scramble miRNA and uninjected groups. The staining of nuclei were recorded and calculated as apoptotic index (API) divided with the total cell number as shown in figure 4.26. No significant difference was observed in the total cell number and neither in TUNEL positive cells among all injected groups.

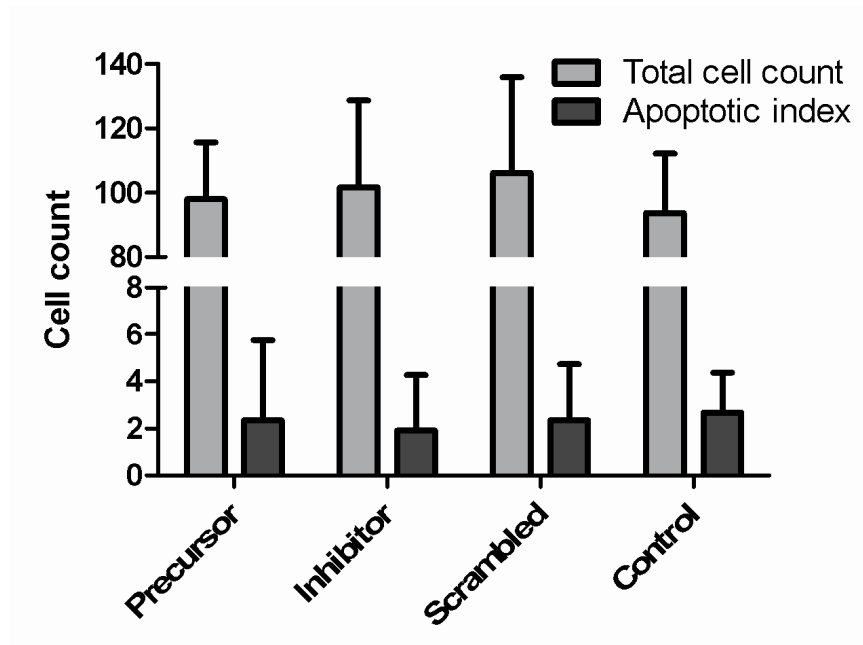


Figure 4.26: The total number of blastocyst cell and apoptotic index of blastocysts stage derived from zygote injected with different treatment groups.

## 5 Discussion

### 5.1 Functional analysis of miRNA in bovine preimplantation

Functional analysis of miRNA is becoming a focus of research in different fields (Chen et al. 2005, Hennebold 2010, Lagos-Quintana et al. 2002, Rosa et al. 2009, Shen et al. 2010b, Xia et al. 2010) but still it leaves a huge area that needs to be explored. In addition, the role of microRNAs in gametogenesis has been evidenced in several reports (Giraldez et al. 2006, McCallie et al. 2010, Tang et al. 2007). Parallel to this, dicer knockout studies showed the importance of the miRNA in oocyte maturation and preimplantation embryo development in mammals (Bernstein et al. 2003, Luense et al. 2008, Ohnishi et al. 2010, Wienholds et al. 2003). But there is no or little research has been conducted to understand the function of specific miRNAs during bovine oocyte maturation or preimplantation embryo development. Therefore, this study was conducted to find the role of miR-130b in bovine oocyte maturation and preimplantation development.

### 5.2 Selection of miRNA for functional analysis study

The oocyte is the gamete contains the half of genetic material and complete cytoplasmic material for an embryo for development (Schultz 2002). These oocytes surrounded with somatic cells and bidirectional communication between the oocytes and their associated follicular somatic cells is essential for the development of both oocytes and cumulus cells (Eppig 2001). For the study of functional analysis of miRNA in oocytes and preimplantation embryo development, miR-130b was selected by referring its expressional pattern between matured and immature oocytes (Tesfaye et al. 2009). According to the authors miR-130b and miR-208 were the miRNAs highly expressed in immature oocyte were selected for further studies. The expression profile of both miR-208 and miR-130b in oocyte companion cells showed the high expression of miR-130b in granulosa and cumulus cells (Figure 4). The focus for study was narrowed to miR-130b due to known bidirectional communication of oocytes and cumulus cells. It is well known that the cumulus cells plays a vital role during maturation (Gilchrist et al. 2004, Gilchrist et al. 2008, Zhang et al. 1995), fertilization and subsequent embryo



development to the blastocyst stage in mammals including bovine (Aparicio et al. 2011, El-Raey et al. 2011, Ge et al. 2008, Huang and Wells 2010, Jin et al. 2006, Wang et al. 2006, Yeo et al. 2009).

### 5.3 Differentially regulation of miR-130 family in oocyte, oocyte surrounding somatic cells and preimplantation embryos

The expression of microRNAs is spatiotemporal, the high expression or reduced expression of some miRNA acts as a marker in different tissue type (Yamamoto et al. 2009, Zubakov et al. 2010). Where as, some prediction of targets specificity was based on the seed sequence which is common for the miRNA family members (Lewis et al. 2003, Lewis et al. 2005) and was validated with the demonstration of reduction in mRNA level in by these family members in a tissue type (Farh et al. 2005, Krutzfeldt et al. 2005, Neilson et al. 2007). Likewise, the let-7 miRNA family was demonstrated to target RAS gene in same tissue (Johnson et al. 2005). To perceive the transcription pattern of the family members of miR-130 (miR-130a, miR-130b, miR-301a and miR-301b), chromosomal localization of the family members was done. miR-130b and miR-301b were located in same chromosome 17 within 10kb where as miR-130a was located on chromosome 15, and miR-301a located at chromosome 19 in bovine according to (miRBase 15) database (Table 8). Although the members of this miRNA family are not located in same chromosome, it was assumed that their regulation may together. To verify this, screening the expression level of miR-130 family was conducted in immature, mature cumulus cells and granulosa cells, immature and mature oocytes and preimplantation embryo. The result has evidenced that miR-130 family don't have any tendency to regulate in same pattern and all miRNA were having its own expression pattern in bovine preimplantation embryo (Figure 4.1, 4.2, 4.4). Although miR-301b was upregulated in zygote to 4-cells stage is required to address the question of functional consequences in early preimplantation stage. It was acknowledged that among the family of miR-130, only miR-130b was abundantly expressed in cumulus cells and granulosa cells (Figure 4.1). Keeping this in mind, miR-130b was further localized in ovarian section, with different stages of follicles. The signal of miR-130b in granulosa cells of antral follicles was predominantly higher compared to the preantral follicular cells and the other ovarian tissues. The high expression of miR-130b by real

time analysis as well as *in situ* hybridization at granulosa and cumulus cells of antral follicles shows the possible role in regulation of granulosa cell secreted factors necessary for granulosa cell function, proliferation, cumulus-oocyte communication and oocyte maturation. The detection of miR-130b was further analyzed for preimplantation stages of bovine embryo. The expression was spatiotemporal and high expression of miR-130b was in 8-cell to the blastocyst stage of preimplantation embryo (Figure 4.4, 4.5). This may suggest that miR-130b could be involved in controlling maternal mRNA and embryonic transcripts. Moreover miR-130b is known to be an embryonic stem cells specific miRNA (Houbaviy et al. 2003, Ma et al. 2010b). This study is the first evidence to localize miR-130b in bovine follicular cells and preimplantation embryo. Taken together, this finding indicates the expression difference of certain miRNA in tissue-specific or cell-specific manner thus emphasizing the intricacy of miRNA-associated regulatory networks and the significance of miRNA functional validation.

#### 5.4 Recognition of miR-130b target genes and their validation

Target genes of miR-130b were selected based on their strong thermodynamics and high score according to *in silico* analysis and their role in cell proliferation, oocyte maturation and embryogenesis. Accordingly, SMAD5, MEOX2, MARCH2, DDX6, EIF2C1, EIF2C4, MSK1 and DOC1R were selected and were experimentally validated. The validation result showed that miR-130b triggered a strong and specific silencing effect on the SMAD5, MEOX2, EIF2C4, MSK1 and DOC1R but no effect on MARCH2, DDX6 and EIF2C1 suggesting *in silico* predicted targets are not always validated experimentally. Interestingly, *In silico* analyzed clone of MSK1, EIF2C4 and MEOX2 were consist of 2 sites with strong 8nt seed complementary from 1-8 but even the luciferase activity was different for each individual gene. The 3'UTR of SMAD5, MARCH2, DOC1R and DDX6 was taken with 2-8 seed sequence (7nt) complementary, here the result showed suppression of SMAD5 and DOC1R by miR-130b but not for MARCH2 and DDX6. It has been already demonstrated that seed sequence sites with as few as 7bp of complementarity to the miRNA 5' end are sufficient to regulate the biologically relevant targets *in vivo* (Doench and Sharp 2004). The experimental validation showed strong reduction of firefly with the clone of MSK1 and SMAD5 (although it has 7bp complementary) where as EIF2C4, DOC1R and MEOX2 were

reduced but comparatively lower than MSK1 and SMAD5. Additionally, MARCH2 and DDX6 (both with 7bp complementary) didn't show any reduction in firefly expression. Similarly, in a study which showed, the 3'UTR of hAT<sub>1</sub>R was computationally validated as a target of several miRNAs including miR-124a, miR-155 and miR-365. To identify the translational repression by each individual miRNA luciferase reporter assay was conducted. Interestingly, only miR-155 could efficiently reduce luciferase activity with specific interaction of the 3'UTR of hAT<sub>1</sub>R mRNA and inhibit translation, where as miR-124a and miR-365 do not interact with the 3'UTR of hAT<sub>1</sub>R mRNAs (Martin et al. 2006). This suggests that validation of target gene computationally is not always applicable for experimental condition, as there are several physiological factors within the cells which work for the complementary of miRNA and its target gene.

Following identification and validation of the target genes of miRNA 130b, the expression pattern of those genes were further investigated during oocyte maturation and preimplantation development stage. Accordingly, the endogenous level of SMAD5 and MSK1 genes were reduced in cumulus cells, morula and blastocyst stage embryos (Figure 4.7, 4.11A-B). These expression patterns of genes with miR-130b were antagonistic. Further protein expression of SMAD5 and MSK1 were estimated in follicular cells and oocytes that showed the same antagonistic pattern with miR-130b in oocytes and companion cells (Figure 4.12). This may imply that endogenous expression of miR-130b involves in the degradation of mRNA. Similarly, antagonistic expression of miRNA and its target genes been described previously by Nielsen et al. they showed during neuronal progenitors about nearly half of the expressed miRNAs were negatively correlated with the expression of their predicted target mRNAs (Nielsen et al. 2009). Another study in *C. elegans* showed lin-4 and let-7 the well known miRNA could lead to significant degradation of their target transcripts of their respective targets that is, lin-14, lin-28, and lin-41 (Bagga et al. 2005). Degradation of mRNA in preimplantation embryo development by miRNA in Zebrafish, showed turnover of maternal mRNAs during early embryogenesis was affected by a single microRNA miR-430. Here they suggested that miR-430 promote the deadenylation and decay of hundreds of target mRNAs that increase the transition between developmental states (Giraldez et al. 2005, Giraldez et al. 2006). This provides more support for the degradation mechanism under physiological conditions. Here, the findings of this study provide the first evidence

experimentally that MSK1, EIF2C4, SMAD5 and MEOX2 are the real target of miR-130b in physiological condition of bovine cumulus cells.

Among EIF2C4, MSK1, MEOX2 SMAD5 and DOC1R the selection of MSK1 and SMAD5 was done on the bases of target validation where high reduction of firefly expression was observed for MSK1 and SMAD5. Furthermore, by peering several reviews MSK1 and SMAD5 were found to be involved in signalling pathway of folliculogenesis, oocyte maturation and cell proliferation (Hirshfield 1991, Hsueh et al. 1984, Knight and Glistler 2003). In addition SMAD is the central gene in the TGF-superfamily signalling (Abecassis et al. 2004, Kawabata and Miyazono 1999). SMAD signalling is also well known for GDF9 and BMP15 in oocyte growth and maturation (Gilchrist et al. 2004, Hussein et al. 2006, McNatty et al. 2007). Implication of SMAD signalling pathway in follicular development, granulosa cell proliferation, terminal differentiation and function is well known (Gilchrist et al. 2004, Hsueh et al. 1984, Hussein et al. 2006, McNatty et al. 2007, Myers and Pangas 2010). SMAD signalling pathway has also been reported for inducing apoptosis in bovine granulosa cells (Zheng et al. 2009, Gilchrist et al. 2003) and in several other cells (Bravo et al. 2003, de Luca et al. 1996, Jang et al. 2002) in human cancer cell lines and inducing G<sub>1</sub> arrest (Lynch et al. 2001, Stuelten et al. 2006). Moreover, MSK1 believed to regulates SMAD signalling pathway by phosphorylating SMAD3 (Abecassis et al. 2004, van der Heide et al. 2011). Other reports showed that MSK1 is reported to induce G<sub>1</sub>/S arrest during neuronal differentiation and neuronal cell death (Hughes et al. 2003, McCoy et al. 2005, Wong et al. 2004). Localization pattern of SMAD5 relatively higher in granulosa cells compared to cumulus cells and oocytes where as MSK1 protein was relatively higher in oocyte compared to follicular granulosa cells and cumulus cells although both SMAD5 and MSK1 protein are located into the nucleus. Therefore the cell specific expression of SMAD5 and MSK1 may suggest that the former may play role in oocyte surround cell proliferation and the later function in oocyte maturation.

The ectopic expression of mir-130b has shown the degradation of mRNA of MSK1 and SMAD5 and also the markable reduction of target protein in oocyte, cumulus cells, granulosa cells and blastocyst. Similarly, there are several evidence which shows the degradation of target mRNA by inducing ectopic miRNA as during retinal development over-expression of miR-124; miR-125 and miR-9 with significant predicted effects upon global mRNA levels resulted in a decrease in mRNA expression of five out of

ACCN2, ETS1, KLF13, LIN28B, NFIB and SH2B3 (Djuranovic et al. 2011). In addition, a report showed in A549 cells the ectopic expression of miR-200c cleaves the mRNA of TCF8 and reduced the endogenous transcript in the cell (Hurteau et al. 2007). In mouse granulosa cells overexpression of miR-224 had shown suppression of SMAD4 where as protein was reduced (Yao et al. 2010a).

### 5.5 The role of miR-130b in oocyte maturation

During oocyte development, synthesis and storage of mRNA was conducted to guide embryo development earlier to the embryonic genomic activation. Oocyte maturation are affected by several factors which is already indicated elsewhere (Amiri et al. 2009, Kren et al. 2004, Vaknin et al. 2001, Wang et al. 2009a, Wang et al. 2009b). To synchronize the stability and activation of these transcriptoms many post-transcriptional regulation also been conducted in oocyte. These ends with several control mechanism at different stages of maturation (Heikinheimo and Gibbons 1998, Luna et al. 2001). Role of miRNA during oocyte maturation was also been studied by many researches (Giraldez et al. 2005, Tang et al. 2007). The predominance of genes was strongly control by miRNAs at the onset of fertilization for the global protein abundance (Nakahara et al. 2005). The Dicer, a protein require for miRNA biogenesis, knockout mice oocytes demonstrated the arrest in meiosis, suggests the importance of miRNA in very earliest stages of development (Murchison et al. 2007). Elsewhere, exhibited the deletion of Dicer from the oocyte blocks cell division in mouse shows the maternal miRNA contribute for zygotic development (Tang et al. 2007). In this study, microinjection of miR-130b precursor in immature oocytes shows the increase of polarbody extrusion where as suppression of miR-130b function significantly ( $p < 0.01$ ) reduction on the first polarbody extrusion (Table 9 and Figure 4.14). The chromosomal staining showed the high number of oocytes arrested at telophase I stage in the inhibition of miR-130b in oocytes but the apparent mechanism was not clear. Microtubule organization and meiotic spindle formation has been shown to be controlled through the MAPK (mitogen activated protein kinase) pathway by phosphorylation of DOC1R protein (Terret et al. 2003). It is well known that MSK1 is a downstream protein of MAPK pathway in oocyte maturation (Hauge and Frodin 2006) which phosphorylates DOC1R protein while oocyte maturation (Terret et al. 2003). The

high regulation of DOC1R protein in young oocyte compared to matured oocyte (Grondahl et al. 2010, Terret et al. 2003) leads to conclude the high amount of the phosphorylated of DOC1R can delays the polarbody extrusion or maturation of oocyte. Mitochondria are known to be the powerhouse of cells which regulates cellular metabolism. Active cell has high cellular metabolism and apoptotic cells drops the activity for the functioning of normal metabolic process and also reduction in the mitochondrial membrane potential (Kroemer et al. 1997). In embryos mitochondria maternally inherited and provide the principal sites for oxidative damage and provide energy production in all embryonic cells leading to regulation of preimplantation embryo development. The current outfinding showed the notably high mitochondrial membrane potential in the oocytes performed with ectopic expression of miR-130b, where as, drop on the fluorescent quenching in miR-130b inhibition injected oocytes (Figure 4.15). Similar work was conducted, to see mitochondrial dysfunction in oocytes was found to be directly responsible for the early arrest of preimplantation embryos *in vitro* (Thouas et al. 2004). Moreover, oocyte mitochondrial damage effects on there development and blastocyst formation (Thouas et al. 2004, Thouas et al. 2006). According to Thouas et al. (2006) blastocyst development *in vitro* is relatively resistant to low levels of mitochondrial injury induced but was intended to identify any delayed developmental effects of this treatment after implantation where as another says that the oocytes with mitochondrial damage can caused for pre- and postimplantation developmental competence and resulted in inhibited zygote formation after fertilization, reduced blastocyst survival and developmental damage for *in vitro* blastocysts generation (Thouas et al. 2004, Thouas et al. 2006).

Although recent reports show the limited role of miRNA in oocyte (Ma et al. 2010a), but our current finding has witnessed the role of miRNA in oocyte maturation and maternal transcript regulation. The injection of miR-130b precursor, inhibitor and scramble has shown a new definition for the presence and regulation of miRNA in preimplantation. The central dogma of gene regulation shows the transcription of gene in any cell type or stage of cell when it require, the same regulation pattern should be for miRNA too, here we have seen a bunch of experiments has shown the different trend of miRNA regulation in oocyte or in preimplantation of several animals (Giraldez et al. 2006, McCallie et al. 2010, Tesfaye et al. 2009, Yang et al. 2008) which witness the regulatory requirement of the miRNA at these stages. Maternal genes are higher in

immature oocyte compared to mature oocyte (Bettegowda and Smith 2007, Fair et al. 2007, Mamo et al. 2011) the signal within the oocyte to regulate the degradation of the excess loaded genes can be miRNA (Giraldez et al. 2005, Ramachandra et al. 2008). The observation of oocyte maturation showed that miR-130b is essential for oocyte maturation. This is the first demonstration for any miRNA functions during bovine oocyte maturation and metabolic activity.

### 5.6 Influence of miR-130b in oocyte surrounding cells proliferation and cholesterol biogenesis

In this study, it was shown miR-130b promotes primary granulosa cell proliferation. To investigate the roles of miR-130b in granulosa cell proliferation, miR-130b was functionally characterized in granulosa and cumulus cells. Ectopic expression of miR-130b significantly increases the proliferation potential of granulosa cells; where as inhibition of miR-130b reduces the proliferation potential. This may indicate that miR-130b could involve in follicular development and granulosa cell proliferation. Parallel to this result, a report showed the overexpression of miR-130b increased cell viability, reduced cell death and decreased expression of *Bim* in TGF- $\beta$  mediated apoptosis, by downregulating the RUNX3 protein expression (Lai et al. 2010). Additionally, a report was showed that miR-130b target TP53INP1 in MT4 cells. The report shows, the knockdown of miR-130b increases TP53INP1 which leads to decreased MT4 cell viability (Yeung et al. 2008). Another work for the same protein showed, the increase of miR-130b decreased TP53INP1 in CD133<sup>-</sup> cells that improve the self renewal and also tumorigenicity *in vivo* (Ma et al. 2010b). Similar to these findings, a recent study has shown that the ectopic expression of miR-224 also promotes mouse granulosa cells proliferation in mouse by targeting SMAD4 (Yao et al. 2010a).

Regulation of cholesterol was not been much affected in cell but cholesterol efflux was comparatively low in miR-130b induced cells. Similar, affect has been found by Lee et al., that miR-130 prevents the unscheduled differentiation of adipocytes by potent repression of PPARgamma, a master regulator of adipogenesis (Lee et al. 2011). Another report showed miR-27 repress PPARgamma in human multipotent adipose-derived stem cells, as well as in mouse preadipocyte model systems, where it was linked to a blockage of adipogenesis (Karbiener et al. 2009, Kim et al. 2010a, Lin et al. 2009).

PPARgamma may play a role in the regulation of granulosa-lutein cells functions through inhibiting proinflammatory factors (Chen et al. 2009). These data suggested that PPAR gamma may be involved in follicular atresia and FSH-stimulated steroidogenesis during follicle development influenced by MAPK signalling pathway (Zhang et al. 2007b). The outfinding has shown high cholesterol level may leads to follicular atresia. Whereas, correlation of the result with these references showed the low expression of cholesterol in media indicates low cholesterol efflux and high cell survival and proliferation in the ectopic expression of miR-130b.

### 5.7 Influence of miR-130b in glycolysis of oocyte surrounding cells

Glycolysis is a metabolic process can be regulated by oxidative and other cellular stresses, fast growing cells or in cancer cells (Elstrom et al. 2004, Shi et al. 2009). Although in cumulus cells high glycolysis is performed for the metabolic requirement for oocytes resumption of meiosis (Biggers et al. 1967, Eppig et al. 2000). In this study, oocyte companion cells transfected with miR-130b showed high lactate production where as inhibition of miR-130b significantly reduced the glycolysis by the reduction of lactate production. It is possible that in bovine presence of endogenous miR-130b in oocyte companion cells induce proliferation through promoting glycolysis. Similarly, lactate levels was measured for the effect of miR-210 on HCT116 cells targets ISCU and COX10 expression which shows the high regulation of lactate in miR-210 treated group compared to negative control (Chen et al. 2010) showed the high metabolic activity and proliferation by the influence of miR-210. Another study shows the metabolic control of cardiomyocytes by miR-133 which regulates the expression of GLUT4 by targeting KLF15 (Horie et al. 2009). In oxidative and cellular stresses, glycolysis was regulated by constitutive activity of the serine/threonine kinase, where both MSK1 and SMAD5 are the members (Elstrom et al. 2004) shows the involvement of miR-130b in direct regulation of lactate production, although the appropriate pathway affected was unclear.

Hence the findings of this study provide the first evidence that miR-130b participates in regulation of bovine antral granulosa cell proliferation and the function of glycolysis by targeting SMAD5 and MSK1.



### 5.8 Effect of miR-130b on blastocyst formation and apoptosis

Selecting embryos with high implantation potential is one of the most important challenges in the field of assisted reproduction. Embryo quality has traditionally been evaluated based on cleavage rate and blastomere morphology (Puissant et al. 1987)). In the present study quantitative expression profiling of miR-130b throughout the preimplantation embryonic stages evidenced that miR-130b is activated from both maternal and embryonic genome. Transcript abundance for miR-130b was high at immature oocytes but down-regulated from mature oocytes until 4-cell stage (but detectable). The amount of miR-130b was relatively increased by 8-cell and reached the peak at the morula and blastocyst stages. The aim was to evaluate the effect of the miR-130b on *in vitro* blastocyst development. Therefore, injection of miR-130b precursor at zygote stage was conducted which didn't show any markable effect on the cleavage rate or development of embryos upto blastocyst formation. Where as suppression of miR-130b at zygotes show arrested embryos at 4-cell by 72 hpi and didn't reach to 8-cells. The blastocyst rate too was affected by suppression of miR-130b at zygote stage and significant reduction of blastocyst was observed. Similar studies in zebrafish development was done, where no endogenous let-7 miRNA expression found in first 48 hours of development observed a specific phenotype upon injection of a double stranded let-7 miRNA in one-cell stage zebrafish embryos. At 26 hours post-fertilization (hpf), the embryos found to be retarded in development. Moreover lack of proper eye development and reduced tail with yolk sac extension was observed. The embryonic death was observed after 2 days (Kloosterman et al. 2004). However a report shows the limited role of miRNA in mouse preimplantation embryo (Ma et al. 2010a, Suh et al. 2010). Similarly, the result shows ectopic expression of miR-130b didn't show any notable changes in preimplantation embryos development and in the phenotype of the embryos. Likewise, the suppression of miR-130b at zygote stage shows no effect on the cleavage rate but post embryonic genomic activation, blastocyst formation was significantly reduced in the miR-130b suppressed embryos. Endogenous expression of miR-130b was high at morula and blastocyst stage which hypothesis the functional role or miR-130b at the late stages of preimplantation stage of bovine embryos. Similarly, the observation shows suppression of miR-130b reduces the formation of morula and blastocyst. Although, total number of blastocyst formation was

reduced in miR-130b inhibitor injected zygotes but there was no significant difference in total cell number in blastocyst and apoptotic index among the blastocysts derived from zygote injected.

The present study has shown the endogenous expression of miR-130b was required for oocyte maturation, granulosa and cumulus cell proliferation and function, and development of embryos after embryonic genome activation. However, further study may be required to understand the involvement of miR-130b in implantation or postimplantation development.

## 6 Summary

The maternal factors associated with the aberrant gene expression in the oocyte maturation and preimplantation embryo development has been one of the major causes of pregnancy failure in cattle. The period of preimplantation development occurs with different timing in various species and been marked by many molecular events including maternal to zygotic transition, morula compaction and the turning point of cell differentiation into the inner cell mass and trophectoderm at the blastocyst stage. Normally, preimplantation development of an embryo relies on the proper genetic programming during preimplantation period starts from the gametogenesis and continues to the zygotic genomic activation. The genetic programming includes the posttranscriptional modification where miRNAs has merged as a major class to fine tune the genomic messengers. Hence, investigating the miRNA in oocyte maturation and preimplantation embryos provides a unique opportunity for generating molecular marker that may be associated with oocyte maturation and embryo preimplantation development. Therefore, in the current study, role of miR-130b was investigated in oocyte maturation and preimplantation embryo development in bovine. As reported, miR-208 and miR-130b were differentially expressed in bovine immature and mature oocytes, both miRNAs were further expression profile in cumulus and granulosa cells using qRT-PCR. The result has shown relatively high expression of miR-130b in granulosa and cumulus cells compared to miR-208. Keeping in mind, the importance of oocyte companion cells in oocyte maturation miR-130b was selected for further study. Additionally, miR-130b share same seed sequence to its family members required to expression profile the miR-130 family in oocyte, cumulus cells, granulosa cells and preimplantation embryos. The expression profiling resulted with the high expression of miR-130b in both cell types as well as in immature oocytes and late preimplantation stage after zygotic genome activation. Furthermore, miR-130b was localized in ovarian section and preimplantation embryos, where it was strongly detected at the granulosa cells of antral follicles compared to the primordial, primary, secondary follicles and other ovarian tissues. The detection of miR-130b was high in cumulus cells of mature and immature oocytes, morula and blastocyst compared to mature oocyte, zygote, 2-cell, 4-cell and 8-cell embryo. High expression of miR-130b indicates that it may have

some role in granulosa cells proliferation or function, oocyte maturation or in scavenging the maternal transcripts.

To identify the appropriate target of miR-130b *in silico* analysis was done and with all threshold criteria RPS6KA5 (MSK1), SMAD5, EIF2C1, EIF2C4, MARCH2, MEOX2, DDX6 and DOC1R were selected for experimental validation. Prior to validation all selected genes were quantified on *in vitro* produced bovine embryos using qRT-PCR. The EIF2C4 and DDX6 were detected at higher level at morula and blastocyst stage embryos compared to early stages of embryo. Expression of MSK1, SMAD5, MARCH2 and EIF2C1 genes were found to be highly abundant at early developmental stages in oocytes to 8-cell compared to morula and blastocyst stage embryos. MEOX2 and DOCR1 were not been detected from mature oocyte to blastocyst stage. The experimental validation was conducted using pmirGLO Dual-Luciferase miRNA Target Expression Vector. Firefly and renilla activity was observed 48 hours post transfection. The results validated that MSK1, SMAD5, EIF2C4, DOCR1 and MEOX2 are the real targets of miR-130b where as EIF2C1, DDX6 and MARCH2 were not validated to be the target of miR-130b.

The high reduction in luciferase efficiency of MSK1 and SMAD5 among the above validated targets and the antagonistic expression relation between miR-130b and gene in preimplantation was kept in mind for the selection of MSK1 and SMAD5 for further studies. MSK1 and SMAD5 were found to be involved in signalling pathway of folliculogenesis, oocyte maturation and cell proliferation. The transcript abundance of MSK1 and SMAD5 in oocyte maturation and corresponding cumulus cells showed both genes were higher in oocytes compared to its corresponding cumulus cells. The protein localization showed SMAD5 and MSK1 were present in oocyte, granulosa cells and cumulus cells.

To analyse the role of miR-130b during oocyte maturation, good quality immature oocytes were categorized into four groups precursor, inhibitor and scramble (injected) and uninjected. From each group after 22 hours of injection (n = 300) oocytes were collected for molecular analysis, (n = 50) oocytes for mitochondrial assay and (n = 150) oocytes for Hoechst staining. To observe the effect of miR-130b in preimplantation development (n = 700) zygotes were categorized for each injected (precursor, inhibitor and scramble) and uninjected groups for investigation. Zygotes were injected and *in*

*vitro* cultured upto blastocyst stage. Day 8 blastocyst were collected for mRNA and protein expression analysis.

To assess the effect of miR-130b in mRNA transcript abundance and protein expression, oocytes were collected after 22 hours of injection and phenotype was observed. The first polarbody was accounted for all injected groups where, precursor showed the higher polarbody extrusion with (86.3%), inhibitor (73.3%) which was significantly reduced compared to scramble (85.13%) and uninjected (84.65%) oocytes. Similarly, 22 hours post injection between (10-12%) of the oocytes were remain at GV stage in all injected groups of oocytes, (22%) of inhibitor injected and (8%) precursor injected groups arrested at Telophase I stage. On the other hand, the proportion of oocytes reached to MII stage was significantly lower in inhibitor injected (60%) ( $p \leq 0.05$ ) compared to the uninjected control group (75%). Where as, miR-130b precursor injected oocyte reached to MII stage was (80%). The mitochondrial fluorescent quenching was observed 22 hours post injection in oocyte which showed a very strong signal in miR-130b precursor injected oocytes where as low in inhibitor injected oocytes compared to scramble or uninjected oocyte groups.

The observation of the transcripts in injected oocytes showed a significant high expression (8000-fold) of miR-130b in precursor injected compared to other groups of injected and uninjected oocytes. However, miR-130b precursor injection was resulted in decreased in MSK1 and SMAD5 transcript abundance where as miR-130b inhibitor injected has significantly ( $p < 0.05$ ) increased compared to uninjected control group. Moreover, immunohistochemistry localization was preformed for all injected and uninjected group oocytes and the result indicated that MSK1 protein expression was reduced by miR-130b overexpression where as suppression of miR-130b has remarkable increased the protein level compared to scramble injected and uninjected control oocytes. Similarly, westernblot analysis showed the reduction of both MSK1 and SMAD5 in precursor injected oocytes where as high expression in inhibitor injected oocytes.

Importance of bidirectional communication between oocytes and surrounding somatic (granulosa and cumulus) cells was well known. The cells ( $2 \times 10^5$ ) were cultured in 24 wells plate and transfected with 30 nM/ml miR-130b precursor, inhibitor and scramble miRNA. Cell viability was observed in 4 replicates using Trypan blue at 24 and 48 hours of transfection. Live cell count was performed under the microscope in

haemocytometer and the live cell count was relatively higher in precursor transfected cells and lower in inhibitor transfected cells compared to scramble and untransfected control groups ( $p \leq 0.05$ ). Following this, cell proliferation assay was conducted to determine the proliferation of cells using MTT assay. Primary granulosa cells were cultured in 96 wells plate ( $7.5 \times 10^4$ ) and transfected with 50 nM/ml of either of miR-130b precursor, inhibitor or scramble. The assay was performed after 24 and 48 hours of transfection. The result showed significant ( $p \leq 0.05$ ) increase in proliferation of cells transfected with miR-130b precursor and reduction in cells transfected with miR-130b inhibitor ( $p \leq 0.05$ ) compared to scramble transfected as well as untransfected cells at 24 and 48 hours time point.

To understand the role of miR-130b in glycolysis the primary granulosa and cumulus cells were transfected and lactate assay was performed 24 hours post transfection in 96 wells plate using multiplate reader. Accordingly, the precursor transfected cells have shown higher ( $p < 0.005$ ) lactate production (nmole) where as inhibitor transfected cells showed a decreased ( $p < 0.01$ ) in lactate production (nmole) compared to scramble and untransfected controls. Effect of miR-130b on cholesterol biosynthesis in granulosa and cumulus cells did not show any significant difference although miR-130b precursor transfected cells showed low cholesterol efflux. The molecular analysis showed reduction of mRNA and protein in miR-130b precursor transfected cells where as high expression in miR-130b inhibitor transfected cells compared to control groups.

The effect of miR-130b in preimplantation embryos was observed by overexpression and suppression of miR-130b at zygote stage. Embryos were collected at 8 days blastocyst and phenotype was collected on specific time intervals. The first cleavage rate was about 75% to 81% for all embryos derived from miR-130b precursor, inhibitor, scramble and uninjected zygotes ( $p > 0.05$ ). After 72 hours, 68% of precursor 58% inhibitor, 65% scramble and 69% uninjected zygotes reached to 8-cell stages. On the other hand, 16% precursor, 28% inhibitor, 19% scramble injected and 18% uninjected controls were at 4-cells. However, the morula rate was ( $p \leq 0.05$ ) reduced in inhibitor injected zygotes compared to uninjected zygotes. The embryos reached to blastocyst in precursor injected zygotes were the highest 22%, inhibitor injected zygotes were 14%, scramble injected 19% and uninjected 20%. A significant reduction was observed in the formation of blastocyst derived from inhibitor injected zygotes ( $p \leq 0.05$ ).

---

In conclusion, the present study shows the functional importance of miR-130b during bovine oocyte maturation and granulosa cell proliferation. The high regulation of miR-130b in granulosa cells of antral follicle leads to the granulosa cell proliferation and increases the metabolic activity by increasing lactate production in oocyte surrounding cells, which may help the oocytes for maturation and further development. During *in vitro* oocyte maturation miR-130b was analyzed to be an important transcript present in abundance and helps the oocytes to undergo maturation and blastocyst formation. The data highlights the potential involvement of miR-130b in oocyte metabolic activity which increases the mitochondrial activity. The overall data provides the significant evidence that transcription of miR-130b is needed during bovine oocyte maturation and granulosa cell proliferation. High expression of miR-130b at morula and blastocyst stage embryo may influence the further embryo implantation. However, in functional depth studies are required whether miR-130b is involved during bovine embryo implantation.

## 7 Zusammenfassung

In der vorliegenden Studie wurde die Rolle der miR-130b in der Oozytenmaturation und in der embryonalen Präimplantationsentwicklung beim Rind untersucht. Die Expression von miR-130b wurde mittels RT-PCR in Kumulus- und in Granulosazellen untersucht. Dabei konnte bei miR-130b sowohl in Kumulus- als auch in Granulosazellen eine höhere Expression detektiert werden als im Vergleich zur miR-208.

Das Expressionsergebnis zeigte eine hohe Expression von miR-130b in beiden Zelltypen sowie in immaturierten Oozyten und im späten Präimplantationsstadium nach zygotischer Genomaktivierung. Darüber hinaus wurde die miR-130b in Bereichen des Eierstockes und in Präimplantationsembryonen lokalisiert. Am stärksten wurde sie in den Granulosazellen des Antrum folliculi im Vergleich zu den primordialen, primären und sekundären Follikeln sowie anderen Ovariengeweben nachgewiesen. Die miR-130b konnte bei Präimplantationsembryonen am stärksten in den Kumuluszellen vom maturierten und immaturierten Oozyten sowie Morula und Blastozysten detektiert werden. Ebenfalls zeigten sich in maturierten Oozyten, Zygoten, 2-Zeller, 4-Zeller und 8-Zeller Embryonen Expression, aber im geringeren Ausmaß. Eine hohe Expression der miR-130b läßt ihre Bedeutung in der Proliferation oder Funktion von Granulosazellen, in der Maturation von Oozyten oder bei der Abfrage von maternalen Genen vermuten. Zur Identifizierung der genauen Ziel Gene der miR-130b wurden *In silico* Analysen durchgeführt. Dafür wurden unter Berücksichtigung der Threshold-Kriterien zur Validierung die Gene RPS6KA5 (MSK1), SMAD5, EIF2C1, EIF2C4, MARCH2, MEOX2, DDX6 und DOC1R ausgewählt. Zur Validierung wurden die Gene in *in vitro* erzeugten Rinderembryonen mittels RT-PCR quantifiziert. EIF2C4 und DDX6 zeigten im Morula- und Blastozystenstadium ein hohes Expressionsmuster, während sie im frühen Embryonenstadium runter reguliert waren. Bei der Expressionsanalyse der Gene MSK1, SMAD5, MARCH2 und EIF2C1 konnte ein hohes Expressionsniveau im frühen Entwicklungsstadium von Oozyten bis zum 8-Zeller beobachtet werden, während im Morula- und Blastozystenstadium ein niedriges Expressionsmuster detektiert wurde. Die Gene MEOX2 und DOC1R konnten nicht während der gesamten Präimplantation (von der maturierten Oozyte bis zur Blastozyste) detektiert werden. Die experimentelle Validierung wurde unter Verwendung des pmirGLO Dual-Luciferase miRNA Target



Expression Vektor durchgeführt. 48 Stunden nach der Transfektion wurde die Firefly und Renilla Aktivität beobachtet. Die Ergebnisse der Validierung erbrachten das MSK1, SMAD5, EIF2C4, DOCR1 und MEOX2 Ziel Gene von miR-130b sind, während dieses für EIF2C1, DDX6 und MARCH2 nicht beobachtet werden konnte.

Von den validierten Genen führte die hohe Reduktion der Luciferase Effizienz von MSK1 und SMAD5 und die antagonistische Beziehung zwischen der miR-130b mit den Genen während der Embryonalentwicklung zu dem Resultat MSK1 und SMAD5 für weitere Untersuchungen auszuwählen. Für die Gene MSK1 und Smad5 konnte festgestellt werden, dass sie in den Pathways der Follikulogenese, Oozytenmaturation und Zellproliferation von Bedeutung sind. Der Vergleich der Expressionsniveaus von MSK1 und SMAD5 während der Oozytenmaturation und ihren dazugehörigen Kumuluszellen zeigte, dass beide Gene in den Oozyten ein höheres Expressionsniveau im Vergleich zu den entsprechenden Kumuluszellen haben. Bei der Proteinlokalisierung konnte eine Expression von MSK1 in Oozyten und Kumuluszellen und für SMAD5 eine höhere Expression bei folliculären Granulosazellen beobachtet werden.

Zur Analyse der Funktion von miR-130b während der Oozytenmaturation, wurden immaturierte Oozyten mit guter Qualität in vier Gruppen Precursor, Inhibitor, Scramble und nicht behandelt eingeteilt. In jeder Gruppe wurden 22 Stunden nach der Injektion Oozyten für die molekulare Analyse (n = 300), Oozyten für mitochondriale Analyse (n = 50) und Oozyten für die Hoechst-Färbung (n = 150) gesammelt. Zur Beobachtung der Wirkung von miR-130b in der Präimplantationsentwicklung (n = 700) wurden Zygoten für jede Behandlungsgruppe (Precursor, Inhibitor und scramble) kategorisiert sowie in injizierte und nicht injizierte für die folgenden Untersuchung eingeteilt. Die Zygoten wurden injiziert, in vitro kultiviert und an Tag 8 des Blastozystenstadiums für die Transkriptions- und Proteinexpressionsanalysen gesammelt. Um den Effekt von miR-130b auf die RNA- und Proteinexpression beurteilen zu können, wurden Oozyten 22 Stunden nach der Injektion gesammelt und der Phänotyp beobachtet. Die ersten Polkörper konnten für alle injizierten Gruppen nachgewiesen werden. Die Precursor injizierten Oozyten zeigten die höchste Polkörper Extrusion mit (86,3%), die Scramble injizierten mit (85,13%), die nicht injizierten Oozyten mit (84,65%) und die Inhibitor injizierten mit (73,3%), was deutlich niedriger war. Ebenso konnte 22 Stunden nach der Injektion bei 10–12 % angefärbten Oozyten aller Behandlungsgruppen das GV Stadium beobachtet werden, während 22 % der Inhibitor

injizierten und 8 % der Precursor injizierten Gruppen in der Telophase I verblieben. Ein signifikant ( $p \leq 0,05$ ) geringerer Anteil der Inhibitor injizierten Oozyten (60%) erreichte die MII Phase im Vergleich zur nicht injizierten Kontrollgruppe (75%) und Precursor injizierten Oozyten (80%). Die mitochondriale Aktivität wurde 22 Stunden nach der Injektion der Oozyten beobachtet. In miR-130b Precursor injizierten Oozyten war ein stärkeres mitochondriales Fluoreszenzsignal und ein niedrigeres bei Inhibitor injizierten Oozyten im Vergleich zu Scramble oder nicht injizierte Oozyten sichtbar.

Die Transkriptionsanalyse der injizierten Oozyten zeigte, dass die Precursor miR-130b injizierten Oozyten signifikant höhere Expression (8000 fache) im Gegensatz zu den anderen Oozytengruppen aufweisen. Die miR-130b Precursor injizierten hatten eine niedrigere Expression des MSK1 Transkriptes. Die miR-130b Inhibitor injizierten hatten eine signifikant höhere MSK1 Expression im Vergleich zur nicht injizierten Kontrollgruppe ( $p < 0,05$ ). SMAD5 zeigte in der Precursor injizierten Gruppe eine 15% verringerte Expression, hingegen zeigten die Inhibitor injizierten Oozyten eine signifikant höhere Expression nach der Maturation als die Kontrollgruppe. Zudem wurde eine immunohistochemische Lokalisierung für alle injizierten und nicht injizierten Oozytengruppen durchgeführt. Die Ergebnisse zeigten, dass die Proteinexpression von MSK1 durch die hohe Expression von miR-130b reduziert wurde. Ebenfalls konnte durch das Ausschalten der miR-130b ein bemerkenswerter Anstieg des MSK1 Proteinlevels im Vergleich zur Scramble injizierten und nicht injizierten Kontrolloozyten ermittelt werden. Durch Westernblot Analysen konnte ebenfalls eine geringere Expression von MSK1 und SMAD5 in Precursor injizierten Oozyten und eine höhere Expression dieser bei Inhibitor injizierten Oozyten ermittelt werden.

Die bidirektionale Kommunikation zwischen Oozyten und ihrer umgebenen somatischen Zellen (Granulosazellen und Kumuluszellen) ist für ihre bedeutende Rolle bekannt. In 24 Wellplatten wurden  $2 \times 10^5$  Zellen kultiviert und mit 30 nM/ml miR-130b Precursor, Inhibitor und Scramble miRNA transfiziert. Die Lebensfähigkeit der Zellen wurde mittels Trypanblau in 6 Wiederholungen 24 und 48 Stunden nach der Transfektion überprüft. Die Zellzahlbestimmung erfolgte unter dem Mikroskop mittels Hämocytometer. Dabei konnte eine höhere Zellzahl bei den Precursor transfizierten Zellen und eine geringere Zahl bei Inhibitor behandelten Zellen im Vergleich zu Scramble und nicht transfizierten Zellen ( $p \leq 0,05$ ) ermittelt werden.

Im Zellproliferationsassay zeigte sich bei beiden Zeitpunkten, 24 und 48 Stunden nach der Transfektion, eine signifikant ( $p \leq 0,05$ ) höhere Zellproliferation in miR-130b Precursor transfizierten und eine reduzierte Zellproliferation in Inhibitor transfizierte Zellen ( $p \leq 0,05$ ), im Vergleich zu Scramble sowie auch in nicht transfizierten Zellen.

Um die Rolle der miR-130b während der Glykolyse besser zu verstehen, wurden sowohl primäre Granulosa- und Kumuluszellen transfiziert und anschließend 24 Stunden nach der Transfektion in 96 Wellplatten mittels eines Multiplate Readers ein Laktat-Assay durchgeführt. Das Resultat zeigte bei Precursor behandelte Zellen eine höhere Laktatproduktion ( $p < 0,005$ ). Bei Inhibitor transfizierte Zellen konnte im Vergleich zur Scramble und der nicht transfizierten Gruppe eine geringere Laktatproduktion beobachtet werden ( $p < 0,01$ ). Es konnten keinen signifikanten Unterschiede zum Einfluss der miR-130b auf die Cholesterin-Biosynthese in Granulosa- und Kumuluszellen festgestellt werden. In der molekulare Analyse konnte in pre-miR-130b transfizierten Zellen eine geringere mRNA- und Proteinexpression detektiert werden. Im Gegensatz dazu zeigte sich eine höhere Expression in anti-miR-130b transfizierten Zellen im Vergleich zur Kontrollgruppe.

Der Einfluss von miR-130b in Präimplantationsembryonen wurde durch eine Überexpression und eine Unterdrückung der miR-130b während des Zygotenstadiums untersucht. Die Embryonen wurden am Tag 8 im Blastozystenstadium gesammelt und deren Phenotypen wurden in bestimmten Zeitintervallen bestimmt. Für alle Embryonen die mit miR-130b Precursor, Inhibitor, Scramble und nicht injizierte Zygoten behandelt wurden, konnte eine erste Teilungsrate um 75 bis 80% beobachtet werden ( $p > 0,05$ ). Nach 72 Stunden erreichten 68% der Precursor, 58% der Inhibitor und 65% der Scramble sowie 69% der nicht injizierten behandelt Zygoten das 8-Zell-Stadium. 16% der Precursor, 28% der Inhibitor und 19% der Scramble sowie 18% nicht injizierten Zygoten verblieben im 4-Zell-Stadium.

Dennoch konnte eine reduzierte Morularate ( $p \leq 0,05$ ) bei Inhibitor injizierten Zygoten im Vergleich zur nicht injizierten Kontrollgruppe beobachtet werden. Die Anzahl an Embryonen die das Blastozystenstadium erreicht hatten, war bei Precursor injizierten Zygoten mit 22% höher als bei Inhibitor injizierten (14%). Scramble injizierte (19%) und nicht injizierten Zygoten (20%) zeigten keinen Unterschied. Des Weiteren konnte eine signifikant verringerte Blastozystenentwicklung bei Inhibitor injizierten Zygoten ( $p \leq 0,05$ ) beobachtet werden.

Zusammenfassend zeigt die vorliegende Studie, dass miR-130b während der Maturation boviner Oozyten und Granulosazellproliferation eine bedeutende Funktion einnimmt. Die hohe Expression der miR-130b in Granulosazellen der antralen Follikel führte zur Proliferation der Granulosazellen und einer erhöhten Stoffwechselaktivität. Während der *in vitro* Oozytenmaturation konnte miR-130b als ein wichtiges Transkript identifiziert werden, das die Oozyten sowohl bei der Maturation als auch bei der Blastozystenbildung unterstützt. Der mögliche Einfluss der miR-130b auf die Stoffwechselaktivität der Oozyten konnte zu einer erhöhten mitochondrialen Aktivität geführt haben. Alle analysierten Daten zeigten, dass die Transkription der miR-130b während der bovinen Oozytenmaturation und Granulosazellproliferation benötigt wird. Des Weiteren könnte eine hohe Expression der miR-130b im Morula- und Blastozystenstadium einen bedeutenden Einfluss auf die Implantation des Embryos haben.

## Reference

Abecassis L, Rogier E, Vazquez A, Atfi A, Bourgeade MF (2004): Evidence for a role of MSK1 in transforming growth factor-beta-mediated responses through p38alpha and Smad signaling pathways. *J Biol Chem* 279, 30474-30479

Abrahante JE, Daul AL, Li M, Volk ML, Tennessen JM, Miller EA, Rougvie AE (2003): The *Caenorhabditis elegans* hunchback-like gene *lin-57/hbl-1* controls developmental time and is regulated by microRNAs. *Dev Cell* 4, 625-637

Ahn HW, Morin RD, Zhao H, Harris RA, Coarfa C, Chen ZJ, Milosavljevic A, Marra MA, Rajkovic A (2010): MicroRNA transcriptome in the newborn mouse ovaries determined by massive parallel sequencing. *Molecular Human Reproduction* 16, 463-471

Ajay SS, Athey BD, Lee I (2010): Unified translation repression mechanism for microRNAs and upstream AUGs. *Bmc Genomics* 11, -

Alvarez-Garcia I, Miska EA (2005): MicroRNA functions in animal development and human disease. *Development* 132, 4653-4662

Amanai M, Brahmajosyula M, Perry AC (2006): A restricted role for sperm-borne microRNAs in mammalian fertilization. *Biol Reprod* 75, 877-884

Ambros V (2004): The functions of animal microRNAs. *Nature* 431, 350-355

Ambros V, Bartel B, Bartel DP, Burge CB, Carrington JC, Chen X, Dreyfuss G, Eddy SR, Griffiths-Jones S, Marshall M, *et al.* (2003a): A uniform system for microRNA annotation. *RNA* 9, 277-279

Ambros V, Lee RC, Lavanway A, Williams PT, Jewell D (2003b): MicroRNAs and other tiny endogenous RNAs in *C. elegans*. *Curr Biol* 13, 807-818

Amiri I, Mirahadi N, Amini A, Parvini M, Heidarbeigi K (2009): The effects of LIF and EGF on mouse oocyte maturation, fertilization and development in vitro. *Iranian Journal of Reproductive Medicine* 7, 189-194

Aparicio IM, Garcia-Herreros M, O'Shea LC, Hensey C, Lonergan P, Fair T (2011): Expression, Regulation, and Function of Progesterone Receptors in Bovine Cumulus Oocyte Complexes During In Vitro Maturation. *Biology of Reproduction* 84, 910-921

Arthur JS, Cohen P (2000): MSK1 is required for CREB phosphorylation in response to mitogens in mouse embryonic stem cells. *FEBS Lett* 482, 44-48

Artzi S, Kiezun A, Shomron N (2008): miRNAMiner: a tool for homologous microRNA gene search. *BMC Bioinformatics* 9, 39

Bagga S, Bracht J, Hunter S, Massirer K, Holtz J, Eachus R, Pasquinelli AE (2005): Regulation by let-7 and lin-4 miRNAs results in target mRNA degradation. *Cell* 122, 553-563

Bartel DP (2004): MicroRNAs: genomics, biogenesis, mechanism, and function. *Cell* 116, 281-297

Bashirullah A, Halsell SR, Cooperstock RL, Kloc M, Karaiskakis A, Fisher WW, Fu WL, Hamilton JK, Etkin LD, Lipshitz HD (1999): Joint action of two RNA degradation pathways controls the timing of maternal transcript elimination at the midblastula transition in *Drosophila melanogaster*. *Embo Journal* 18, 2610-2620

Berezikov E, van Tetering G, Verheul M, van de Belt J, van Laake L, Vos J, Verloop R, van de Wetering M, Guryev V, Takada S, *et al.* (2006): Many novel mammalian microRNA candidates identified by extensive cloning and RAKE analysis. *Genome Res* 16, 1289-1298

- Bernstein E, Kim SY, Carmell MA, Murchison EP, Alcorn H, Li MZ, Mills AA, Elledge SJ, Anderson KV, Hannon GJ (2003): Dicer is essential for mouse development. *Nat Genet* 35, 215-217
- Besecker MI, Harden ME, Li G, Wang XJ, Griffiths A (2009): Discovery of herpes B virus-encoded microRNAs. *J Virol* 83, 3413-3416
- Bettegowda A, Smith GW (2007): Mechanisms of maternal mRNA regulation: implications for mammalian early embryonic development. *Front Biosci* 12, 3713-3726
- Biggers JD, Whittingham DG, Donahue RP (1967): The pattern of energy metabolism in the mouse oocyte and zygote. *Proc Natl Acad Sci U S A* 58, 560-567
- Bilodeau-Goeseels S (2003): Effect of oocyte quality on the relative abundance of specific gene transcripts in bovine mature oocytes and 16-cell embryos. *Can J Vet Res* 67, 151-156
- Bjork JK, Sandqvist A, Elsing AN, Kotaja N, Sistonen L (2010): miR-18, a member of Oncomir-1, targets heat shock transcription factor 2 in spermatogenesis. *Development* 137, 3177-3184
- Borgdorff V, Leonart ME, Bishop CL, Fessart D, Bergin AH, Overhoff MG, Beach DH (2010): Multiple microRNAs rescue from Ras-induced senescence by inhibiting p21(Waf1/Cip1). *Oncogene* 29, 2262-2271
- Bouhallier F, Allioli N, Laval F, Chalmel F, Perrard MH, Durand P, Samarut J, Pain B, Rouault JP (2010): Role of miR-34c microRNA in the late steps of spermatogenesis. *Rna-a Publication of the Rna Society* 16, 720-731
- Bracht J, Hunter S, Eachus R, Weeks P, Pasquinelli AE (2004): Trans-splicing and polyadenylation of let-7 microRNA primary transcripts. *RNA* 10, 1586-1594

Bravo SB, Pampin S, Cameselle-Teijeiro J, Carneiro C, Dominguez F, Barreiro F, Alvarez CV (2003): TGF-beta-induced apoptosis in human thyrocytes is mediated by p27kip1 reduction and is overridden in neoplastic thyrocytes by NF-kappaB activation. *Oncogene* 22, 7819-7830

Brennecke J, Hipfner DR, Stark A, Russell RB, Cohen SM (2003): bantam encodes a developmentally regulated microRNA that controls cell proliferation and regulates the proapoptotic gene hid in *Drosophila*. *Cell* 113, 25-36

Burmistrova OA, Goltsov AY, Abramova LI, Kaleda VG, Orlova VA, Rogaev EI (2007): MicroRNA in schizophrenia: genetic and expression analysis of miR-130b (22q11). *Biochemistry (Mosc)* 72, 578-582

Bushati N, Cohen SM (2007): microRNA functions. *Annu Rev Cell Dev Biol* 23, 175-205

Bushati N, Stark A, Brennecke J, Cohen SM (2008): Temporal reciprocity of miRNAs and their targets during the maternal-to-zygotic transition in *Drosophila*. *Current Biology* 18, 501-506

Byrne MJ, Warner CM (2008): MicroRNA expression in preimplantation mouse embryos from Ped gene positive compared to Ped gene negative mice. *J Assist Reprod Genet* 25, 205-214

Cai X, Lu S, Zhang Z, Gonzalez CM, Damania B, Cullen BR (2005): Kaposi's sarcoma-associated herpesvirus expresses an array of viral microRNAs in latently infected cells. *Proc Natl Acad Sci U S A* 102, 5570-5575

Calin GA, Sevignani C, Dumitru CD, Hyslop T, Noch E, Yendamuri S, Shimizu M, Rattan S, Bullrich F, Negrini M, *et al.* (2004): Human microRNA genes are frequently located at fragile sites and genomic regions involved in cancers. *Proc Natl Acad Sci U S A* 101, 2999-3004



Carletti MZ, Fiedler SD, Christenson LK (2010): MicroRNA 21 Blocks Apoptosis in Mouse Periovarian Granulosa Cells. *Biology of Reproduction* 83, 286-295

Castro FO, Sharbati S, Rodriguez-Alvarez LL, Cox JF, Hultschig C, Einspanier R (2010): MicroRNA expression profiling of elongated cloned and in vitro-fertilized bovine embryos. *Theriogenology* 73, 71-85

Chang H, Brown CW, Matzuk MM (2002): Genetic analysis of the mammalian transforming growth factor-beta superfamily. *Endocr Rev* 23, 787-823

Chang S, Johnston RJ, Jr., Frokjaer-Jensen C, Lockery S, Hobert O (2004): MicroRNAs act sequentially and asymmetrically to control chemosensory laterality in the nematode. *Nature* 430, 785-789

Chen K, Rajewsky N (2007): The evolution of gene regulation by transcription factors and microRNAs. *Nat Rev Genet* 8, 93-103

Chen PY, Manninga H, Slanchev K, Chien M, Russo JJ, Ju J, Sheridan R, John B, Marks DS, Gaidatzis D, *et al.* (2005): The developmental miRNA profiles of zebrafish as determined by small RNA cloning. *Genes Dev* 19, 1288-1293

Chen QJ, Sun XX, Chen JL, Cheng LA, Wang J, Wang YW, Sun ZG (2009): Direct rosiglitazone action on steroidogenesis and proinflammatory factor production in human granulosa-lutein cells. *Reproductive Biology and Endocrinology* 7, -

Chen X (2005): MicroRNA biogenesis and function in plants. *FEBS Lett* 579, 5923-5931

Chen Y, Gorski DH (2008): Regulation of angiogenesis through a microRNA (miR-130a) that down-regulates antiangiogenic homeobox genes GAX and HOXA5. *Blood* 111, 1217-1226

- Chen Z, Li Y, Zhang H, Huang P, Luthra R (2010): Hypoxia-regulated microRNA-210 modulates mitochondrial function and decreases ISCU and COX10 expression. *Oncogene* 29, 4362-4368
- Chendrimada TP, Gregory RI, Kumaraswamy E, Norman J, Cooch N, Nishikura K, Shiekhattar R (2005): TRBP recruits the Dicer complex to Ago2 for microRNA processing and gene silencing. *Nature* 436, 740-744
- Choe J, Cho H, Lee HC, Kim YK (2010): microRNA/Argonaute 2 regulates nonsense-mediated messenger RNA decay. *Embo Reports* 11, 380-386
- Choi Y, Qin Y, Berger MF, Ballow DJ, Bulyk ML, Rajkovic A (2007): Microarray analyses of newborn mouse ovaries lacking Nobox. *Biol Reprod* 77, 312-319
- Choi Y, Rajkovic A (2006): Genetics of early mammalian folliculogenesis. *Cell Mol Life Sci* 63, 579-590
- Christenson L.K. (2010). MicroRNA control of ovarian function. *Anim. Reprod*, v.7, n.3, 129-133.
- Cifuentes D, Xue HL, Taylor DW, Patnode H, Mishima Y, Cheloufi S, Ma EB, Mane S, Hannon GJ, Lawson ND, *et al.* (2010): A Novel miRNA Processing Pathway Independent of Dicer Requires Argonaute2 Catalytic Activity. *Science* 328, 1694-1698
- Cook MS, Munger SC, Nadeau JH, Capel B (2011): Regulation of male germ cell cycle arrest and differentiation by DND1 is modulated by genetic background. *Development* 138, 23-32
- Coutinho LL, Matukumalli LK, Sonstegard TS, Van Tassell CP, Gasbarre LC, Capuco AV, Smith TPL (2007): Discovery and profiling of bovine microRNAs from immune-related and embryonic tissues. *Physiological Genomics* 29, 35-43

Crist CG, Montarras D, Pallafacchina G, Rocancourt D, Cumano A, Conway SJ, Buckingham M (2009): Muscle stem cell behavior is modified by microRNA-27 regulation of Pax3 expression. *Proc Natl Acad Sci U S A* 106, 13383-13387

Curry E, Ellis SE, Pratt SL (2009): Detection of Porcine Sperm MicroRNAs Using a Heterologous MicroRNA Microarray and Reverse Transcriptase Polymerase Chain Reaction. *Molecular Reproduction and Development* 76, -

Daniels SM, Melendez-Pena CE, Scarborough RJ, Daher A, Christensen HS, El Far M, Purcell DF, Laine S, Gagnol A (2009): Characterization of the TRBP domain required for dicer interaction and function in RNA interference. *BMC Mol Biol* 10, 38

Davis BN, Hilyard AC, Lagna G, Hata A (2008): SMAD proteins control DROSHA-mediated microRNA maturation. *Nature* 454, 56-61

de Luca A, Weller M, Fontana A (1996): TGF-beta-induced apoptosis of cerebellar granule neurons is prevented by depolarization. *J Neurosci* 16, 4174-4185

de Vantery Arrighi C, Campana A, Schorderet-Slatkine S (2000): A role for the MEK-MAPK pathway in okadaic acid-induced meiotic resumption of incompetent growing mouse oocytes. *Biol Reprod* 63, 658-665

Dean W, Santos F, Stojkovic M, Zakhartchenko V, Walter J, Wolf E, Reik W (2001): Conservation of methylation reprogramming in mammalian development: aberrant reprogramming in cloned embryos. *Proc Natl Acad Sci U S A* 98, 13734-13738

Dekel N, Aberdam E, Goren S, Feldman B, Shalgi R (1989): Mechanism of action of GnRH-induced oocyte maturation. *J Reprod Fertil Suppl* 37, 319-327

Djuranovic S, Nahvi A, Green R (2011): A Parsimonious Model for Gene Regulation by miRNAs. *Science* 331, 550-553

- Doench JG, Sharp PA (2004): Specificity of microRNA target selection in translational repression. *Genes Dev* 18, 504-511
- Du T, Zamore PD (2005): microPrimer: the biogenesis and function of microRNA. *Development* 132, 4645-4652
- Dumont J, Umbhauer M, Rassinier P, Hanauer A, Verlhac MH (2005): p90Rsk is not involved in cytostatic factor arrest in mouse oocytes. *J Cell Biol* 169, 227-231
- Ealy AD, Yang QE (2009): Control of interferon-tau expression during early pregnancy in ruminants. *Am J Reprod Immunol* 61, 95-106
- El-Raey M, Geshi M, Somfai T, Kaneda M, Hirako M, Abdel-Ghaffar AE, Sosa GA, El-Roos ME, Nagai T (2011). Evidence of melatonin synthesis in the cumulus oocyte complexes and its role in enhancing oocyte maturation in vitro in cattle. *Mol Reprod Dev* 78, 250-262.
- Elstrom RL, Bauer DE, Buzzai M, Karnauskas R, Harris MH, Plas DR, Zhuang H, Cinalli RM, Alavi A, Rudin CM, *et al.* (2004): Akt stimulates aerobic glycolysis in cancer cells. *Cancer Res* 64, 3892-3899
- Elvin JA, Yan C, Matzuk MM (2000): Oocyte-expressed TGF-beta superfamily members in female fertility. *Mol Cell Endocrinol* 159, 1-5
- Enright AJ, John B, Gaul U, Tuschl T, Sander C, Marks DS (2003): MicroRNA targets in *Drosophila*. *Genome Biol* 5, R1
- Eppig JJ (1985): Oocyte-somatic cell interactions during oocyte growth and maturation in the mammal. *Dev Biol (N Y)* 1985, 1, 313-347
- Eppig JJ (2001): Oocyte control of ovarian follicular development and function in mammals. *Reproduction* 122, 829-838

- Eppig JJ, Hosoe M, O'Brien MJ, Pendola FM, Requena A, Watanabe S (2000): Conditions that affect acquisition of developmental competence by mouse oocytes in vitro: FSH, insulin, glucose and ascorbic acid. *Molecular and Cellular Endocrinology* 163, 109-116
- Fabian MR, Sonenberg N, Filipowicz W (2010): Regulation of mRNA Translation and Stability by microRNAs. *Annual Review of Biochemistry*, Vol 79 79, 351-379
- Fair T, Carter F, Park S, Evans AC, Lonergan P (2007): Global gene expression analysis during bovine oocyte in vitro maturation. *Theriogenology* 68 Suppl 1, S91-97
- Fan HY, Huo LJ, Chen DY, Schatten H, Sun QY (2004): Protein kinase C and mitogen-activated protein kinase cascade in mouse cumulus cells: cross talk and effect on meiotic resumption of oocyte. *Biol Reprod* 70, 1178-1187
- Farh KK, Grimson A, Jan C, Lewis BP, Johnston WK, Lim LP, Burge CB, Bartel DP (2005): The widespread impact of mammalian MicroRNAs on mRNA repression and evolution. *Science* 310, 1817-1821
- Ferreira EM, Vireque AA, Adona PR, Meirelles FV, Ferriani RA, Navarro PA (2009): Cytoplasmic maturation of bovine oocytes: structural and biochemical modifications and acquisition of developmental competence. *Theriogenology* 71, 836-848
- Fields SD, Hansen PJ, Ealy AD (2011): Fibroblast growth factor requirements for in vitro development of bovine embryos. *Theriogenology* 75, 1466-1475
- Fire A, Xu S, Montgomery MK, Kostas SA, Driver SE, Mello CC (1998): Potent and specific genetic interference by double-stranded RNA in *Caenorhabditis elegans*. *Nature* 391, 806-811
- Fissore RA, He CL, Vande Woude GF (1996): Potential role of mitogen-activated protein kinase during meiosis resumption in bovine oocytes. *Biol Reprod* 55, 1261-1270

Forstemann K, Tomari Y, Du T, Vagin VV, Denli AM, Bratu DP, Klattenhoff C, Theurkauf WE, Zamore PD (2005): Normal microRNA maturation and germ-line stem cell maintenance requires Loquacious, a double-stranded RNA-binding domain protein. *PLoS Biol* 3, e236

Friedman RC, Farh KK, Burge CB, Bartel DP (2009): Most mammalian mRNAs are conserved targets of microRNAs. *Genome Res* 19, 92-105

Fujino Y, Ozaki K, Yamamasu S, Ito F, Matsuoka I, Hayashi E, Nakamura H, Ogita S, Sato E, Inoue M (1996): DNA fragmentation of oocytes in aged mice. *Hum Reprod* 11, 1480-1483

Galvin KE, Travis ED, Yee D, Magnuson T, Vivian JL (2010): Nodal Signaling Regulates the Bone Morphogenic Protein Pluripotency Pathway in Mouse Embryonic Stem Cells. *Journal of Biological Chemistry* 285, 19747-19756

Gao J, Yang T, Han J, Yan K, Qiu X, Zhou Y, Fan Q, Ma B (2011). MicroRNA expression during osteogenic differentiation of human multipotent mesenchymal stromal cells from bone marrow. *J Cell Biochem*

Gavin AC, Ni Ainle A, Chierici E, Jones M, Nebreda AR (1999): A p90(rsk) mutant constitutively interacting with MAP kinase uncouples MAP kinase from p34(cdc2)/cyclin B activation in *Xenopus* oocytes. *Mol Biol Cell* 10, 2971-2986

Ge L, Han D, Lan GC, Zhou P, Liu Y, Zhang X, Sui HS, Tan JH (2008): Factors affecting the in vitro action of cumulus cells on the maturing mouse oocytes. *Mol Reprod Dev* 75, 136-142

Gilchrist RB, Lane M, Thompson JG (2008): Oocyte-secreted factors: regulators of cumulus cell function and oocyte quality. *Hum Reprod Update* 14, 159-177

Gilchrist RB, Morrissey MP, Ritter LJ, Armstrong DT (2003): Comparison of oocyte factors and transforming growth factor-beta in the regulation of DNA synthesis in bovine granulosa cells. *Mol Cell Endocrinol* 201, 87-95

Gilchrist RB, Ritter LJ, Armstrong DT (2001): Mouse oocyte mitogenic activity is developmentally coordinated throughout folliculogenesis and meiotic maturation. *Dev Biol* 240, 289-298

Gilchrist RB, Ritter LJ, Armstrong DT (2004): Oocyte-somatic cell interactions during follicle development in mammals. *Anim Reprod Sci* 82-83, 431-446

Giraldez AJ, Cinalli RM, Glasner ME, Enright AJ, Thomson JM, Baskerville S, Hammond SM, Bartel DP, Schier AF (2005): MicroRNAs regulate brain morphogenesis in zebrafish. *Science* 308, 833-838

Giraldez AJ, Mishima Y, Rihel J, Grocock RJ, Van Dongen S, Inoue K, Enright AJ, Schier AF (2006): Zebrafish MiR-430 promotes deadenylation and clearance of maternal mRNAs. *Science* 312, 75-79

Golan D, Levy C, Friedman B, Shomron N (2010): Biased hosting of intronic microRNA genes. *Bioinformatics* 26, 992-995

Gotoh Y, Nishida E (1995): Activation mechanism and function of the MAP kinase cascade. *Mol Reprod Dev* 42, 486-492

Gottesman S (2004): The small RNA regulators of *Escherichia coli*: roles and mechanisms\*. *Annu Rev Microbiol* 58, 303-328

Gougeon A (1996): Regulation of ovarian follicular development in primates: facts and hypotheses. *Endocr Rev* 17, 121-155

Gregory RI, Chendrimada TP, Cooch N, Shiekhattar R (2005): Human RISC couples microRNA biogenesis and posttranscriptional gene silencing. *Cell* 123, 631-640

Gregory RI, Yan KP, Amuthan G, Chendrimada T, Doratotaj B, Cooch N, Shiekhattar R (2004): The Microprocessor complex mediates the genesis of microRNAs. *Nature* 432, 235-240

Griffiths-Jones S (2004): The microRNA Registry. *Nucleic Acids Res* 32, D109-111

Grondahl ML, Andersen CY, Bogstad J, Nielsen FC, Meinertz H, Borup R (2010): Gene expression profiles of single human mature oocytes in relation to age. *Human Reproduction* 25, 957-968

Grotowski W, Lecybyl R, Warenik-Szymankiewicz A, Trzeciak WH (1997): [The role of apoptosis of granulosa cells in follicular atresia]. *Ginekol Pol* 68, 317-326

Grun D, Wang YL, Langenberger D, Gunsalus KC, Rajewsky N (2005): microRNA target predictions across seven *Drosophila* species and comparison to mammalian targets. *PLoS Comput Biol* 1, e13

Gutierrez CG, Campbell BK, Webb R (1997): Development of a long-term bovine granulosa cell culture system: induction and maintenance of estradiol production, response to follicle-stimulating hormone, and morphological characteristics. *Biol Reprod* 56, 608-616

Han J, Lee Y, Yeom KH, Kim YK, Jin H, Kim VN (2004): The Drosha-DGCR8 complex in primary microRNA processing. *Genes Dev* 18, 3016-3027

Han J, Lee Y, Yeom KH, Nam JW, Heo I, Rhee JK, Sohn SY, Cho Y, Zhang BT, Kim VN (2006): Molecular basis for the recognition of primary microRNAs by the Drosha-DGCR8 complex. *Cell* 125, 887-901

Hauge C, Frodin M (2006): RSK and MSK in MAP kinase signalling. *J Cell Sci* 119, 3021-3023



Hawkins SM, Matzuk MM (2010): Oocyte-somatic cell communication and microRNA function in the ovary. *Annales D Endocrinologie* 71, 144-148

Hayashi K, Chuva de Sousa Lopes SM, Kaneda M, Tang F, Hajkova P, Lao K, O'Carroll D, Das PP, Tarakhovsky A, Miska EA, *et al.* (2008): MicroRNA biogenesis is required for mouse primordial germ cell development and spermatogenesis. *PLoS One* 3, e1738

Hayashita Y, Osada H, Tatematsu Y, Yamada H, Yanagisawa K, Tomida S, Yatabe Y, Kawahara K, Sekido Y, Takahashi T (2005): A polycistronic microRNA cluster, miR-17-92, is overexpressed in human lung cancers and enhances cell proliferation. *Cancer Res* 65, 9628-9632

Hehl S, Stoyanov B, Oehrl W, Schonherr R, Wetzker R, Heinemann SH (2001): Phosphoinositide 3-kinase-gamma induces *Xenopus* oocyte maturation via lipid kinase activity. *Biochem J* 360, 691-698

Heikinheimo O, Gibbons WE (1998): The molecular mechanisms of oocyte maturation and early embryonic development are unveiling new insights into reproductive medicine. *Mol Hum Reprod* 4, 745-756

Hennebold JD (2010): Preventing Granulosa Cell Apoptosis Through the Action of a Single MicroRNA. *Biology of Reproduction* 83, 165-167

Herrera-Esparza R, Pacheco-Tovar D, Avalos-Diaz E (2008): GW bodies: from RNA biology to clinical implications in autoimmunity. *Expert Rev Clin Immunol* 4, 21-25

Hirai H, Verma M, Watanabe S, Tastad C, Asakura Y, Asakura A (2010): MyoD regulates apoptosis of myoblasts through microRNA-mediated down-regulation of Pax3. *Journal of Cell Biology* 191, 347-365

Hirshfield AN (1991): Development of follicles in the mammalian ovary. *Int Rev Cytol* 124, 43-101

Hoeffler CA, Cowansage KK, Arnold EC, Banko JL, Moerke NJ, Rodriguez R, Schmidt EK, Klosi E, Chorev M, Lloyd RE, *et al.* (2011): Inhibition of the interactions between eukaryotic initiation factors 4E and 4G impairs long-term associative memory consolidation but not reconsolidation. *Proceedings of the National Academy of Sciences of the United States of America* 108, 3383-3388

Homa ST (1995): Calcium and meiotic maturation of the mammalian oocyte. *Mol Reprod Dev* 40, 122-134

Hong X, Luense LJ, McGinnis LK, Nothnick WB, Christenson LK (2008): Dicer1 is essential for female fertility and normal development of the female reproductive system. *Endocrinology* 149, 6207-6212

Horie T, Ono K, Nishi H, Iwanaga Y, Nagao K, Kinoshita M, Kuwabara Y, Takanabe R, Hasegawa K, Kita T, *et al.* (2009): MicroRNA-133 regulates the expression of GLUT4 by targeting KLF15 and is involved in metabolic control in cardiac myocytes. *Biochemical and Biophysical Research Communications* 389, 315-320

Hossain MM, Ghanem N, Hoelker M, Rings F, Phatsara C, Tholen E, Schellander K, Tesfaye D (2009): Identification and characterization of miRNAs expressed in the bovine ovary. *BMC Genomics* 10, 443

Houbaviy HB, Murray MF, Sharp PA (2003): Embryonic stem cell-specific MicroRNAs. *Dev Cell* 5, 351-358

Hsueh AJ, Adashi EY, Jones PB, Welsh TH, Jr. (1984): Hormonal regulation of the differentiation of cultured ovarian granulosa cells. *Endocr Rev* 5, 76-127

Huang Y, Zou Q, Song H, Song F, Wang L, Zhang G, Shen X (2010). A study of miRNAs targets prediction and experimental validation. *Protein Cell* 1, 979-986

- Huang ZW, Wells D (2010): The human oocyte and cumulus cells relationship: new insights from the cumulus cell transcriptome. *Molecular Human Reproduction* 16, 715-725
- Hughes JP, Staton PC, Wilkinson MG, Strijbos PJLM, Skaper SD, Arthur JSC, Reith AD (2003): Mitogen and stress response kinase-1 (MSK1) mediates excitotoxic induced death of hippocampal neurones. *Journal of Neurochemistry* 86, 25-32
- Hunter AG, Moor RM (1987): Stage-dependent effects of inhibiting ribonucleic acids and protein synthesis on meiotic maturation of bovine oocytes in vitro. *J Dairy Sci* 70, 1646-1651
- Huntzinger E, Izaurralde E (2011): Gene silencing by microRNAs: contributions of translational repression and mRNA decay. *Nature Reviews Genetics* 12, 99-110
- Hurteau GJ, Carlson JA, Spivack SD, Brock GJ (2007): Overexpression of the microRNA hsa-miR-200c leads to reduced expression of transcription factor 8 and increased expression of E-cadherin. *Cancer Res* 67, 7972-7976
- Hussein TS, Thompson JG, Gilchrist RB (2006): Oocyte-secreted factors enhance oocyte developmental competence. *Dev Biol* 296, 514-521
- Hutt KJ, Albertini DF (2007): An oocentric view of folliculogenesis and embryogenesis. *Reprod Biomed Online* 14, 758-764
- Hutvagner G, Simard MJ, Mello CC, Zamore PD (2004): Sequence-specific inhibition of small RNA function. *PLoS Biol* 2, E98
- Jang CW, Chen CH, Chen CC, Chen JY, Su YH, Chen RH (2002): TGF-beta induces apoptosis through Smad-mediated expression of DAP-kinase. *Nat Cell Biol* 4, 51-58
- Jia WZ, Li Z, Lun ZR (2008): Discoveries and functions of virus-encoded MicroRNAs. *Chinese Science Bulletin* 53, 169-177

- Jiang J, Gusev Y, Aderca I, Mettler TA, Nagorney DM, Brackett DJ, Roberts LR, Schmittgen TD (2008): Association of MicroRNA expression in hepatocellular carcinomas with hepatitis infection, cirrhosis, and patient survival. *Clin Cancer Res* 14, 419-427
- Jiang SA, Zhang HW, Lu MH, He XH, Li Y, Gu H, Liu MF, Wang ED (2010): MicroRNA-155 Functions as an OncomiR in Breast Cancer by Targeting the Suppressor of Cytokine Signaling 1 Gene. *Cancer Research* 70, 3119-3127
- Jin S, Zhang M, Lei L, Wang C, Fu M, Ning G, Xia G (2006): Meiosis activating sterol (MAS) regulate FSH-induced meiotic resumption of cumulus cell-enclosed porcine oocytes via PKC pathway. *Mol Cell Endocrinol* 249, 64-70
- Jin W, Grant JR, Stothard P, Moore SS, Guan LL (2009): Characterization of bovine miRNAs by sequencing and bioinformatics analysis. *BMC Mol Biol* 10, 90
- Johnson SM, Grosshans H, Shingara J, Byrom M, Jarvis R, Cheng A, Labourier E, Reinert KL, Brown D, Slack FJ (2005): RAS is regulated by the let-7 microRNA family. *Cell* 120, 635-647
- Johnston DS, Wright WW, DiCandeloro P, Wilson E, Kopf GS, Jelinsky SA (2008): Stage-specific gene expression is a fundamental characteristic of rat spermatogenic cells and Sertoli cells. *Proceedings of the National Academy of Sciences of the United States of America* 105, 8315-8320
- Jung JH, Seo PJ, Park CM (2009): MicroRNA biogenesis and function in higher plants. *Plant Biotechnology Reports* 3, 111-126
- Kahata K, Hayashi M, Asaka M, Hellman U, Kitagawa H, Yanagisawa J, Kato S, Imamura T, Miyazono K (2004): Regulation of transforming growth factor-beta and bone morphogenetic protein signalling by transcriptional coactivator GCN5. *Genes Cells* 9, 143-151

- Karbiener M, Fischer C, Nowitsch S, Opriessnig P, Papak C, Ailhaud G, Dani C, Amri EZ, Scheideler M (2009): microRNA miR-27b impairs human adipocyte differentiation and targets PPAR gamma. *Biochemical and Biophysical Research Communications* 390, 247-251
- Kawabata M, Miyazono K (1999): Signal transduction of the TGF-beta superfamily by Smad proteins. *Journal of Biochemistry* 125, 9-16
- Kedde M, Strasser MJ, Boldajipour B, Vrieling JAFO, Le Sage C, Nagel R, Voorhoeve PM, Van Duijse J, Orom UA, Lund AH, *et al.* (2007): RNA-binding protein Dnd1 inhibits microRNA access to target mRNA. *Cell* 131, 1273-1286
- Ketting RF, Fischer SE, Bernstein E, Sijen T, Hannon GJ, Plasterk RH (2001): Dicer functions in RNA interference and in synthesis of small RNA involved in developmental timing in *C. elegans*. *Genes Dev* 15, 2654-2659
- Khatib H, Maltecca C, Monson RL, Schutzkus V, Rutledge JJ (2009): Monoallelic maternal expression of STAT5A affects embryonic survival in cattle. *BMC Genet* 10, 13
- Khvorova A, Reynolds A, Jayasena SD (2003): Functional siRNAs and miRNAs exhibit strand bias. *Cell* 115, 209-216
- Kim GH, Samant SA, Earley JU, Svensson EC (2009): Translational Control of FOG-2 Expression in Cardiomyocytes by MicroRNA-130a. *Plos One* 4, -
- Kim SK, Nam JW, Rhee JK, Lee WJ, Zhang BT (2006): miTarget: microRNA target gene prediction using a support vector machine. *Bmc Bioinformatics* 7, -
- Kim SY, Kim AY, Lee HW, Son YH, Lee GY, Lee JW, Lee YS, Kim JB (2010a): miR-27a is a negative regulator of adipocyte differentiation via suppressing PPAR gamma expression. *Biochemical and Biophysical Research Communications* 392, 323-328

Kim YJ, Ku SY, Rosenwaks Z, Liu HC, Chi SW, Kang JS, Lee WJ, Jung KC, Kim SH, Choi YM, *et al.* (2010b): MicroRNA Expression Profiles are Altered by Gonadotropins and Vitamin C Status During In Vitro Follicular Growth. *Reproductive Sciences* 17, 1081-1089

Kim YK, Kim VN (2007): Processing of intronic microRNAs. *EMBO J* 26, 775-783

Kloosterman WP, Wienholds E, Ketting RF, Plasterk RHA (2004): Substrate requirements for let-7 function in the developing zebrafish embryo. *Nucleic Acids Research* 32, 6284-6291

Knight PG, Glister C (2003): Local roles of TGF-beta superfamily members in the control of ovarian follicle development. *Anim Reprod Sci* 78, 165-183

Knight PG, Glister C (2001): Potential local regulatory functions of inhibins, activins and follistatin in the ovary. *Reproduction* 121, 503-512

Koscianska E, Baev V, Skreka K, Oikonomaki K, Rusinov V, Tabler M, Kalantidis K (2007): Prediction and preliminary validation of oncogene regulation by miRNAs. *BMC Mol Biol* 8, 79

Krek A, Grun D, Poy MN, Wolf R, Rosenberg L, Epstein EJ, MacMenamin P, da Piedade I, Gunsalus KC, Stoffel M, *et al.* (2005): Combinatorial microRNA target predictions. *Nat Genet* 37, 495-500

Kren BT, Wong PY, Sarver A, Zhang X, Zeng Y, Steer CJ (2009): MicroRNAs identified in highly purified liver-derived mitochondria may play a role in apoptosis. *RNA Biol* 6, 65-72

Kren R, Ogushi S, Miyano T (2004): Effect of caffeine on meiotic maturation of porcine oocytes. *Zygote* 12, 31-38

- Krichevsky AM, King KS, Donahue CP, Khrapko K, Kosik KS (2003): A microRNA array reveals extensive regulation of microRNAs during brain development. *RNA* 9, 1274-1281
- Kroemer G, Zamzami N, Susin SA (1997): Mitochondrial control of apoptosis. *Immunol Today* 18, 44-51
- Krol J, Sobczak K, Wilczynska U, Drath M, Jasinska A, Kaczynska D, Krzyzosiak WJ (2004): Structural features of MicroRNA (miRNA) precursors and their relevance to miRNA biogenesis and small interfering RNA/Short hairpin RNA design. *Journal of Biological Chemistry* 279, 42230-42239
- Krug PJ, Riffell JA, Zimmer RK (2009): Endogenous signaling pathways and chemical communication between sperm and egg. *Journal of Experimental Biology* 212, 1092-1100
- Krutovskikh VA, Herceg Z (2010): Oncogenic microRNAs (OncomiRs) as a new class of cancer biomarkers. *Bioessays* 32, 894-904
- Krutzfeldt J, Rajewsky N, Braich R, Rajeev KG, Tuschl T, Manoharan M, Stoffel M (2005): Silencing of microRNAs *in vivo* with 'antagomirs'. *Nature* 438, 685-689
- Kurosaka S, Eckardt S, McLaughlin KJ (2004): Pluripotent lineage definition in bovine embryos by Oct4 transcript localization. *Biol Reprod* 71, 1578-1582
- Lagos-Quintana M, Rauhut R, Lendeckel W, Tuschl T (2001): Identification of novel genes coding for small expressed RNAs. *Science* 294, 853-858
- Lagos-Quintana M, Rauhut R, Meyer J, Borkhardt A, Tuschl T (2003): New microRNAs from mouse and human. *RNA* 9, 175-179
- Lagos-Quintana M, Rauhut R, Yalcin A, Meyer J, Lendeckel W, Tuschl T (2002): Identification of tissue-specific microRNAs from mouse. *Curr Biol* 12, 735-739
- Lai EC (2004): Predicting and validating microRNA targets. *Genome Biol* 5, 115

- Lai EC, Tam B, Rubin GM (2005): Pervasive regulation of *Drosophila* Notch target genes by GY-box-, Brd-box-, and K-box-class microRNAs. *Genes Dev* 19, 1067-1080
- Lai KW, Koh KX, Loh M, Tada K, Subramaniam MM, Lim XY, Vaithilingam A, Salto-Tellez M, Iacopetta B, Ito Y, *et al.* (2010): MicroRNA-130b regulates the tumour suppressor RUNX3 in gastric cancer. *European Journal of Cancer* 46, 1456-1463
- Lall S, Grun D, Krek A, Chen K, Wang YL, Dewey CN, Sood P, Colombo T, Bray N, Macmenaminutes.P, *et al.* (2006): A genome-wide map of conserved microRNA targets in *C. elegans*. *Curr Biol* 16, 460-471
- Landgraf P, Rusu M, Sheridan R, Sewer A, Iovino N, Aravin A, Pfeffer S, Rice A, Kamphorst AO, Landthaler M, *et al.* (2007): A mammalian microRNA expression atlas based on small RNA library sequencing. *Cell* 129, 1401-1414
- Landthaler M, Yalcin A, Tuschl T (2004): The human DiGeorge syndrome critical region gene 8 and its *D. melanogaster* homolog are required for miRNA biogenesis. *Curr Biol* 14, 2162-2167
- Lau NC, Lim LP, Weinstein EG, Bartel DP (2001): An abundant class of tiny RNAs with probable regulatory roles in *Caenorhabditis elegans*. *Science* 294, 858-862
- Lecellier CH, Dunoyer P, Arar K, Lehmann-Che J, Eyquem S, Himber C, Saib A, Voinnet O (2005): A cellular microRNA mediates antiviral defense in human cells. *Science* 308, 557-560
- Lee CT, Risom T, Strauss WM (2007): Evolutionary conservation of microRNA regulatory circuits: an examination of microRNA gene complexity and conserved microRNA-target interactions through metazoan phylogeny. *DNA Cell Biol* 26, 209-218



Lee EK, Lee MJ, Abdelmohsen K, Kim W, Kim MM, Srikantan S, Martindale JL, Hutchison ER, Kim HH, Marasa BS, *et al.* (2011): miR-130 Suppresses Adipogenesis by Inhibiting Peroxisome Proliferator-Activated Receptor gamma Expression. *Molecular and Cellular Biology* 31, 626-638

Lee HS, Kim EY, Kim KH, Moon J, Park KS, Kim KS, Lee KA (2010): Obox4 critically regulates cAMP-dependent meiotic arrest and MI-MII transition in oocytes. *Faseb Journal* 24, 2314-2324

Lee RC, Feinbaum RL, Ambros V (1993): The *C. elegans* heterochronic gene *lin-4* encodes small RNAs with antisense complementarity to *lin-14*. *Cell* 75, 843-854

Lee Y, Jeon K, Lee JT, Kim S, Kim VN (2002): MicroRNA maturation: stepwise processing and subcellular localization. *EMBO J* 21, 4663-4670

Lee Y, Kim M, Han J, Yeom KH, Lee S, Baek SH, Kim VN (2004): MicroRNA genes are transcribed by RNA polymerase II. *EMBO J* 23, 4051-4060

Lei L, Jin SY, Gonzalez G, Behringer RR, Woodruff TK (2010): The regulatory role of Dicer in folliculogenesis in mice. *Molecular and Cellular Endocrinology* 315, 63-73

Lewis BP, Burge CB, Bartel DP (2005): Conserved seed pairing, often flanked by adenosines, indicates that thousands of human genes are microRNA targets. *Cell* 120, 15-20

Lewis BP, Shih IH, Jones-Rhoades MW, Bartel DP, Burge CB (2003): Prediction of mammalian microRNA targets. *Cell* 115, 787-798

Lieberfarb ME, Chu T, Wreden C, Theurkauf W, Gergen JP, Strickland S (1996): Mutations that perturb poly(A)-dependent maternal mRNA activation block the initiation of development. *Development* 122, 579-588

- Liehman P, Greve T, Xu KP (1986): Nuclear and cytoplasmic maturation of bovine oocytes cultured with dbc AMP, FSH and hCG. *Acta Vet Scand* 27, 566-574
- Lim LP, Glasner ME, Yekta S, Burge CB, Bartel DP (2003a): Vertebrate microRNA genes. *Science* 299, 1540
- Lim LP, Lau NC, Weinstein EG, Abdelhakim A, Yekta S, Rhoades MW, Burge CB, Bartel DP (2003): The microRNAs of *Caenorhabditis elegans*. *Genes Dev* 17, 991-1008
- Lin Q, Gao ZG, Alarcon RM, Ye JP, Yun Z (2009): A role of miR-27 in the regulation of adipogenesis. *Febs Journal* 276, 2348-2358
- Lin SL, Chang D, Ying SY (2005): Asymmetry of intronic pre-miRNA structures in functional RISC assembly. *Gene* 356, 32-38
- Lin SY, Johnson SM, Abraham M, Vella MC, Pasquinelli A, Gamberi C, Gottlieb E, Slack FJ (2003): The *C. elegans* hunchback homolog, *hbl-1*, controls temporal patterning and is a probable microRNA target. *Dev Cell* 4, 639-650
- Liu HC, Tang YX, He ZY, Rosenwaks Z (2010): Dicer is a key player in oocyte maturation. *Journal of Assisted Reproduction and Genetics* 27, 571-580
- Livak KJ, Schmittgen TD (2001): Analysis of relative gene expression data using real-time quantitative PCR and the  $2^{-\Delta\Delta C_t}$  method. *Methods* 25, 402-408
- Long JE, Chen HX (2009): Identification and Characteristics of Cattle MicroRNAs by Homology Searching and Small RNA Cloning. *Biochemical Genetics* 47, 329-343
- Louafi F, Martinez-Nunez RT, Sanchez-Elsner T (2010): MicroRNA-155 Targets SMAD2 and Modulates the Response of Macrophages to Transforming Growth Factor-beta. *Journal of Biological Chemistry* 285, 41328-41336

- Luna HS, Ferrari I, Rumpf R (2001): Influence of stage of maturation of bovine oocytes at time of vitrification on the incidence of diploid metaphase II at completion of maturation. *Animal Reproduction Science* 68, 23-28
- Lund E, Guttinger S, Calado A, Dahlberg JE, Kutay U (2004): Nuclear export of microRNA precursors. *Science* 303, 95-98
- Lykke-Andersen K, Gilchrist MJ, Grabarek JB, Das P, Miska E, Zernicka-Goetz M (2008): Maternal Argonaute 2 is essential for early mouse development at the maternal-zygotic transition. *Mol Biol Cell* 19, 4383-4392
- Lynch MA, Petrel TA, Song H, Knobloch TJ, Casto BC, Ramljak D, Anderson LM, DeGross V, Stoner GD, Brueggemeier RW, *et al.* (2001): Responsiveness to transforming growth factor-beta (TGF-beta)-mediated growth inhibition is a function of membrane-bound TGF-beta type II receptor in human breast cancer cells. *Gene Expr* 9, 157-171
- Ma J, Flemr M, Stein P, Berninger P, Malik R, Zavolan M, Svoboda P, Schultz RM (2010a): MicroRNA Activity Is Suppressed in Mouse Oocytes. *Current Biology* 20, 265-270
- Ma S, Tang KH, Chan YP, Lee TK, Kwan PS, Castilho A, Ng I, Man K, Wong N, To KF, *et al.* (2010b): miR-130b Promotes CD133(+) Liver Tumor-Initiating Cell Growth and Self-Renewal via Tumor Protein 53-Induced Nuclear Protein 1. *Cell Stem Cell* 7, 694-707
- Maatouk DM, Loveland KL, McManus MT, Moore K, Harfe BD (2008): Dicer1 is required for differentiation of the mouse male germline. *Biology of Reproduction* 79, 696-703
- Madan P, Bridges PJ, Komar CM, Beristain AG, Rajamahendran R, Fortune JE, MacCalman CD (2003): Expression of messenger RNA for ADAMTS subtypes

changes in the periovulatory follicle after the gonadotropin surge and during luteal development and regression in cattle. *Biol Reprod* 69, 1506-1514

Maddox-Hyttell P, Gjorret JO, Vajta G, Alexopoulos NI, Lewis I, Trounson A, Viuff D, Laurincik J, Muller M, Tveden-Nyborg P, *et al.* (2003): Morphological assessment of preimplantation embryo quality in cattle. *Reprod Suppl* 61, 103-116

Malzkorn B, Wolter M, Liesenberg F, Grzendowski M, Stuhler K, Meyer HE, Reifenberger G (2010): Identification and Functional Characterization of microRNAs Involved in the Malignant Progression of Gliomas. *Brain Pathology* 20, 539-550

Mamo S, Carter F, Lonergan P, Leal CLV, Al Naib A, McGettigan P, Mehta JP, Evans ACO, Fair T (2011): Sequential analysis of global gene expression profiles in immature and in vitro matured bovine oocytes: potential molecular markers of oocyte maturation. *Bmc Genomics* 12, -

Martin MM, Lee EJ, Buckenberger JA, Schmittgen TD, Elton TS (2006): MicroRNA-155 regulates human angiotensin II type 1 receptor expression in fibroblasts. *J Biol Chem* 281, 18277-18284

Matsuda F, Inoue N, Maeda A, Cheng YA, Sai T, Gonda H, Goto Y, Sakamaki K, Manabe N (2011): Expression and Function of Apoptosis Initiator FOXO3 in Granulosa Cells During Follicular Atresia in Pig Ovaries. *Journal of Reproduction and Development* 57, 151-158

McCallie B, Schoolcraft WB, Katz-Jaffe MG (2010): Aberration of blastocyst microRNA expression is associated with human infertility. *Fertility and Sterility* 93, 2374-2382

McCoy CE, Campbell DG, Deak M, Bloomberg GB, Arthur JSC (2005): MSK1 activity is controlled by multiple phosphorylation sites. *Biochemical Journal* 387, 507-517

McNatty KP, Hudson NL, Whiting L, Reader KL, Lun S, Western A, Heath DA, Smith P, Moore LG, Juengel JL (2007): The effects of immunizing sheep with different BMP15 or GDF9 peptide sequences on ovarian follicular activity and ovulation rate. *Biol Reprod* 76, 552-560

Medina PP, Nolde M, Slack FJ (2010): OncomiR addiction in an *in vivo* model of microRNA-21-induced pre-B-cell lymphoma. *Nature* 467, 86-U119

Meister G, Landthaler M, Dorsett Y, Tuschl T (2004a): Sequence-specific inhibition of microRNA- and siRNA-induced RNA silencing. *RNA* 10, 544-550

Miah AG, Salma U, Sinha PB, Holker M, Tesfaye D, Cinar MU, Tsujii H, Schellander K (2011): Intracellular signaling cascades induced by relaxin in the stimulation of capacitation and acrosome reaction in fresh and frozen-thawed bovine spermatozoa. *Anim Reprod Sci* 125, 30-41

Min H, Yoon S (2010): Got target?: computational methods for microRNA target prediction and their extension. *Experimental and Molecular Medicine* 42, 233-244

Mineno J, Okamoto S, Ando T, Sato M, Chono H, Izu H, Takayama M, Asada K, Mirochnitchenko O, Inouye M, *et al.* (2006): The expression profile of microRNAs in mouse embryos. *Nucleic Acids Res* 34, 1765-1771

Mosakhani N, Guled M, Lahti L, Borze I, Forsman M, Paakkonen V, Ryhanen J, Knuutila S (2010): Unique microRNA profile in Dupuytren's contracture supports deregulation of beta-catenin pathway. *Modern Pathology* 23, 1544-1552

Moss EG, Lee RC, Ambros V (1997): The cold shock domain protein LIN-28 controls developmental timing in *C. elegans* and is regulated by the *lin-4* RNA. *Cell* 88, 637-646

Mourelatos Z, Dostie J, Paushkin S, Sharma A, Charroux B, Abel L, Rappsilber J, Mann M, Dreyfuss G (2002): miRNPs: a novel class of ribonucleoproteins containing numerous microRNAs. *Genes Dev* 16, 720-728

- Mtango NR, Potireddy S, Latham KE (2008): Oocyte quality and maternal control of development. *Int Rev Cell Mol Biol* 268, 223-290
- Murchison EP, Stein P, Xuan Z, Pan H, Zhang MQ, Schultz RM, Hannon GJ (2007): Critical roles for Dicer in the female germline. *Genes Dev* 21, 682-693
- Myers M, Pangas SA (2010): Regulatory roles of transforming growth factor beta family members in folliculogenesis. *Wiley Interdiscip Rev Syst Biol Med* 2, 117-125
- Nagaraja AK, Andreu-Vieyra C, Franco HL, Ma L, Chen R, Han DY, Zhu H, Agno JE, Gunaratne PH, DeMayo FJ, *et al.* (2008): Deletion of Dicer in somatic cells of the female reproductive tract causes sterility. *Mol Endocrinol* 22, 2336-2352
- Nakahara K, Kim K, Sciulli C, Dowd SR, Minden JS, Carthew RW (2005): Targets of microRNA regulation in the *Drosophila* oocyte proteome. *Proc Natl Acad Sci U S A* 102, 12023-12028
- Nakamura K, Maki N, Trinh A, Trask HW, Gui JA, Tomlinson CR, Tsonis PA (2010): miRNAs in Newt Lens Regeneration: Specific Control of Proliferation and Evidence for miRNA Networking. *Plos One* 5, -
- Neilson JR, Zheng GX, Burge CB, Sharp PA (2007): Dynamic regulation of miRNA expression in ordered stages of cellular development. *Genes Dev* 21, 578-589
- Nganvongpanit K, Muller H, Rings F, Gilles M, Jennen D, Holker M, Tholen E, Schellander K, Tesfaye D (2006): Targeted suppression of E-cadherin gene expression in bovine preimplantation embryo by RNA interference technology using double-stranded RNA. *Molecular Reproduction and Development* 73, 153-163
- Ni M, Shu WJ, Bo XC, Wang SQ, Li SG (2010): Correlation between sequence conservation and structural thermodynamics of microRNA precursors from human, mouse, and chicken genomes. *Bmc Evolutionary Biology* 10, -

Nicholson BJ (2003): Gap junctions - from cell to molecule. *J Cell Sci* 116, 4479-4481

Nielsen JA, Lau P, Maric D, Barker JL, Hudson LD (2009): Integrating microRNA and mRNA expression profiles of neuronal progenitors to identify regulatory networks underlying the onset of cortical neurogenesis. *Bmc Neuroscience* 10, -

Nyholt de Prada JK, Lee YS, Latham KE, Chaffin CL, VandeVoort CA (2009): Role for cumulus cell-produced EGF-like ligands during primate oocyte maturation in vitro. *Am J Physiol Endocrinol Metab* 296, E1049-1058

O'Donnell L, Robertson KM, Jones ME, Simpson ER (2001): Estrogen and spermatogenesis. *Endocr Rev* 22, 289-318

Obernosterer G, Martinez J, Alenius M (2007): Locked nucleic acid-based in situ detection of microRNAs in mouse tissue sections. *Nat Protoc* 2, 1508-1514

Ohashi S, Naito K, Sugiura K, Iwamori N, Goto S, Naruoka H, Tojo H (2003): Analyses of mitogen-activated protein kinase function in the maturation of porcine oocytes. *Biol Reprod* 68, 604-609

Okamura K, Ishizuka A, Siomi H, Siomi MC (2004): Distinct roles for Argonaute proteins in small RNA-directed RNA cleavage pathways. *Genes Dev* 18, 1655-1666

Olsen PH, Ambros V (1999): The lin-4 regulatory RNA controls developmental timing in *Caenorhabditis elegans* by blocking LIN-14 protein synthesis after the initiation of translation. *Dev Biol* 216, 671-680

Otsuka F, McTavish KJ, Shimasaki S (2011): Integral Role of GDF-9 and BMP-15 in Ovarian Function. *Molecular Reproduction and Development* 78, 9-21

Otsuka M, Zheng M, Hayashi M, Lee JD, Yoshino O, Lin S, Han J (2008): Impaired microRNA processing causes corpus luteum insufficiency and infertility in mice. *J Clin Invest* 118, 1944-1954

Oubrahim H, Stadtman ER, Chock PB (2001): Mitochondria play no roles in Mn(II)-induced apoptosis in HeLa cells. *Proc Natl Acad Sci U S A* 98, 9505-9510

Palmer A, Gavin AC, Nebreda AR (1998): A link between MAP kinase and p34(cdc2)/cyclin B during oocyte maturation: p90(rsk) phosphorylates and inactivates the p34(cdc2) inhibitory kinase Myt1. *EMBO J* 17, 5037-5047

Palmer A, Nebreda AR (2000): The activation of MAP kinase and p34cdc2/cyclin B during the meiotic maturation of *Xenopus* oocytes. *Prog Cell Cycle Res* 4, 131-143

Pan Q, Chegini N (2008): MicroRNA signature and regulatory functions in the endometrium during normal and disease states. *Semin Reprod Med* 26, 479-493

Panigel M, Kraemer DC, Kalter SS, Smith GC, Heberling RL (1975): Ultrastructure of cleavage stages and preimplantation embryos of the baboon. *Anat Embryol (Berl)* 147, 45-62

Paradis F, Vigneault C, Robert C, Sirard MA (2005): RNA Interference as a tool to study gene function in bovine oocytes. *Mol Reprod Dev* 70, 111-121

Parrish JJ, Susko-Parrish J, Winer MA, First NL (1988): Capacitation of bovine sperm by heparin. *Biol Reprod* 38, 1171-1180

Pasquinelli AE, Reinhart BJ, Slack F, Martindale MQ, Kuroda MI, Maller B, Hayward DC, Ball EE, Degnan B, Muller P, *et al.* (2000): Conservation of the sequence and temporal expression of let-7 heterochronic regulatory RNA. *Nature* 408, 86-89

Paulini F, Melo EO (2011): The Role of Oocyte-Secreted Factors GDF9 and BMP15 in Follicular Development and Oogenesis. *Reproduction in Domestic Animals* 46, 354-361

Pepling ME (2010): A Novel Maternal mRNA Storage Compartment in Mouse Oocytes. *Biology of Reproduction* 82, 807-808



Perez GI, Knudson CM, Leykin L, Korsmeyer SJ, Tilly JL (1997): Apoptosis-associated signaling pathways are required for chemotherapy-mediated female germ cell destruction. *Nat Med* 3, 1228-1232

Pfeffer S, Zavolan M, Grasser FA, Chien M, Russo JJ, Ju J, John B, Enright AJ, Marks D, Sander C, *et al.* (2004): Identification of virus-encoded microRNAs. *Science* 304, 734-736

Picton H, Briggs D, Gosden R (1998): The molecular basis of oocyte growth and development. *Mol Cell Endocrinol* 145, 27-37

Pillai RS, Bhattacharyya SN, Artus CG, Zoller T, Cougot N, Basyuk E, Bertrand E, Filipowicz W (2005): Inhibition of translational initiation by Let-7 MicroRNA in human cells. *Science* 309, 1573-1576

Portela VM, Zamberlam G, Price CA (2010): Cell plating density alters the ratio of estrogenic to progestagenic enzyme gene expression in cultured granulosa cells. *Fertil Steril* 93, 2050-2055

Pratt AJ, MacRae IJ (2009): The RNA-induced silencing complex: a versatile gene-silencing machine. *J Biol Chem* 284, 17897-17901

Pregel P, Bollo E, Cannizzo FT, Rampazzo A, Appino S, Biolatti B (2007): Effect of anabolics on bovine granulosa-luteal cell primary cultures. *Folia Histochem Cytobiol* 45, 265-271

Pretheeban T, Gordon M, Singh R, Perera R, Rajamahendran R (2009): Differential mRNA expression in *in vivo* produced pre-implantation embryos of dairy heifers and mature cows. *Mol Reprod Dev* 76, 1165-1172

Puissant F, Vanrysselberge M, Barlow P, Deweze J, Leroy F (1987): Embryo Scoring as a Prognostic Tool in Ivf Treatment. *Human Reproduction* 2, 705-708

- Ramachandra RK, Salem M, Gahr S, Rexroad CE, 3rd, Yao J (2008): Cloning and characterization of microRNAs from rainbow trout (*Oncorhynchus mykiss*): their expression during early embryonic development. *BMC Dev Biol* 8, 41
- Reinhart BJ, Slack FJ, Basson M, Pasquinelli AE, Bettinger JC, Rougvie AE, Horvitz HR, Ruvkun G (2000): The 21-nucleotide let-7 RNA regulates developmental timing in *Caenorhabditis elegans*. *Nature* 403, 901-906
- Reinhart BJ, Weinstein EG, Rhoades MW, Bartel B, Bartel DP (2002): MicroRNAs in plants. *Genes Dev* 16, 1616-1626
- Ro S, Park C, Sanders KM, McCarrey JR, Yan W (2007a): Cloning and expression profiling of testis-expressed microRNAs. *Dev Biol* 311, 592-602
- Ro S, Park C, Song R, Nguyen D, Jin J, Sanders KM, McCarrey JR, Yan W (2007b): Cloning and expression profiling of testis-expressed piRNA-like RNAs. *RNA* 13, 1693-1702
- Rodriguez A, Griffiths-Jones S, Ashurst JL, Bradley A (2004): Identification of mammalian microRNA host genes and transcription units. *Genome Res* 14, 1902-1910
- Rogler CE, Levoci L, Ader T, Massimi A, Tchaikovskaya T, Norel R, Rogler LE (2009): MicroRNA-23b cluster microRNAs regulate transforming growth factor-beta/bone morphogenetic protein signaling and liver stem cell differentiation by targeting Smads. *Hepatology* 50, 575-584
- Rosa A, Spagnoli FM, Brivanlou AH (2009): The miR-430/427/302 Family Controls Mesendodermal Fate Specification via Species-Specific Target Selection. *Developmental Cell* 16, 517-527
- Rosenkrans CF, Jr., First NL (1994): Effect of free amino acids and vitamins on cleavage and developmental rate of bovine zygotes in vitro. *J Anim Sci* 72, 434-437

- Salama S, Arbo E, Lamazou F, Levailant JM, Frydman R, Fanchin R (2010): Reproducibility and reliability of automated volumetric measurement of single preovulatory follicles using SonoAVC. *Fertility and Sterility* 93, 2069-2073
- Sanbuissho A, Coskun S, Lin YC (1992): Role of cyclic adenosine monophosphate (cAMP) in vitro on bovine oocyte maturation. *Theriogenology* 38, 153-163
- Sasseville M, Ritter LJ, Nguyen TM, Liu F, Mottershead DG, Russell DL, Gilchrist RB (2010): Growth differentiation factor 9 signaling requires ERK1/2 activity in mouse granulosa and cumulus cells. *Journal of Cell Science* 123, 3166-3176
- Sato E, Matsuo M, Miyamoto H (1990): Meiotic maturation of bovine oocytes in vitro: improvement of meiotic competence by dibutyl cyclic adenosine 3',5'-monophosphate. *J Anim Sci* 68, 1182-1187
- Schier AF (2007): The maternal-zygotic transition: death and birth of RNAs. *Science* 316, 406-407
- Schultz RM (2002): The molecular foundations of the maternal to zygotic transition in the preimplantation embryo. *Hum Reprod Update* 8, 323-331
- Schwarz DS, Zamore PD (2002): Why do miRNAs live in the miRNP? *Genes Dev* 16, 1025-1031
- Sempere LF, Sokol NS, Dubrovsky EB, Berger EM, Ambros V (2003): Temporal regulation of microRNA expression in *Drosophila melanogaster* mediated by hormonal signals and broad-Complex gene activity. *Dev Biol* 259, 9-18
- Sen GL, Blau HM (2005): Argonaute 2/RISC resides in sites of mammalian mRNA decay known as cytoplasmic bodies. *Nat Cell Biol* 7, 633-636

- Sheedy FJ, Palsson-McDermott E, Hennessy EJ, Martin C, O'Leary JJ, Ruan QG, Johnson DS, Chen YH, O'Neill LAJ (2010): Negative regulation of TLR4 via targeting of the proinflammatory tumor suppressor PDCD4 by the microRNA miR-21. *Nature Immunology* 11, 141-U159
- Shen QL, Cicinnati VR, Zhang XY, Iacob S, Weber F, Sotiropoulos GC, Radtke A, Lu MJ, Paul A, Gerken G, *et al.* (2010a): Role of microRNA-199a-5p and discoidin domain receptor 1 in human hepatocellular carcinoma invasion. *Molecular Cancer* 9, -
- Shen XH, Han YJ, Cui XS, Kim NH (2010b): Ago2 and GW182 expression in mouse preimplantation embryos: a link between microRNA biogenesis and GW182 protein synthesis. *Reproduction Fertility and Development* 22, 634-643
- Shi DY, Xie FZ, Zhai C, Stern JS, Liu Y, Liu SL (2009): The role of cellular oxidative stress in regulating glycolysis energy metabolism in hepatoma cells. *Mol Cancer* 8, 32
- Shi W, Gerster K, Alajez NM, Tsang J, Waldron L, Pintilie M, Hui AB, Sykes J, P'ng C, Miller N, *et al.* (2011): MicroRNA-301 Mediates Proliferation and Invasion in Human Breast Cancer. *Cancer Research* 71, 2926-2937
- Sirotkin AV, Ovcharenko D, Grossmann R, Laukova M, Mlyncek M (2009): Identification of microRNAs controlling human ovarian cell steroidogenesis via a genome-scale screen. *J Cell Physiol* 219, 415-420
- Smitz JE, Cortvrindt RG (2002): The earliest stages of folliculogenesis in vitro. *Reproduction* 123, 185-202
- Sontheimer EJ (2005): Assembly and function of RNA silencing complexes. *Nat Rev Mol Cell Biol* 6, 127-138
- Starbuck MJ, Dailey RA, Inskeep EK (2004): Factors affecting retention of early pregnancy in dairy cattle. *Anim Reprod Sci* 84, 27-39

Stark A, Brennecke J, Russell RB, Cohen SM (2003): Identification of *Drosophila* MicroRNA targets. *PLoS Biol* 1, E60

Stark MS, Tyagi S, Nancarrow DJ, Boyle GM, Cook AL, Whiteman DC, Parsons PG, Schmidt C, Sturm RA, Hayward NK (2010): Characterization of the Melanoma miRNAome by Deep Sequencing. *Plos One* 5, -

Strozzi F, Mazza R, Malinverni R, Williams JL (2009): Annotation of 390 bovine miRNA genes by sequence similarity with other species. *Anim Genet* 40, 125

Stuelten CH, Buck MB, Dippon J, Roberts AB, Fritz P, Knabbe C (2006): Smad4-expression is decreased in breast cancer tissues: a retrospective study. *Bmc Cancer* 6, -

Su YQ, Sugiura K, Wigglesworth K, O'Brien MJ, Affourtit JP, Pangas SA, Matzuk MM, Eppig JJ (2008): Oocyte regulation of metabolic cooperativity between mouse cumulus cells and oocytes: BMP15 and GDF9 control cholesterol biosynthesis in cumulus cells. *Development* 135, 111-121

Suh MR, Lee Y, Kim JY, Kim SK, Moon SH, Lee JY, Cha KY, Chung HM, Yoon HS, Moon SY, *et al.* (2004): Human embryonic stem cells express a unique set of microRNAs. *Dev Biol* 270, 488-498

Suh N, Baehner L, Moltzahn F, Melton C, Shenoy A, Chen J, Belloch R (2010): MicroRNA Function Is Globally Suppressed in Mouse Oocytes and Early Embryos. *Current Biology* 20, 271-277

Sun Y, Wu J, Wu SH, Thakur A, Bollig A, Huang Y, Liao DJ (2009): Expression profile of microRNAs in c-Myc induced mouse mammary tumors. *Breast Cancer Res Treat* 118, 185-196

Sutton ML, Cetica PD, Beconi MT, Kind KL, Gilchrist RB, Thompson JG (2003): Influence of oocyte-secreted factors and culture duration on the metabolic activity of bovine cumulus cell complexes. *Reproduction* 126, 27-34

- Tadros W, Goldman AL, Babak T, Menzies F, Vardy L, Orr-Weaver T, Hughes TR, Westwood JT, Smilbert CA, Lipshitz HD (2007): SMAUG is a major regulator of maternal mRNA destabilization in *Drosophila* and its translation is activated by the PAN GU kinase. *Developmental Cell* 12, 143-155
- Tam OH, Aravin AA, Stein P, Girard A, Murchison EP, Cheloufi S, Hodges E, Anger M, Sachidanandam R, Schultz RM, *et al.* (2008): Pseudogene-derived small interfering RNAs regulate gene expression in mouse oocytes. *Nature* 453, 534-538
- Tang F, Kaneda M, O'Carroll D, Hajkova P, Barton SC, Sun YA, Lee C, Tarakhovskiy A, Lao K, Surani MA (2007): Maternal microRNAs are essential for mouse zygotic development. *Genes Dev* 21, 644-648
- Tanzer A, Stadler PF (2004): Molecular evolution of a microRNA cluster. *J Mol Biol* 339, 327-335
- Terret ME, Lefebvre C, Djiane A, Rassinier P, Moreau J, Maro B, Verlhac MH (2003): DOC1R: a MAP kinase substrate that control microtubule organization of metaphase II mouse oocytes. *Development* 130, 5169-5177
- Tesfaye D, Regassa A, Rings F, Ghanem N, Phatsara C, Tholen E, Herwig R, Un C, Schellander K, Hoelker M (2010): Suppression of the transcription factor MSX1 gene delays bovine preimplantation embryo development in vitro. *Reproduction* 139, 857-870
- Tesfaye D, Worku D, Rings F, Phatsara C, Tholen E, Schellander K, Hoelker M (2009): Identification and expression profiling of microRNAs during bovine oocyte maturation using heterologous approach. *Mol Reprod Dev* 76, 665-677
- Thouas GA, Trounson AO, Jones GM (2006): Developmental effects of sublethal mitochondrial injury in mouse oocytes. *Biol Reprod* 74, 969-977

Thouas GA, Trounson AO, Wolvetang EJ, Jones GM (2004): Mitochondrial dysfunction in mouse oocytes results in preimplantation embryo arrest in vitro. *Biol Reprod* 71, 1936-1942

Tripurani SK, Xiao CD, Salem M, Yao JB (2010): Cloning and analysis of fetal ovary microRNAs in cattle. *Animal Reproduction Science* 120, 16-22

Vaknin KM, Lazar S, Popliker M, Tsafiriri A (2001): Role of meiosis-activating sterols in rat oocyte maturation: effects of specific inhibitors and changes in the expression of lanosterol 14alpha-demethylase during the preovulatory period. *Biol Reprod* 64, 299-309

Valencia-Sanchez MA, Liu J, Hannon GJ, Parker R (2006): Control of translation and mRNA degradation by miRNAs and siRNAs. *Genes Dev* 20, 515-524

van der Heide LP, van Dinther M, Moustakas A, ten Dijke P (2011): TGF beta Activates Mitogen- and Stress-activated Protein Kinase-1 (MSK1) to Attenuate Cell Death. *Journal of Biological Chemistry* 286, 5003-5011

van Rooij E, Olson EN (2007): MicroRNAs: powerful new regulators of heart disease and provocative therapeutic targets. *J Clin Invest* 117, 2369-2376

Vella MC, Choi EY, Lin SY, Reinert K, Slack FJ (2004): The *C. elegans* microRNA let-7 binds to imperfect let-7 complementary sites from the *lin-41* 3'UTR. *Genes Dev* 18, 132-137

Wang C, Xie H, Song X, Ning G, Yan J, Chen X, Xu B, Ouyang H, Xia G (2006): Lanosterol 14alpha-demethylase expression in the mouse ovary and its participation in cumulus-enclosed oocyte spontaneous meiotic maturation in vitro. *Theriogenology* 66, 1156-1164

- Wang C, Xu B, Zhou B, Zhang C, Yang J, Ouyang H, Ning G, Zhang M, Shen J, Xia G (2009a): Reducing CYP51 inhibits follicle-stimulating hormone induced resumption of mouse oocyte meiosis in vitro. *J Lipid Res* 50, 2164-2172
- Wang LL, Zhang Z, Li Q, Yang R, Pei X, Xu Y, Wang J, Zhou SF, Li Y (2009b): Ethanol exposure induces differential microRNA and target gene expression and teratogenic effects which can be suppressed by folic acid supplementation. *Hum Reprod* 24, 562-579
- Wang NL, Zhang P, Guo XJ, Zhou ZM, Sha JH (2011): Hnrnpk, a Protein Differentially Expressed in Immature Rat Ovarian Development, Is Required for Normal Primordial Follicle Assembly and Development. *Endocrinology* 152, 1024-1035
- Watanabe T, Imai H, Minami N (2008): Identification and expression analysis of small RNAs during development. *Methods Mol Biol* 442, 173-185
- Watanabe T, Takeda A, Tsukiyama T, Mise K, Okuno T, Sasaki H, Minami N, Imai H (2006): Identification and characterization of two novel classes of small RNAs in the mouse germline: retrotransposon-derived siRNAs in oocytes and germline small RNAs in testes. *Genes Dev* 20, 1732-1743
- Watashi K, Yeung ML, Starost MF, Hosmane RS, Jeang KT (2010): Identification of Small Molecules That Suppress MicroRNA Function and Reverse Tumorigenesis. *Journal of Biological Chemistry* 285, 24707-24716
- Wienholds E, Kloosterman WP, Miska E, Alvarez-Saavedra E, Berezikov E, de Bruijn E, Horvitz HR, Kauppinen S, Plasterk RH (2005): MicroRNA expression in zebrafish embryonic development. *Science* 309, 310-311
- Wienholds E, Koudijs MJ, van Eeden FJM, Cuppen E, Plasterk RHA (2003): The microRNA-producing enzyme Dicer1 is essential for zebrafish development. *Nature Genetics* 35, 217-218



Wienholds E, Plasterk RH (2005): MicroRNA function in animal development. *FEBS Lett* 579, 5911-5922

Wiggin GR, Soloaga A, Foster JM, Murray-Tait V, Cohen P, Arthur JS (2002): MSK1 and MSK2 are required for the mitogen- and stress-induced phosphorylation of CREB and ATF1 in fibroblasts. *Mol Cell Biol* 22, 2871-2881

Wightman B, Ha I, Ruvkun G (1993): Posttranscriptional regulation of the heterochronic gene *lin-14* by *lin-4* mediates temporal pattern formation in *C. elegans*. *Cell* 75, 855-862

Wong DS, Zhang JY, Awasthi Y, Sharma A, Rogers L, Matlock EF, Van Lint C, Karpova T, McNally J, Harrod R (2004): Nerve growth factor receptor signaling induces histone acetyltransferase domain-dependent nuclear translocation of p300/CREB-binding protein-associated factor and hGCN5 acetyltransferases. *Journal of Biological Chemistry* 279, 55667-55674

Xia HF, Jin XH, Song PP, Cui Y, Liu CM, Ma X (2010): Temporal and Spatial Regulation of miR-320 in the Uterus during Embryo Implantation in the Rat. *International Journal of Molecular Sciences* 11, 719-730

Xu P, Vernooij SY, Guo M, Hay BA (2003): The *Drosophila* microRNA *Mir-14* suppresses cell death and is required for normal fat metabolism. *Curr Biol* 13, 790-795

Xu YF, Li EL, Han YD, Chen L, Xie ZA (2010): Differential expression of mRNAs encoding BMP/Smad pathway molecules in antral follicles of high- and low-fecundity Hu sheep. *Animal Reproduction Science* 120, 47-55

Yamamoto Y, Kosaka N, Tanaka M, Koizumi F, Kanai Y, Mizutani T, Murakami Y, Kuroda M, Miyajima A, Kato T, *et al.* (2009): MicroRNA-500 as a potential diagnostic marker for hepatocellular carcinoma. *Biomarkers* 14, 529-538

- Yan N, Lu Y, Sun H, Qiu W, Tao D, Liu Y, Chen H, Yang Y, Zhang S, Li X, *et al.* (2009): Microarray profiling of microRNAs expressed in testis tissues of developing primates. *J Assist Reprod Genet* 26, 179-186
- Yang Y, Bai W, Zhang L, Yin G, Wang X, Wang J, Zhao H, Han Y, Yao YQ (2008): Determination of microRNAs in mouse preimplantation embryos by microarray. *Dev Dyn* 237, 2315-2327
- Yao GD, Yin MM, Lian J, Tian H, Liu L, Li X, Sun F (2010a): MicroRNA-224 Is Involved in Transforming Growth Factor-beta-Mediated Mouse Granulosa Cell Proliferation and Granulosa Cell Function by Targeting Smad4. *Molecular Endocrinology* 24, 540-551
- Yao N, Yang BQ, Liu Y, Tan XY, Lu CL, Yuan XH, Ma X (2010b): Follicle-stimulating hormone regulation of microRNA expression on progesterone production in cultured rat granulosa cells. *Endocrine* 38, 158-166
- Yekta S, Shih IH, Bartel DP (2004): MicroRNA-directed cleavage of HOXB8 mRNA. *Science* 304, 594-596
- Yeo CX, Gilchrist RB, Lane M (2009): Disruption of bidirectional oocyte-cumulus paracrine signaling during in vitro maturation reduces subsequent mouse oocyte developmental competence. *Biol Reprod* 80, 1072-1080
- Yeung ML, Yasunaga J, Bennasser Y, Dusetti N, Harris D, Ahmad N, Matsuoka M, Jeang KT (2008): Roles for microRNAs, miR-93 and miR-130b, and tumor protein 53-induced nuclear protein 1 tumor suppressor in cell growth dysregulation by human T-cell lymphotropic virus 1. *Cancer Res* 68, 8976-8985
- Yi R, Qin Y, Macara IG, Cullen BR (2003): Exportin-5 mediates the nuclear export of pre-microRNAs and short hairpin RNAs. *Genes Dev* 17, 3011-3016

Yu YS, Sui HS, Han ZB, Li W, Luo MJ, Tan JH (2004): Apoptosis in granulosa cells during follicular atresia: relationship with steroids and insulin-like growth factors. *Cell Res* 14, 341-346

Yu ZR, Raabe T, Hecht NB (2005): MicroRNA Mirn122a reduces expression of the posttranscriptionally regulated germ cell transition protein 2 (Tnp2) messenger RNA (mRNA) by mRNA cleavage. *Biology of Reproduction* 73, 427-433

Zamah AM, Hsieh M, Chen J, Vigne JL, Rosen MP, Cedars MI, Conti M (2010): Human oocyte maturation is dependent on LH-stimulated accumulation of the epidermal growth factor-like growth factor, amphiregulin(dagger). *Human Reproduction* 25, 2569-2578

Zeng Y, Yi R, Cullen BR (2003): MicroRNAs and small interfering RNAs can inhibit mRNA expression by similar mechanisms. *Proc Natl Acad Sci U S A* 100, 9779-9784

Zhang B, Pan X, Cannon CH, Cobb GP, Anderson TA (2006): Conservation and divergence of plant microRNA genes. *Plant J* 46, 243-259

Zhang B, Pan X, Cobb GP, Anderson TA (2007a): microRNAs as oncogenes and tumor suppressors. *Dev Biol* 302, 1-12

Zhang H, Kolb FA, Jaskiewicz L, Westhof E, Filipowicz W (2004): Single processing center models for human Dicer and bacterial RNase III. *Cell* 118, 57-68

Zhang H, Li Q, Lin H, Yang Q, Wang H, Zhu C (2007b): Role of PPARgamma and its gonadotrophic regulation in rat ovarian granulosa cells in vitro. *Neuro Endocrinol Lett* 28, 289-294

Zhang L, Jiang S, Wozniak PJ, Yang X, Godke RA (1995): Cumulus cell function during bovine oocyte maturation, fertilization, and embryo development in vitro. *Mol Reprod Dev* 40, 338-344

Zhang N, Bevan MJ (2010): Dicer controls CD8(+) T-cell activation, migration, and survival. *Proceedings of the National Academy of Sciences of the United States of America* 107, 21629-21634

Zhao Y, Srivastava D (2007): A developmental view of microRNA function. *Trends Biochem Sci* 32, 189-197

Zheng X, Boerboom D, Carriere PD (2009): Transforming growth factor-beta1 inhibits luteinization and promotes apoptosis in bovine granulosa cells. *Reproduction* 137, 969-977

Zheng X, Price CA, Tremblay Y, Lussier JG, Carriere PD (2008): Role of transforming growth factor-beta1 in gene expression and activity of estradiol and progesterone-generating enzymes in FSH-stimulated bovine granulosa cells. *Reproduction* 136, 447-457

Zubakov D, Boersma AWM, Choi Y, van Kuijk PF, Wiemer EAC, Kayser M (2010): MicroRNA markers for forensic body fluid identification obtained from microarray screening and quantitative RT-PCR confirmation. *International Journal of Legal Medicine* 124, 217-226

Zuker M (2003): Mfold web server for nucleic acid folding and hybridization prediction. *Nucleic Acids Res* 31, 3406-3415

---

“Om Bhagavate Vasudevaya Namah”

At the outset, I would like to take the opportunity to convey my sincere thanks to all who have played their respective roles in contributing to the success of my project. It's indeed a privilege to have been selected for a position to pursue my Ph.D. under Prof. Dr. Karl Schellander, Institute of Animal Breeding And Husbandry Group, University of Bonn, Germany.

During my doctoral study, I have worked with a sizable number of people and thus their contribution in their own unique way to the research and this thesis deserves special mention.

Firstly, I would like to record my sincere gratitude to Prof. Dr. Karl Schellander for his advice and guidance from the very early stage of this research as well as in imparting his enriching experiences throughout the work. At all times of need, he has provided me unflinching encouragement and support in various ways. His scientific and innovative approach towards every task has imbibed in me an eternal ocean of ideas and the passion to excel in the field of science which is the dream of every student, researcher and scientist. His never ending zeal and enthusiasm in research has motivated me more than ever towards fruitful research which makes him an unforgettable person. He has not only guided me as student but also considered me as a part of his family. He has claimed his rightful place in my mind as a guardian and a constant source of inspiration to help me to proceed, achieve and excel not only in the field of research but in life as a whole. I am proud to record that I had opportunities to work with an exceptionally experienced scientist like him and I am highly indebted to him for the same.

I am thankful of Prof. Dr. Jens Léon, Institute of Crop Science and Resource Conservation (INRES), University of Bonn for his acceptance to be my second supervisor, valuable advice and evaluation of my work.

I gratefully acknowledge Dr. Dawit Tesfaye for his advice, supervision and key contribution, which formed the backbone of this research and thus to this thesis. His involvement combined with his innovativeness has triggered and nourished my intellectual maturity which will benefit me for a long time to come. His strong and dynamic leadership have played their part in cultivating and sharpening my scientific abilities. I owe my special thanks to him and hope to maintain our collaboration in future too. I also benefited by the outstanding work from Dr. Dessie Salilew Wondim, Dr. Nasser Ghanem, Dr. M Ulas Mehmet Cinar, Dr. Abdul Gaffer Miah and Dr. Umme Salma who helped with their special skills and their price less suggestions for the completion of this thesis. I wish to acknowledge Ms. Franca Rings and Ms. Eva Held for their technical support and contribution in embryos and phenotype collection in Frankenforst.

It is a pleasure to pay tribute to Prof. Dr. Christian Looft, Dr. Michael Hölker and Dr. Ernst Tholen for their constant encouragement and useful comments. I am much grateful of all

---

administrative members of the Institute of Animal Science, especially Ms. Bianca Peters and Ms. Ulrike Schröter for their kind helps with documentation, Mr. Peter Müller and Ms. Christine Große-Brinkhaus for their help and support in computer assistance. Many thank goes to all technical assistants especially Ms. Nadine Leyer, Mrs. Claudia Müller, Ms Helga Brodeßer, Mrs. Birgit Koch-Fabritius, Mr. Heinz, Mr. Simon and Mr. Stefan Knauf for their continuous technical help. I am grateful of Dr. rer. nat. Jochen Reinsberg, Universitätsklinikums Bonn, Dr. Bernhard Fuss, LIMES and Dr. Stephanie Buchholz, Life and Brain GmbH for necessary equipment access.

Collective and individual acknowledgments are also well deserved by my colleagues, Dr. Kanokwan Kaewmala, Dr. Autschara Kayan, Dr. Watchara. Laenoi, Dr. Munir Hossain, Dr. Abdollah Mohammadi Sangcheshmeh, Dr. Dagnachew Hailemariam, Dr. Alemu Hunde Regassa, Ms. Anke Brings, Ms. Hanna Heidt, Mrs. Simret Weldenegodguad, Mrs. Walaa Abd-El-Naby, Ms. Sally Rashad Elsaid Ibrahim, Mr. Heiko Buschbell, Mr. Muhammad Jasim Uddin, Mr. Huitao Fan, Mr. Md Ahmed Yehia Gad., Mr. Luc Frieden, Mr. Ijaz Ahmad, Mr. Ariful Islam, Mr. Sudeep Sahadevan, Mr. Sina Seifi Noferesti, Md. Mahmodul Hasan Sohel, Mr. Asep Gunawan, Mr. Ahmed Abdelsamad Zaki Amin, Mr. Jianfeng Liu.

My heartly thanks go to sweet ladies, Ms. Christiane Neohoff and Ms. Maren Julia Pröll, without whom the German translation part of this thesis would not have been possible.

I am at loss of words to express my feelings for my husband, Mr. Bimal Kumar Sinha, for his endless love, never ending support & encouragement during the entire course of my study in abroad without which it would not have been possible. He is the person from whom I have learned proactive thoughts and hard work. Being a mother it was very tough for me to leave an 11 month baby for studies but it has been possible only with the support of my lovable daughter, Ms. Vaishnawi Sinha, who still doesn't know her real mother, I don't know how to thank her. Your Germany Momma always missed you my sweetheart. I would like to give my sincere thanks to the family of Mrs. & Mr. Makhan who pampered & nourished my daughter as their beloved ones. My heartfull thanks to my elder sister Mrs. Savita Sinha and her husband Mr. D.N. Sinha how encouraged me during entire study period and nourished my child as they did in my childhood to obtained first in class.

Last but not the least, with deep reverence, I offer my sincere "Pranaam" to my father who rests in peace in the arms of the Cosmic Beloved but always looks upon me offering his eternal blessings and guidance. Further, I offer my respects to my mother, elders & in-laws for their blessings and the entire family for their continual encouragement. I shouldn't forget my Bachelor and Master friends who were always stood with me when I needed them.

Above all, I offer my prayers and homage at the feet of The Eternal Ultimate who has given me a happy family, a great career and all happiness in life.



---

**Publication:**

Manoharan K., Mishra G., Sathishkumar R., **Pritam Bala Sinha**, Karuppanapandian T., Agrawal S., Jagannathan V. (2005). Induction of embryogenic callus and direct plantlet regeneration in black gram (*Vigna mungo* (L.) Hepper). *J Swamy Bot-CI*. 22: 39-46.

Manoharan K., Karuppanapandian T., **Pritam Bala Sinha**, Prasad R. (2005). Membrane degradation, accumulation of phosphatidic acid, stimulation of catalase activity and nuclear DNA fragmentation during 2,4-D-induced leaf senescence in mustard. *J Plant Biol*. 48(4): 394-403.

Karuppanapandian T., Karuppudurai T., **Pritam Bala Sinha**, Kamarul Haniya A., Manoharan K. (2006). Genetic diversity in green gram [*Vigna radiata* (L.) landraces analyzed by using random amplified polymorphic DNA (RAPD). *Afr J Biotechnol*. 5(13): 1214-1219.

Karuppanapandian T., **Pritam Bala Sinha**, Premkumar G., Manoharan K. (2006). Chromium toxicity: Correlated with increased in degradation of photosynthetic pigments and total soluble protein and increased peroxidase activity in green gram (*Vigna radiata* L.) seedlings. *J Swamy Bot-CI*. 23: 117-122.

Karuppanapandian T., **Pritam Bala Sinha**, Kamarul Haniya A., Manoharan K. (2006). Differential antioxidative responses of ascorbate-glutathione cycle enzymes and metabolites to chromium stress in green gram (*Vigna radiata* L. Wilczek) leaves. *J Plant Biol*. 49(6): 440-447.

Karuppanapandian T., **Pritam Bala Sinha**, Kamarul Haniya A., Premkumar G., Manoharan K. (2006). Aluminium-induced changes in antioxidative enzyme activities, hydrogen peroxide content and cell wall peroxidase activity in green gram (*Vigna radiata* L. cv. Wilczek) roots. *J Plant Biol*. (India) 33(3): 241-246.

Karuppanapandian T., Karuppudurai T., **Pritam Bala Sinha**, Kamarul Haniya A., Manoharan K. (2006). Phylogenetic diversity and relationships among cow pea (*Vigna unguiculata* L. Walp.) landraces using random amplified polymorphic DNA markers. *Gen Appl Plant Physiol*. 32(3-4): 141-152.



---

**Pritam Bala Sinha**, Karuppanapandian T., Kamarul Haniya A., Manoharan K. (2007). Hydrogen peroxide-induced oxidative damage occurs on senescence green gram (*Vigna radiata* L.) leaves. *Internat J Plant Sci.* 2(1): 175-177.

Karuppanapandian T., Karuppudurai T., **Pritam Bala Sinha**, Kamarul Haniya A., Manoharan K. (2007). Random amplified polymorphic DNA markers variability and relationships among black gram (*Vigna mungo* L. Hepper) landraces. *J Plant Biol.* 34(2): 79-85.

Karuppanapandian T., **Pritam Bala Sinha**, Kamarul Haniya A., Manoharan K. (2009). Chromium-induced accumulation of peroxide content, stimulation of antioxidative enzymes and lipid peroxidation in green gram (*Vigna radiata* L. cv. Wilczek) leaves. *Afr J Biotechnol.* 8 (3), 475-479.

**Pritam Bala Sinha**, Hossain MM, Rings F, Hoelker M, Phatsara C, Tholen E, Schellander K, Tesfaye D (2010). Functional characterization of miR-130 family during bovine preimplantation development. *Reproduction Fertility and Development*, Volume: 22 Issues: 1 Page: 283-283, Published: 2010, Abstract: 252.

Miah AG, Salma U, **Pritam Bala Sinha**, Holker M, Tesfaye D, Cinar MU, Tsujii H, Schellander K (2011). Intracellular signaling cascades induced by relaxin in the stimulation of capacitation and acrosome reaction in fresh and frozen-thawed bovine spermatozoa. *Anim Reprod Sci.* (ahead of print).